Chapter 1.

Background and Literature Review.

1.1 Epidemiology of Alzheimer's disease, and HIV associated dementia.

Dementia is a term used to denote collectively a set of symptoms such as cognitive disabilities, neurological and psychological malfunctions caused by a multitude of disease conditions resulting from damage to the CNS or disorders of the brain (Ghafouri et al. 2006). AD, HAD, multiple sclerosis (MS), amyloidopathies and head injury related dementia are the leading forms of dementias affecting a significant population of the world. AD affects mostly the aged both in the developed and developing nations to the extent that the president of the United States declared November 2004 as a national AD awareness month. More than 18 million people in the world were living with AD in 2000 which constitutes about 60 to 70 % people suffering from any form of dementia (Prince 1997, Prince 2000, Wimo et al. 2003). By 2020, it is estimated to increase to 30-40 million (Prince 2000, Wimo et al. 2003). Prevalence of AD can be directly correlated to age as most of the patients suffering from AD are above 65 (Prince et al. 2006). Although AD is still more prevalent in the developed world, it is predicted that the prevalence of AD in the developing countries is increasing at a frightening rate. By 2040, with the increasing aged population in the developing world, the number of individuals with dementia will rise to 71 % of the total dementia cases in the world (Ferri et al. 2005, Kalaria et al. 2008). The majority of the cases will be AD as at present out of the total cases of dementia, 60 – 70 % cases account for AD.

Amongst the developing countries, China and Latin America are the worst hit by AD. Although AD is reported to be less prevalent in India, and sub-Saharan Africa, there could be underestimation due to less concrete diagnostic machinery, less awareness, and not reporting to the doctors due to poor socioeconomic backgrounds. The prevalence of AD amongst the African-American population is higher than that of the sub-Saharan African population. In US, the yearly direct and indirect cost of AD and other dementias is $ 148 billion (AD facts and figures 2008), whereas in developing countries, it is estimated to be $ 73 billion (Kalaria et al. 2008).

The second largest 21st century brain disorder after AD and vascular dementia with a significant impact on the society in the African continent as well as the other developing and developed nations is a dementia associated with HIV. HIV related dementia or HIV dementia, HIV associated dementia, AIDS dementia Complex, and neuroAIDS are commonly used acronyms to indicate the cognitive deficit associated with AIDS. In some research articles, HIV-1-associated dementia is abbreviated to HAD (Goodkin et al. 1997, Hinkin et al. 2001). For the purpose of this thesis, HAD is used to denote all these interrelated terms which are used to indicate dementia associated with HIV. The prevalence of HIV is increasing rapidly all over the world. According to the World Health Organisation (WHO) report in 2003, out of more than 40 million people suffering from HIV/AIDS worldwide, about 26.6 million people are from sub-Saharan Africa (Nath and McArthur 2004). 2.7 million new AIDS cases and 2 million deaths have been reported in Africa in the year 2005 (Robertson et al. 2008). HIV infection has direct and indirect impact on the CNS and life of an individual. One of the routes that HIV spreads from one individual to the other is via sharing of needles amongst drug users. Although in hospitals and medical care centres, effective measures have been taken to reduce the spread of HIV via blood transfusion or other iatrogenic routes, but many drug addicts, under the influence of drugs share the

needles, and this has resulted in the spread of HIV infection. There is a correlation between the epidemiology of cocaine addiction (with and without needle use) and HIV neuropathogenesis or HAD (Goodkin et al. 1997). It is hypothesized that the HAD prevalence might be enhanced by convergence with cocaine use (Goodkin et al.1998). Most of the people suffering from AIDS don't have access to the anti-retrovirals in poor or underdeveloped nations, but the overall access to the retroviral therapy is increasing, although at a very low pace. The increased access to the highly active anti-retroviral therapy (HAART) has also increased the life expectancy of the individuals suffering from AIDS. Prior to the HAART era, the prevalence of HIV dementia was 7 %, and the lifetime risk for an individual was 5 to 20 % (McArthur et al. 1993). After access to the HAART therapy, initially there was a drop in HAD or HIV dementia cases (McArthur 2004). However, later in the post HAART era, the percentage of people with HAD and other HIV related neurological symptoms is increasing at an alarming rate (McArthur 2004, Nath and McArthur 2005). It is postulated that HAART may reduce the incidence of HAD, but may increase the prevalence of the disease due to longer life span of an individual (Sacktor et al. 2001). This increase could create second epidemic of cognitively impaired individuals in sub-Saharan Africa (Wong et al. 2007). Thus, HAD could emerge as the second largest disorder of the brain next to AD and vascular dementia.

In order to develop new treatment strategies, it is necessary to understand the aetiology of these neuroinflammatory disorders. The aetiology of these two highly prevalent disorders is discussed in the following section.

1.2 Primary factors involved in the aetiology of AD and HAD.

In the last century, Alois Alzheimer identified a form of dementia associated with plaques, which was later defined as AD. As discussed in the previous section, AD affects mostly aged individuals above 65, but at least in 10% cases it affects young individuals from the age of 40 to 60 yrs. Depending upon the age group it most affects, AD is classified as an early onset AD (or familial form of AD), and late onset AD (or Sporadic form of AD). Both these forms of AD share some common pathological features. The most important pathological hallmark of AD is amyloid plaques. In order to develop a drug for the treatment of AD, it is important to understand the plaque pathology, formation of plaques and pathogenic proteins involved in the aetiology of AD. A vast amount of literature is available in this regard, (Blennow et al. 2006, Nixon 2007, Haddad et al. 2004). Amyloid precursor protein (APP) plays an important role in synapse formation (Priller et al. 2006), and synaptic plasticity (Turner 2003) under normal circumstances. It is metabolised by the α, β and γ secretases. APP is processed to Aβ 40, but in AD, it is converted into Aβ42. This Aβ42 is insoluble and results in the formation of plaques. These plaques are the primary pathological features of AD. In the familial form of AD, there is an over expression of mutated APP (Hardy 2006) and the rate of production of amyloid proteins exceeds the rate of clearance or metabolism of APP with the net result of deposition of amyloid plaques, whereas in the sporadic form of AD, although there is no over expression of APP, the rate of clearance of amyloid protein is slower than that of its production rate which results in the deposition of plaques. The other

pathological determinants of sporadic form of AD are discussed later in the appropriate section. The plaques and oligomers are further involved in the activation of the proinflammatory mediators, neurofibrillary tangle (NFT) formation which subsequently leads to dementia. The overall process is simplified, and discussed in a recent review on AD in Lancet (Blennow et al. 2007).

Another pathological hallmark of AD is a family of microtubule proteins (six isoforms) referred as tau proteins, which are normally expressed within neurons (Himmler et al. 1989). Hyperphosphorylated tau proteins are evident in NFTs in APPsw/tau transgenic mice as well as in the brains of patients suffering from AD (Perez et al. 2008). In AD tau is hyperphosphorylated due to many factors. It is reported that mitochondrial oxidative stress is responsible for the hyperphosporylation of tau in AD (Melov et al. 2007). It is also reported that Aβ proteins are responsible for the hyperphosphorylation of tau, and a family of kinases is involved in the phosphorylation (Williamson et al. 2002). Tau dependent AD pathology is also mediated by extracellular prefibrillar amyloid proteins (King et al. 2006). Recently, it was also shown that the soluble Aβ oligomers (ADDLs) are involved in the aetiology of AD independent of the fibrillar proteins. These oligomers stimulated phosphorylation of tau in neuroblastoma cell lines and hippocampal neurons (De Felice et al. 2008). It was also shown in the same study that ADDLs extracted from the brains of AD patients were able to stimulate the hyperphosphorylation of tau, but not the ones extracted from non AD patients. The hyperphosphorylated tau protein is responsible for the pathophysiology of AD through its ability to degenerate neurons (A´ Vila et al. 2004, De Felice et al. 2008). Once hyperphosphorylated, it disrupts the neuronal trafficking, and is also responsible for oxidative stress which leads to neurodegeneration (Stamer et al. 2002). Tau is an important constituent of NFTs which are directly correlated with AD. However, a quantitative and immunohistochemical study of the supragranular layer of the middle temporal neocortex revealed non-tau based neuronal degeneration in 2 patients with AD (van De Nes et al. 2008). This tau independent mechanism might be responsible for the decay in the dysfunction at cellular level in the neocortex which subsequently leads to dementia.

The other protein which plays an important role in the pathophysiology of AD is Apo lipoprotein E4 (ApoE4). ApoE is a component of triglyceride rich lipoproteins, and is involved in the catabolism of cholesterol, triglycerides, and lipoproteins in plasma under normal condition (Weisgraber et al. 1994, Mahley 1996, Mahley and Ji 1999). It is mainly localised, and synthesized in the liver, and in the brain. In the brain, it is synthesized independent of liver. It exists in three different isoforms (2, 3, and 4), and the isofroms ApoE3 and ApoE4 bind to ciliary neurotrophic growth factor (CNTF) to facilitate neural repair (Gutman et al. 1997). It also downregulates production of inflammatory cytokines TNF-α and IL6 by glial cells of the brain, and thereby prevents inflammation (Laskowitz 1997, Lynch 2000). However, it has been genetically linked to the late onset familial and sporadic form of AD and poses a greatest risk of inheritance (Corder et al. 1993, Strittmatter et al. 1993). ApoE4 has also been correlated with small blood vessel disorders including amyloid angiopathy (Tiraboschi et al. 2004). In the same study, it was found that there was a correlation between ApoE4 and amyloid senile plaques. No correlation was observed between NFT and ApoE4 in their study. However, some

investigators found correlation between ApoE4 with the phosphorylation of tau and formation of NFTs (Strittmatter et al. 1994). Through its interactions with tau, it was implicated in the pathophysiology of AD. Neuron specific proteolysis of ApoE4 was also found to be involved in the phosphorylation of tau protein in transgenic APP expressing mice (Brecht et al. 2004). In short, amyloid, tau and ApoE4 are the primary pathological hallmarks of AD. According to a new hypothesis, the behavioural deficit in AD patients is observed much earlier before the formation of insoluble Aβ or plaques, and therefore the role of ADDLs is not restricted just to the formation of insoluble amyloid proteins, but have certain direct involvement in the pathophysiology of AD as evidenced by the inhibition of long term potentiation by them (walsh et al. 2002). So amyloid protein, ADDLs, tau, and ApoE4 are the primary factors involved in the aetiology of AD.

HIV-1 enters the brain of HIV +ve patients in early stages of infection. HAD is characterised by motor, behavioural and cognitive deficit, and at least some of its symptoms can be correlated to AD (Minagar et al. 2004, Shapshack et al. 2008). In HAD, HIV and its pathogenic protein are responsible for the pathogenesis. The proteins Tat1, gp 120, and Nef 41 are known to play an important role in the pathophysiology of HAD (Sheng et al 2000, Rempel and Pullium 2005, Saha and Pahan 2007, van Marle et al. 2004). Recently, HIV-1 Vpr was also found to cause apoptosis and neurodegeneration (Jones et al. 2007).

1.3 Similarities and differences in the aetiologies of AD and HAD.

Although there is a basic difference in the primary pathophysiology of AD and HAD, there are striking similarities in the pathogenic factors associated with them. These two disorders share so many things in common that the title of one recently published article was, “The coming problem of HIV-associated Alzheimer's disease” (Alisky 2007). The primary factors in the aetiology of AD such as amyloid and presenillin are the secondary factors activated by the primary factors (virus and its proteins) in HAD. HAD could also result from the CNS infections due to weakened immune system in later stages of AIDS. Most of these are opportunistic infections in an immunocompromised environment.

1.4 Similarity between AD and HAD at Genetic Level.

Recently, a study was done where genetic comparison was made between AD and NeuroAIDS using the National Centre for Biotechnology (NCBI), Entrez and other websites. The comparison was made at three levels such as structure, function, and expression of genes in these two disorders to explore the relationship between AD and HAD without ignoring the differences. It was found that Aβ and HIV associated genes shared chromosomal locations (4, 5, 11, and 17). There was a similar association in the chromosomal locations of presenilin genes and HIV related genes, and these two shared the locations on chromosomes 1, 2, 3, and 14. However, the ApoE4 gene shares no loci relationship with HIV related genes (Shapshak et al. 2008). Thus, aetiological features associated with these two disorders of the brain show similarity at biochemical and genetic level.

1.5 Immune Activation and Inflammatory Processes in AD and HAD.

Both AD and HAD show activation of the immune system and involvement of common pro-inflammatory mediators. The activation of cells of the immune system and residual brain cells, although beneficial initially, results in release and/or activation of several pro-inflammatory mediators, which are responsible for damage to the brain tissue. Activation of astrocytes and microglia can be found in most of the brain disorders including AD and HAD (Carson et al. 2006). The common pro-inflammatory mediators found in most of the neurodegenerative disorders are free radicals, NF-κB, cyclooxygenases (COX), and most importantly, the complement system (Phillis et al. 2006, Chiarugi et al. 2003, Bonifati and Kishore 2007). In AD aggregation of primary pathogenic proteins in the cholinergic target areas is also associated with the degeneration of basal forebrain cholinergic neurons, and these form one of the major treatment strategies aimed at AD (Lahiri et al. 2003a). Amyloid plaques in AD are responsible for the activation of pro-inflammatory mediators and up-regulation of the complement system (Tacnet-Delorme et al. 2001). Both HIV and its pathogenic proteins along with amyloid protein are responsible for up-regulation of the complement system **(**Vehmas et al. 2004). Besides the complement system, other pro-inflammatory mediators are also involved in the neuroinflammation in AD and HAD. These are free radicals, eicasonoids, nitric oxide, leukotrienes, cytokines, and cyclooxygenases (Kubis and Janusz 2008, Li et al. 2003, Rotilio et al. 2003, Consilvio et al. 2004). These pro-inflammatory mediators, in synergy with each other, and/ or independent of each other mediate neuroinflammation These neuroinflammatory processes are at the core of many neurodegenerative disorders including AD and HAD.

1.6 Current treatment strategies for AD, HAD, and other neuroinflammatory disorders, and their drawbacks.

At the base of these neuroinflammatory processes are the activated microglia, phagocytic, immune cells, or other cells of the CNS which can generate most of these proinflammatory molecules. As discussed earlier, apart from their direct actions, complement components play indirect roles in mediating the actions of proinflammatory molecules, particularly those that are released or expressed by glial or other immune cells. It is evident from the fact that complement is involved in the activation and chemotaxis of glial and other cells involved in neuroimmune activation. In addition, some enzymes like cyclooxygenases are probably associated with the complement system or its receptors, and mediate inflammation by activating the complement system. This is evident from the recent findings where it was shown that C1q levels were high in mice over expressing COX-2 (Spielman et al 2002). COX inhibitors inhibit complement mediated glomerular epithelial cell injury in Heyman nephritis which further supports association between COX-2 and the complement system (Takano et al. 2003). However, there is no complement regulatory agent available on the market for the treatment of inflammation in general and neuoinflammation in particular (Makrides 1998). Anti-inflammatory drugs, which include non steroidal anti-inflammatory drugs (NSAIDs), such as indomethacin, and the other cyclooxygenase-1 (COX-1) inhibitors like rofecoxib, celecoxib, naproxen, and aspirin, are being tried

and found to have some neuroprotective role, but at present no currently available agent offers significant neuroprotection in the neurodegenerative disorders (Aisen et al. 2003, Scharf et al. 1999). Recently rofecoxib was withdrawn from the market because of undesirable cardiovascular side effects which makes the case that drugs need to be very carefully screened before clinical use. These findings might lead one to question the significance of inflammation in neurodegenerative disorders. However, the reason for their failure can be attributed to their inability to directly inhibit the complement system. On the other hand, steroids like estrogens and progesterone have been tested for their neuroprotective roles (Hilton et al. 2004, Gonzalez-Deniselle et al. 2002).

Although aforementioned disorders are affecting a significant world population, there is no effective treatment available for the treatment of these disorders. The initiatives to develop a vaccine against AD have failed. In one of the clinical trials where amyloid proteins were targeted using antibodies against them, the treatment resulted in aggravation of the neuroinflammatory response instead of neuroprotection (Karkos et al. 2004). Estrogen mediates its action by direct inhibition of microglial activation (Bruce-Keller et al. 2000). Recently, attempts were made to develop estrogen based hormone therapy for treating women affected by AD as the prevalence of AD is higher in women than in men. Prednisone and estrogen treatment in the controlled trial of AD patients failed (Aisen et al. 2000, Reichman 2000). This raises a grave concern regarding the therapeutic utility of these agents in allied disorders. A recent study revealed that the hormone therapy with estrogen works only if the therapy starts immediately after cessation of menopause in women. If the treatment with estrogen starts at an old age, it might not have any effect (Sherwin 2006). AD is associated with neuroinflammation, and many NSAIDs have been tested for their clinical effectiveness in the treatment of AD. Indomethacin (Rogers et al. 1993) and Nimesulide (Aisen et al. 2002) were found to be effective in a clinical trial and a random pilot study of AD. However, more controlled clinical trials revealed no beneficial effects of NSAIDs in treatment of AD. Rofecoxib (Reines et al. 2004) and diclofenac / misoprostol (Scharf et al. 1999) failed to show significant improvement in AD treatment in controlled clinical trials. NSAIDs control inflammation through their ability to inhibit cyclooxygease enzymes (COX-1 and COX-2). The importance of COX enzymes in the brain, and side effects associated with the inhibition of COX enzymes are discussed in a recent review (Minghetti 2004). COX-2 is mainly involved in inflammation, and COX-1 is present in the gut. Most of the NSAIDs are mixed inhibitors of COX, and thus chronic treatment may lead to severe gastrointestinal problems such as ulcers. COX-2 isozyme is involved in memory consolidation and COX-1 is involved in memory formation. COX-2 is involved in the production of harmful prostaglandins in normal nociceptive response, but it leads to the formation of PGE_2 in the hippocampus, which is involved in the regulation of membrane excitability and synaptic transmission (Chen and Bazan 2005).

1.7 Treatment of HAD.

Although neuroinflammation is evident in HAD, generally the therapy is aimed at controlling HIV-1 using anti-retrovirals or more recently using the highly active anti-retroviral therapy (HAART).

HAART has shown definite beneficial effects, but still better agents need to be developed. Abacavir is one of the antiretrovirals with an ability to cross BBB. It was tested for its effectiveness in the treatment of HAD in a double blind placebo controlled clinical trial on 105 HIV positive patients who were already on a combination of anti-retroviral. There was a slight improvement in the cognitive functions of Abacavir treated patients, but the improvement was not statistically significant (Brew et al. 2006). Proper design of the study with the inclusion of two or three anti-retrovirals, better understanding of the relationship between mild to severe forms of dementia are some of recommendations for future clinical trial (Ellis 2007). Zydovudine was recently tested for its effectiveness in HAD due to its ability to cross the BBB. It was found to improve the cognitive symptoms in HAD. However, even in the post HAART era, the prevalence of HAD is increasing at an alarming rate (McArthur 2004, Nath and McArthur 2005, Sacktor et al. 2001). As discussed in the epidemiology section, this could result in the second largest pandemic in sub-Saharan Africa (Wong et al. 2007). The patients on HAART has also shown increased incidence of peripheral neuropathy, and the HAART treatment is also associated with the increased levels of C3 and C4 in the plasma of the patients (Spear et al. 1999, Datta and Rappaport 2006). This indicates the importance of development of alternative strategies for the control or the treatment of HAD.

As discussed in the section on aetiology, like AD, inflammation plays a damaging role in HAD. Therefore, development of alternative strategies for the treatment of these two disorders is essential. Gene therapy, although a good option, is still at the stage of infancy. The bottom line is that the specific pharmacological treatment of the primary cause of most of the neuroinflammatory disorders is currently not available and NSAIDs available on the market have a limited scope and/or undesirable side effects. The development of suitable neuroprotective agents therefore is strategically important and demands urgent attention.

1.8 Other possible treatment strategies under development.

Apart from steroids and NSAIDs, several agents are under development. A few of them mediate their actions through receptors (agonist/antagonists), nitric oxide synthesis inhibitors, or free radical scavengers (Kristin et al. 2003) Nitrones are also shown to have a neuroprotective role (Floyd 2002). Cannabinoids acting via their own receptors, D3/D2 agonists in PD, serine protease inhibitors like FUT-175, phenolic thiazoles, phosphodiesterase inhibitors and calcium channel blockers also offer neuroprotection (Mizuno et al. 2004, Harnett et al. 2004, Blake 2004, Toyoda et al. 2004, Kastumata et al. 2003). However, most of these agents are directed towards a single component involved in neuroinflammation and a few of them show some indirect or direct actions against the complement. As mentioned earlier, neurons are more prone to attack by the complement components, as they produce very low levels of complement regulatory proteins. A few agents like cannabinoids might play some neurodegenerative role apart from neuroprotecive roles (Sarne and Keren 2004). Most of these agents show no direct activity against complement and they might not be of significant help in several neuroinflammatory disorders, where complement plays a major role. Hence, for effective

neuroprotection, development of and/or search for the agents with complement regulatory activity as a major activity is a matter of urgency. Complement regulatory proteins offer hope in this context. This is evident from the recent findings that a complement regulatory protein, sCrry, plays an important role in the treatment of MS (Davoust et al. 1999). However, the same agent failed in the treatment of AD (Wyss-Coray et al. 2002). Attention to this contradiction should not be neglected.

In order to develop the complement regulatory neuroprotective agents for the treatment of AD and HAD, it is essential to further understand the basics of the complement system, its roles in neuroinflammation in general, and in AD and HAD in particular.

1.9 The Complement System.

The complement system is a well defined host defense mechanism against invading microorganisms. It consists of nearly 20 proteins (C1 (q, r, s) to C9, properdin factor B, factor H) which are involved in non-specific immune response. The roles of complement proteins as the body's defense system as well as in the brain are well documented by many (Barnum 1995, Makrides 1998). In addition to these 20 proteins comprising of enzymes, coenzymes or peptides mostly circulating in the body in an inactive form, 10 more membrane bound proteins of the complement system which act as complement regulatory proteins also form a part of the complement system (Barnum 1995). The role of various complement components in the pathophysiology of several disorders has been well studied in the past two decades. The activation of this critical system takes place through three pathways, CP, AP, and the lectin mediated pathway (LMP). Out of these three, CP and AP are the major pathways of complement activation involved in the aetiology of CNS disorders. The process of activation of these two pathways is summarized in Fig 1.1 below.

Activation of the AP and CP in AD, HAD and other neuroinflammatory disorders.

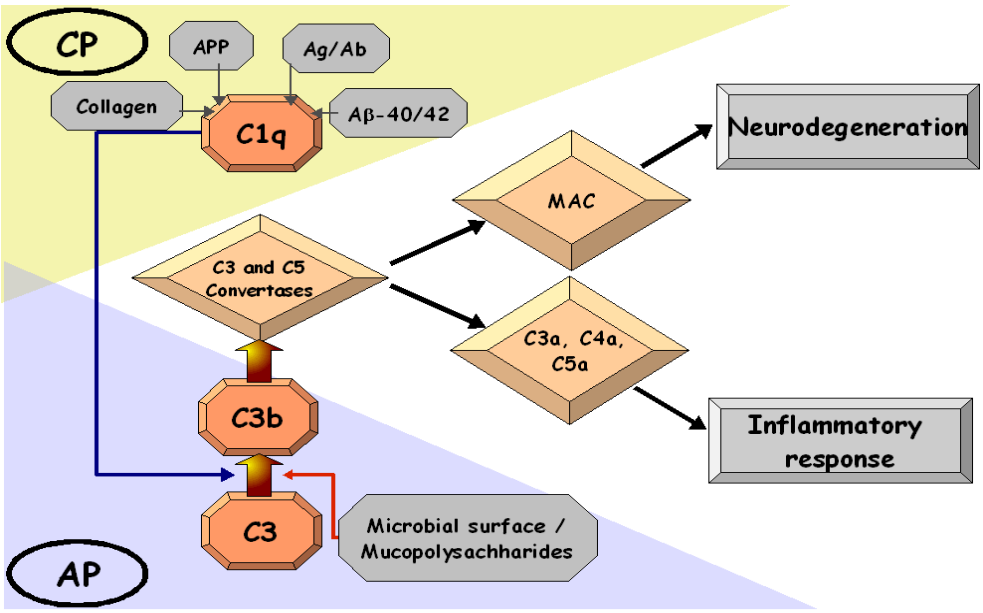

Figure 1.1. *Activation of the classical pathway (CP; Shown by yellow background and a blue line) and the alternative pathway (AP; shown by violet background and a red line) of complement activation. In AD, HAD and other neuroinflammatory disorders, CP is activated by binding of pathogenic proteins such as Aβ-40, Aβ-41, amyloid precursor protein (APP), antigen antibody complex (Ag/Ab) to the complement component C1q which leads to the activation of C3). The activation of AP is initiated by binding of microbial surface proteins and polysaccharides to complement components C3 and C3b. C3 and C3b are central to complement activation, and are involved in the formation of C3 and C5 convertases which leads to the formation of anphylatoxins (C3a, C4a, and C5a), and membrane attack complex (MAC) which in turn leads to neuroinflammation and neurodegenerartion*

The complement proteins circulate in the body in an inactive form. Whenever a foreign molecule attacks the host, the complement system gets activated by either of these pathways. The antigen-antibody complex activates C1q component of the classical complement cascade and a series of proteolytic steps are mediated leading to activation of C3 and C5 convertases, and subsequent production of anaphylatoxins (McGeer and McGeer 1998).

AP, however, is activated by the surface of microorganisms and lipopolysaccharides. The final consequence of complement activation by either of these pathways is the formation of membrane attack complex (MAC) and generation of anaphylatoxins. MAC is involved in the removal of foreign molecules or pathogens. It also mediates cell lysis. The various components of the complement system are involved in the process of inflammation. The roles of the various pathways of complement activation and the various components of the complement system generated as a result of complement activated neuroinflammation are discussed in the following section.

1.9.1 The complement pathways and neuroinflammation.

Activation of the CP through C1q component of the complement is evident in neurodegenerative disorders, such as AD (Webster et al. 1995). Once activated, C1 cleaves both C4 and C2 to generate C4a and C2a fragments, which combine to form the C3 convertase of CP, and are involved in the cleavage of component C3 to form C3a and C3b. C3a is an anaphylatoxin and acts via various receptors present on the cellular surfaces. C3b combines with C4a and C2a to form C5 convertase, which leads to the formation of C5a and C5b. The former is an anaphylatoxin and the latter is involved in the production of terminal complement components, C6 to C9. C5b, with these terminal complement components, results in the formation of MAC (Muller-Eberhard 1988). The AP also results in the formation of complement anaphylatoxins and MAC, but activated through C3 component, requires factor B to form C3 convertase and C5 convertase. The overall process of complement activation by the AP, and CP, and the role of complement regulatory molecules in their control are described in detail by many (Makrides 1998, Stoiber et al. 2005, Datta and Pappaport 2006). The activation of complement system in neurodegenerative disorders such as AD leading to neuroinflammation is outlined in Fig 1.1.

1.9.2 Anaphylatoxins and Neuroinflammation.

As noted previously, activation of complement by the major pathways involved in the neurodegeneration process results in the formation of anaphylatoxins. C3a and C5a are the potent anaphylatoxins. These are found to be associated with several neurodegenerative disorders. The role of anaphylatoxins in inflammation is complex and not fully understood. Recent reports suggest that complement anaphylatoxins might play a neuroprotective role (Mukherjee and Pasinetti 2000, Mukherjee and Pasinetti 2001, van Beek et al 2001). Anaphylatoxin 5a plays a neuroprotective role by mitogen-activated protein kinase inhibition of caspase-3 (Mukherjee and Pasinetti 2001). The complement anaphylatoxin C3a is also found to have some neuroprotective role in N-methyl d-aspartate (NMDA) induced neurotoxicity (van Beek et al. 2001). Anaphylatoxin C5a is found to be beneficial in kainic acid toxicity and reduces the levels of glutamate, a neurotoxic agent found to be elevated in neurodegenerative disorders (Osaka et al. 1999). However, C3a does not protect against kainic toxicity though it has been shown to have neuroprotective actions in NMDA-induced cell death (van Beek et al. 2001). The beneficial effects of complement anaphylatoxins must be balanced against their detrimental effects to understand the exact role played.

1.9.3 The complement regulatory molecules.

As the terminal products generated after complement activation are damaging to the cell, and therefore needs to be tightly regulated. There are several complement regulatory molecules whose role in complement regulation is discussed in many reviews (Datta and Rapoport 2006, Makrides 1998). These complement regulatory molecules are expressed at a very low level in neurons, and therefore up-regulation of the complement system in the CNS leads to neuroinflammatory consequences (Singhrao et al. 2000). HIV is known to inhibit the complement regulatory molecules as discussed later in the

section. This highlights the need for suitable complement regulatory molecules for the treatment of these disorders.

1.9.4 Dual nature of the complement system.

From the above discussion, it is evident that the complement system plays a major role in the pathogenesis of several neuroinflammatory disorders. Although in most instances, the effects of complement system are detrimental, their beneficial roles, especially in glutamate and kainate toxicity should not be neglected (Osaka et al. 1999, Mukherjee and Pasinetti 2001, van Beek et al. 2001). The role of complement in neurodegeneration is a double-edged sword (Singhrao et al. 2000). This dual nature of the complement system suggests the necessity of thorough investigation of the roles played by various complement components. The dual nature played by the complement system may depend critically on the form of the disease and period of exposure to various complement components. In the normal immune response, in which an exposure to complement components is for a short period of time, the tissue repairing roles played by complement components are beneficial. However, chronic exposure results in their detrimental effects. An added complexity is that an acute exposure, as observed in accidental injury to the brain or spinal cord, is also destructive. The overall time and concentration-dependent actions of complement components can be diagrammatically represented by the minute, second, and hour hands of a clock (Fig 1.2).

Time dependent actions of the complement system in neuroinflammatory disorders of the CNS.

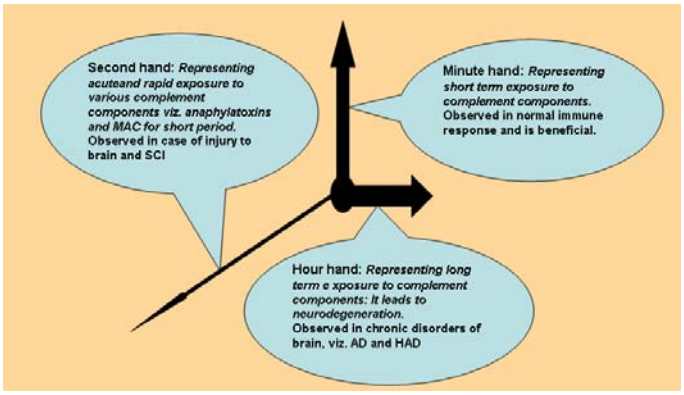

Figure 1.2. *Hands of a clock representation of time dependent actions of complement components in neurodegenerative disorders. The complement exposure in AD and HAD represented by the Hour hand.*

1.9.5 The complement system and AD.

In AD, amyloid plaques activate the CP of complement system. In transgenic mice lacking C1q, there is less neuropathology than in amyloid producing transgenic mice models (Fonesca et al. 2004). In these mice deficient of C1q, there is a low level of glial activation as compared to the transgenic mice expressing C1q, which means that amyloid protein activate glial cells via activation of the CP of complement. In AD patients, mRNA levels of the complement component C1q was increased from 11

to 80 % in the entorhinal cortex, hippocampus, and midtemporal gyrus, and the level of complement component C9 from 10 to 27% (Yasojima et al. 1999). These are the regions were the accumulation of Aβ and NFT was dense. NFTs, associated tau, and other proteins are also involved in the activation of complement (Shen et al. 2001, Fonseca et al. 2004). The complement opsonins and MAC are involved in the etiology of AD (van Beek et al. 2003, McGeer and McGeer 2003). In AD, the complement system plays a dual role, and is explained by the "Yin and Yang" hypothesis (Shen and Meri 2003). Initially, the opsonin complements (i.e., iC3, C3b, etc.) play a beneficial role in the clearance of plaques, but in later stages of AD, particularly in sporadic AD, the upregulation of various inflammatory components (anaphylotoxins and MAC) results in neurodegeneration, which is associated with dementia (Webster et al. 1995). Cox-1 is involved in AD and is found to be associated with the complement system. The complement components are involved in the activation of cells of the CNS and the migration of macrophage and leukocyte from periphery to the CNS, thereby playing an important role in the pathogenesis. There is now evidence that the AP is activated in the frontal cortex of AD patients, where factor B plays an important role (Strohmeyer et al. 2000) not only amyloid plaques, and fibrils, but also Aβ oligomers activate the complement system in prions disease (Andreas et al. 2008, Sjoberg et al. 2008). Aβ oligomers which are also involved in the pathophysiology of AD might also play a similar role. According to a recently proposed oligomer hypothesis, not only amyloid plaques and proteins, but soluble β-oligomers are at the core of the neuropathological features of AD. In addition, cytokines, such as IL-1α and IL- 1β, upregulate APP expression leading to Aβ depositions, which itself can trigger the cascade of inflammatory pathway (Lahiri et al. 2003b). Recent evidence showed that there is polymorphism in the complement factor H (CFH), which influences the risk of AD (Zetterberg et al 2008). Also, an interaction between ApoE4 alleles and CFH was observed which may predispose the AD patients to morbidity. C3 and C4 are expressed in C1q sufficient and deficient mice in AD (Zhou et al. 2008). The levels of C3 and C4 are also elevated in AD with mild to severe clinical symptoms with a low level of expression of complement regulatory molecules (Zanzani et al. 2005).

1.9.6 The complement system and HAD.

Immediately after the entry into the host body, HIV has to survive antibody-mediated neutralisation of the virus by complement (Huber et al. 2006). This mechanism is essential to reduce viremia during the initial stage of the disease, but the virus manages to escapes the complement mediated neutralisation. Once HIV enters the body of the host, it immediately gains access to the brain even at the early stage of the disease. The virus not only evades the immune response, but also uses the components of the immune system for its benefit. The complement opsonised-HIV is correctly described as a "free rider on its way to infection of the cells" (Stoiber et al. 2005). In this review article it is proposed that HIV binds to the complement component C3 which in time gets converted to C3b and iC3b (opsonin). This iC3b-HIV complex then passes from erythrocytes to B cells and from B cells to T cells. Thus, according to this hypothesis, HIV is not only capable of protecting itself from the complement attack, but effectively uses the complement components to infect T-cells which has a profound impact on the HIV mediated

pathogenesis. The interaction of HIV and complement, complement mediated entry, evasion of virolysis as well as inhibition of complement regulation by the virus, and consequences in neuroAIDS are extensively reviewed in a recent review (Datta and Rappaport 2006). Briefly, HIV and its proteins gp41 and Nef1 induce the synthesis of the complement component C3 by upregulating the C3 promoter activity in astrocytes. The complement components are normally expressed at low level in the brain. However, HIV-1 and its pathogenic proteins Nef and gp41 also induce the expression of C3 by astrocytes and neurons (Speth et al. 2002). HIV virion, and its pathogenic proteins gp41 and Nef activate the transcription factor C/EBPδ. This activation on one hand enhances the replication of virus in the brain, and on the other hand results in the enhanced expression of C3 resulting in the stimulation of neuroinflammation in the brain and subsequent neurodegeneration (Bruder 2003). HIV-1 is also responsible for the increased synthesis of C1q by microglia, and macrophage during the infectious phase (Depboylu et al. 2005). HIV is also associated with the increase in the level of C4 in the brain (Jongen et al. 2000). gp120, a viral protein is known to mediate the complement dependent toxicity of sensory ganglion neurons (Apostolski 1994).

1.10 Vaccinia virus complement control protein (VCP), a role model for the treatment of neuroinflammatory disorders.

The complement regulatory protein encoded by vaccinia virus, commonly known as VCP is a regulator of both the pathways of complement activation. The possible involvement of different mechanisms in the neuroprotective roles of such agents must also be considered because complement inhibitor C1q-INH mediates its neuroprotective roles through mechanisms independent of C1q (De Simoni et al. 2004). New complement inhibitors must be evaluated for their neuroprotective value in neuroinflammatory disorders. The complement regulatory protein molecules of microbial origin which they express, able to evade the immune response, might be of great help in this context. Delivery of these proteins to the brain or their gene delivery to express the protein of therapeutic interest in the CNS to enable expression over a prolonged period of time would be a better option in the treatment of neurodegenerative disorders, where long-term treatment is required.

VCP is a major protein secreted by vaccinia virus, and could be a drug of choice in the treatment of neurodegenerative disorders, where complement plays an important role. The role of VCP in various disorders is well documented in a recent review (Jha and Kotwal 2003). Briefly, it is a 28.8 kDa protein secreted by vaccinia virus mimics the human complement control proteins and was the first compound of viral origin to show complement regulation (Kotwal and Moss 1988). It is composed of four complement control protein modules called sushi domains. The four sushi domains (or modules) of VCP bear more than 30 % amino acid identity to the human complement control proteins C4b-BP, decay-accelerating factor (DAF), membrane cofactor protein (MCP; Kotwal et al. 1990, Earl and Moss 1989). It was shown to inhibit the CP of complement activation (Kotwal et al. 1990)

Through its ability to bind C3 and C4 and ability as a cofactor of factor I to cleave C3b and C4b, it inhibits the CP with greater potency than human C4b-BP (McKenzie et al. 1992). VCP is also

known to inhibit factor-B dependent complement-enhanced neutralization of antibody-sensitized virus, suggesting a regulatory role of this protein in the AP of complement activation. A possible mechanism involved might be an acceleration of the decay C3 convertase of the AP or through the cleavage of C3b into iC3b by acting as a cofactor for factor I (Sahu et al. 1998).

Although, VCP regulates both the pathways of complement activation, the concentration required to inhibit the AP is much higher than that for inhibiting the CP. Regulation of these two pathways by VCP results in the reduction in the generation of complement anaphylatoxins, which besides playing an important role in the neuroinflammatory disorders, also inhibits MAC.

In addition to its complement regulatory roles, VCP has also shown the ability to bind heparin and heparan sulphate proteoglycan molecules (HSPGs) (Smith et al. 2000, Ganesh et al. 2004). The heparin binding ability of VCP explains several physiologically interesting roles of VCP, for example, uptake by mast cells, attachment to the endotelial cells, inhibition of complement-mediated killing of endothelial cells and blockade of interaction between (pig aortic) endothelial cells, neutrophils and natural killer cells thereby preventing cell death, (Reynolds et al. 2000, Al-Mohana et al. 2001).

All these actions mediated by VCP promote it as a potent anti-inflammatory agent. As discussed above, the anti-inflammatory activity of VCP involves multiple actions, complement inhibitory action being the major one. VCP inhibits more than one component involved in neuroinflammation and neuroimmune activation, its major action being complement regulation, which makes it a strong neuroprotective agent in the treatment of neurodegenerative disorders such as AD and HAD. Unlike several herbal ingredients, *in vitro* and *in vivo* activity of this protein in several neurodegenerative disorders is well established using rodent models.

VCP is also known to restore spatial memory deficit in MWM model in rats (Hicks et al. 2002) and might play an important role in dementia associated with AD (Kotwal et al. 2002). Consequently, its role as a neuroprotective agent in animal models mimicking other neurodegenerative disorders involving head injury, TBI, and SCI are well established (Pillay et al. 2005, Pillay et al. 2007, Hicks et al. 2002, Reynolds et al. 2003).

1.10.1 Alzheimer's Disease (AD).

The pathogenic proteins in the etiology of AD, for example, tau protein and Aβ derived from the amyloid precursor protein, are involved in the activation of the CP of the complement system. As mentioned earlier, the AP is also involved in the pathogenesis of AD. By virtue of its ability to inhibit the in-vitro activation of the complement system by amyloid protein, it was hypothesized that VCP might play an important role in the prevention and treatment of dementia associated with AD (Daly and Kotwal 1998, Hicks et al. 2002). When VCP was administered intracranially in young APPswe transgenic mice showing early onset familial form of AD (2 to 3 months and 6.5 to 7.5 months old), thus showed improvement in the ChBM learning compared to their transgenic controls (Pillay et al. 2008). This suggests the beneficial roles of VCP in the treatment of familial form of AD in mice.

1.10.2 Traumatic Brain Injury (TBI).

TBI involves complement and HSPG, a heparin conjugate. The injury and inflammation of the brain tissue in TBI is associated with cognitive dysfunction. VCP, with its ability to bind heparin like molecules and complement inhibitory activity, was found to be effective in a rodent model of TBI (Hicks et al. 2002). VCP was found to be effective in the treatment of spinal cord injury (SCI) in rodent SCI model (Reynolds et al. 2003, Reynolds et al. 2004). Neutrophil influx in association of the complement component C3 was evident in a rat fluid percussion injury model (FPI; Keeling et al. 2000). VCP was also found to improve sensorimotor function after fluid percussion injury in rats (Pillay et al. 2007). Improvement in the spatial learning of rodents was observed after the direct administration of VCP in a mild injury model (Pillay et al. 2005).

Hence, the use of novel strategies, by use of poxviruses (Kotwal 2000) and mediation by molecules like VCP with complement regulation as a key activity, might be a promising approach in the treatment of several neuroinflammatory disorders for which no suitable therapy is currently available. These compounds have an advantage of inhibiting a wide range of complement components involved in the neuroinflammation. However, it also appears that inhibition of anaphylatoxins by the complement pathway regulators may actually play a devastating role in glutamate and kainate toxicity, since anaphylatoxins have shown protective effects in these toxicities (Mukherjee et al. 2008, Osaka et al. 1999). Bearing in mind some of the controversial findings, it may be possible that regulators of both complement pathways can be effectively used in the treatment of neurodegenerative disorders.

In addition to its effectiveness in the treatment of these disorders of the brain, VCP has many biological roles. Its biological roles have been thoroughly reviewed, and it was correctly described as a "potential wonder drug" (Jha and Kotwal 2003). It was found to be effective in the treatment of atherosclerosis, and in blocking xenorejection (Thorbjornsdottir et al. 2005, Jha et al 2003, Anderson et al. 2003.). It was also found to bind the heparin and heparan sulphate proteoglycans (HPSG; Smith et al. 200, Smith et al. 2003, Ganesh et al. 2004). In fact, it is the only regulator of the complement from microbial source with this activity reported thus far. These findings have certain implications in the anti-neuroinflammatory roles of VCP. HSPG is known to play an important role in AD. It is found to be associated with ApoE4. Consequently, ApoE4 is also involved in atherosclerosis. HSPG mediate enhanced binding of ApoE4 to lipoproteins, and the roles of HSPG and ApoE4 in the lipoprotein metabolism, and their clinical implications are thoroughly reviewed by Mahley and Ji (1999). VCP may well be targeting this HSPG-ApoE4 association, and it could be the main action of VCP in atherosclerosis and AD in addition to complement regulation. To further support this hypothesis it is important to consider the role of VCP 2,3,4, a truncated analogue of VCP commonly called as tVCP, in the rodent brain injury model (Hicks et al. 2002). tVCP does not inhibit the complement system or is not known to bind the complement components, but is known to bind heparin (Smith et al 2000. Smith et al. 2003). Therefore, the question of VCP's mode of action in the treatment of neuroinflammation can be attributed to more than one action, and therefore the need of including appropriate controls in further unravelling the complexities of its action.

1.11 VCP and tVCP Delivery to the Brain.

In all the reported experiments to date where VCP and tVCP were tested for their therapeutic effectiveness in the treatment of rodent CNS disorders, they were administered directly into the brain by focal injection. For VCP to be therapeutically beneficial, it is necessary to deliver it to the brain using less invasive and more convenient route of administration.

VCP, being a protein molecule cannot be administered orally to treat brain disorders, as it most likely will be degraded like most other proteins due to the high activity of the metabolic enzymes. Moreover, the cost of VCP expression and purification is also very high. The oral route would also require large amounts to be given, and therefore use of this route was considered being inappropriate. The systemic administration of VCP to reduce the dose is possible, but VCP has never been administered systemically to test its bioavailability in the brain. However, a further problem is its large size (28.8 kDa). Consequently it might not be able to cross the blood brain barrier (BBB), which is permeable to molecules upto 700 Da. In CNS disorders where there is a compromised BBB, VCP could gain access, but there is no evidence to show that there is a compromise of BBB in the early stage of AD.

The other possibility is that VCP through its ability to bind heparin and HSPG is able to bind to the endothelial cells and macrophages. In CNS disorders, macrophages are reported to migrate to the brain, and VCP through its ability to bind macrophages may gain access to the brain. However, the delivery of VCP in those cases is possible only in advanced stages of the disease when the migration of macrophages is evident. It could also be hypothesized that due to its ability to bind endothelial cells, it might bind to the brain endothelial cells of BBB, and as with some other drug molecules, due to transendothelial migration, it may be transferred to the brain. One other alternative is to facilitate VCP's transfer into the brain by pharmacological manipulation of BBB.

1.11.1 Opening of BBB for VCP delivery.

VCP could also be delivered to the brain by opening the BBB. This reflects the compromised BBB stage observed in most of the inflammatory CNS disorders (Stahel et al. 2001). Various approaches are currently being employed for the pharmacological opening of BBB. The pharmacological agents such as papaverine (Bhattacharjee et al., 2002) and lipopolysachharides (Gillard et al. 2003) were used to open BBB. The osmotic opening of BBB and then maintaining it open in the same state for some period of time as done by others (Ikeda et al. 2002) can also be used to deliver VCP to the CNS. For the osmotic opening of BBB, mannitol (Intra-arterial injection of 1.1 M cold solution of mannitol) is generally used (Ikeda et al. 2002). The other possibility is use of pegylated liposomes, which are stable in the blood and therefore retained for a long period of time. The use of this system enhances the stability of the incorporated drug particles. If VCP is incorporated into these particles, it would be stable in the blood, and would be retained for a longer period of time, thus increasing its chances of interaction with the endothelial cells and macrophages, which could later then enter into the brain.

However, all these approaches either need manipulation of BBB and/or other formulations of VCP. It is not known whether manipulation of VCP for delivery may alter its pharmacological profile, although under normal circumstances, it is stable to extremes of temperature and pH as discovered by Smith et al. (2002). While further research is required to explore these options, the alternative routes of administration could be exploited for the delivery of VCP to the brain. One of the basis of all the evidence the delivery of VCP via intranasal route is worthy of further investigation. The best alternative route of administration that could be tried for the delivery of VCP is the intranasal route of administration.

1.11.2 Intranasal route of administration for drug delivery to the CNS.

It is general knowledge that the skin protects the body from microbial invasion. The stratified epithelial layer of the skin acts as a barrier, and protects the body from invading macromolecules, toxic substances, and microorganisms. Yet, some of these microorganisms are able to sneak through the "loopholes" in the barrier. The nasal cavity is one of those "loopholes" which the microorganisms have been using to enter the human body. Many viruses such as herpes simplex virus (HSV; Mori et al. 2005), mouse hepatitis virus (Barnett et al. 1993), and stomatitis virus (Hunneycutt et al. 1994) are reported to use this route to infect the CNS. Many toxic substances are also known to enter the brain via this route. The same route could also be exploited to deliver the drugs to the CNS. Many reviews are available on the delivery of drugs to the CNS using this route of administration (Illum 2000, Talegaonkar and Mishra 2004, Constantino et al. 2007, Hussain 1998, Gozes 2001, Thorne and Frey 2001, Vyas et al. 2005). The intranasal delivery of many small sized and large sized molecules is discussed by them. The physical factors, and the advantages as well as drawbacks of this route of administration could be found in a recent review (Talegaonkar and Mishra 2004). In a more recent review the patient compliance, regimen, patient population, physicochemical properties of drug and other factors of intranasal administration are discussed using case examples (Constantino et al. 2007). Indeed this route offers great therapeutic potential for drug delivery to the CNS. In these reviews as well as in the recently published online PhD thesis (Jansson 2004T), the nasal physiology, and the routes a drug can take to reach the brain are discussed. The physiolology of the nasal epithelium, and the possible ways drugs delivered by this route taken up by the CNS are briefly summarised in the following section.

1.11.3 The nasal physiology and the possible routes taken by drugs to reach the brain.

The nasal cavity is lined by epithelium like all other cavities of the body, and anatomically the nasal epithelium can broadly be divided into two parts, the respiratory mucosa and the olfactory epithelium. The olfactory epithelium (OE) deals with the odorants. For drug delivery purpose, the respiratory epithelium (RE) which covers the anterior portion and is rich in blood flow, is exploited to deliver drugs into the systemic circulation and many nasal formulations are available on the market for the delivery of drugs into the systemic circulation via nasal route. The OE on the other hand offers a

great potential to deliver the drugs to the CNS. At least one preparation (peptide formulation Lexicon Pharmaceuticals) is available on the market where the formulation for nasal delivery has been exploited to treat the clinical symptoms in neuroinflammatory disorders. This site however offers a potential entry point of toxicants as well as microorganisms, and is physically protected from them by directing most of the air away from this area. As toxicants can enter the CNS via this route, it also offers an important entry point for the drug delivery.

The drug administered intranasally can reach the brain via the intraneuronal, extraneuronal, and /or systemic route.

1.11.4 Extraneuronal and intraneuronal routes.

As of the last century, several compounds have been delivered into the CNS via the intranasal route, and there is no doubt that drugs are taken up in the brain or CSF after being delivered by this route (Jansson 2004T). The next obvious question concerns the route taken by these drugs to reach the brain. Until 2004 the intranasal delivery of drugs to the CNS was based on a belief that there is a connection between the nasal lymphatics (NL) and CSF in the brain, but no concrete evidence is available to substantiate this. The connection between CSF and NL prior to 2004 was not well established although there were some reports indicating some association between NL and CSF from the subarachnoid space (SAS). However, recently, using microfil, a substance which allows 3D imaging after being transported through an organ or tissue, the connection between the CSF, olfactory nerve (ON) and NL was confirmed for the first time (Johnston et al. 2004). When this compound was administered into the CSF compartment, it preferred nasal lymphatics (NL) over venous route, and stained the cribriform plate (cp) and ON leading to nasal submucosa (NSM). This study confirmed that CSF is transported from the CSF compartments to ON, and cp, and NL. It might be drained into NL. Recently, it has also been shown that this flow is not unidirectional, but CSF can also be transported from NL to the CSF compartments via ON (Johnston et al. 2005). These two research articles further support the intranasal delivery of drugs to the CNS through the connection between NL, ON and SAS. The drugs are shown to be taken up into the brain or CSF via ON. It is also believed that these drugs can be taken up into the CNS via trigeminal nerve (TGN). If the transfer occurs via these two nerve fibre tracts, it is termed as axonal or neuronal transport of the drugs. Sometimes, a drug can be found in the CNS within minutes after being delivered intranasally, and this could be due to the extraneuronal transport via the cp, or through perineural space (PNS), which is formed by perineural cells surrounding the ON fibre bundles in NL and is continuous with the SAS. Therefore, the drugs which are directly transferred to CSF are believed to take this route which is independent of neuronal transport, and is therefore termed as extraneuronal or extracellular or perineuronal transport. The extracellular transport is reported to take place by three routes (Thorne et al. 2004). The first route is taken by the small molecules which are found in the peripheral olfactory system within minutes after administration. The second route is via olfactory PNS. The drugs gaining access by this route mainly concentrate in the olfactory lobe (Olf). Recently, it was shown that a drug can reach the spinal cord, and brain stem via

Trigeminal extracellular (TE) or PNS-Trigeminal pathway (Thorne et al. 2004). Insulin-like growth factor-1(IGF-1) has been shown to be taken up by all the three routes. The transport of drug via intraneuronal and extraneuronal routes is schematically represented in a Fig 1.3 below.

1.11.5 Systemic route.

Some drugs, instead of being transferred to the CNS directly through the intraneuronal or extraneuronal route, first gain access to the systemic circulation, and then cross BBB, and reach the brain. The small sized lipid soluble compounds may take this route.

Transfer of drugs to the brain after intranasal administration.

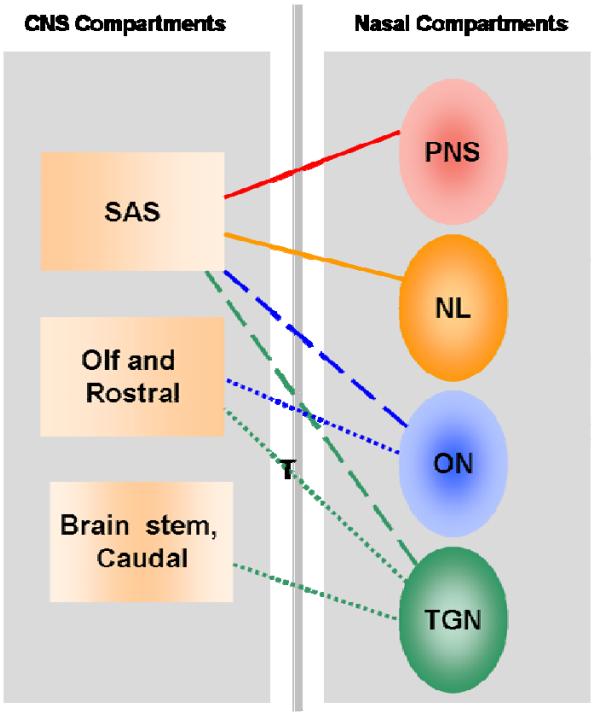

Figure 1.3. *Schematic representation of transfer of drug from the nasal compartments to the CNS compartments. The nasal compartments [perineural space (PNS), nasal lymphatics (NL), olfactory nerve (ON), and trigeminal nerve (TGN)] are shown by different coloured ellipses, and the CNS compartments [subarachnoid space (SAS), olfactory lobes (Olf), Caudal] are shown by the rectangles with distinct colour patterns. The transfer of drugs from the nasal compartments to the CNS compartments is shown by colour coded lines. The colour of the line matches with the colour of the nasal compartment from where the drugs transfer to the CNS. The solid lines indicate direct transfer into CSF or SAS from NL and PNS. The neuronal transport via ON and TGN to the rostral parts of the brain such as olf is shown by dotted lines. The transfer of drugs from ON and TGN into SAS or CSF is shown by broken lines. From TGN, drugs reaches the brain stem and the caudal parts of the CNS as shown by dotted lines. Thorne et al (2004) also showed the uptake into the rostral part and Olf via this route (T).*

1.11.6 Compounds delivered to the brain intranasally.

Delivery of drugs to the CNS using intranasal delivery is not a new concept, although it is gaining popularity only recently. Compounds such as dopamine (Dahlin 2000, Dahlin 2001, Jansson 2004T), estrogen (Kaya et al. 2008, Firat et al. 2008), morphine (Westin et al. 2005 and Westin et al. 2006) Lidocaine (Chou and Donovan 1998), Budesonide (Yilmaz et al. 2000), cephalexin (Sakane et al. 1991), methotrexate (Wang et al. 2003), melanocortin and insulin (Born et al. 2002) have been detected either in the brain or CSF after being delivered intranasally. Many peptides (Gozes 2001) and neurotrophic growth factors (NGF; Thorne and Frey 2001) have been delivered through this route of administration and their therapeutic utility was assessed. NGF was also administered intranasally and was shown to be effective in mouse model of AD. Insulin-like growth factor-1 (IGF-1) was administered in focal ischemia (Liu et al. 2001). The delivery of peptides for the treatment of neurodegenerative disorders such as AD, HAD, and applications of AVP peptide, GnRH, isulin and possible roles of many other peptides in the treatment of neurodegenerative disorders using this route have been extensively reviewed by Gozes (2001). Thorne and colleagues have also reviewed the intranasal delivery of NGFs and their applications in the treatment of neurodegenerative disorders (Thorne and Frey 2001). These studies are indicative of this route of administration being thoroughly investigated for its utility in the treatment of neurodegenerative disorders. Intranasal application of a neuromodulatory and nuroprotective peptide developed from the adrenocorticotrophic hormone (ACTH) for the treatment of ischemia (Semax, Lexicon) is available on the market. This demonstrates the potential therapeutic utility and proof of the concept since at least one intranasal formulation is available on the market for the treatment of CNS disorders. The route was also exploited for the CNS delivery of proteins in 1971, when HRP was detected in the mice olfactory vesicles and supporting cells 15 min after the intranasal administration (Kristensson and Olsson 1971). Since then, many protein molecules and peptides have been delivered to the brain, and the therapeutic effectiveness of some of them is also proven in preclinical studies. Horse raddish peroxidase (HRP) is a 40 kDa molecule which was delivered to the brain by a direct or extracellular route of administration in its native form (Kristensson and Olsson 1971). When it was coupled with wheat germ agglutitnin (WGA-HRP), the resulting 62 kDa conjugate was delivered to the brain although via a different mechanism called adsorptive endocytosis, and was taken into the olfactory glomerular cell layer and simultaneously detected in ON (Broadwell and Balin 1985, Thorne et al. 1995). Evans blue labelled albumin was also delivered to the CNS after being administered intranasally (Kristensson and Olsson 1971, Jansson 2004T). Delivery of green fluorescence protein (29 kDa) and subsequent intracellular transduction shows that large sized proteins are not only delivered to the brain, but can be taken up by the brain cells if formulated appropriately (Loftus et al. 2006). The IGF-1 delivered intranasally to the brain is more than 7 kDa protein. Dextran 3kDa (Jansson and Bjork 2002), and high molecular weight dextrans (4 to 40 kDa; Sakane et al. 1995) were also delivered intranasally to the brain. The delivery to the brain was dependent upon the molecular weights of dextrans (Sakane et al. 1995). Thus there is evidence that proteins from 7 kDa to 62 kDa can be delivered to the brain, with or without conjugation with other

proteins. Heparin binding epidermal growth factor (22 kDa) delivered intranasally was found to be effective in neurogenesis (Jin et al. 2003). Fibroblast growth factor 2, a 210 amino acid protein was also delivered intranasally, and was found to be effective in neurogenesis (Jin et al. 2003). The HRP was delivered to the brain with intact biological activity as discussed earlier. Thus, there is ample evidence that the nasal route can be used to deliver the large molecular weight protein molecules without loss of their biological activity.

1.11.7 Practical considerations of intranasal delivery with reference to tVCP, VCP, and the ingredients of herbal origin.

Both the small sized (e.g. Cur) as well as high molecular weight compounds (tVCP and VCP) used in the current investigation will be delivered intranasally to study their distribution and subsequent therapeutic efficacy. According to the literature, intranasal delivery of VCP and tVCP to the CNS has not yet been reported. Cur that is used in the investigation will be dissolved in PBS. Many drugs have previously been dissolved in PBS, saline or water for the intranasal delivery and were delivered to the brain without any modifications as illustrated by the following; NGF in PBS by Capsoni et al. (2002); amphetamine derivative and cocaine in water by De Souza Silva et al. (1997); Dopamine in PBS by Dahlin et al. (2001), Cholera toxin subunit (CT-B) in PBS by van Ginkel et al. (2000). Consequently, PBS will be used in the current investigation to dilute VCP, tVCP and Cur to deliver them to the CNS.

Another advantage of this route is that hydrophilic drugs can be delivered to the brain (Talegaonkar and Mishra 2005, Illum 2000, and Hussain 1998). The third advantage is that although the metabolic enzymes are present in the nasal mucosa, they affect nasal absorption only to a minimal extent (Hussain 1998). After being administered intraperitoneally, VCP as such was detected in the serum even after 8 h (Jha et al. 2003). This shows stability of VCP in biological fluids, and its resistance to metabolic enzymes of liver. Also, it is a physically stable molecule which survives high temperature and pH conditions (Smith et al. 2002), and the chances of being degraded by nasal enzymes are negligible. Therefore, these compounds will be diluted in PBS, and will be delivered intranasally in rats and transgenic mice to study their distribution patterns and therapeutic effectiveness, respectively in the current investigation.

1.12 Development of small sized complement regulatory proteins as an alternative to high molecular weight VCP to the rat brain.

VCP is approximately 28.8 kDa protein molecule. As discussed earlier, the first objective of the thesis was to deliver VCP and test its effectiveness in the treatment of neurodegenerative disorders. The second objective was the development of a small sized complement regulatory molecule which could be delivered easily to the brain to control neuroinflammation. For centuries, ingredients of natural origin have been known to offer great potential in the process of drug development. During the last two decades, several ingredients of herbal origin have been tested for their complement inhibitory potential. To gain some perspective with a view to developing suitable complement inhibitory molecules from

naturally occurring compounds, some of the active constituents of medicinal plants with complement inhibitory activity *in vitro* in most cases, are discussed below.

1.12.1 Medicinal plants with complement inhibitory ingredients.

The flavonoids in *Juglans mandshurica*, afzelin and quercitrin have been shown to inhibit the complement system. The galloyl residues, tetragalloyl glucose and trigalloyl glucose present in the plant also showed complement regulatory activity (Min et al. 2003). *Glycyrrhiza glabra* is well documented in Ayurvedic literature for its antiinflammatory potential. The active constituents, β-glycyrrhetinic acid and glycyrrhizin have shown complement regulatory activity. Both of them induced conformational changes in C3 (Kawakami et al. 2003). β-glycyrrhetinic acid was also shown to inhibit CP by inhibiting C2 rather than C4 and C1q (Kroes et al. 1999). Glycirrhizin inhibited the C3 component of the complement anaphylatoxin C3a and C3b (Kawakami et al. 2003). The triterpene lupeol from *Crataeva nurvala.* is an active constituent of this medicinal plant. Both lupeol and a compound synthesized from it, that is, lupeol linoleate, were considered to reduce C3 convertase activity (Geetha and Varalakshmi 1999). Further elaboration of the complement inhibitory activity is essential. The ethanolic extracts of *Ligustrum vulgare* and *Phillyrea latifolia* Leaves, and the active constituents isolated from the extract (flavonoids apigenin, luteolin, and their glucosides) were found to have complement inhibitory activity (Pieroni et al. 2000). A plant from the African continent, *Morinda morindoides* from the Democratic Republic of Congo and is used traditionally to alleviate rheumatic pain. Qur and MO15 present in this plant inhibited both the AP and CP of complement activation. In addition to this, some other constituent also showed inhibition of CP of complement activation (Cimanga et al. 1995). The plant also contain iridoids, gaertneroside, acetylgaertneroside, and gaertneric acid which inhibited CP but failed to inhibit AP of complement activation in an *in-vitro* study (Cimanga et al. 2003). The mature leaves of *Osbeckia aspera*, an Ayurvedic medicinal plant have been used traditionally to treat liver disease in Srilanka. The whole plant extract was found to have a dose-dependent effect on both the CP and the AP of complement activation, and the effect was more pronounced on the CP (Nicholl et al. 2001). The fresh leaf extracts of *Cedrela lilloi* and *Trichilia elegans* from Argentina were found to have complement inhibitory activity on both the pathways of complement activation (Nores et al. 1997). RA from *Rosmarinus officinalis* was also found to be an effective inhibitor of complement (Peake et al. 1991, Sahu et al. 1999, Cimanga et al.1995). It inhibited C3, and C3b, and was shown to inhibit both the CP and AP of complement activation. The effect of various ingredients of herbal origin on the components of complement system is outlined in Fig 1.4.

From this discussion, it is evident that ingredients of herbal origin offer a great potential in the development of neuroprotective agents for the treatment of disorders of the brain where complement components play a damaging role. As shown in the Fig 1.4, these ingredients inhibit both the pathways of complement activation very efficiently. The small size of these compounds is advantageous, and depending upon their physicochemical properties, they may cross BBB. Therefore as a part of this study

it was decided to exploit ingredients of herbal origin for the development of suitable complement regulatory molecules.

Interaction of ingredients of herbal origin with the complement components.

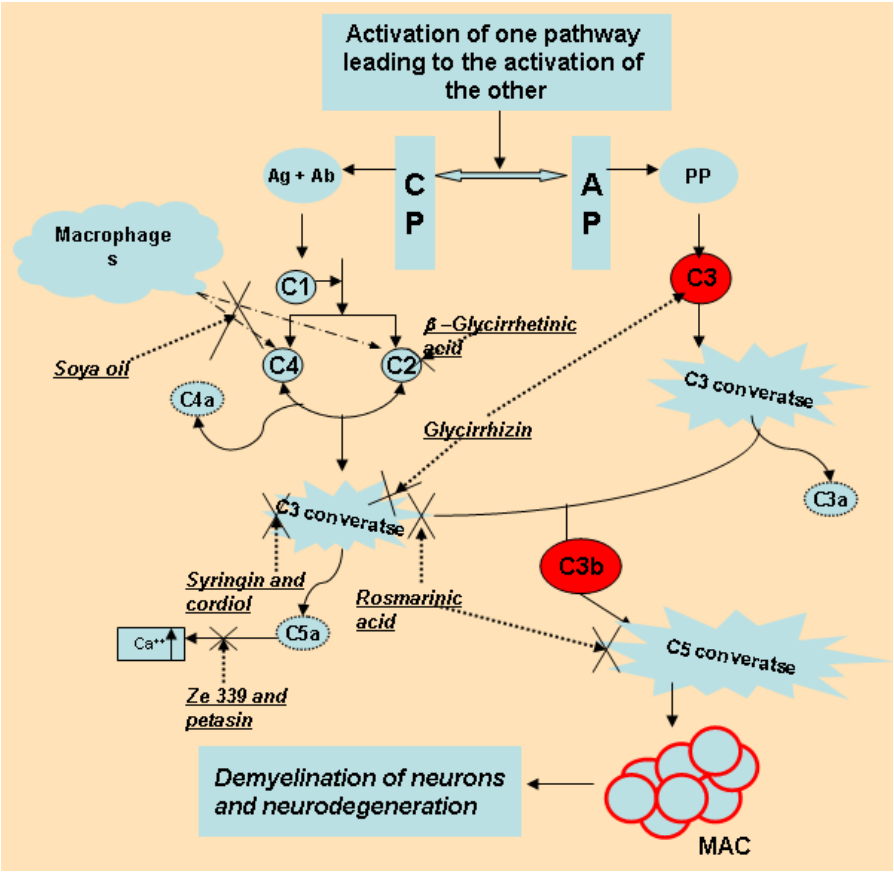

Figure 1.4. *The complement components activated by the CP and AP, and inhibition of complement activation by various ingredients of herbal origin. The key components central to the activation of both the pathways are shown as solid red circles. The activation of one pathway may lead to the activation of the other pathway. The ingredients of herbal origin interact with the complement components (C1, C2, C3, C3b, C4), anaphylatoxins C4a, C3a, C5a, and AP and CP converatses (C3 and C5) resulting in the prevention of formation of MAC and the subsequent demyelination of neurons and neurodegeneration by them. Some of them act at more than one site, whereas some others chelate ions such as* Ca^{++} *required for the complement activation.*

1.12.2 Selection of compounds for the development of complement regulatory neuroprotective agents.

In the current investigation, it was not possible to test all of them for screening the best complement regulatory molecule. Therefore, it was decided to select some of the structurally similar compounds for the sake of proper comparison of their complement regulatory activity. Consequently, in addition to the complement regulatory compounds of herbal origin discussed in the above section, in a recent study, it was found that polyhydroxy compounds of natural origin were found to inhibit the complement system (Sahu and Pangburn 1996). It was found by them that dopamine, salicylhydroxamic

acid, epinephrine and norepinephrine all inhibit the complement components with great efficacy. It was also proposed that the drugs like salicylhydroxamic acid used in the study would be effective in the treatment of AD and other neurological disorders of the brain by virtue of their complement inhibition. RA from *Rosmariunus officinalis* and Qur from a plant of African origin (Cimanga et al. 1995) which were found to inhibit both the AP and CP of the complement system are also polyhydroxy phenolic compounds. Subsequently, RA and Qur were also found in other African plants (Kumatou 2005, Cimanga et al 1995, Snijman et al. 2007). Qur is found Rooibos tea (*Aspalathus linearis*), which is highly popular in South Africa for its health benefits (Snijman et al. 2007). Based on their biological activity and therapeutic effectiveness, when ingredients of herbal origin were tested for their effectiveness, curcumin (Cur) was found to be the most thoroughly studied biological compound with reported anti-inflammatory activity. More than 2400 articles could be found on pubmed using the search word "curcumin". Its anti-inflammatory and biological roles at molecular level include chemoprevention (Gafner et al. 2004), inhibition of IκB-kinase activity and inhibitory effect on nuclear factor kappa- β (NF-κβ; Jobin et al. 1999), extracellular signal-regulated-kinase activity (ERK; Chun et al. 2003) and inhibition of NF-κβ to an extent that exceeds the currently used NSAIDs (Sandur et al. 2007). Due to Cur's broad spectrum of activities at molecular level, it has been reported in the literature for its effectiveness in the treatment of inflammatory disorders, anticancer, antineuroinflammatory activities by many (Aggarwal 2008, Goel et al. 2008a, Shishodia et al. 2007, Sandur et al. 2007). It was reported to be safe in phase-I clinical trial (Chainani-Wu 2003). The compound is thoroughly reviewed from its applications in the form of turmeric, reported in the ancient Ayurvedic literature, kitchen, laboratory, and is currently under clinical trials of many disorders from cancer, psoriasis to Alzheimer's disease (Goel et al. 2008b, Strimpakos and Sharma 2008, Hatcher 2008, Tomillero and Moral 2008a, Tomillero and Moral 2008b). This compound which is an ingredient of turmeric was found to be structurally related to RA, and is also a polyhydroxy phenolic compound. However, it has not reported in the literature for its complement regulatory activity. The compound is known to have widespread anti-inflammatory activity, and is reported in the literature to be effective in many neuroinflammatory disorders. As discussed previously, the complement system is found to be involved in many inflammatory disorders, and known to be proinflammatory on its own as well as by mediating the actions of other pro-inflammatory mediators. Subsequently, due to structural similarity with RA, a complement regulatory molecule, it was hypothesized that Cur would inhibit the complement system. Therefore, these three structurally similar compounds abundantly reviewed in the literature as well as in the natural resources were selected for the comparison of their complement regulatory activity with that of VCP, tVCP, and the large sized molecules of microbial origin.

1.12.3 Study of complement inhibition by Cur, Qur and RA and comparison with that of VCP.

An haemolysis assay, and other enzymatic assays are available for the comparison of the effect of compounds on AP and CP of complement activation. These assays which will be discussed in the appropriate chapter, will be used to compare the effect of these ingredients of herbal origin on the

complement system with that of VCP and tVCP. The compound inhibiting both the pathways of complement activation with efficiency will then be selected to study their effect on the central components of complement activation, C3 and C3b, which are found to be involved in the aetiology of AD and HAD, and are central to the activation of AP and CP. A relatively new technology based on QCM-D monitoring will then be exploited to study the effect of these compounds on C3 and C3b.

1.13 The Central hypothesis.

Bioactive compounds such as VCP and the compounds of natural origin (curcumin) could be delivered to the brain to modulate neuroinflammation and provide neuroprotection in neurodegenerative disorders.

1.14 Specific objectives.

- Comparison of VCP, tVCP and Small Sized Molecules of Herbal Origin for their *in-vitro* Complement Regulatory Activities.
- Investigation of the Interaction of VCP, tVCP and Curcumin With the Complement Components C3 and C3b Using Quartz Crystal Microbalance With Dissipation Monitoring (QCM-D) Technology.
- Distribution of Intracranially and Intranasally Administered VCP, and its Comparison with the Intranasally Administered tVCP and Curcumin.
- Intracranial Administration of VCP, tVCP and Curcumin in MO/HU APPswe PS1δE9 Mice to Investigate the Effect on Associative Learning Using a Cheese Board Maze Model.
- To Investigate the Effect of Intranasally Administered VCP, tVCP, and Curcumin on Anxiety and Exploratory Behaviour in MO/HU APPswe PS1δE9 Mice.
- To Investigate the Effect of Intranasally Administered VCP, tVCP, and Curcumin on Spatial Learning, Spatial Reversal Learning And Spatial Working Memory in MO/HU APPswe PS1δE9 Mice.
- Intranasal Administration of VCP, tVCP and Curcumin in MO/HU APPswe PS1δE9 Mice to Investigate the Effect on Paired Associative Learning Using a Novel Cheese Board Maze Model.

Chapter 2.

Comparison of VCP, tVCP and small sized molecules of herbal origin for their *in-vitro* complement regulatory activities.

2.1 Introduction.

Vaccinia virus complement control protein has previously been extensively studied for its effect on the complement system. It was found to regulate both the pathways of the complement activation (Kotwal and Moss 1988, Kotwal et al. 1990, McKenzie et al. 1992). Its complement regulatory activity and other biological roles have been studied extensively by researchers across the globe in the last decade. After establishing its *in-vitro* complement regulatory activity, VCP was further investigated using *in-vivo* models of neuroinflammatory disorders. It was found to be effective in several models of rodent brain disorders where complement plays an important role. In all these rodent models of CNS disorders, where VCP was found to be effective, it was administered directly into the rodent brain. tVCP, a structural analogue of VCP has also previously been reported to improve TBI after direct administration into the rat brain. The next step in developing the therapeutic potential of VCP, its analogue tVCP, and other potential candidates of herbal origin was to investigate routes of delivery to the brain which are non-invasive.It was therefore necessary to deliver VCP to the brain using non-invasive approaches. An alternative approach is to develop small sized complement regulatory molecules which could be delivered to the brain after being administered by conventional route(s) of administration as a first stage approach to test their anti-inflammatory properties in neurodegenerative disorders

Most of the polydroxy phenolic compounds of herbal origin are small sized complement regulatory molecules which offer a great potential in the development of small sized neuroprotective agents with an ability to cross BBB. It has previously been shown that polyhydroxy phenolic compounds regulate the complement system (Sahu and Pangburn 1996). Cur is also a polyhydroxy phenolic compound from turmeric. Cur could be regarded as the, “golden yellow pear” due to its golden yellow colour and medicinal value reported in the literature. As discussed in the literature review, from NF-kappa to COX, it is known to inhibit most of the pro-inflammatory mediators at the root of neuroinflammatory disorders (Aggarwal et al. 2008, Mukhopadhyay et al. 1982, and Yang et al. 2005). Amongst the polyhydroxy phenolic compounds, RA shares structural similarity with Cur (Fig F1.1, Appendix F). Both RA and Cur show anti-inflammatory activities. It was found to dissolve Aβ plaques like RA (Yang 2005). RA has previously been reported to inhibit both the AP and CP of complement activation (Cimanga et al. 1995, Peake et al. 1991, Sahu et al. 1999). Qur is another polyhydroxy phenolic compound found in a Rooibos tea which is popular in South Africa (Snijman 2007). It has been reported to inhibit both the CP, and AP of complement activation, and was compared with RA for its effect on these pathways of complement activation (Cimanga et al. 1995). There are no reports in the literature of Cur being investigated for its effect on the complement system or compared with RA, although it is structurally related to RA, and shows similar anti-inflammatory activity profile as that of RA. Cur is known to inhibit many pro-inflammatory mediators including NF-κβ, and cyclooxygenases (Jobin et al. 1999, Gafner et al. 2004, Chun et al. 2003) as discussed in the literature review, but its effect on the complement system has not been reported as discussed previously.

As discussed in the literature review, the complement system is implicated in many disorders of the brain. Cur is a potent anti-neuroinflammatory compound currently being studied for its effectiveness in the clinical trials of AD and other diseases (Strimpakos and Sharma 2008, Hatcher 2008). The other NSAIDs have failed in clinical trials of AD patients (Reines et al. 2004, Aisen et al. 2003), although this group of compounds inhibited many pro-inflammatory mediators but most of them have not been shown to have the complement regulatory activity. The reason for their failure could be attributed to their inability to inhibit the complement system. As discussed in the literature review, the complement system activates many pro-inflammatory mediators such as NF-κβ, microglial activation, and cyclooxygenases. In order to discover a potent small sized complement regulatory molecule with an ability to cross BBB, as an alternative to the delivery of large sized complement regulatory proteins such as VCP, it is necessary to compare the complement regulatory activities of all these compounds with VCP. Exploring the potential of small sized complement regulatory agents with neuroprotective properties may therefore lead to the development of effective treatment of complement mediated neuroinflammatory disorders.

With these goals in mind, the objectives of this investigation were as follows:

2.2 Objectives.

1) To express tVCP using *P. pastoris,* and along with VCP use it for the subsequent characterisation of complement inhibition
2) To compare the effect of Cur with that of RA, Qur, and VCP on CP of complement activation using a haemolysis assay
3) To compare the effect of Cur, RA, and Qur on AP of complement activation

2.3 VCP and tVCP gene.

The fragment encoding amino acids 82-262 of VCP (VCP2, 3, 4 or tVCP) genes cloned in *pPIC9* vectors were used for the expression of tVCP. For the diagrams of vectors, please refer Appendix F (Fig F1.2, Appendix F). These clones were kindly provided by Prof. Paul Barlow, UK. VCP expressed in *P. pastoris* is commonly referred as rVCP (corresponding to amino acids 18-262 of VCP), but in subsequent chapters VCP R is used to denote VCP treated rats, therefore it will be referred as VCP throughout the thesis. Highly pure, endotoxin free VCP expressed in *P. pastoris* was kindly provided by Prof. Girish Kotwal. tVCP clones provided were highly expressing, and tVCP was expressed using *p. pastoris* yeast expression system, and was purified and was made free from endotoxin by the same method used for VCP expression and purification.

2.4 Materials and Methods.

2.4.1 Expression of tVCP using *P. pastoris* yeast expression system.

tVCP was expressed using *P. pastoris* by a method described elsewhere (Smith 2000, and Smith 2003). Briefly, a single colony which showed the presence of tVCP insert during pre-screening was selected from the yeast extract peptone dextrose (YPD) or minimal methanol + histidine (MMH) plate (please refer to Appendix for the composition), and was inoculated into 5 to 25 ml of buffered glycerol-complex medium (BMGY) in a 100 to 250 ml flask with a rubber stopper. The flask was then incubated at $30^{O}C$ in a rotary incubator shaker at 200 rpm till the OD_{600} reached between 2 to 3. This was used as a starter culture, and was inoculated in BMGY medium (500 ml to 1 L), incubated at 200 rpm and $30^{O}C$ for about 48 h or till the OD_{600} was between 2 to 6. The cells were then harvested at 4000 rpm for about 15 min. About 1 ml supernatant was stored at $-20^{O}C$, and the remaining cell supernatant was discarded. The cells were then resuspended in BMMY medium for the induction. The volume of buffered methanol-complex medium (BMMY) used was about 4 to 5 times less the volume of BMGY used for the initial cell growth. After every 24 h, 1 ml of supernatant was collected, spun at 13200 rpm for one minute. The pellet was discarded, and the supernatant was kept for the analysis of tVCP expression. It also served as a double check for the screening of the clones for the expression of tVCP. After 96 h, all the supernatants were analysed for the expression of tVCP using Sodium dodecyl sulphate-polyacrylamide gel electrophoresis (SDS-PAGE) analysis. The procedure was repeated until such time as tVCP was expressed as indicated by a band in the range of tVCP in the gel. After, the initial SDS-PAGE analysis, the cells were harvested at 4000 rpm for 15 min. The supernatant was collected and subjected to centrifugation at 10000 rpm, filtered using 0.22 μ filter and stored at $-20^{O}C$ for further purification, and characterisation.

2.4.2 SDS-PAGE analysis of the samples.

Method (Sambrook and Russell 2001)**:** Please refer to Appendix S for the preparation of solutions, reagents and composition of gel. 10 to 12 % SDS-PAGE resolving gels were poured using the Bio-Rad or Peqlab apparatus. The composition of the gel and preparation of the solutions was as described in the Appendix S (Table S2.1). The gel was allowed to polymerise for 30 to 45 min with an overlay of isobutanol (BDH) or water. After polymerisation of the gel, the overlay was poured off, and the top of the gel was washed several times with deionised double distilled water (dd water). The remaining water was removed with a paper towel. The stacking gel was prepared with the composition mentioned in the table S2.1 of Appendix S. While pouring the gel, wells were made in the stacking gel using a comb. The samples were mixed with gel loading buffer (3 parts sample + 4X gel loading buffer by Nu PAGE), and loaded into the wells. The gel was run at 60 to 70 V until the time the gel front had moved into the resolving gel (as shown by the colour of the bromophenol blue), and after that it was run at100 V to 120 V. The gel was then stained with staining solution, and destained subsequently using a solution of methanol, water, and glacial acetic acid (MWGAA).

2.4.3 Concentration and purification of the supernatants.

tVCP was expressed at high level, and only one band is visible in the gel. tVCP, therefore, was concentrated, desalted and purified by passing through a pellicon cut off filter (5 kDa) using 100 mM salt solutions. After this, the solution was tested for heparin binding activity according to method of Smith and colleagues (2000). Briefly, supernatant containing tVCP was passed through heparin Hi-trap column (1 or 5 ml capacity by Amersham Biosciences). The column was washed with pure millipore dd water. VCP and its fragments were eluted using 500 mM to 750 mM salt solution fractions (Smith et al. 2000). Therefore, tVCP was also eluted at 500 mM to 750 mM concentration after washing the column with millipore ddwater. tVCP eluted with 500 mM to 750 mM salt solutions was then desalted, purified, concentrated by passing several times through the 5 kDa cut off filter by pellicon, and subjected to SDS-PAGE analysis.

2.4.4 Endotoxin removal from the supernatants.

tVCP was made endotoxin free by passing through Detoxi-Gel Affinity Pak TM Pre-packed columns (by Pierce, Rockford, IL) according to their instructions. The Detoxi-Gel endotoxin removing gel uses polymixin-B immobilised by cross linking to beaded agarose. This polymixin-B binds to the lipopolysaccharide portion of the endotoxins and removes pyrogens from proteins and DNA samples or other pharmacologically important molecules. In order to purify the samples, first, the columns were regenerated by washing with 1% sodium deoxycholate, and washed several times with pyrogen free saline, and equilibrated with endotoxin free autoclaved 0.154 mM saline. The samples were applied to the column, and allowed to incubate for at least 30 min, and eluted with the endotoxin free saline. Further analysis of the eluted sample was done by SDS-PAGE electrophoresis as discussed previously.

2.4.5 Estimation of protein concentration by Bio-Rad kit.

The concentration was determined by using a Bio-rad kit (Bio-rad, California, USA). The kit was based on the Bradford method of protein estimation (Bradford, 1976). BSA protein standards (0.125 mg / ml to 2 mg/ml) used were from Pierce, Rockford, IL. 5 µl of each sample and protein standards were added to different wells of a 96 well plate, and mixed with 25 µl of reagent-A supplied in the kit using a multi channel pipette. 75 µl of the reagent B was added to this mixture. After 15 -20 min, the OD_{595} (Optical density at 595 nm) values of the samples and standards were measured and plotted. The concentration of different samples was estimated by comparing to the OD_{595} of standards.

2.4.6 Haemolysis Assay.

The method described by Kotwal et al. (1990) with a few modifications was followed. For this assay, 20 µl of VCP and tVCP, respectively at different dilutions were added to 75 µl of ssRBCs. After this, 5 µl of appropriate dilutions of serum causing lysis of 95 % of ssRBCs (Diamedix) was added to each sample, and the mixture incubated for an hour at $37^{O}C$. After one hour the eppendorf tubes were subjected to centrifugation at 700 rpm for 30 seconds. The pellet was discarded, and the supernatant was

analysed at 405 nm using a microplate reader (Anthos-labtec, Salzburg, Austria). From this the percentage inhibition by VCP, and tVCP could be determined.

2.4.7 Modified Haemolysis Assay.

The Cur, RA, and Qur are coloured compounds. The colour of these compounds may interfere with the measurement of OD_{405} of the assay due to absorption at this wavelength. Therefore, for the detection of the complement inhibition by these coloured compounds, the normal haemolysis assay was modified. For the assay, eppendorf tubes were covered with an aluminium foil for protecting the photo degradation of Cur. All the steps mentioned in the haemolysis assay above till the centrifugation steps were followed. After centrifugation, instead of discarding the pellet, the supernatant was discarded. The cell pellet was then washed with 100 µl of gelatine veronal-buffered saline. The cells were then haemolysed using 100 µl of double-distilled water (ddH2O). 75 µl of this solution comprising lysed RBCs was then analyzed at 405 nm using 96 well microplate reader (Anthos-labtec, Salzburg, Austria). The OD_{405} values obtained were later used to determine the percentage of cells that were not lysed during the assay. From this, the percentage complement inhibition by Cur, Qur, and RA was calculated, and compared with that of VCP. The schematic diagram representing the modified haemolysis assay is as shown in the Fig 2.1 below:

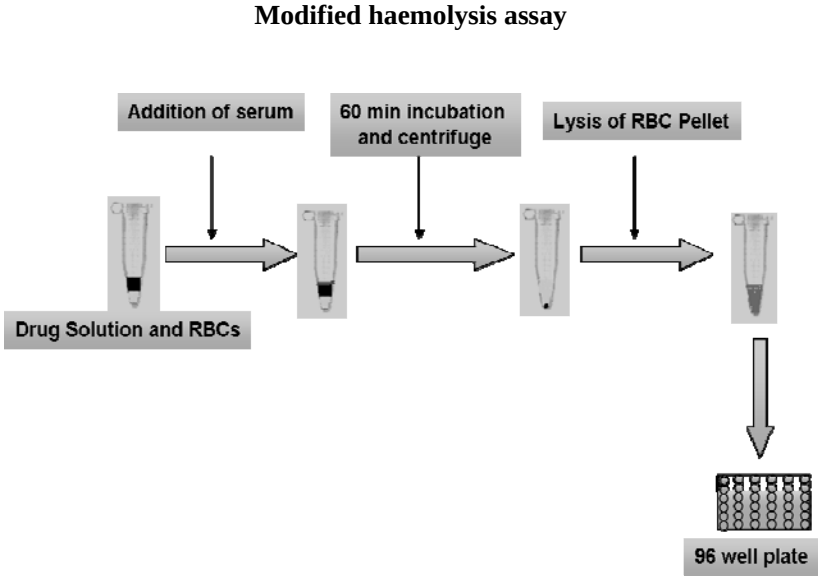

Figure 2.1. *Procedure for Modified Haemolysis assay for the detection of complement inhibition by Cur, Qur, and RA*

2.4.8 Effect of Cur on the AP of complement activation.

An enzyme immunoassay kit (Quidel Corporation) for the quantification of Bb fragment of factor B was used. The kit was modified by Ghebremariam and Kotwal for studying the effect of humanized recombinant VCP (hrVCP) on the zymosan activated AP of complement (Ghebremariam et

al. 2005). This modified version was employed to examine effect of Cur, RA, and Qur on the AP of complement activation.

Principle of the assay: Zymosan activates the AP of complement activation. This results in the production of Bb fragment from factor B by C3b. The level of this Bb fragment is measured by using the Quidel kit supplied by Quidel Corporation. By assessing the level of factor B in the presence of complement regulatory molecule, one can assess the effect of the complement regulatory molecules on the alternative pathway of complement activation.

Method: 10 µl of Cur, RA and Qur, were incubated for an hour at 37°C with normal human serum (undiluted, 10 µl) and/or heat-inactivated serum in the presence of 1.25 µl of zymosan solution (10 mg/ml) pre-sonicated before use. All the solutions were used in duplicates. 10 µl of each solution was then diluted with the specimen diluent (Quidel Corporation) to 100 µl and incubated for 30 minutes with mouse anti-Bb monoclonal antibody in pre-washed eight-well microplate assay strips (Quidel Corporation). The amount of Bb (in the sample and controls) was detected by adding 50 µl of horseradish peroxidase (HRP)–conjugated goat anti-human Bb antibody and the colour developed by 1/20 diluted chromogenic substrate. The colour developed was quantitated using 96 well microplate reader at 405 nm. From these values, the percentage inhibition of the AP by these Cur RA, and Qur was determined. The concentration of Qur, RA and Cur used for the study was 640 µM as maximum inhibition of haemolysis of ssRBCs by Qur and Cur was observed using this concentration as shown in the results section. It was found that Cur showed better inhibition of AP at this concentration in this assay, and therefore it was selected for further analysis. The effect of Cur on AP was determined at different concentrations using the Quidel enzyme immunoassay kit by the same method. The percentage inhibition of AP at different concentrations was determined and plotted on a log scale to determine the IC_{50} value of Cur.

2.5 Results.

2.5.1 SDS-PAGE analysis of VCP.

SDS-PAGE analysis of VCP.

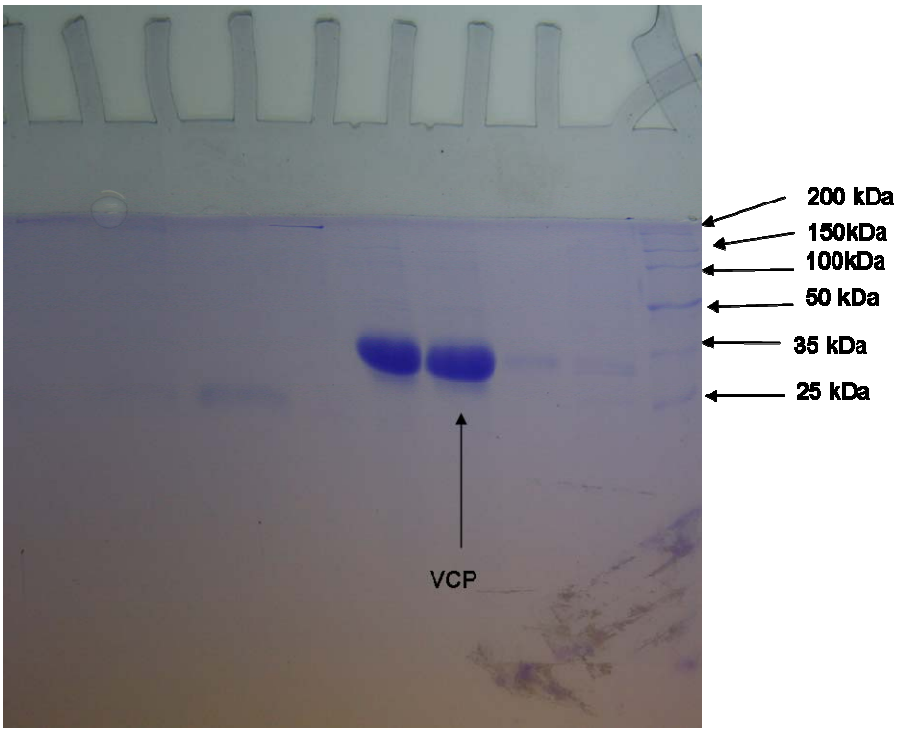

Figure 2.2. *SDS-PAGE analysis of VCP (Lanes: 1 = protein marker, 2, 3, 4 and 5 = Pure endotoxin free VCP used for characterisation. 4 and 5 represent the band of VCP at high concentration; 2 and 3 represent VCP band at low concentration).*

Results: The pure and endotoxin free VCP supplied by Prof Kotwal was used for the study. It appears as a band between 25 kDa and 35 kDa as shown in Fig 2.2. The pure VCP fractions were used for the *in-vitro* characterisation, Q-sense study as well as in the *in vivo* behavioural study.

2.5.2 Expression and purification of tVCP.

tVCP expression using *Pichia pastoris.*

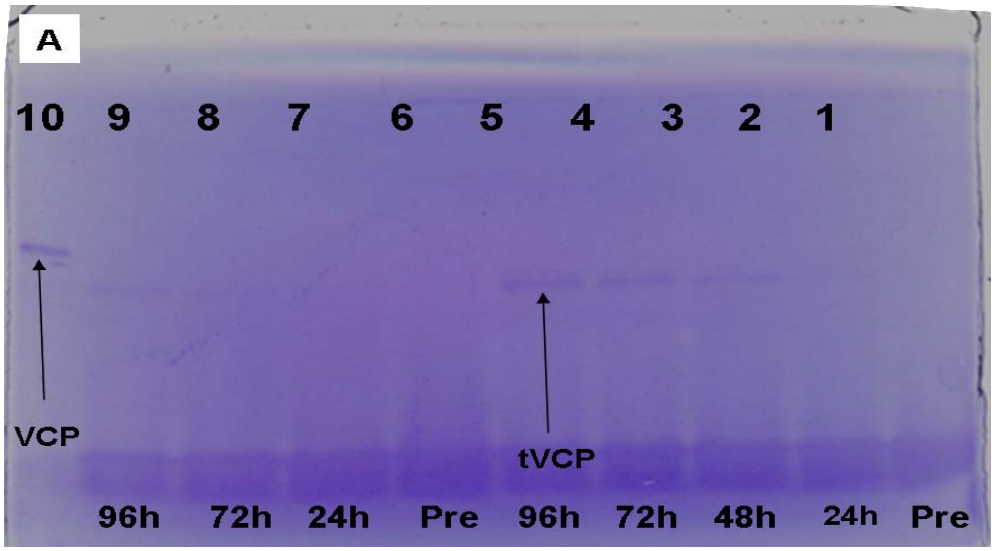

Figure 2.3. A. *Induction of tVCP expression in P. pastoris using methanol. Equal volume of the starter culture was inoculated into 250 ml of BMMY in two different 2.5 L flasks X and Y. X was induced with 2.5 ml of methanol / 24 h and Y was induced with 1.25 ml of methanol/ 24 h for 96 h ([Lanes 1= Preinduction medium X; 2, 3, 4, and 5 = 24 h, 48 h, 72 h and 96 h after the induction for X] [lanes 6 = Preinduction Y; 7, 8, and 9 = 24h, 72 h, and 96 h after the induction with methanol for Y])*

.

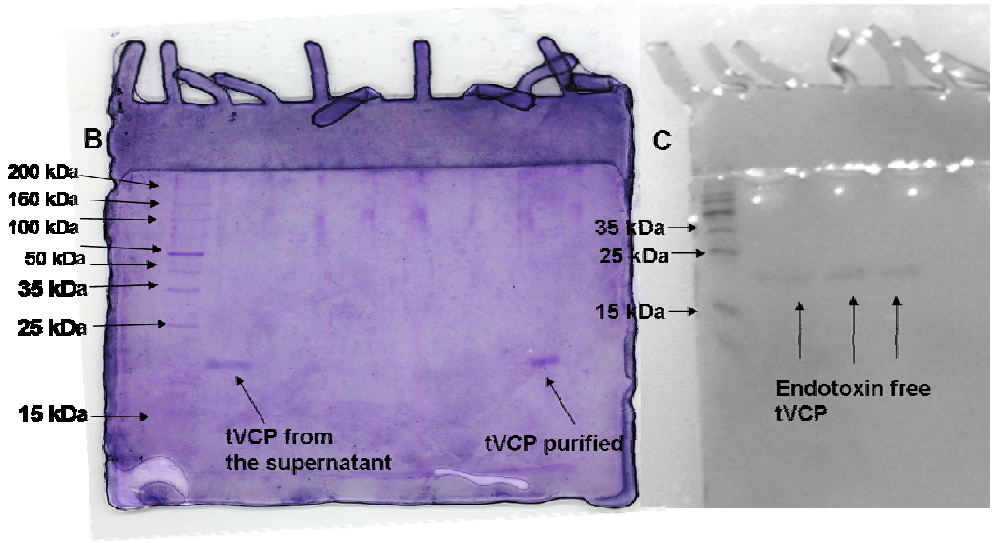

B. *Purification, and subsequent SDS-PAGE analysis of pure tVCP samples (Lanes (from left to right): 2 = Protein marker, 3 = tVCP in supernatant, 9 = pure, desalted and concentrated tVCP).* ***C.*** *Various fractions of tVCP, which were purified, concentrated, and passed through Detoxi-Gel Affinity Pak TM Pre-packed columns for endotoxin removal (Lanes (From left to right): 1 = protein marker, 2, 3, and 4 = Endotoxin free tVCP. This tVCP was used for further characterisation and binding studies using Q-sense as well as behavioural assessment.*

Results: tVCP was successfully expressed, and the method of expression using *P. pastoris* yeast expression system was optimised. Using this method, tVCP was expressed as a single pure band (Fig 2.3 A) during 24 h to 96 h after induction. The expression was directly proportional to the concentration of methanol used for the induction. When 1 % methanol (2.5 ml / 24h) was used for induction, the amount of tVCP expressed was more than that of 0.5 % methanol (1.25 ml / 24 h). A single band of tVCP after purification (Fig 2.3 B), and endotoxin removal (Fig 2.3 C) suggested that tVCP was purified, and freed from endotoxin without a significant loss. This was after being passed through 5 kDa cut off filter and Detoxi-Gel Affinity Pak TM Pre-packed columns for endotoxin removal. The protein concentration of various fractions of tVCP after being concentrated and purified was found to be 5.5 to 11.55 mg / ml. After endotoxin removal of tVCP fractions of 5.55 mg / ml, the concentrations were between 2.775 to 4.62 mg / ml. This means that the percentage yield was about 50 to 80 % of the initial concentration.

As far as VCP is concerned, highly pure VCP was supplied either as 2.76 mg of lyophilised powder or solutions of different concentrations of VCP.

2.5.3 Comparison of complement inhibition by VCP, and tVCP using haemolysis assay.

Complement inhibition by VCP and tVCP.

Sr	(A) Sample	(B) OD_{405}	(C) Percentage lysis of ssRBCs	(D) Percentage Complement Inhibition (C2-C3 for tVCP or C2-C4 for VCP)
1	-VE Control (PBS)	0.086	------	------
2	+ VE Control (Serum)	0.418	100 %	------
3	tVCP + Serum	0.337	75.45 %	24.55 %
4	VCP + Serum	0.136	14.55 %	85.45 %

Table 2.1. *Complement inhibition by VCP, and tVCP [OD_{405} (column B) and the percentage complement inhibition by VCP and tVCP (Column D) calculated from the percentage lysis of the ssRBCs caused by serum in the presence of tVCP and VCP (column 3). Sr = Serial number. – VE ctrl = PBS (5 µl), and + VE control = Serum*

2.5.4 Effect of VCP and tVCP on the serum mediated haemolysis of ssRBCs.

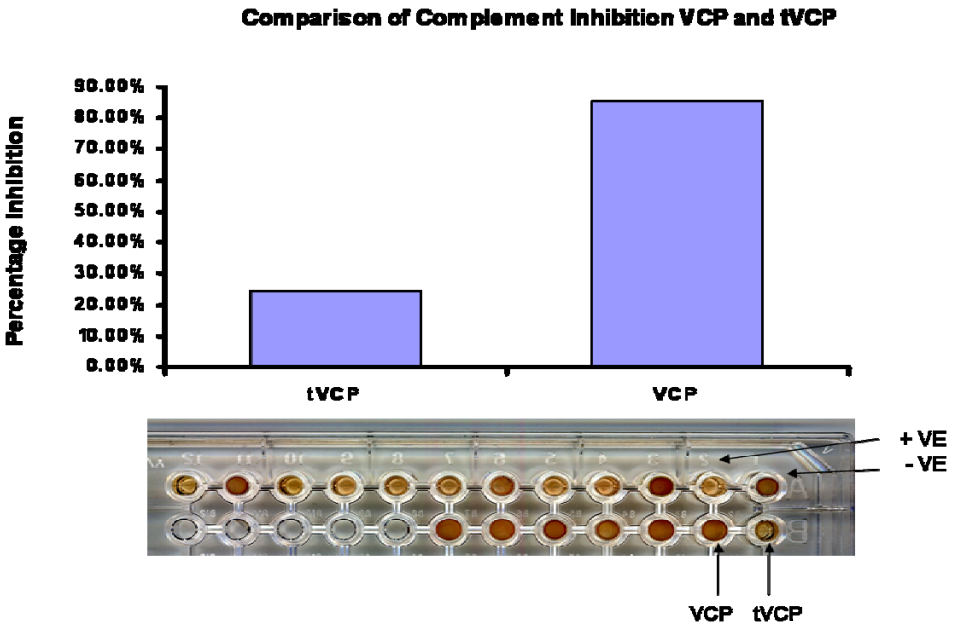

Figure 2.4. *Diagrammatic representation of the effect of VCP and tVCP on the complement mediated lysis of ssRBCs (+VE = +VE Control, -VE = - VE Control). Yellow coloured well indicates complete lysis of ssRBCs mediated by complement components from serum. Red colour indicates the intact ssRBCs as a measure of complement inhibition. The Percentage inhibition (Y- axis) by VCP and tVCP are shown by a bar graph above the wells.*

Results: When tVCP was subjected to the haemolysis assay, tVCP showed about 24.55 % of complement inhibition at 1 mg / ml concentration (Table 2.1). These findings are similar to the findings by other investigators (Smith et al. 2000, Smith et al. 2003) who showed the inability of tVCP to prevent complement mediated haemolysis. For this reason, tVCP was not further tested for complement inhibition using the *in-vitro* assays.

When subjected to the haemolysis assay, at the same time, under similar circumstances, VCP showed about 85.45 % complement inhibition (Table 2.1). When, the 96 well plate, as shown in Fig 2.4, was kept at $4^{O}C$ to settle the ssRBCs, and photographed, it is evident that the colour of the well to which VCP was added is dark red matching the negative control indicating intact ssRBCs, and consequently complement inhibition by VCP (Fig 2.4). In contrast to this, the well to which tVCP was added showed yellow colouration similar to +VE control due to its inability to prevent serum (complement) mediated lysis of ssRBCs. VCP was further subjected to a haemolysis assay for the determination of IC_{50} value.

2.5.5 Determination of IC_{50} value of VCP using haemolysis assay.

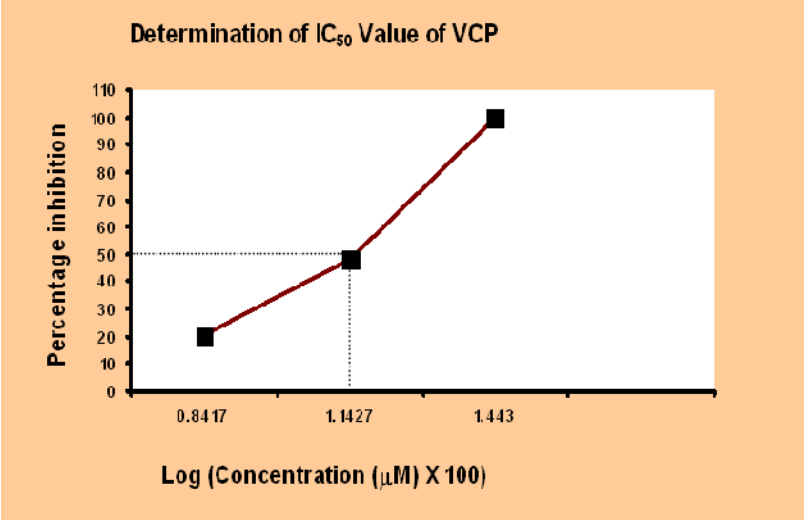

Figure 2.5. *The IC_{50} value, that is the concentration of VCP required for 50 % inhibition of the complement system was determined by plotting percentage inhibition (Y axis) vs log of 100 X μM conc. of VCP (X axis)*

Result: The IC_{50} value of VCP, as determined by plotting the percentage inhibition by VCP against the log of conc. of VCP was found to be 0.145 μM (Fig 2.5 and Table R2.1, Appendix R).

2.5.6 Determination of IC_{50} values of Cur, RA and Qur using modified haemolysis assay.

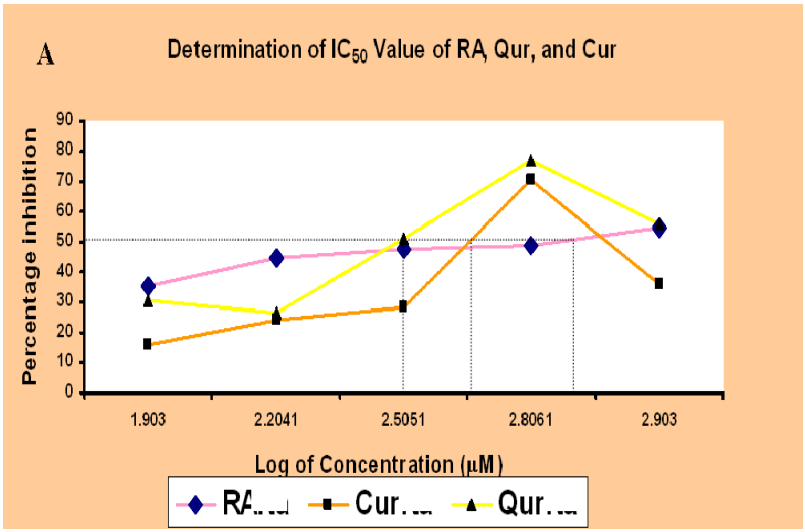

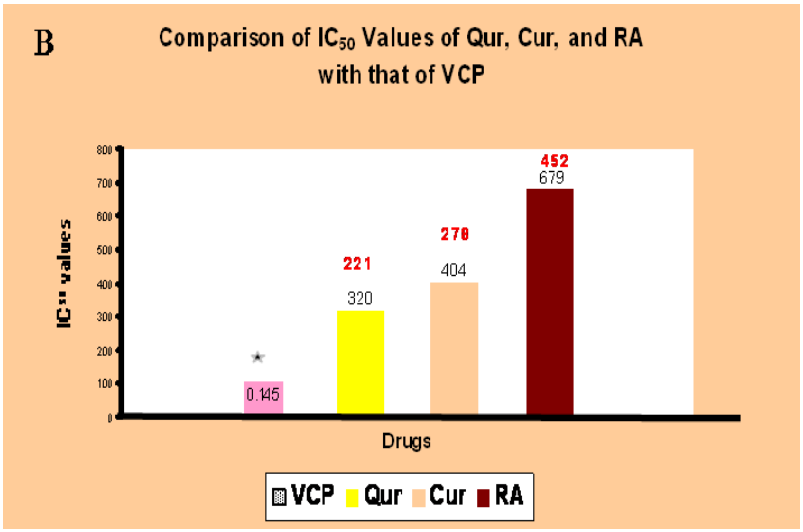

Figure 2.6A. *Determination of IC_{50} values by plotting log of µM concentrations of RA, Qur, and Cur (X axis) against the percentage complement inhibition (Y axis) by each of them as shown by the modified haemolysis assay. The IC_{50} values were determined by dropping a line (fine dotted grey) onto the X axis where the line coincides with the three line graphs.* ***B*** *The comparison of the IC_{50} values (Y-Axis) of Qur, RA, and Cur with that of VCP. The IC_{50} values are shown in black, and the multiple fold activity of VCP is shown using red font. The asterisk in 2.6B is used to show thousand fold less value than all the other compounds used in the assay*

Results: The IC_{50} values of RA, Qur, and Cur were found to be 679 µM, 320 µM, and 404 µM, respectively (Fig. 2.6A, Table R2.2, Appendix R). When compared with VCP, VCP was found to be 2212, 2786, and 4520 times more potent at inhibiting the complement system in haemolysis assay than that of RA, Qur, and Cur, respectively (Fig 2.6B).

2.5.7 Inhibition of the CP of complement activation by the ingredients of herbal origin.

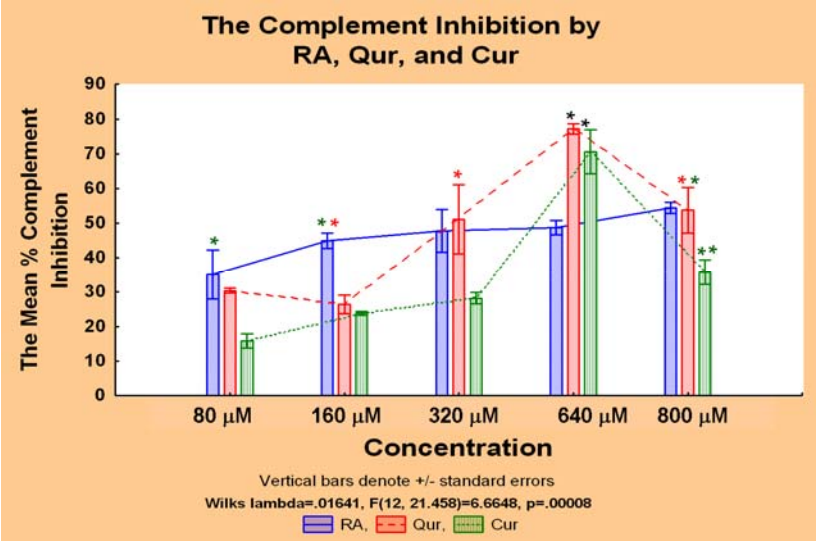

Figure 2.7. *The mean percentage complement inhibition by using the modified haemolysis assay (Y axis) at different concentrations of RA, Qur, and Cur (X axis) as shown by the bar graphs. The bars from the same group at different concentration are connected by a line of the same colour as that of the bars being connected. Repeated measures ANOVA with post hoc test (Neuman-Keul's multiple comparison) were used for the statistical analysis. The significant difference between the treatment groups at the same concentration, as well as between the different concentrations of the same drug are shown by colour coded asterisks. The significant difference between the two drugs at the same concentration is shown by the colour coded asterisks whose colour matches with the colour of the bar being compared. The significant difference between the higher and lower concentrations of the same drug is shown by placing an asterisk on the bar representing the higher concentration of that drug. In this case the asterisk colour is the same as that of the colour of the bar. The black coloured asterisks indicate a significant difference in the values from all the other drugs and concentrations with the exception of the other bar(s) bearing the black asterisk(s).*

Results: As shown in Fig 2.7 and Appendix R (Table R2.3), at lower concentrations (80 to 160 µM), RA showed better complement inhibition than that of Cur, and Qur, however at higher concentrations (320 µM for Qur, and 640 µM for Cur), there was a sharp rise in the complement inhibition by Cur and Qur. There was no difference in the complement inhibition by RA at all the concentrations. Cur and Qur showed dose dependent complement inhibition as indicated by the modified haemolysis assay, and the graph is typical sigmoid-like for both of them. There was a sudden rise in the complement inhibition at 640 µM by them which rapidly decreased there-after at 800 µM concentration. The decline in the complement inhibition by Cur at higher concentration was sharper than that of Qur.

2.5.8 The effect of Cur, Qur, and RA on the AP of complement activation.

The IC_{50} value for the complement inhibition by RA was close to 640 µM, and it showed the same degree of complement inhibition at all the other concentrations. Both Cur, and Qur showed maximum complement inhibition at this concentration. Consequently, these concentrations were therefore selected for studying the effect of these compounds for the initial screening of them for their effect on the AP of complement activation, using a Quidel enzyme immunoassay kit as mentioned in the methods section. All the samples were used in duplicates at this concentration.

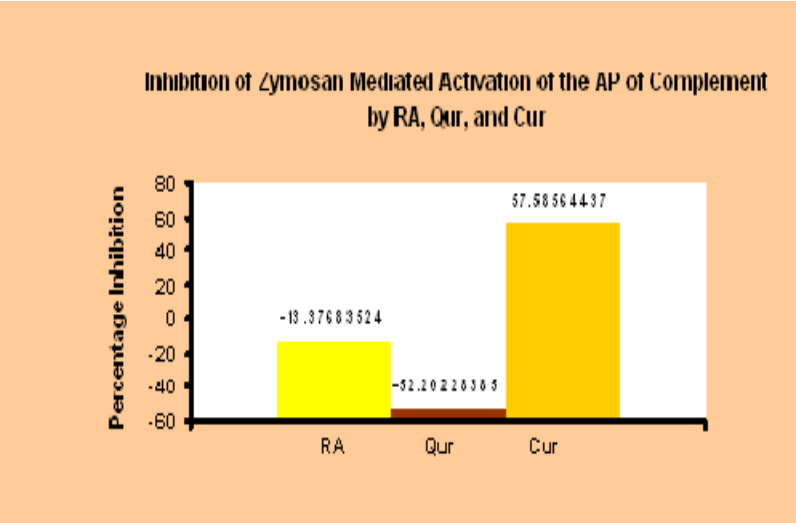

Figure 2.8. *The percentage inhibition of zymosan mediated activation of AP of complement (Y axis) by RA, Qur, and Cur at 640 μM Concentration (X axis). The Y axis crosses the X axis at -60 as the OD of Qur and RA was less than that of the Positive control. This results in the negative values of complement activation.*

Results: Cur showed approximately 58 % inhibition of AP of the complement activation at 640 μM. The OD of RA was close to the positive ctrl, which means that it could not inhibit AP of complement activation. In the case of Qur, the OD was exceptionally high, even higher than that of the positive control which results in the negative value. The role of VCP on AP has already been well established by others, and use of the same kit has been reported previously (Ghebremariam et al. 2005). Therefore, VCP was not used to investigate its effect on AP. Since only Cur showed inhibition of zymosan activated AP at this concentration, it was selected for further measuring its concentration dependent effect on AP of complement activation, and determination of its IC_{50} values.

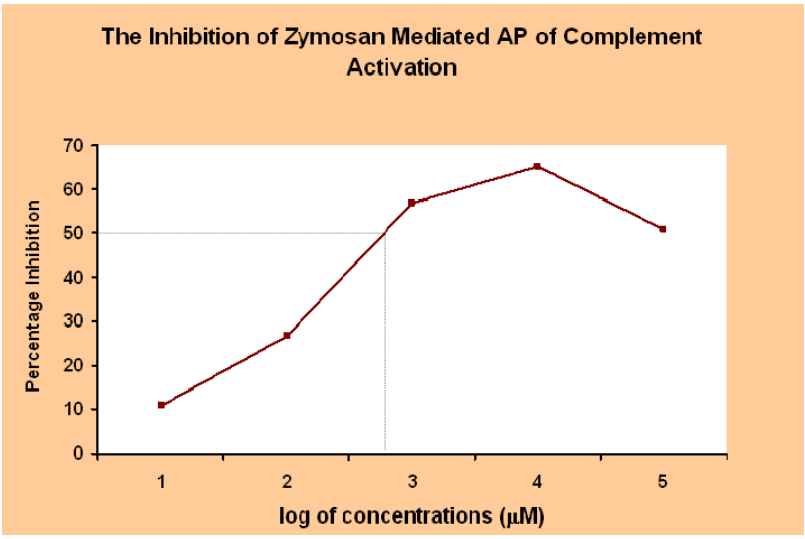

Figure 2.9. *The effect of Cur on zymosan mediated activation of AP in terms of percentage inhibition (Y axis) at log values of different concentrations (X axis). The IC_{50} value is determined by dropping a vertical line (fine dotted grey) onto X axis. The different concentrations of Cur used were 160 μM, 320 μM, 640 μM, 960 μM, and 1280 μM.*

Result: The IC_{50} value of Cur for the inhibition of zymosan mediated activation of AP was found to be 630 μM (Fig 2.9). It is almost twice the concentration of Cur required for the inhibition of CP.

2.5.9 Summary of Results.

Sr	Experiment	Results	Conclusion
1	Expression of VCP, tVCP, and subsequent analysis using SDS-PAGE, concentration and purification (Figs 2.2 and 2.3)	SDS-PAGE for VCP = a band between 35 kDa and 25 kDa, as well as other bands. VCP supplied = just one band corresponding to VCP. tVCP= Only one band corresponding to 18.8 kDa.	VCP, and tVCP were expressed. tVCP expressed in large quantity. VCP supplied was highly pure with only one band on gel.
2	Haemolysis Assay (Table 2.1 and Fig 2.4 and 2.5)	VCP showed serum mediated lysis of RBCs. tVCP did not show complement inhibition in haemolysis assay.	VCP inhibited the CP of complement activation with IC_{50} value of VCP = 0.145 μM.
3	Modified haemolysis Assay (Figs 2.1, 2.6 A and B and 2.7)	RA, Qur, and Cur inhibited CP. The shape of the graph for RA was linear, and sigmoid-like for the other two. The IC_{50} values for Cur, Qur, and RA were 404 μM, 320 μM, and 679 μM, respectively.	Qur, Cur, and RA inhibit the CP of complement activation.They were several times less potent that that of VCP.
4	Quidel Enzyme Immunoassay (Figs 2.8, and 2.9)	RA and Qur = No effect at 640 μM. Cur = Inhibition of AP with sigmoid-like curve. IC_{50} value for AP inhibition = 630 μM.	Cur dose dependently inhibits AP.

2.6 Discussion.

As shown in the gel, highly pure endotoxin free VCP appears as a single band between 25 kDa and 35 kDa band in SDS- PAGE. Consequently this VCP was used in the current investigation as well as subsequent *in-vitro* and *in-vivo* studies. tVCP was expressed using *P. pastoris* yeast expression system. The tVCP clones used in the study were highly expressing. Using these strain, tVCP was expressed as a highly pure single band (Fig 2.3A). It was further purified and made free of endotoxin (Fig 2.3B and C).

When these compounds were subjected to haemolysis assay (functional assay) for measuring their *in-vitro* complement regulatory activity, as expected, tVCP inhibited the complement mediated haemolysis to a very much lesser extent as opposed to VCP, which showed significant inhibition of complement (Fig 2.4 and table 2.1). This supports the finding by other investigators who found that tVCP does not bind the complement components and therefore does not inhibit the complement activation (Smith et al. 2000, Smith et al. 2003). As evidenced by the photographs of the 96 wells used to study the haemolysis assay of VCP, and tVCP, tVCP could not inhibit the complement mediated lysis of ssRBCs, and therefore, the lysed ssRBCs appear as a yellow coloured solution. This is similar to the positive control where serum was used to lyse the ssRBCs (Fig 2.4). That VCP inhibited the complement mediated lysis is shown by the red colour of intact ssRBCs (Fig 2.4).

The haemolysis assay used in the current investigation is widely used to screen compounds for their ability to inhibit the CP of complement activation (Kotwal et al. 1990, Smith et al. 2000). tVCP and VCP showed complement inhibition as observed by the other investigators. This assay was used in the current investigation to confirm that the protein bands corresponding to their size shown in Figs 2.2 and 2.3 are actually of tVCP, and VCP, respectively. The similar functional profile shown by the proteins expressed in the current investigation, as well as SDS-PAGE analysis, thus confirm the expression of these compounds.

Using this assay, IC_{50} value of VCP was found to be 0.145 μM (Fig 2.5). tVCP at the concentration used in the study (about 1 mg / ml) showed only 24.55 % inhibition of complement, and therefore its IC_{50} value could not be determined.

When the attempts were made to screen the small sized complement regulatory molecules, RA, Cur, and Qur for their ability to inhibit the CP of complement activation, the absorption by these compounds due to their colour in the same range is problematical. The assay was therefore modified as discussed in the methodology, and shown in Fig 1 of the chapter. Using this method, it was found that RA, Qur, and Cur showed inhibition of the CP of complement activation. RA (Peake et al. 1991, Sahu et al. 1999), and Qur (Cimanga et al. 1995) have previously been screened for their complement regulatory activity and similar results were observed in this study, which further validates the findings of the investigation using modified haemolysis assay.

Qur is also known to inhibit both the CP and AP of complement activation (Cimanga et al. 1995). The effect of Cur on CP of complement activation is reported for the first time in the current investigation. As shown in Fig 2.6, the IC_{50} values for Cur, Qur, and RA was found to be 404 μM,

320 μM, and 679 μM, respectively. When the complement inhibition by these compounds was compared at different concentrations (Fig 2.7), it was found that at lower concentration, RA inhibited the complement system to a greater extent than that of Qur, and Cur. Further analysis of the results suggested that RA inhibited the CP to the same extent at all the concentrations, and the dose dependent increase in the complement inhibition by RA was not significant. However, both Qur, and Cur used in the study show dose dependent inhibition of the complement up to 640 μM concentration after which, there was a sudden drop in their complement regulatory activity. This drop in the activity could be explained on the basis of cooperative effect. Previously, when VCP was being compared for the complement inhibition with C4b binding protein (C4b-BP), C4b-BP showed a similar sigmoidal graph (Kotwal 1994) as shown by Cur in the current investigation. In their study, the shape of the graph was attributed to the cooperative effect, and thus the activity of Cur observed in the current investigation could also be explained on the same basis. This sigmoid-like shape shown by Cur can also be attributed to the intermolecular and intramolecular bonding shown by Cur (Tonnesen et al.1982). It is possible that at lower concentration, the intermolecular bonding by Cur predominates over the intramolecular binding. Thus, Cur binds strongly to the complement components, and inhibits them, but at higher concentration, the intramolecular bonding may overcome this intermolecular binding, resulting in the decrease in the affinity of Cur towards the complement components.

RA and Qur have previously been shown to inhibit both the CP, and AP of complement activation. However, in the current investigation, these compound could not inhibit the AP as shown in Fig 2.8. This could be attributed to the way their solutions were prepared in those studies. In the previous studies where these compounds have shown the complement regulatory activity (Peake et al. 1991, Cimanga et al. 1995, Sahu et al. 1999), these compounds were not used as their sodium salts compared to the current study. Preparation of their solutions in PBS and NaOH used in the current investigation might have affected their activity. In the previous investigations (Cimanga et al. 1995), RA was found to be a better inhibitor of complement than Qur in contrast with our results. This could be attributed to the differences in the methodology as well as preparation of solutions, and their use of different concentrations.

When Cur was investigated for its effect on zymosan mediated activation of the AP of complement activation, it was found to inhibit it dose dependently (Fig 2.9). The IC_{50} of inhibition was found to be 630 μM, which is almost twice than that for the inhibition of the CP (404 μM). The Quidel Bb fragment enzyme immunoassay used in the current investigation to test the effect of Cur on inhibition of AP of complement activation is based on quantitative estimation of Bb. Bb is a cleavage product of factor B in human serum. Bb factor is an index of complement activation by the AP. Therefore, it could be concluded that in the current investigation, Cur dose-dependently inhibited the formation of Bb. Bb is a fragment of factor B involved in the activation of the AP (Xu et al. 2001, Le et al. 2007). This dose-dependent inhibition of complement activation can be attributed to a reduction in the formation of Bb by Cur through different mechanisms. Formation of Bb from factor B is a two-step process, which requires Mg^{++} ions and factor D.

Cur shows the phenolic hydroxy groups and it is known that the phenolic hydroxy moieties might result in the formation of phenoxide ions (Wade 1995) which is a negatively charged moiety. This phenoxide moiety may chelate the Mg^{++} ions and thereby prevent the cleavage of factor B. However, Cur's inhibitory action on the AP of complement activation cannot be solely attributed to this chelation effect, as Mg^{++} ions are not an absolute requirement for the formation of the AP convertases (Pryzdial and Isenman 1986). Therefore, the effect of Cur on other factors which mediate the activation of AP needs to be investigated. As found in the current investigation, Cur inhibits both the CP and AP of complement activation. Both C3, and C3b are central to the activation of the AP and CP. Therefore, the effect of Cur on these components being central to the complement activation needs to be further investigated.

The sigmoid type graph for AP inhibition (Fig 2.9) by Cur may also be explained on the basis of a cooperative effect and intermolecular / intramolecular hydrogen bonding by Cur discussed previously.

The *in-vitro* complement regulation by Cur can be used to further explain its anti-inflammatory activities. In most of the *in-vitro* studies, Cur was dissolved using DMSO or other organic solvent. The use of these solvents is not practical if Cur is to be used for the clinical studies. Cur solubilised using PBS and NaOH used in the current investigation might be an effective solution to this problem. Indeed when sodium salt of Cur was used to study the effect of Cur on the inhibition of inflammation (Mukhopadhyay et al. 1982), it showed the anti-inflammatory activity. The activity of the sodium salt of Cur was better than that of the parent compound, and phenylbutazone, a standard anti-inflammatory compound. In the same investigation, it was found that Cur did not show this activity due to inhibition of prostaglandin synthesis or the release of steroids from the adrenal cortex. The inflammatory activity by Cur shown by Mukhopadhyay et al. (1982) could be attributed to the complement regulatory activity by Cur as observed in the current investigation.

When the effect of Cur, Qur, and RA was compared with that of VCP, it was found that the IC_{50} values of Cur (404 μM), Qur (320 μM), and RA (630 μM) were found to be 2785, 2212, and 4520 times more than that of VCP (0.145 μM) (Fig 2.6A and B). This means that VCP is thousands of times more potent in haemolysis assay of than that of these compounds. This observation might have certain consequences on the pharmacological activity of these compounds. VCP could show biological activity at an extremely low concentration, but has not been shown to be able to cross BBB and thus as discussed in the literature review and general introduction, there is a requirement to deliver it to the brain by alternative means. Cur, although is able to cross BBB (Yang et al. 2005), showed complement inhibition at high concentration. Therefore, an approach could be to prepare complement regulatory analogues of Cur with better complement regulatory activity.

In conclusion, tVCP was expressed, and purified using the *P. pastoris* expression system. VCP, but not tVCP showed regulation of the CP of complement activation. RA and Qur inhibited the CP of complement activation, but not the AP. The effect of RA on the CP was not dose dependent, but Qur showed dose dependent complement inhibition with a sigmoidal graph. Cur showed complement regulatory activity with an inhibitory effect on both the AP and CP of complement activation. Its effect

on C3 and C3b, the complement components central to the activation of complement, needs further investigation. Thus, Cur which is shown to inhibit both the AP and CP of complement system may possibly be used in the treatment of disorders of the brain where up-regulated complement components play a devastating role.

In the present investigation Cur inhibited both the pathways of complement activation, and therefore it will be compared with that of VCP and tVCP for its ability to bind complement components using Q-sense. This will reveal its mode of action on the complement system.

Chapter 3.

Investigation of Interaction of VCP, tVCP and Cur With the Complement Components C3 and C3b Using Quartz Crystal Microbalance With Dissipation Monitoring (QCM-D) Technology.

3.1 Introduction.

The complement regulatory molecules might prove beneficial in the prevention of damage to the CNS from up-regulated complement components in chronic as well as acute neurodegenerative disorders. With the objective of investigating small sized complement regulatory molecules with an ability to regulate the complement system, VCP was compared to phenolic hydroxy compounds of herbal origin RA, Qur and Cur as reported in the previous chapter by using *in vitro* techniques. Similar to VCP, Cur was found to inhibit both the CP and AP of complement activation. In the last two decades, VCP has been thoroughly investigated for its effect on components of the complement system. VCP was reported to inhibit both the CP and AP two decades ago (Kotwal and Moss 1988, Kotwal 1990, Mckenzie et al 1992). It was found to inhibit these pathways by inhibiting the third and fourth components of the complement (Kotwal et al. 1990, McKenzie et al. 1992). VCP is known to be structurally similar to C4Bbp, but functionally to CR1, a human complement regulatory molecule known to bind C3b. VCP has previously been shown to bind to C3b using surface plasmon resonance (SPR; Smith et al. 2003). As Cur was found to inhibit both the CP and AP of complement activation, it is likely that it may also inhibit these pathways through its ability to interact with C3b. In the previous chapter (2), Cur was shown to inhibit the AP activation through its ability to prevent the cleavage of factor B to Bb in the previous chapter. It was hypothesized that it might have done so either through binding to Mg^{++}, or through binding to factor D which cleaves factor B to generate Bb fragments. It was also hypothesized that it might be able to inhibit formation of C3 convertases. It may inhibit stabilization of C3 convertase by properdin or it may have more than one sites of action on the complement components. The complement components that Cur might bind could be the complement components which are central to the activation of CP and AP. Properdin can bind to C3 (H_2O) and C3b for the assembly of the C3 convertase. Complement factor B and Bb bind to C3 (H_2O) for the formation of C3 convertase (Hinshelwood et al. 1999).

Based on our previous results, and the information in the aforementioned articles, it can be argued that Cur may bind to C3 (H2O) and/or C3b. By doing so, it may prevent binding of properdin or Bb to C3 and C3b, and thereby inhibit the formation of the AP convertase. C3 in the form of C3 (H_2O) also acts as a central component of complement activation, which circulate in the body in its inactive form. Upon activation, it is converted into its active fragments such as C3b, C3a, C3c and C3d as discussed in several reviews (Makrides 1998, Datta and Rappaport 2006). C3b and C3a are reported to play a damaging role in inflammatory disorders as discussed in the literature review. HIV and its proteins are known to increase the expression of C3 in the the neurons and strocytes (Speth et al. 2002). Recently, it was also proposed that HIV uses complement opsonin iC3b, a C3b or C3 fragment, and this opsonised HIV infects T cells (Stoiber et al. 2005). HAART is also associated with peripheral neuropathy and elevation of complement components C3 and C4 (Spear et al 1999, Datta and Rappaport 2006). C3 is also implicated in several neuroinflammatory disorders. C3 and C4 are expressed in C1q sufficient

and deficient mice (Zhou et al. 2008). The levels of C3 and C4 are also elevated in AD with mild to severe clinical symptoms with a low level of expression of complement regulatory molecules (Zanzani et al. 2005). Therefore, there is little doubt that the activated complement components need to be regulated and compounds inhibiting C3 and C3b need to be discovered to prevent the detrimental effects of these complement components. VCP is known to inhibit both C3b and C4. However, VCP's ability to bind to C3 has not been reported. Similarly, Cur's ability to bind C3 and C3b has also not been reported. It was therefore consider important to investigate and compare the effect of these components central to the activation of complement by use of specialized techniques.

There are many techniques available for protein adsorption or interaction (Ramsden 1993). In order to carry out the protein binding study, it was decided to use QCM-D based Q-sense (D-300), a Swedish based technology thoroughly studied and developed for the protein adsorption studies at Chalmers University of Technology, Goteberg, Sweden (Höök 2004T). In Q-sense, the change in frequency (dF) of a quartz based sensor crystal resonating at its resonant frequency (*f*) upon adsorption of an adsorbing moiety (AM) is correlated with the change in mass of AM. The energy dissipated during this adsorption is also recorded and measured in terms of disspation factor (D). The changes in dissipation (dD) and dF are specific for a particular system comprising an AM. The ratio dD/dF gives information regarding the viscoelastic properties and adsorption kinetics of a system (Höök 2004T). The QCM-D technique offers the advantage of real time monitoring, rapidity, simplicity, sensitivity, and economy, compared to the other routinely used techniques. The potential of QCM as a biosensor, and its sensitivity was found to be comparable to that of surface plasma resonance (SPR; Kosslinger et al. 1995, Höök 2004T), a commonly used technique for protein binding studies. Using bare gold crystals of QCM, it was shown to be as sensitive as ELISA (Aberl et al. 1994) when compared with gp41 based HIV-ELISA offering an advantage of real time monitoring and rapidity (10 min to 2 h versus several hours to 1-2 days in ELISA) without loosing sensitivity. It does not involve labeling of protein molecules and therefore the chances of changes in conformation of the protein under proper experimental conditions are less. It also takes into account D values or dD/dF values. These values can be used to study the nature (rigid vs reversible) as well as kinetics of protein binding. The many advantages of QCM-D technology over the other routinely employed techniques as discussed above was the deciding factor for employing q-sense D-300 (q-sense) to study the interaction of VCP and Cur with the complement components.

QCM-D has previously been employed to study the interaction of the complement system with biomaterials. Jonas Anderson from the University of Uppsala, Sweden studied the interaction of complement components with the of biomaterial surface (Andersson et al. 2002). Using QCM-D, it was also shown that the polystyrene surface activates the AP of complement activation. C3 deposited on the polystyrene surface can form C3 convertase and activates the AP of complement activation (Andersson et al. 2002). QCM-D was also compared to ELISA

technique to show that biomaterial surfaces activate the complement system and this activation can be inhibited by complement regulatory molecules such as factor H (Andersson et al. 2001). The technique was also used to study the interaction of the complement components with complement inhibitory molecules such as C1q inhibitor CRI. Thus Q-sense based on QCM-D may be employed to investigate the complement regulatory molecules of therapeutic importance. In order to confirm binding characteristics, more than one surface was used to ensure proper comparison. In the current study the gold and polystyrene sensor (PS) crystals were used to study the interaction of with the complement system in hydrophilic and relatively hydrophobic environments, respectively. PS surface is also known to activate the complement system via C3 offering a special advantage in the study. Cur is known to interact with BSA (Barik et al 2003, Sahoo et al. 2008) and therefore it was used as a positive control for the interaction of Cur with C3 and C3b.

3.2 Objectives.

The overall objectives of the present investigation are to compare the interactions of VCP, tVCP and Cur with C3 and C3b on the gold and PS surfaces. The specific aims are to;

a. Compare the nature of binding of VCP, tVCP and Cur with that of C3 and C3b using gold and PS surfaces.
b. Compare the adsorption kinetics of interaction of VCP, tVCP and bovine serum albumin (positive control for Cur) with the gold and PS.
c. Compare the interaction of C3 and C3b with the aforementioned surfaces as well as with VCP and tVCP adsorbed onto these surfaces.
d. Investigate the modulation of binding of Cur to C3 and C3b bound to the gold and PS surfaces by VCP and tVCP.

3.3 Basic principles of QCM, terminologies used, and description of Q-sense.

QCM is used to measure the interaction between protein or adsorbing molecules and that of the surface as well as with each other, employing a piezoelectric sensor crystal. The word Piezoelectricity (greek: Piezein = press) is referred to as the property of certain materials such as quartz to generate an electric potential in response to an applied stress. For the QCM studies, this piezoelectric sensor crystal is coated with a very thin layer of gold on both the sides which serve as electrodes which are used to apply an AC voltage. This results in oscillation of the sensor crystal at its resonant frequency *f*. This inherent *f* of the quartz crystal changes upon adsorption of a thin layer of an AM. In QCM, this change in frequency (dF) is correlated with the change in mass (ΔM or dM). The amount of a substance deposited on the crystal surface is determined from this change in frequency using Sauerbrey's equation (Höök 2004T, Sauerbrey 1956):

$$\frac{\Delta m}{A} = \frac{N_q \rho_q}{\pi Z f_L} \tan^{-1}\left[Z \tan\left(\pi \frac{f_U - f_L}{f_U}\right)\right]$$

Equation 2 – Z-match method

f_L – Frequency of loaded crystal (Hz)

f_U – Frequency of unloaded crystal, i.e. Resonant frequency (Hz)

N_q – Frequency constant for AT-cut quartz crystal (1.668×10^{13} Hz.Å)

Δm – Mass change (g)

A – Piezoelectrically active crystal area (Area between electrodes, cm^2)

ρ_q – Density of quartz ($\rho_q = 2.648$ g/cm^3)

$$Z = \sqrt{\left(\frac{\rho_q \mu_q}{\rho_f \mu_f}\right)}$$

μ_q – Shear modulus of quartz ($\mu_q = 2.947 \times 10^{11}$ g/cm.s^2)

μ_f - Shear modulus of film (Varies: units are g/cm.s^2)

The Sauerbrey's equation is based on a few assumptions as mentioned below.

1) The AM should be rigidly deposited on the crystal.
2) The AM should be distributed evenly.
3) The added mass is smaller than the weight of the crystal.

The study of interaction of VCP, tVCP and Cur with that of C3 and C3b was based on these assumptions. Fit analysis was carried out in some of the experiments to check whether the experiments were following the assumptions based on Sauerbrey's equation.

3.4 Q-sense: Practical considerations (Q-sense Reference manual, Höök 2004T).

The equipment used for the current investigation Q-sense (model D-300) makes use of QCM-D technology as discussed above. The basic layout of the equipment is as shown in the Fig 3.1. It consists of four basic components viz. sensor crystal, measurement chamber, electronics unit, and acquisition software.

The Q-sense (D-300) apparatus and its components.

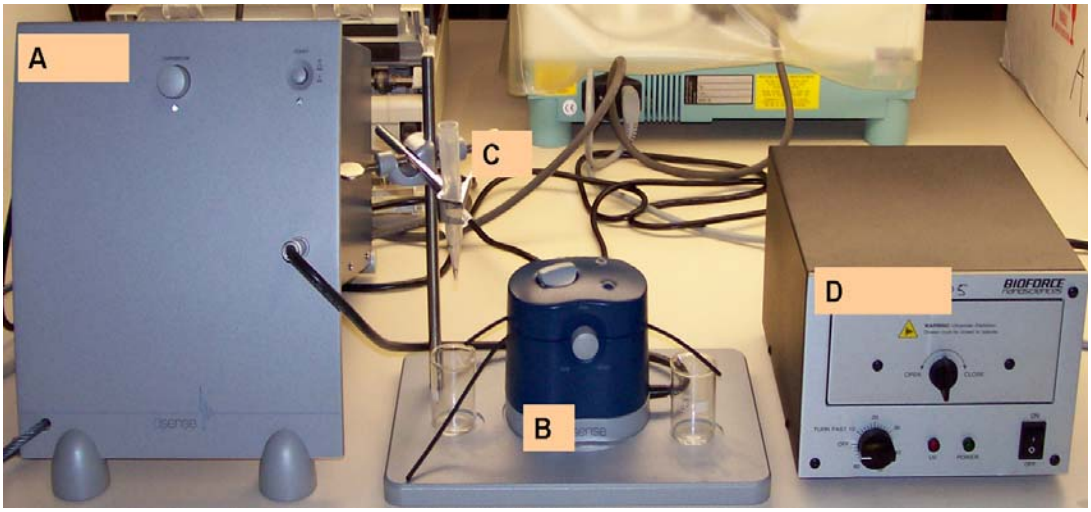

Figure 3.1. *The components of Q-sense (D-300) equipment at UCT showing the electronic unit (A), measurement chamber (B)sample holder (C), and the UV chamber for activating the crystal surface (D)*

In most of the Q-sense based experiments, temperature needs to be controlled appropriately by use of the controller knob of the electronic unit. The experiments are carried out at room temperature (+ 25^{O}C) as extremes of temperature may induce aberrant changes in frequency (Q-sense manual). The temperature inside the chamber for all the experiments was maintained at 24.7^{O}C. Inside this chamber (Fig 3.2), the AT-cut crystals (gold or polystyrene coated; Fig 3.3) operated in thickness shear mode at 5 MHz *f* were mounted as per the instructions in the manual.

The Q-sense chamber.

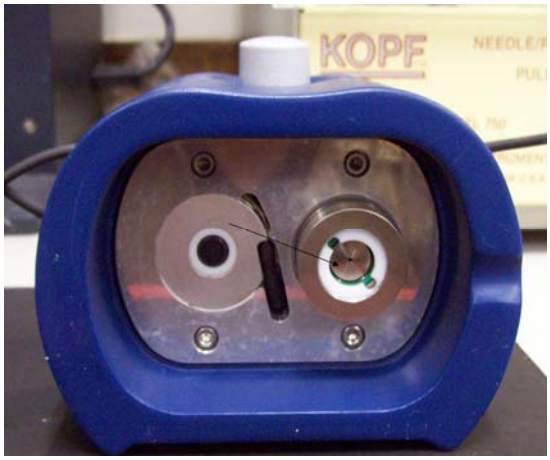

Figure 3.2. *The Q-sense chamber where the sensor crystal is mounted (shown by an arrow)*

The Sensor crystals used for Q-sense study.

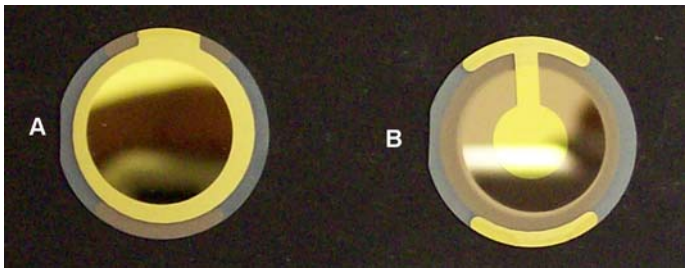

Figure 3.3. *The gold or PS sensor crystal used in the Q-sense study (A = Smooth surface exposed to chamber when mounted at the position shown by an arrow in Fig 3.2; B = The surface connected to the electronic unit (A) in Fig 3.1)*

The smooth surface of the crystal is used for the measurements, and the opposite side of the crystal is connected to A/C supply of the electrical unit and operated in a shear thickness mode. The measurement chamber also consists of a sample holder, the position of which can be adjusted to optimize the flow rate (Fig 3.1 C). The solution of the AM is kept in this sample holder and it can either be added to the "temperature loop" or to the "sensor crystal" using a controller knob on the measurement chamber. About 2 ml of solution is passed on the sensor crystal for an accurate measurement.

The chamber is connected to a PC and the change in *f* and D is monitored online at different overtones using q-soft software. The q-tools software provided with the equipment is used for the analysis of the data captured using q-soft. Using q-tools, it is first confirmed whether the adsorption of the AM follows the Sauerbrey law (Refer section 3.3) using fit analysis. If the adsorption doesn't follow the Sauerbrey equation, a method called Z-match and / or viscoelastic modeling is recommended. As discussed earlier, the change in frequency upon adsorption is correlated with the mass adsorbed on the sensor crystal to study the adsorption of AMs used in the study.

3.5 Dissipation factor in QCM.

In advanced QCM, the important factor that needs to be taken into consideration is the "Q factor". This Q factor is determined experimentally as the ratio of the resonance frequency (*fr*) to the bandwidth (denoted by "w" being the difference between the maximum and minimum cut-off frequencies). This ratio when inversed (w/*f*) gives information regarding the energy lost during one complete oscillation and is defined as the D factor. The D factor is calculated by measuring the decay of the oscillation amplitude of the electrode after the AC voltage is disconnected. The faster the decay, the higher the dissipation.

The D factor gives information regarding the energy dissipated during one oscillation after adsorption of the AM on the crystal. This factor is very important when considering dissipative losses introduced by the mass load in an oscillating system. When the change in dissipation factor is divided

by the change in frequency (dD/dF), it gives information regarding the rigidity of the binding. The low values of this ratio indicate stronger binding. The D-shifts or change in D values are attributed to dissipation at three interfaces (Rodahl et al. 1996, Höök 1998a, Höök 1998b): Dissipation at; 1) the protein-surface interface 2) protein-liquid interface, and 3) within the proteins and/or protein layer including effects of trapped liquid. The dD / df ratio is the lowest for the globular proteins and increases for the complex multidomain proteins. The factors that affect D values and therefore rigidity of binding are; 1) Irreversible structural changes due to interaction with the surface (Brash and Horbett 1995). 2) Water entrapped in pores between adsorbed proteins. 3) Viscoelastic properties of the proteins. 4) The way proteins or adsorbing moieties interact with the surface. 5) Size of the proteins. For smaller proteins (<50 kDa), the f and D values give a physically realistic interpretation of the dissipative mechanism (Rodahl et al. 1997).

3.6 Materials.

2 mg/ml of Cur solution was prepared freshly prior to adsorption during each experiment as shown in the Appendix S. To prepare VCP solution, approximately 50 µl of 1.2 mg/ml of endotoxin free extra pure rVCP was diluted to 2 ml using ice cold PBS solution at the time of experiment. The tVCP used in the study was purified by desalting and by washing with PBS and concentrated by passing the solution several times through a 5 kDa cut-off filter. The final concentration of tVCP was 1.8767 times higher than that of VCP supplied and its molecular weight (18.8 kDa) is 1.5319 times less than that of rVCP (28.8 kDa). In order to prepare tVCP of the same concentration, 40.82 µl to 76.06 µl of tVCP was dissolved in 2 ml of PBS solution prior to experimentation. C3 and C3b solution of the same molar strength were used. To prepare C3 and C3b solution, 15 µl of 2 mg / ml C3 was diluted in 2 ml and 20 µl of approximately 1.6 mg/ ml of C3b was diluted in 2 ml in PBS prior to the experiment. BSA used in the experiment was prepared by diluting 42.2 µl of 2 mg/ml of BSA in 2 ml of PBS. PBS (Gibco, Invitrogen or prepared in the laboratory; 0.154 M; pH 7.2). The solutions were passed through a 0.22 µM filter and degassed prior to use. Two sensor crystals [gold (g) and polystyrene (PS)] were used in the experiments. Hydrogen peroxide (30% approx), Liquid ammonia, concentrated HCl used for washing the sensor crystals were either of analytical or molecular grade. The water used in the experiment and/or to wash the sensor crystal surface was of deionized double distilled Millipore grade (dd H_2O), and it was degassed prior to use.

3.7 Methods.

3.7.1 Preparing the surface and the chamber prior to use.

Just before starting the experiment, and after completion of the experiment, the sensor crystal was washed in appropriate cleansing solution as mentioned in the instruction manual. For washing PS crystal, piranha solution (HCl: H_2O_2: H_2O) was used. A cocktail of ammonia: water: hydrogen peroxide was used for washing the gold crystal. The chamber was washed with 1 % Hellmanex-II solution. After

each washing step, the sensor crystals as well as the chamber were dried using nitrogen gas. The sensor crystal was exposed to UV light for 5-10 minutes to destroy impurities on the sensor surface. It was ensured that resonant frequencies of the crystals matched the values as per the instruction manual. For all the experiments, only the crystals showing comparable and similar pattern of F and D values were used. The final volume of each AM used was 2 ml. PBS was used to obtain a baseline before starting each experiment as well as prior to each adsorption.

3.7.2 Experiments.

Prior to the adsorption of AM, a baseline for the resonance frequency of the crystal was obtained by adding PBS (pH =7.2; 154 mM) to the surface. PBS was added until there was no further drop in the frequency. The surfaces, adsorbing moieties used, and the sequence of adsorbing moieties are as described in the table 3.1. As shown in the table, VCP and tVCP were adsorbed on either PS or gold surface and their interaction with C3 and C3b was measured. In the case of Cur, first C3 and C3b were deposited on the surface of the sensor crystal and Cur was adsorbed. After adsorption of the first compound on the sensor crystal for a particular period of time (approximately 30 – 50 min), 2 ml of the second AM was added to the sensor surface to adsorb on the first AM. The adsorption was continued for approximately the same period. The third step was either final washing and / or continuation of the experiment by adsorbing the third AM on the second AM. Generally the 3rd AM adsorption was used after the adsorption of C3 or C3b onto tVCP or VCP, which in turn was bound to the gold or PS surface. In these cases, Cur was adsorbed onto C3 or C3b. This was done to check whether Cur can bind to C3 or C3b adsorbed onto VCP or tVCP to investigate whether Cur and these drugs share common binding sites. The *df* and dD values were measured online and plotted using Q-soft software. The dD / *df* ratios were calculated to get information regarding rigidity of binding molecules. dD values (Y axis) at different time intervals were plotted against *df* values at the same interval to get information regarding the kinetics of binding. Avogadro's formula (shown in the sections d and e of the terminology section) was used to calculate the number of molecules of one compound. However, in the current experiment, as the water binding capacity of VCP, tVCP, and Cur was not known, the number of molecules bound to each other and with the surface is not true reflection, but an approximate value. As discussed later in the appropriate section, 30% mass accounts for the water bound to protein molecules, and therefore it was deducted from the final mass of AMs interacting with the surfaces or other AMs. As this was not the main objective, and also that viscoelastic modelling of more than 30 experiments was beyond the scope of the objectives in this study, the results for approximate binding of molecules are included in the tables in the tables R3.1 to R3.4 of Appendix R.

The outline of the Q-sense experiments.

Sr	Surface	AM (AM) I	AM II	AMIII	No of experiments performed (n)
1	Gold	VCP	C3	Cur	2
2	Gold	VCP	C3b	Cur	2
3	PS	VCP	C3	Cur	2
4	PS	VCP	C3b	Cur	1
5	Gold	tVCP	C3	Cur	2
6	Gold	tVCP	C3b	Cur	1
7	PS	tVCP	C3	Cur	2
8	PS	tVCP	C3b	Cur	2
9	PS	C3	VCP	----	1
10	Gold	C3	Cur	---	2
11	Gold	C3b	Cur	---	2
12	PS	C3	Cur	---	2
13	PS	C3b	Cur	---	1
14	Gold	BSA	Cur	---	2
15	Gold	BSA	Cur	---	2
16	PS	BSA	Cur	---	2
17	PS	BSA	Cur	---	2

Table 3.1. Showing the surface coating of the crystal, and the sequence of AMs (AMI, AMII, and AMIII) and the number of experiments performed per serial number (Sr.)

3.7.3 Terminology used in the results and discussion.

1) As discussed in the above section, there were two to three AMs used for the study. AMI = AM bound to the surface of the sensor crystal (gold or PS). Therefore, AMI is indicated by putting the first letter of the surface (g = gold; ps = polystyrene) in lower case, next to AMI. The abbreviations used in the results and discussion are as mentioned below:
    a. Where AM is bound to the surface of the sensor crystal (AMI), where it is either gold or PS, the abbreviations are VCPg, VCPps, tVCPg, tVCPps, C3g, C3ps, C3bg, C3bps, BSAg, and BSAps.
    b. Where AMII is bound to AMI bound to the surface of the sensor crystal (g or ps) as shown in the table 3.1, the abbreviations are C3-VCPg, C3-VCPps, Cur-C3g, Cur-C3bps, etc.
    c. Where AMIII is bound to the AMII adsorbed onto AMI as described above and shown in the table 3.1, the abbreviations are Cur-C3VCPg, Cur-C3VCPps, Cur-C3tVCPg, etc.
2) Most of the experiments were carried out for 30 min, therefore, dF_{30} and dD_{30} refers to dF and dD values after 30 min, respectively. dF_{30} and dD_{30} values for AMs were calculated as follows:

    a. dF_{30} = dF at 30 min – $dF_{initial}$, where $dF_{initial}$ refers to the baseline or initial f or D values prior to the adsorption of AMs.
    b. In some of the experiments, the adsorption was continued for more than 30 min (and

rarely less than 30 min). In those cases, in addition to dF_{30} or dD_{30} values, dF_{fin} or dD_{fin} values were also calculated. These values were recorded after washing the surface with PBS after the adsorption was over and were calculated as: dF_{fin} = Final dF (or dD) values after washing with PBS – $dF_{initial}$ (or $dD_{initial}$).

c. Using these dD and dF values, dD/dF ratios were calculated to get the information regarding the rigidity (affinity) or viscoelasticity of binding.

d. No. of molecules of AM adsorbed onto the crystal surface or onto the other AM = 6.022 X 1023 X mass adsorbed (ng/cm^2) / molecular weight of the AM.

e. Molecular weights of C3, C3b, Cur, BSA, and tVCP in nanograms (ng) were 1900 X 10^{11}, 1800 X 10^{11}, 3.6839 X 10^{11}, 680 X 10^{11}, 188 X 10^{11}, and 288 X 10^{11}, respectively. These values were taken either from Calbiochem catalogue (C3 and C3b), Sigma-Aldrich (Cur) or from the literature (VCP and tVCP).

3.7.4 Instructions for the interpretations of the figures 3.4 to 3.7: These figures comprise of the primary and secondary axes. The primary X and Y axes are shown by black lines, whereas the secondary X and Y axes are shown by red lines. The primary X axis represents AMs (Please refer the terminology section above to understand the meanings of the abbreviations used for AMs). The primary Y axis shows dD/dF ratios for AMs shown on the primary axis. Two different sets of dD/dF values for the AMs are shown by violet and red coloured bars. The violet coloured bars indicate the average values after 30 min (dD30avg/dF30avg) and the red coloured bars indicate the average final values after washing the sensor surfaces once the experiments are over (dDFinavg/dFfinavg). The secondary Y axis represents dF values for the AMs shown on the primary X axis. The gradient yellow brown bars plotted on the secondary X and Y axes represent dF30 values. The dF30 values are also displayed on the secondary axis for a quick reference. The orange dots connected by a thick turquoise line are used to show the dFfin values of AMs on the primary X axis. It should be noted that for some of the AMs, dF30 or dFfin values plotted on the secondary X axis in these graphs were high and the bars for these values were overlapping with the dD/dF bars plotted on the primary axis. In order to avoid this overlapping, the point of origin of the graphs is in negative although such negative values don't have any physical reality.

3.7.5 Instructions for the interpretations of the figures 3.8 to 3.11: In order to discuss the results of the kinetics of binding of AMs, dD values (Y-axis) at five different time points were plotted against dF values (X-axis) at the same time points. dD vs dF graphs are plotted to avoid time dependency and to know about the shapes of the graph to study the phases of adsorption. Therefore the zero values used in the current graphs don't indicate time point or data pointnd the start point of the graph was kept zero.

3.8 Results.

3.8.1 Binding of AMs to C3 on PS.

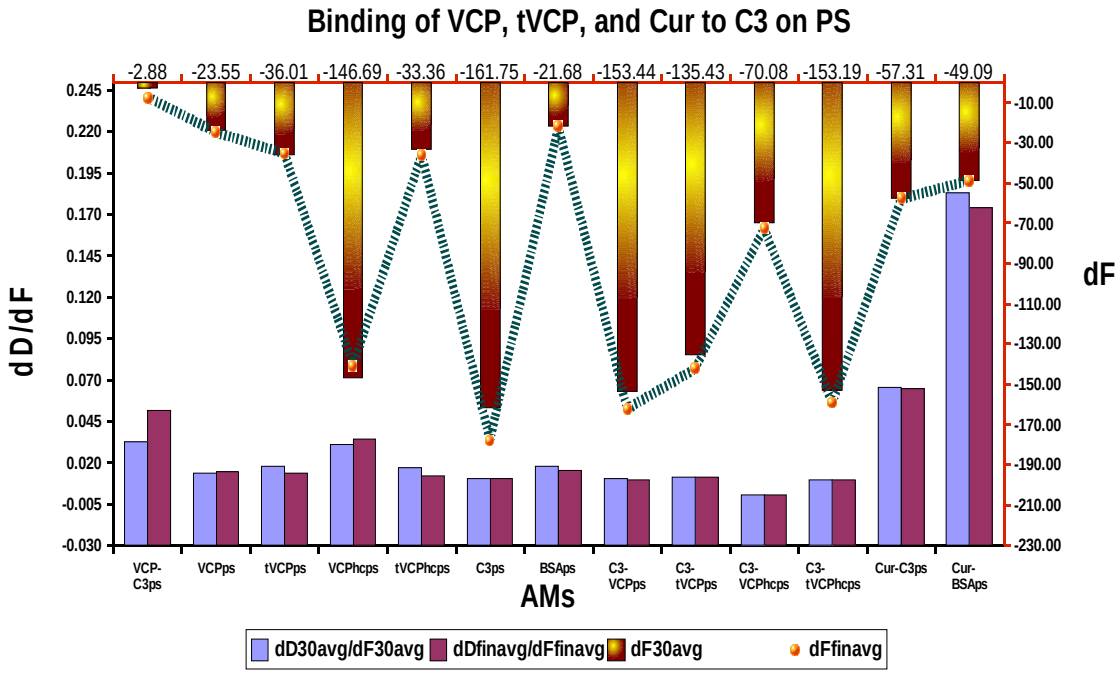

Figure 3.4. *dD/dF ratios (the primary X and Y axis) and dF values (the secondary Y axis and the secondary X axis shown in red) for binding of VCP, tVCP, Cur and C3 on PS. dD/dF ratios at 30 min interval are shown in blue whereas final dD/dF ratios are shown in red color. The dF_{30} values are shown by a gradient yellow-brown bar whereas the dF_{fin} values are shown by turquoise line with orange dots ( ). The dF and dD values shown indicate the average values obtained from the two experiments.*

Results: As shown in Fig 3.4 and the Table R3.1, Appendix R and, dD/dF ratio for the binding of VCP adsorbed on PS to C3 is very low (0.0005 after 30 minutes and 0.0002 after the final binding and washing with PBS) suggesting a very strong binding. As shown in Fig 3.4 (and Table R3.1, Appendix R), the order for dD/dF ratios for the different binding moieties is: C3 vs VCPps <<< C3 vs tVCPps < VCP vs C3ps < Cur vs C3ps < Cur vs BSAps. The ratio was the lowest for C3 vs VCP and it was the highest for Cur vs BSAps. dF_{30} and dF_{fin} were of the following order: C3 vs tVCP > C3 vs VCP > Cur vs C3ps > Cur vs BSAps. The dD/dF ratios for the adsorption on PS were of the following order: C3 > BSA > tVCP > VCP. The dF_{30} and dF_{fin} values were the highest for C3 and the lowest for BSA (C3 > VCP > tVCP > BSA).

3.8.2 Binding of AMs to C3 on gold surface.

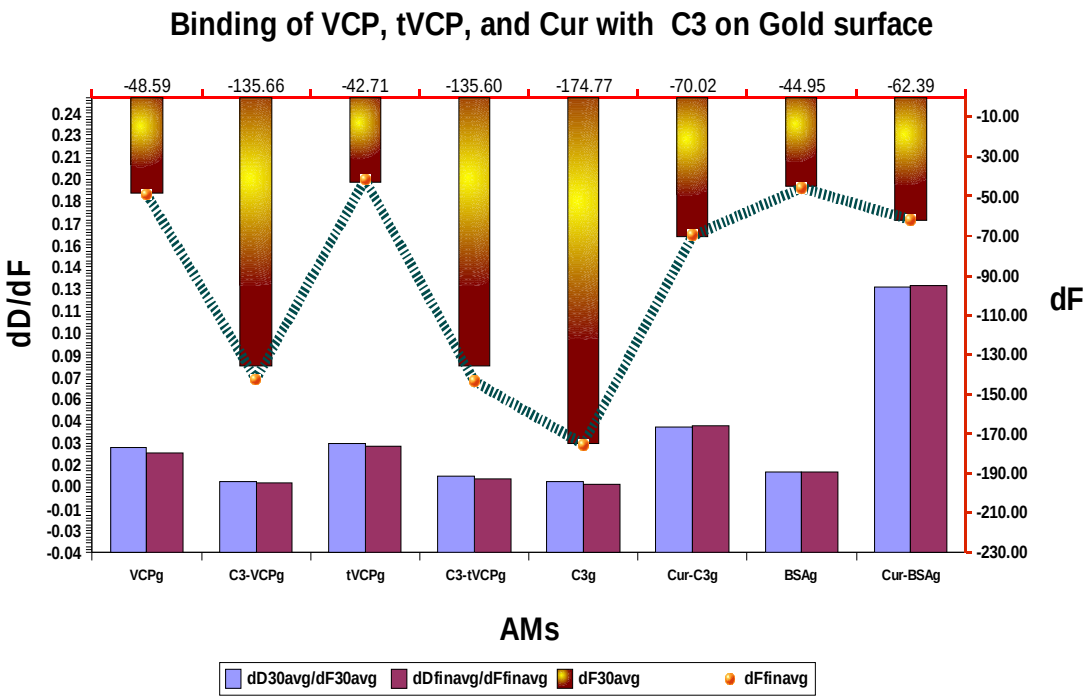

Figure 3.5. *dD/dF ratios (the primary X and Y axis) and dF values (the secondary Y axis and and secondary X axis shown in red) for binding of VCP, tVCP, Cur and C3b on PS are as shown in this figure. dD/dF ratios at 30 min interval are shown in blue whereas final dD/dF ratios are shown in red colour. The dF_{30} values are shown by gradient yellow-brown bars whereas the final dF values are shown by the turquoise line bearing orange dots ( ). The dD/dF ratios and dF values indicate average of the values obtained from the two experiments.*

Results (Fig 3.5 and Table R3.3, Appendix R).

dD/dF ratios were in the following order: C3b vs tVCP $\leq$ C3b vs VCP < Cur vs C3bps < Cur vs BSAps, and for the dF values the order was C3b vs VCPps > Cur vs BSAps > Cur vs C3bps. For the dD/dF values for the adsorption on PS, the order was C3bps < VCP < tVCP < BSA, and the dF values for the adsorption on PS were found to be C3b >> VCP > tVCP > BSA.

3.8.3 Binding of AMs to C3b on PS

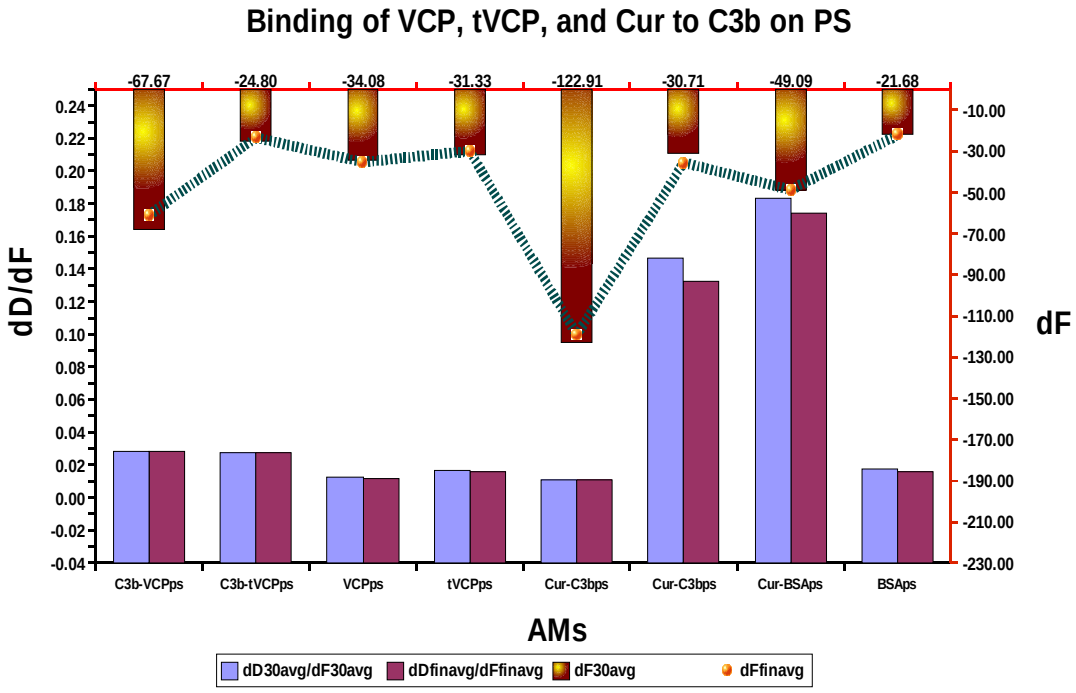

Figure 3.6: *dD/dF ratios (the primary X [bottom] and Y axis [black; left]) and dF values (the secondary Y axis shown in red and the secondary X axis is shown at the top) for the binding of VCP, tVCP, Cur and C3 on the gold surface are as shown in this figure. dD/dF ratios at 30 min interval are shown in blue whereas final dD/dF ratios are shown in red colour. The dF_{30} values are shown by a gradient yellow-brown bar whereas the final dF values are shown by the turquoise line with orange dots ( ). All the dD/dF ratios and dF values indicate average of the values obtained from two experiments.*

Results (Fig 3.6 and Table R 3.2, AppendixR)**:** The dD/dF values for the adsorbing moieties were found to be of the following order:

C3 vs VCPg < C3 vs tVCP < Cur vs C3g < Cur vs BSAg and the dF_{30} and dF_{final} values were found to be highest for C3 - VCPg and lowest for Cur vs BSAg (order: C3 vs VCPg > C3 vs tVCPg > Cur vs C3g > Cur vs BSAg. The order of affinity of AMs under investigation for C3 as indicated by their dD/dF values tested for the adsorption on gold surface was: tVCP > VCP > BSA > C3, and the dF the values were of the following order: C3>> VCP$\geq$ tVCP > BSA.

3.8.4 Binding of AMs to C3b on gold surface.

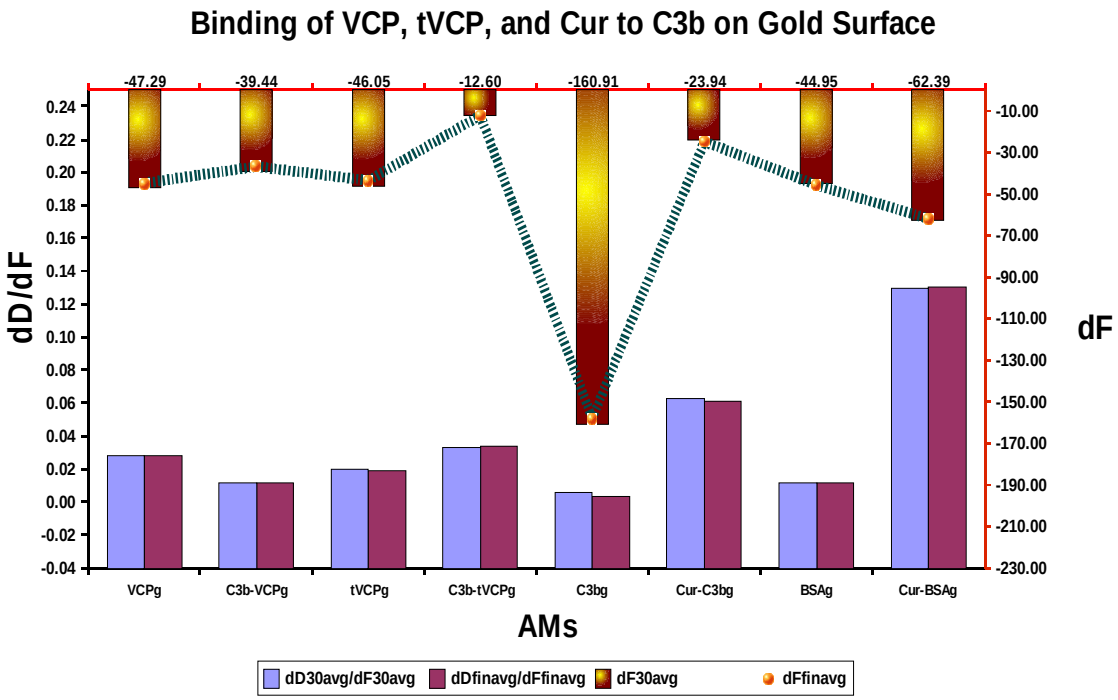

Figure 3.7: *dD/dF ratios (Primary X [bottom] and Y axis [black, left]) and dF values (secondary Y axis [Red; right] and the secondary X [top]) for binding of VCP, tVCP, Cur and C3b on gold surface are as shown in this figure. dD/dF ratios at 30 min interval are shown in blue whereas final dD/dF ratios are shown in red. The dF_{30} values are shown by gradient yellow-brown bars whereas the final dF values are shown by an turquoise line with orange dots (). dF values (dF30 = blue bars; dFfin = red bars) are shown on the primary X axis. dD/dF ratios and dF values indicate an average of the values obtained from two experiments.*

Results: The order of dD/dF values (Table R3.4, Appendix R and Fig 3.7) for the binding to C3b on the gold surface is VCP vs C3bg < tVCP vs C3b < Cur vs C3bg < Cur vs BSAg. As far as the dF value is concerned, Cur vs BSA > VCP vs C3b > VCP vs Cur > tVCP vs C3b. dF30 values for the adsorption on the gold surface are C3b >>> VCP $\geq$ tVCP $\geq$ BSA. dD/dF ratios for these AMs are C3b < BSA < tVCP < VCP.

3.8.5 Adsorption kinetics for the AMs on gold and PS surfaces.

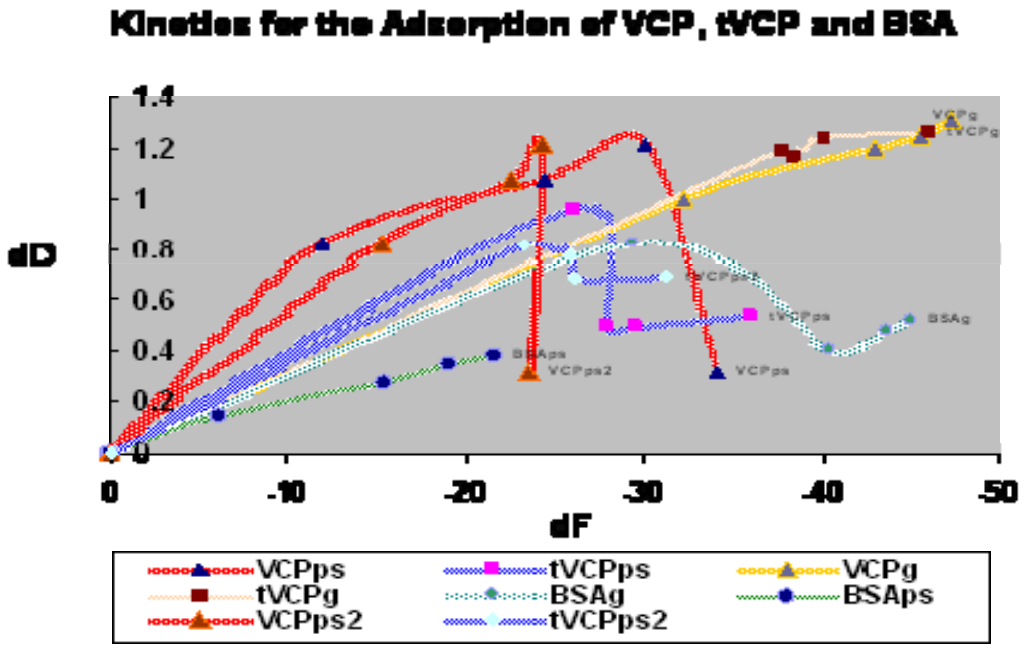

Figure 3.8. *dF values (X-axis) and dD values (Y-axis) of VCP, tVCP and Cur on g and PS at five different time points are plotted in this figure. The suffix "ps2" in the subscript of the AM indicates the values for the second set of experiment where the experiments were repeated.*

Results: As shown in Fig 3.8, the adsorption of VCP on PS is a two phase phenomenon as shown by similar graphs obtained for two different sets of experiments (each set = two experiments) shown as VCPps and VCPps2 series (red lines with brown and blue triangles, respectively). In the first phase, dD values increase almost linearly with the decrease in dF values up to -24 to -30 Hz, and at the adsorption maximum, a typical curve ("elephant head") is obtained after which there is a rapid decline in dD values with a slow decrease in dF values (VCPps) or almost steady (VCPps2) dF values. For tVCPps, the adsorption is a three phase phenomenon (tVCPps and tVCPps2 shown as dark blue lines with pink and blue squares). There is a steady rise in dD values with the decrease in dF values during the phase I of adsorption (up to 20- 25Hz), followed by a sudden drop and then again steady dD values with the decrease in dF values (from 25 Hz and onwards) which results in the formation of "Z shaped graph". For BSAps (green line with blue circles), the dD values increase linearly with the decline in dF values for all the data points suggesting that it is a single phase phenomenon. The dD values for VCPg and tVCPg increase linearly with the increase in dF values throughout the adsorption although towards the end of the experiment, there is a slight change in the rate of change of dD values per unit change in dF. For BSAg, the dD values increase linearly with a decrease in dF values up to -30 Hz (phase I). After this there is a steady decline in the dD values per unit change in dF values till 40 Hz (Phase II), and again there is a slow but steady rise in dD values per unit decline in dF values (Phase III).

3.8.6 Adsorption kinetics for VCPhc and tVCPhc adsorption on PS.

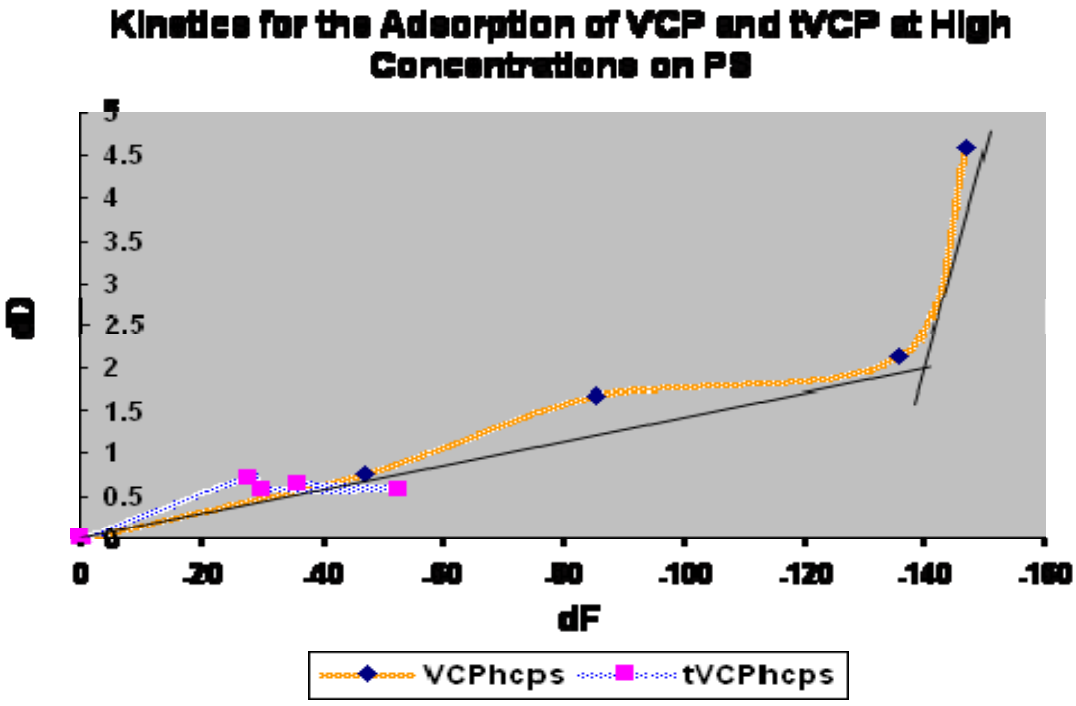

Figure 3.9. *dF values (X-axis) for VCPhcps and tVCPhcps at five different time points are plotted against dD values (Y-axis) at the same time points. The two adsorption phases for VCPhcps are shown by black lines.*

Results: VCPhc, which was 1.25 times more concentrated than VCP showed a different pattern of adsorption onto PS than that of VCP. dD values increased slowly and almost linearly up to -135 Hz (Phase I), after which there was a sharp increase in the dD values with the increase in dF values. dD_{15} / $dF_{15\ ratio}$ for VCPhcps was found to be 0.01570 and ($dD_{30} - dD_{15}$) / $dF_{30} - dF_{15}$) was found to be 0.21564 indicating that the latter was about 13.735 times higher than the former. This suggests that VCP has 14 times stronger affinity for PS than tVCP. Even after increasing the concentration of tVCP by about five times, there was not much difference in the dF30 values of tVCP. For tVCP, although adsorption was a three phase phenomenon, there was a difference in the pattern of adsorption graph shown by VCP and tVCP. During the first phase, increase in the dD values was linear with the decrease in dF values (upto -23Hz), after which dD values per unit change in dF values were almost unchanged up to - 55 Hz (Phase II). Although dD values were steady, thereafter there was an increase in the dF value which constituted the third phase for tVCP adsorption.

3.8.7 Adsorption kinetics for the interaction of AMs with C3 and C3b.

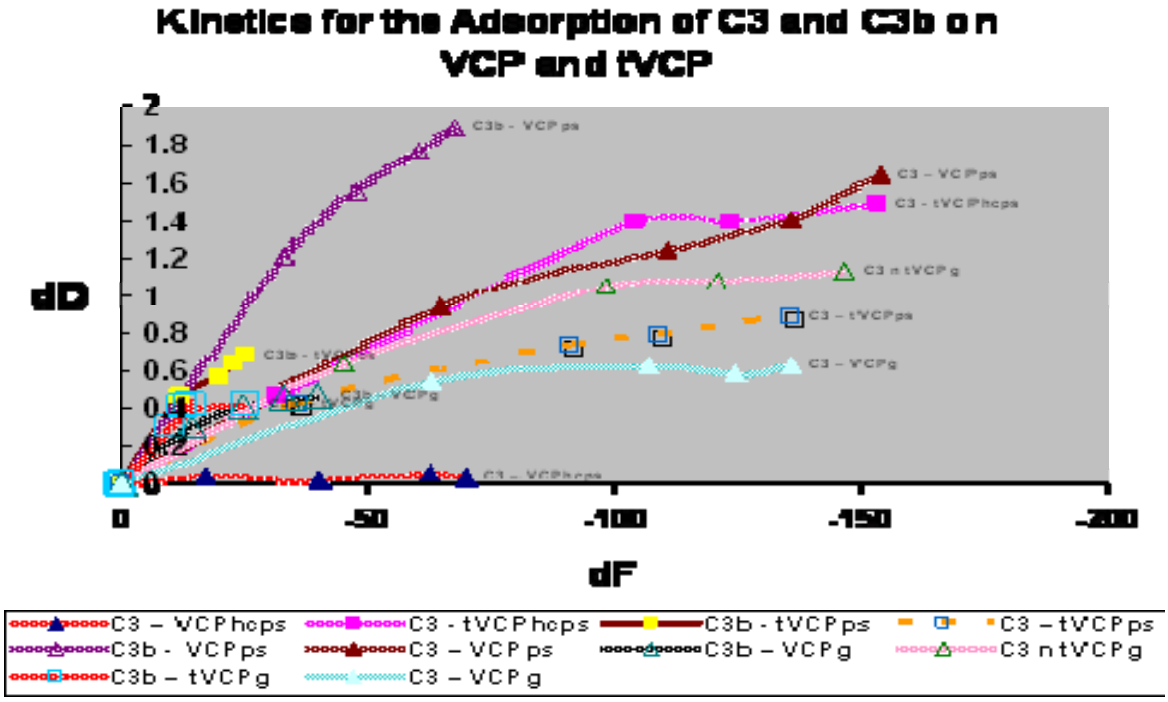

Figure 3.10. *dF values for the interaction of VCP and tVCP adsorbed either on g or ps with C3 and C3b (X-axis) were plotted against dD values (Y-axis) (Markers for data points: triangle = VC, and squares = tVCP). The data label for each series indicates AM (Series: C3-VCPhcps, C3-tVCPhcps, C3-tVCPps, C3-VCPg indicates adsroption of C3 on VCPhcps, tVCPhcps,tVCPps, and VCPg, whereas C3b-VCPps, C3b-VCP, C3b-tVCPps, C3b-tVCPg indicate adsorption of C3b on VCPps, VCPg, tVCPps and tVCPg. hc prior to ps in the case of VCP denote VCP at high concentration)*

Results: When VCP (AMII) was adsorbed on C3 bound to PS (AMI), it did not get adsorbed on C3 (see table 2, Sr. 6). Similar results were obtained when the attempts were made to adsorb on C3 and C3b bound to gold and PEG-COOH crystal surface (Ms. Philippa Randall, BSc Honours project (unpublished data). Therefore, in the current investigation, VCP and tVCP were first adsorbed on g or PS, and C3 and C3b were then adsorbed on them.

In almost all the experiments for the adsorption of C3 on gold, PS, VCP and tVCP, the dD vs Df graphs were linear during the initial stages of adsorption which constitute phase I of the adsorption. It is followed by the second phase where dD values changed only slightly with dF. The adsorption of C3 on VCPhcps however was a single phase phenomenon as shown by a linear graph. For VPhcps, throughout the adsorption, the dD values were close to zero and the dF values dropped up to -72 Hz in 30 min.

In most of the experiments with C3b, adsorption was a linear phenomenon as dD values show a steady rise per unit decline in dF values. The final dF30 values for the adsorption of C3b arebetween -25

Hz to -40 Hz for all the adsorptions with an exception of C3b-VCPps (above -60 Hz). Also, for the adsorption of C3b on VCP, there is a steady increase in dD values with the decrease in dF values till -40 Hz, however the rate of change of dD values per unit change in f dropped to a certain extent resulting in the second phase of adsorption. The decline during this second phase of C3b-VCPps adsorption was not as sharp as the decline during C3-VCPps adsorption. The graphic evidence shows that for most of the C3b adsorptions, the dD values per unit dF values are higher than that for the adsorption of C3.

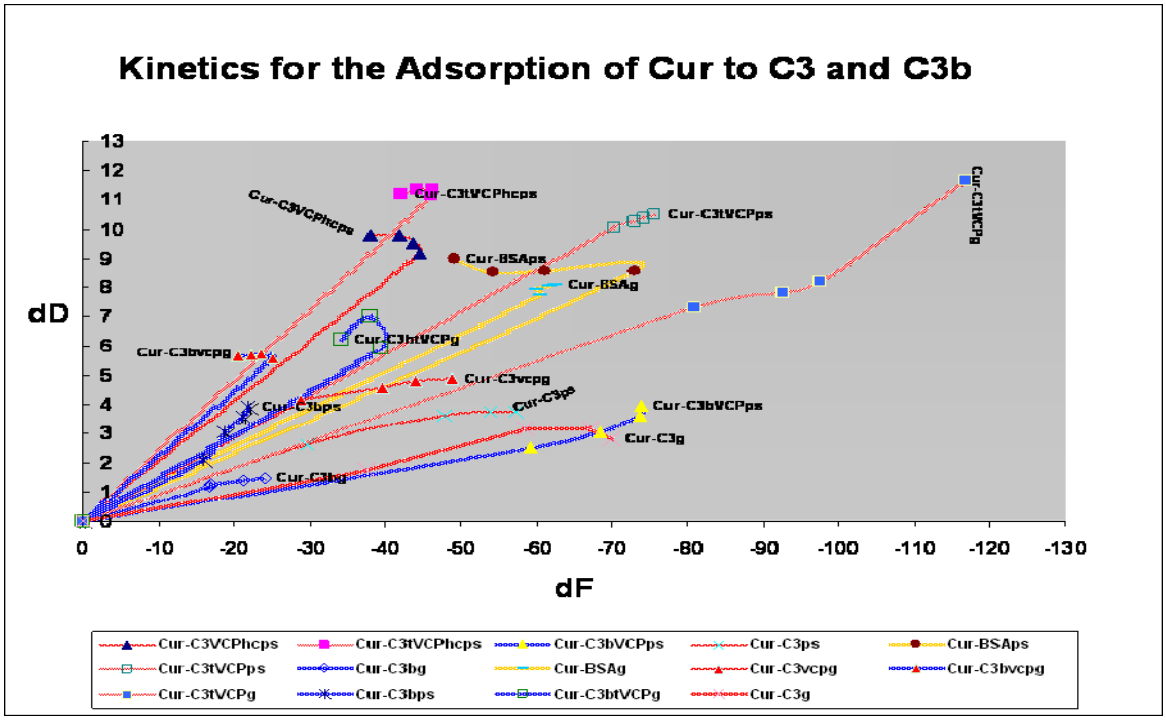

Figure 3.11. *dF values (X-axis) at five different data points for the adsorption of Cur on C3, C3b and BSA adsorbed on gold, PS and VCP or tVCP adsorbed on gold and PS are plotted against dD values (Y-axis) The data labels are used to show AMs. The suffix g or PS in the subscript of an AM indicates that the AM is adsorbed onto either gold or PS surface)*

Results: The adsorption of Cur on C3, C3b and BSA was either a single phase or two phase phenomenon. For Cur-C3g, Cur-C3bg Cur-C3ps, Cur-C3bps, Cur-BSAg, Cur-C3tVCPg, and Cur-C3tVCPhcps, the second phase started at -60 Hz, -20 Hz, -50 Hz ,– 15 Hz., -70 Hz, -90 Hz, and -30 Hz, respectively. Cur-C3VCPhcs, Cur-C3btVCPg , and cur-C3tVCPg also showed similar two phase adsorption, the second phase starting at -40 Hz (dD = Approx 9), -28 Hz (dD = Approx 5.7), and -40 Hz (dD = Approx 6 Hz), respectively. For Cur-C3VCPg, during the first phase of adsorption, there was a rise in dD values until the start of the second phase which started at about -28 Hz. After this, there was a decrease in dD values. The final dD values (about 4.87) were higher than that of Cur-C3g (about 2.82), but much lower than that of Cur-C3tVCPg (11.67). For Cur-C3tVCPps, the graph is linear showing only one phase of adsorption with a high dD value (10.5). For Cur-C3bVCPps, the adsorption is almost linear. The final dD values (3.95) were close to Cur-C3b (3.94) but a drop in dF values (-73.89) was much higher than that of Cur -C3b (-21.91).

3.8.8 Summary of Results.

Sr	Expmt	Results	Conclusion
1	Binding of VCP, tVCP and Cur to C3 on PS surface (Fig 3.4)	**dD/dF ratio** for VCP to C3ps = (0.0005 after 30 minutes and 0.0002 after PBS). **dD/dF ratios order (AMI):** C3 vs VCPps <<< C3 vs tVCPps < VCP vs C3ps < Cur vs C3ps < Cur vs BSAps. **dF30 and dFfin (AMII):** C3 vs tVCP > C3 vs VCP > Cur vs C3ps > Cur vs BSAps. **dD/dF ratios (AMI):** C3 > BSA > tVCP > VCP.	VCP binds very strongly to C3. Cur binds to C3 with higher affinity than that BSA. The binding of Cur to C3 on PS is less rigid than that of VCP and tVCP.
2	Binding of VCP, tVCP and Cur to C3b on PS surface (Fig 3.5)	**dD/dF ratios for AM II:** C3b vs tVCP ≤ C3b vs VCP < Cur vs C3bps < Cur vs BSAps **dF values for AM II:** C3b vs VCPps > Cur vs BSAps > Cur vs C3bps. **dD/dF values for AM I:** C3bps < VCP < tVCP < BSA, **dF values for AM I:** C3b >> VCP > tVCP > BSA.	tVCP and VCP bind to C3b with almost equal affinity, but the amount of VCP adsorbed is more than that of tVCP. Cur binds to C3b with a greater affinity than to BSA but the amount of Cur adsorbed onto BSA is more than that on C3b. VCP and tVCP bind more strongly to C3b than Cur.
3	Binding of VCP, tVCP and Cur to C3 on gold surface (Fig 3.6)	**The dD/dF values (AMII):** C3 vs VCPg < C3 vs tVCP < Cur vs C3g < Cur vs BSAg **dF values**: order: C3 vs VCPg > C3 vs tVCPg > Cur vs C3g > Cur vs BSAg. **dD/dF values (AMI):** tVCP > VCP > BSA > C3. **dF (AMI)**: C3>> VCP> tVCP > BSA.	The order of affinity of different compounds for C3g: VCP > tVCP > Cur > BSA.
4	Binding of VCP, tVCP and Cur to C3b on PS surface (Fig 3.7)	**dD/dF values (AMII):** VCP vs C3bg < tVCP vs C3b < Cur vs C3bg < Cur vs B SAg. **dF values (AMII):** Cur vs BSA > VCP vs C3b > VCP vs Cur > tVCP vs C3b. **dD/dF values (AMI):** for these moieties are C3b < BSA < tVCP < VCP. **dF values (AMI):** C3b >>> VCP ≥ tVCP ≥ BSA.	The binding of VCP to C3b is stronger than that of tVCP and Cur. Cur binds to C3b with more affinity than that of BSA. A greater amount of VCP adsorbs on PS than that of tVCP, but the rigidity of binding is nearly the same for them but greater than that of BSA.
5	Adsorption kinetics of VCP, tVCP, and BSA on gold surface (Fig 3.8)	VCP on PS is a two phase phenomenon., a typical curve "elephant head" is obtained at adsorption maximum with steady dF values and sudden drop in dD. For tVCPps, the adsorption is a three phase phenomenon with "Z shaped graph". For BSAps, it is a single phase phenomenon.	Drop in dD values during the second phase of VCP addition suggests change in conformation favouring strong adsorption by VCP. Similarly for tVCP, the binding is less strong than that of VCP as drop in dD values was not as sharp as VCP.
6	Adsorption kinetics of VCPhc and tVCPhc on PS (Fig 3.9)	The adsorption of VCP on PS is a two phase, concentration dependent phenomenon. tVCP, reaches saturation maximum earlier than that of VCP, and does not further add to the surface.	VCP shows more affinity to the PS than that of tVCP at higher concentration.
7	Adsorption kinetics of C3 and C3b on VCP and tVCP on gold and PS (Fig 3.10)	tVCP and VCP do not adsorb onto C3 deposited on gold or PS, but C3 binds to VCP and tVCP bound to the gold or PS surfaces. VCP binds very strongly to C3. Both VCP and tVCP showed more affinity to C3 than that of C3b. A greater amount of C3b is adsorbed onto VCP than onto tVCP. All the adsorptions were two phase phenomenon with a short second phase at the end suggesting changes in the conformation during this phase. For VCP, it was almost linear.	VCP binds more strongly to C3 than to C3b. Both VCP and tVCP show more affinity to C3 than to C3b. Adsorptions are a two phase phenomenon except for adsorption of C3 on VCPhc. VCP binds to C3 very strongly.
8	Adsorption kinetics for the adsorption of Cur on C3 and C3b bound to different surfaces and adsorbed onto VCP and tVCP. (Fig 3.11)	Cur adsorbs onto C3 and C3b bound to the gold, PS as well as on tVCP, VCP and BSA adsorbed onto gold and PS with a varying affinity. dD/dF ratios were the highest for C3 and C3b adsorbed onto tVCP, and lowest when they were adsorbed directly on the surface, but the values were intermediate for VCP	Cur and tVCP probably share common adsorbing sites. VCP shares some binding sites with Cur for C3 to a lesser degree, but to an even lesser degree to C3b. VCP + Cur could possible be mixed for regulation of the activated complement pathways.

3.9 Discussion.

QCM studies correlate dF values with that of the mass of moiety adsorbed based on the Sauerbrey relation as discussed in the principle of QCM. The adsorption of a protein layer on the crystal surfaces may violate the Sauerbrey relationship (Thompson et al 1986, Ward and Buttry 1990). The mass adsorbed cannot be estimated using the dF values in those cases (Höök et al. 2004T, Caruso et al. 1997). However, the frequency shift can be reliably interpreted using another factor called dissipation or D factor (Höök et al. 1998a). Therefore in QCM-D, in addition to dF values, the most important factor that can be studied using Q-sense is the dissipation factor which provides information regarding the rigidity of protein binding. dD/dF ratios have been used previously to investigate the rigidity of protein binding (Höök et al 2004, Höök et al 1998a, Höök et al. 1998b). These studies show that the lower the ratio, the stronger the binding. The dD/dF ratios for the adsorption of VCP on C3ps in the current investigation were found to be very low; consequently a very strong binding of VCP with that of C3ps is indicated. Using SPR, it is established that VCP inhibits the complement system through its ability to bind C3b (Smith et al. 2003). The current findings have added a new dimension to the mode of action of VCP. VCP and tVCP were used at two concentrations in the current study. At lower concentration (2 nm), the amount of VCP adsorbed on C3 was about 670 ng/cm^2 with dD /dFfin ratio corresponding to about 0.0099, whereas the amount of C3 adsorbed on tVCP was about 587.46 ng/ cm^2 with dD/dF ratio of 0.0110 suggesting that VCP binds more strongly to C3 than that of tVCP. When the concentration of VCP was increased by 1.25 times (VCPhc), the amount of VCPhc adsorbed on PS was significantly higher than that of VCP at a low concentration. (Series 4, Table R3.1, Appendix R and Fig 3.9).

When the binding of VCP and tVCP to C3 was compared on the PS surface, dD/dF values for C3-VCPps were less by as much as twice than that of tVCP. However, the number of molecules of C3 binding to VCP and tVCP and the amount of C3 adsorbed on them were found to be the nearly the same (Table R3.1, Appendix R).

The dD/dF ratios for the adsorption of Cur on C3 were greater than that of VCP and tVCP, but about 2.8 times smaller than that of Cur-BSAps (Table R3.1 of Appendix R, Fig 3.7). Similar results were observed on the gold surface (Table R3.3 of Appendix R, Fig 3.5). dD / dF_{30} ratio for Cur-C3g binding was three times less than that of Cur-BSAg. Cur showed greater affinity for C3g than that of C3ps. However, a greater amount of Cur was adsorbed on C3g than that of C3ps. Also, on both gold and PS, the amount of Cur adsorbed on C3 was more than that on BSA. Previous studies have shown that BSA binds to Cur, and therefore this combination was included as a positive control in the current study. The dD/dF ratios were more for Cur-BSA that that of Cur-C3, an also the amount of Cur adsorbed onto C3 was more than that onto BSA. Therefore, it is concluded that Cur shows binding to C3 in the current investigation.

The dD/dF ratios for VCPps-C3b and tVCPps - C3b did not differ significantly from each other (Fig 3.6, Table R3.2, Appendix R). This suggested that both VCPps and tVCPps have an equal affinity for C3b at the concentration used in the study. Previous studies using SPR revealed that tVCP does not

bind to C3b (Smith et al. 2003). This could be attributed to the difference in the concentration used by them, and variation in their methodology. They used amine coupling, as opposed to the adsorption onto PS. The dd/dF ratios for C3b-VCPps and C3b-tVCPps were significantly higher than that of C3-VCPps and C3-tVCPps (Table R3.2, Fig 3.6). This suggested that both VCP and tVCP show greater affinity for C3 than that of C3b on PS. On the gold surface, the amount of C3 adsorbed onto VCPg is three times more C3 than that for tVCPg (Table R3.3, Appendix R and Fig 3.5).

The dD/dF ratio for C3b-VCPg was found to be approximately 2.8 times less than that of C3b-tVCPg, and the amount adsorbed in ng / cm^2 was found to be about three times more for C3b-VCPg than that for C3b-tVCPg. These results on the gold and PS surfaces suggested that VCP binds to C3b to a greater extent than that of tVCP. These results, as opposed to the study on PS, compare with the findings by Smith et al. (2003) where they have shown binding of VCP to C3b using SPR. The dD/dF ratios for the adsorption of C3b onto VCP and tVCP bound to gold and PS surfaces were found to be more than that for C3 on both the surfaces. This suggests that both VCP and tVCP bind to C3 more strongly than that of C3b. VCP binds to C3 and C3b to a greater extent than that of tVCP. These data support the findings, where VCP has been shown to inhibit the complement system in a haemolysis assay to a greater extent than that of tVCP (Chapter 2).

When cur was tested for its ability to bind to C3bps, dD/dF ratios for Cur-C3bps was found to be less than that for Cur-BSAps, which suggested stronger binding of Cur to C3bps. However, dF values as well as the amount of Cur adsorbed onto C3bps was less than that of BSAps (Table R3.2, Fig 3.6). The results were similar for the adsorption of Cur on C3bg and BSAg, where the dD/dF ratio was found to be less for Cur-C3bg and the amount in ng/cm^2 of Cur adsorbed on C3bg was less than that on BSAg (Fig 3.7, Table R3.4, Appendix R). The results indicate that Cur binds to C3b with more affinity, but the binding is weaker than that of Cur-C3. These findings suggest that the inhibition of the CP and AP shown by Cur in the Chapter 2 using the haemolysis assay and the Quidel kit could therefore be attributed to the ability of Cur to bind to both C3 and C3b, but it binds to C3 with more affinity than to C3b.

The current study has also revealed important information regarding the nature of binding of VCP, tVCP, C3, C3b and BSA to the gold and PS surface as reflected by dF values, and dD/dF ratios in Figs 3.4 to 3.7. The lower dD/dF ratios of both VCP and tVCP for the adsorption on PS compared to the adsorption on gold suggest their greater affinity for PS than for the gold surface, whereas C3, C3b, and BSA all showed greater affinity for the gold surface. C3 and C3b add to a different extent on the gold and PS surfaces, the former being adsorbed to a greater extent than the latter, however with nearly the same dD/dF ratios. The observed variation in the extent of adsorption could be attributed to the structural differences between them.

The amount of BSA adsorbed onto the gold surface is twice the amount adsorbed on PS. The amount of VCP and tVCP adsorbed onto the gold surface is 1.5 times more than onto PS, but with the subsequent increase in dD/dF ratio, it suggests a weaker binding by them to the gold surface than to the PS surface.

In previous studies (Höök et al. 1998a and Höök et al.1998b), dD and dF values at different time points were be plotted on a X-Y scatter plot to give an information regarding the binding kinetics of the adsorbing moieties. These X-Y scatter plots gave information regarding the phases of adsorption, which in turn provides insight into the nature of adsorption, molecular arrangement or change in conformation during adsorption which might have an impact on the adsorption of the second AM. Therefore, in the current investigation, dD vs dF graphs were plotted to get an information regarding binding kinetics of the adsorbing moieties. As shown in the Fig 3.8, VCPps shows a peculiar graph with a sharp decline in dD values during the second phase of adsorption suggesting the change in confirmation of VCPps during the second phase of adsorption. tVCPps also shows three phases of adsorption suggesting some molecular rearrangement. However, both VCPg and tVCPg add almost linearly on the surface. BSAps showed a single phase adsorption, with low final dF_{30} values suggesting adsorption to a limited extent on PS. BSAg adsorbs in three phases showing some change in conformation during the second and third phases of adsorption.

VCPhcps shows adsorption kinetics and the pattern of adsorption different from that of VCPps, suggesting that the kinetics of VCP adsorption changes during the course of adsorption, and thus this is dependent upon the concentration of VCP (Fig 3.9). This might be due the ability of VCP to form a dimer as shown by the others (Liszewski et al. 2006). During the second phase of adsorption of VCP, the dD values increase sharply indicating loose binding or bilayer formation on the already adsorbed VCP on PS at higher concentration.

As shown in Fig 3.9, tVCPhcps adsorbs in three phases, and during the third phase of adsorption, there is rapid increase in frequency with steady dD values suggesting the desorption of tVCP bound loosely to the PS surface. This finding also suggests that VCP can form a bilayer, but that tVCP cannot. The difference in the adsorption behaviour could be attributed to the lack of one module in tVCP.

The adsorption kinetics for the interaction of VCP and tVCP with that of C3 and C3b adsorbed onto the gold and PS surfaces is shown in Fig 3.10. Here, C3 adsorbs in two phases, with the exception of C3-VCPhcps. As discussed in the results section and shown in Fig 3.9, the kinetics of VCPhcps adsorption suggests a very strong binding of VCPps with that of C3. In all the cases for the adsorption of C3 on VCP and tVCP on both the surfaces, the dF values for the last data points are more than -140 Hz (except for VCPhcps), and that for the adsorption of C3b being less than -40 Hz, except for C3b-VCPps. The adsorption kinetics also suggests that dD values per unit change in dF values are quite high for the adsorption of C3b on both C3 and C3b.

The adsorption kinetics for the adsorption of C3 and C3b on VCP and tVCP suggest that both VCP and tVCP have better affinity for C3 than that of C3b. C3b shows better adsorption kinetics for VCP than that of tVCP. The lack of module one in tVCP as well as structural difference between C3 and C3b may be attributed to the differences in the adsorption kinetics of these AMs.

The adsorption kinetics for the adsorption of Cur on C3 and C3b adsorbed onto gold, PS, VCPps, VCPg, tVCPps, and tVCPg is shown in Fig 3.11. As shown in the results section as well as Fig

3.11, the dD values per unit change in dF values are very high for Cur-C3 and Cur-C3b adsorption compared to that of VCP and tVCP. When Cur was adsorbed onto C3 and C3b bound to VCP or tVCP, there was a sharp increase in dD values, and the values were on the higher side for Cur-C3tVCPps/g (or Cur-C3btVCPps/g) than that of Cur-C3VCPps/g (or Cur-C3bVCPps/g). For Cur-C3bVCPps the final dD values were same as that of Cur-C3bps with a greater decline in dF values. Similarly, the adsorption kinetics pattern and the final dD values for Cur-C3VCPg were quite close to Cur-C3g. This could be attributed to either an enhanced binding ability of Cur to C3 and C3b bound to VCP, or both VCP and Cur share different binding sites on C3 and C3b which might have resulted in the similar dD values in the respective cases. In the case of adsorption of Cur on C3 and C3b bound to tVCP, there was a sharp rise in dD values suggesting a very loose binding of Cur. This could be due to sharing of common binding sites by tVCP and Cur.

The mass of AMs adsorbed onto the other AM or onto the gold or PS surface in the QCM-D, could be used to estimate the number of molecules of the binding moieties interacting with each other. In the current investigation, using the Avogadro's formula, the number of molecules interacting with each other was estimated, and reported in the tables (R3.1 to R3.4) in the Appendix R. However, it should be noted that these estimated values are not accurate as the exact mass of water trapped within the AMs used in the study is unknown. Generally about 30 % of water is trapped within the proteins (Saenger 1987, Höök et al.1998a). Consequently, this 30 % value was deducted from the final mass of AMs adsorbed onto various surfaces and the other AMs obtained in the current studies. However, water trapped within Cur molecules as well as VCP, and tVCP is not known. Further research is required in this direction. Also in the case of Cur, dD values were very high in some of the experiments which violate the Sauerbrey law, and therefore the exact amount of these compounds interacting with each other could not be determined.

However, the dD/dF ratios and other information reported in this investigation certainly has implications in the development of complement based pharmacotherapeutic agents in the treatment of neuroinflammatory disorders. The binding of VCP and Cur to C3 and C3b found in the current investigation can be correlated with their complement inhibition in the previous chapter. VCP was found to be thousand times better than that of Cur in inhibiting the complement mediated haemolysis (Chapter 2), and this could be attributed to better ability of VCP to bind both to C3 and C3b than that of Cur as observed in the current investigation. tVCP, which inhibited the CP to a less extent in the Chapter 2, could be attributed to the fact that although it adsorbs onto C3 and C3b, the binding is variable, and it does not inhibit C3 as strongly as VCP. As discussed in the introduction, polystyrene activates C3, and VCP, tVCP and Cur were able to inhibit the same. These compounds inhibited C3 to abetter extent than that of C3b.

In conclusion, in the current study, QCM-D was successfully employed to obtain information regarding the interaction of VCP, tVCP, and Cur with C3 and C3b. VCP showed greater binding affinity for both the C3 and C3b than Cur and tVCP. The binding of VCP and tVCP to C3 and C3b was orientation dependent. In addition, it was shown that Cur binds to both C3 and C3b. However, all these

compounds show greater affinity for C3 than C3b. VCP and Cur probably share different binding sites and may possibly be combined. VCP is a thousand fold stronger inhibitor of complement than Cur, and is known to inhibit amyloid mediated complement activation (Daly and Kotwal 1998). Cur is a weak inhibitor of complement, but dissolves plaques (Yang et al. 2005). The current investigation suggests that both these compounds probably share different binding sites on C3 and C3b, and thus may not interfere with each others actions on the complement system. Due to their broad spectrum anti-inflammatory activities covering different aspects of inflammation, further research is recommended in the direction of developing a "synergestic cocktail" by mixing Cur and VCP to prevent the complement mediated neurodegeneration in amyloidopathies. Before making such an attempt, it would be necessary to a suitable mouse model of AD or amyloidopathies to test this assumption.

Chapter 4.

Distribution of Intracranially and Intranasally Administered VCP, and its Comparison with the Intranasally Administered tVCP and Curcumin.

4.1 Introduction.

The *in-vitro* investigation in the previous chapters using haemolysis assay, Quidel kit, and Q-sense revealed complement regulatory activities of VCP and Cur. VCP was found to be a thousand times more potent complement regulatory agent than Cur (Chapter 2). This strong ability of VCP to regulate the complement system, as well as the other biological actions of VCP created the possibility of a "potential wonder drug" in the prevention and treatment of many inflammatory disorders (Jha and Kotwal 2003). It was found to be effective in the prevention and treatment of neuroinflammatory disorders in a number of rodent models after being directly (intrathecally) administered into the brain (Hicks et al. 2002, Reynolds et al. 2003, Pillay et al. 2007). Neuroinflammatory roles of VCP are well studied, but the only reported study concerning tVCP is by Hicks et al (Hicks et al. 2002) on the effect of tVCP in TBI. Both VCP and tVCP were found to be equally effective in the treatment of TBI. However, in all these studies VCP (and tVCP in TBI) was administered directly into the brain. The direct administration into the brain is invasive, and not advisable in actual therapy. Consequently, it is necessary to optimise the delivery of VCP to the brain. Due to the large size of VCP, it was assumed that it might not be able to cross BBB. As discussed in the literature review, many proteins and peptide molecules have previously been delivered to the brain using the intranasal route of administration (Gozes 2001, Thorne and Fery 2001). As discussed in the literature review, NGF, a 20 kDa protein, when delivered intranasally, was found to improve cognitive performance in mice (Capsoni et al. 2002). HRP as well as colloidal gold, have previously been delivered to the CNS using this route of administration. VCP (28.8 kDa) is smaller than HRP (40 kDa) and some other proteins that have been delivered to the CNS via this route. It is therefore argued that on the basis of their size that VCP will reach the brain after delivered intranasal delivery.

Cur has previously been shown to cross BBB when administered systemically (Yang et al. 2005). Yang and colleagues have also shown that Cur reaches the brain when it was mixed with the mice food pellets. However, Cur used in the previous studies differs from the Cur used in the current investigation in so far as it was dissolved with the aid of ethanol or DMSO or was mixed with food (Yang et al. 2005). In the present investigation it was dissolved in PBS with the aid of NaOH. Once Cur is dissolved in aqueous solution such as PBS, it was thought that after systemic administration, its bioavailability in the brain would be very much less due to increased polarity of Cur in PBS than the Cur dissolved in organic solvents. It was therefore necessary to deliver Cur to the brain by using a route of administration previously has been used in the delivery of water soluble compounds to the CNS. The intranasal route is potentially the most suitable route and has previously been used to deliver small sized water soluble compounds.

Localization of VCP in different parts of the brain after direct administration (intrathecal) has so far been reported only by Hicks et al. **(**2002). Only one or two doses of VCP are found to be effective in treating neuroinflammatory disorders (Hicks et al. 2002, Pillay et al. 2005, Pillay et al. 2008). It is detectable after 8 h in the systemic circulation following i.p. administration in rodents (Jha et al 2003), but its retention time in the brain tissue or CSF has not been reported. After intranasal administration of

VCP, it was surmised to reach the brain in low concentration. It is not known whether VCP is stable or is metabolised by the metabolic machinery of the brain. There are no reported appropriate positive controls available to confirm its presence in the brain. Consequently, in this study it is important to investigate whether VCP is detectable in CSF several hours after inytrnasal administration. It is also considered necessary to investigate whether it is stable in the brain, and whether it can be retained for relatively long periods after being administered directly into brain. It is also considered necessary to develop positive controls for the immunohistochemical detection of VCP in the rat brain.

Consequently, since one of the main objectives of the thesis is to study the possible therapeutic efficacy of these compounds and their delivery to the brain by a less invasive route of administration in transgenic mouse models, these properties need to be explored. Before carrying out the experiments in mice which present a different set of technical problems, it was first necessary to study the distribution of these compounds in rats, which are also considered to be the best models (Jansson 2004T) due to their large size, and the relative ease of collection of CSF samples.

4.2 Objectives.

The objectives of the investigation are therefore as follows:

1) Administration of VCP directly into different parts of the brain such as lateral ventricle, hippocampus, and olfactory lobe.
2) Administration of VCP, tVCP, and Cur via the intranasal route.
3) Collection of CSF and the brain tissue from different treatment groups.
4) Optimising and development of an *in-vitro* method to detect Cur following intranasal administration.
5) Optimising a method of detecting VCP, and tVCP in CSF samples intranasal or direct delivery into the brain, and measuring the levels of these compounds using enzyme linked immunosorbent assay (ELISA).
6) Immunohistochemical analysis of the rat brains for the detection of VCP, and tVCP in the respective treatment groups.

4.3 Procedure for the Distribution study.

The procedures used for the distribution study are outlined in a schematic diagram (Fig 4.1) shown below. For the distribution study, rats were divided into different treatment groups described in the section below. Depending upon the treatment or control groups, saline, VCP, tVCP or Cur were administered to rats. VCP was administered directly either into the left lateral ventricle of the rats or into the hippocampus or olfactory lobes via a stereotaxic procedure. For the intranasal administration, the position of the rat's head was between 70 to 90 degrees to the heating pad on which the rat was laid on its back (Fig 4.1). After the administration of these complement regulatory molecules or saline to

different treatment groups, CSF samples collected were from the cisterna magna at different time intervals. At the end of the study, the rats were transcardially perfused, and their brains were subjected to immunohistochemical analysis. The CSF samples were frozen at -80^{O}C and later subjected either to ELISA (tVCP / VCP), or fluorimetry (Cur). Before optimising the ELISA protocol, a small volume of CSF from the VCP treated group was also subjected to SDS-PAGE, and western blot. In the case of Cur treated rats, their brains were frozen. A few rat brains acting as negative control were also processed similarly.

The Distribution Study.

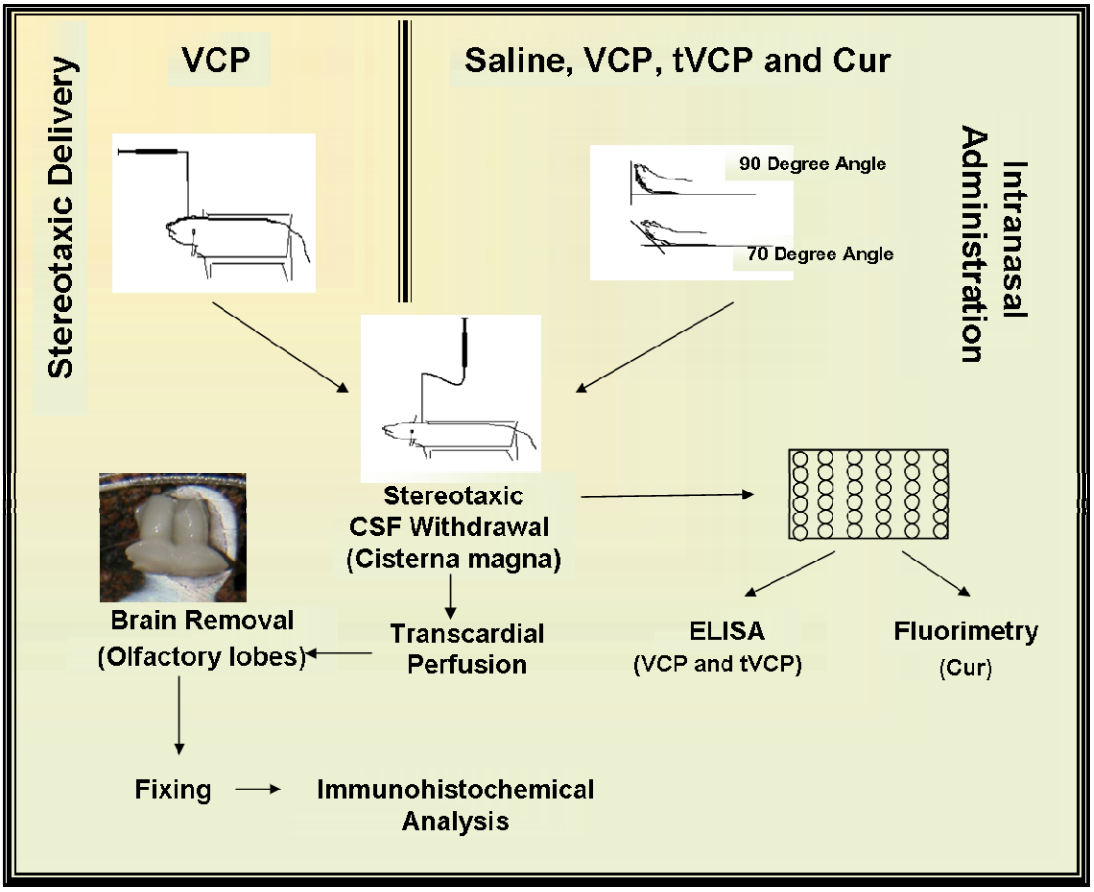

Figure 4.1. *Diagrammatic representation of a plan outlining the study of distribution of VCP, tVCP, and Cur in the rat brain and CSF. Intranasal administration using a head to surface angle between 70 to 90 degree with the rat supine. Direct administration of VCP to the rat brain using a Hamilton syringe connected to a thin tube and stereotaxic placement of the needle. CSF analysis using 96 well plate (ELISA for VCP and tVCP detection, and fluorimetry for Cur), and brain removal with special emphasis on the olfactory lobes for immunohistochemical analysis.*

4.4 Methods.

4.4.1 Grouping of rats: In order to study the distribution of VCP after intracranial and intranasal administration, rats were divided into five groups. To the first group, VCP was administered directly into the left lateral ventricle (4 rats), the olfactory lobe (one rat), and into the hippocampus (one rat). For the intranasal administration, the rats were divided into four different groups (n = 6), namely saline treated (SNT R), VCP treated (VCP R), tVCP treated (tVCP R) and Cur treated (Cur R). (Note: "R" in each group rats. Symbol is used to differentiate them from the transgenic mice treatment groups which will be described later).

4.4.2 Intranasal administration to different treatment groups.

Materials.

VCP, tVCP (expressed in *P pastoris*), and Cur (Sigma). 300 g Wistar rats, thermoregulatory heating pad, Terumo [Neolus] dental surgical needles (27G x 1/2" [0.4x13mm], Cliniscience Medical Distributors, SA; thin tubing (Technicon); stereotaxic apparatus, microscope (Carl Zeiss, Germany); The rat brain atlas (Paxinos and Watson 1982); ketamine hydrochloride [Anaket-V], and xylazine [Rompun 2%] (Centaur Labs, Business of Bayer (pvt) Ltd., Animal Health Division, Bayer, Germany); rats (Wistar male; 300g); Endotoxin free normal saline.

Method.

A group of six rats (approximately 300g) was selected for the study. The rats were anesthetised with approximately 300 µl (either i.m. or i.p.) of standard ketamine-xylazine mixture. 50 to 70 µl (140 to 210 µg) of VCP and / or tVCP was administered intranasally to each rat. 10 mg / ml Cur stock solution was freshly prepared as mentioned in the Appendix S. (Note: For the development of a method for detection of Cur in CSF, Cur was prepared either in EtOH or using PBS and NaOH. For simplification, Cur prepared using PBS and NAOH will be referred as CurNa or Cur and Cur solution prepared in EtOH will be referred as CurEt for this chapter. In the subsequent behavioural study, only Cur solution in PBS is used and therefore it will be referred as Cur). After being anaesthetized, the rat was laid on its back on a thermoregulatory pad with the head positioned 70 to 90 degree angle to the surface as shown in Fig 4.1. Using thin flexible gel loading pipette tips by Eppendorf, VCP, tVCP or CurNa was administered to the respective treatment groups (n=6). It was administered into both nostrils sequentially over a period of 20 min. After this the CSF samples were collected as described in the protocol for the collection of CSF samples (See 4.4.4).

4.4.3 Intracranial administration of VCP into the rat brain.

Materials.

50 µl Hamilton syringe (50 µl by Hamilton Co, Reno, Nevada, USA), syringe pump model 341 A (SAGE thermoregulatory instruments, Division of Orion Research Incorporation, Cambridge, MA, USA). Needles, anaesthetic and saline were the same as discussed above.

Method.

The rats were anaesthetised using standard ketamine xylazine mixture (See 4.4.2 for method). Once the rat was surgically anaesthetised and its head shaven, its head was fixed in the stereotaxic apparatus with the ear bars. Before fixing the rat's head in the stereotaxic apparatus, the position of the inter aural line (IAL) was marked. The dental needle was fixed into the stereotaxic apparatus and using thin tubing, its blunt end was connected to a Hamilton syringe fixed to a syringe pump. Normal saline was drawn into the syringe via the sharp needle tip. A small amount of air was drawn into the needle after this. VCP solution was then drawn into the syringe. Using the brain co-ordinates shown in Table 1 with reference to interaural line (IAL), 10 µl (25 µg) of VCP was administered into the left lateral ventricle of each rat. The minute bubble serves as a visual marker for the delivery of the VCP solution.

One of the aims of this investigation was to characterise the distribution pattern of intranasally delivered VCP into the rat brain. Previous studies have shown that some of the proteins e.g. cholera toxin protein adjuvant delivered intranasally are concentrated in the olfactory lobe of the rat brain (van Ginkel et al. 2000). In order to study the distribution pattern of intranasally delivered VCP, it was necessary to find out whether VCP directly administered into different parts of the brain localises and can be detected in that part of the brain. For this in one of the rats, VCP was directly administered into the hippocampus, and in the other rat it was administered directly into the olfactory lobe to observe the staining pattern in this part of the brain. The co-ordinates used for the administration of VCP into the rat brain are as indicated in the Table 4.1 below.

Stereotaxic coordinates for VCP administration.

Sr	Part of the brain	AP	ML	DV
1	Lateral Ventricle	7.7	1.6	3.1
2	Hippocampus	4.48	2.2	2.8
3	Olfactory lobe	13.7	1.6	3.1

Table 4.1. *Brain areas, and the stereotaxic coordinates (Anteroposterior [AP], Mediolateral [ML], and Dorsoventral [DV]) used for the direct administration of VCP via 27.5 G needle into various parts of the brain using IAL as a reference line (Sr represents serial number).*

4.4.4 The collection of CSF samples.

Many methods for the collection of CSF samples from the rat brain are discussed in the literature. Some researchers have cannulated the cisterna magna for the frequent sampling, whereas others have relied on the cisternal puncture (Frankman 1986, van den Berg et al. 2002). The drug level in the cisterna magna indicates its circulation in different parts within the ventricular system of the brain since CSF drains into the cisterna magna. Consequently, it was decided to collect CSF by cisternal puncture.

A simple method was developed to withdraw CSF. In the current investigation, instead of using the commonly used reference points such as bregma, lamda, or IAL, the dorsal posterior ridge of the cranium was used as a reference point after making a skin incision to target the cisterna magna stereotaxically. Immediately after the intracranial administration, with or without removing the rat fur, the upper ridge of the cranium was located with the help of the blunt end of the scalpel. The dental needle was positioned 1 to 1.2 mm posterior to this point, 0.8 to 1 mm mediolaterally, and inserted ventrally about 9 mm to13 mm or until it punctured the atlanto-occipital membrane above the cisterna magna, and CSF appeared into the needle. Initially the length of the needle required to reach to the cisterna magna varied from rat to rat, depending upon the degree of lowering of the incisor bar and therefore the altered head angulation. Lowering the incisor bar to an optimal degree helps better expose the atlanto-occipital membrane covering the cisterna magna facilitating withdrawal of CSF. There are numerous variations of the method of CSF withdrawal (Frankman 1986, van den Berg et al. 2002) depending upon the design of the experiment. The chronic cannulation of the cisterna magna is possible for the serial collection of the samples, but this may lead to breaking of the BBB (Frankman 1986 and van den Berg et al. 2002). As the rats were immediately killed after the collection of CSF, they were maintained on anaesthesia and the needle was allowed to remain in the same position while on the stereotaxic apparatus. With this method, it was possible to collect aliquots of CSF over a period of 5 to 6 h, and in a very few cases for longer than 6 hours. The amount of clear CSF withdrawn was between 40 to 50 µl. The simplicity of the method is an advantage and the method is useful when the rat can be anaesthetised to collect the serial CSF samples. If appropriate measures are not taken to immediately anaesthetise the animal before it recovers, it may disturb the position of the needle. This may result in the need to reposition the needle, and may also damage the membrane and possibly contaminate CSF. Therefore, constant monitoring of the rat and maintaining anaesthesia is required. Almost all (about 90%) the samples were clear and free from blood contamination. While collecting the last CSF samples, if there was any blood contamination, the sample was immediately spun at 3200 rpm for a minute or less, and clear supernatant removed. The collection of the CSF samples was stopped after the first appearance of blood. The CSF samples were collected for about 4 h after direct administration into the lateral ventricles and the olfactory lobe. The samples were later stored at -20^{O}C (or -80^{O}C for long term storage) for further analysis. The rat to which VCP was administered directly into the hippocampus, the first sample was contaminated with blood, it was thus discarded and no further samples were collected. In the case of intranasal administration of VCP, tVCP, and Cur, it was planned to collect CSF at 8

different intervals 30 min to 1 h apart. However, in most of the samples, a maximum of six samples were collected, and rarely were samples 7 and 8 collected. Therefore only samples at six different intervals from six different rats of the treatment groups were pooled for the analysis. For the Control groups, some of the samples were used as a control for Cur R group, and the remaining samples were used as control for the detection of VCP, and tVCP.

4.4.5 Development of methods to detect Cur in CSF samples.

In order to detect Cur in the CSF samples, it was first necessary to develop a sensitive technique for the detection of Cur. Therefore attempts were made to develop two different techniques based on two different principles. The first technique was based on the principle of colourimetry, and the second one was based on fluorimetry. The principles, methods and results of these two methods are as discussed below.

4.4.5.1 Development of a colourimetric method for the detection of Cur.

Principle: Cur has previously been used to detect boric acid in biological samples (Yoshida et al 1989a, Yoshida et al. 1989b). It was also used to detect boric acid content in shrimp (Ogawa 1979). The protocol by Yoshida et al. (1989a and 1989b) was based on the reaction of protonated Cur with boric acid to give a red coloured rosacyanin which was quantitated using colourimetry at 550 nm. Using the same principle, in this study, saturated solution of boric acid was used to detect Cur.

Method: 0.5 g of Boric acid was dissolved in 9 ml of deionised double distilled water. The undissolved boric acid was discarded, and the solution was then filtered through 0.22 μ filter. 10 mg / ml solution of Cur was prepared in 0.154 mM PBS and 0.5M NaOH just to dissolve it. The solution was prepared on ice and the tube in which Cur solution was prepared was covered with an aluminium foil in order to avoid degradation. 25 μl of various dilutions of Cur dissolved in the above manner was added to the 96 well plate in triplicate. To this 30 μl of glacial acetic acid and 10 μl of concentrated sulphuric acid was added and it was thoroughly mixed to give protonated Cur. 25 μl of boric acid prepared in the above manner was added to this mixture. It was thoroughly mixed and the mixture was kept on a shaker at room temperature (RT). After 30 min, 10 μl of EtOH was added, mixed properly, and the OD of the mixture at 550 nm was recorded (OD_{550}). The assay was repeated in triplicate and the average OD values (OD_{550avg}) were calculated at different concentration as shown in the following Fig 4.1 below (Table R4.1, Appendix R). (Note, in one or two cases, where OD values were outliers due to experimental error, the closest two OD values were averaged, and shown in the table R4.1 Appendix R and in the Fig 4.2).

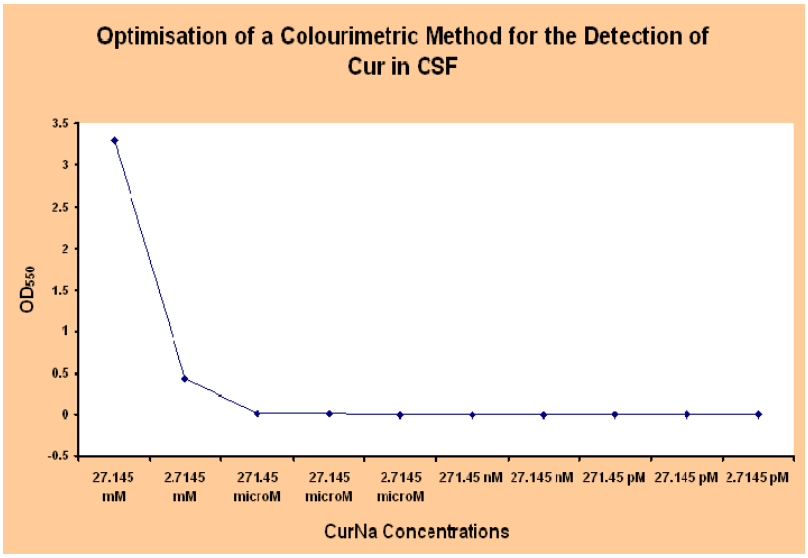

Figure 4.2. *The OD_{550} values (Y axis) indicating the formation of rosacyanin as a measure of different concentrations of CurNa (X axis).*

Results: There was a sudden drop in the OD_{550} values when the concentration was decreased from 27.145 mM (10 mg / ml) to 2.7145 mM (1mg/ml). The OD_{550} of Cur at 271.145 μM was found to be 0.00743, and at 2.7145 μM it is equivalent to or less than blank (Table R4.1 of Appendix R). Therefore, the assay was sensitive for the detection of Cur only in mM range.

4.4.5.2 Development of a fluorimetric method for the detection of Cur.

Principle and development of the assay.

Since the sensitivity of the colourimetric method for detection of Cur was only in mM concentration, and Cur was expected to reach the CSF at a very low concentration, it was necessary to be able to detect Cur at microgram to nanogram levels. For this, it was necessary to develop a more sensitive technique for the detection of Cur in the brain. There are several methods available for the detection of Cur in biological or other samples. Recently, Cur was detected and quantitated in mouse lung cancer cells at the level of 2.5 nM range by matrix assisted laser desorption ionization time of flight mass spectrometry (May et al. 2004). It was also detected in tumor and normal cells by a fluorimetric method at picomolar concentration (Kunwar et al. 2006). A new method to enhance the fluorescence of Cur by 33 fold was also developed recently (Wang et al. 2006). Using this method it was shown that fluorescence of Cur was not affected even in the presence of foreign substances such as cations, anions, fructose, glucose, and proteins (BSA and HAS), and thus this method was advocated for the detection of Cur in biological samples. This method was based on the formation of micelles of Cur in the solution using mixture of cationic and anionic surfactants, sodium dodecyl benzene sulfonate (SDBS) and cetyl trimethyl ammonium bromide (CTAB). The sensitivity of this method was also very high, but the SDBS and CTAB used by the investigators were not readily available in our laboratories. Using the principle that the ionic surfactants can be used to enhance the fluorescence spectra of Cur, it was decided to enhance the fluorescence of Cur using the commonly used surfactants available in most

molecular biology laboratory. While optimising the fluorescence enhancement in the aforementioned article, SDS was found to enhance the fluorescence to a lesser extent than that of SDBS. It was also shown that the anionic, cationic, and non-ionic surfactants used in their experiments enhanced the fluorescence, and their mixture had a synergistic effect. The commonly used surfactants which are readily available in most molecular biology laboratories are Tween-20 and SDS. Tween-20 was not used in the aforementioned protocol (Wang et al. 2006), and therefore it was necessary to detect whether it enhances the fluorescence of Cur.

In the same assay, it was also shown by Wang et al. that pH and solvent affect the fluorescence of Cur, and pH below 4 was recommended. The recommended solvent system was HOAc-NaOAc (acetic acid and sodium acetate). In their experiment, Cur was detected in aqueous solution prepared using DMSO. In our experiment, Cur was dissolved using NaOH and therefore it was thought that addition of acetic acid may result in the formation of NaOAc. Therefore, only HOAc was used in the current assay. The λmax_{exc} for cur used in the fluorimetric methods of Cur were around 420 nm.

Method.

Two assays were performed. The first one was performed to establish the concept and optimise the protocol. The second assay was performed for the detection of Cur in CSF.

Assay 1.

For this assay, Cur solutions of different dilutions [1:10 (b), 1:100 (c), 1:1000 (d), and1:10000 (e)] were prepared using 2.00 mg / ml of stock solution (a) of Cur by dissolving it either in ethanol (CurEt) or using PBS + NaOH dilution medium (CurNa) as mentioned in the colourimetric assay. The concentration of CurNa / CurET was randomly selected, and was close to 2 mg / ml. The stock solution was 2.667 mg / ml, and it was diluted to b, c, d and e. 30 µl of each of these dilutions were added in duplicates to the 96 wells plate. To this either 20 µl of SDS, Tween-20 (20% or 10%, freshly prepared in PBS [CurNaTw20]), Tween-20-GAA [i.e. mixture of Tween-20 and glacial acetic acid (10 µl each)], Tween-SDS-GAA [mixture of Tween-20 (10 µl), glacial acetic acid (5 µl), and 10% SDS (5 µl)] were added. To CurNa, 5 µl GAA, and 5 µl EtOH [CurNa-GAA-EtOH] were also added. The plate was covered with an aluminium foil, and placed on ice enclosed by a Styrofoam box which was kept on a shaker for 5-10 min for proper mixing of the solutions in the 96 well plate. Immediately after this, the fluorescence of Cur solutions was recorded at four different wavelengths. The excitation, and emission combinations tried were 420-484, 423-490, 425-495, and 426-492 using 10 nm slit of Cary Eclipse fluorimeter.

Results: Using the combination of wavelengths, the maximum fluorescence emission wavelength (λmax_{em}) was found to be at 495 nm when it was excited at 425 nm. In short, the combination 425-495 nm worked better than all the other combinations and only the data at this combination of excitation and emission wavelength is shown in the Figs R.3 A and B, and tables R4.2A and B of Appendix R.

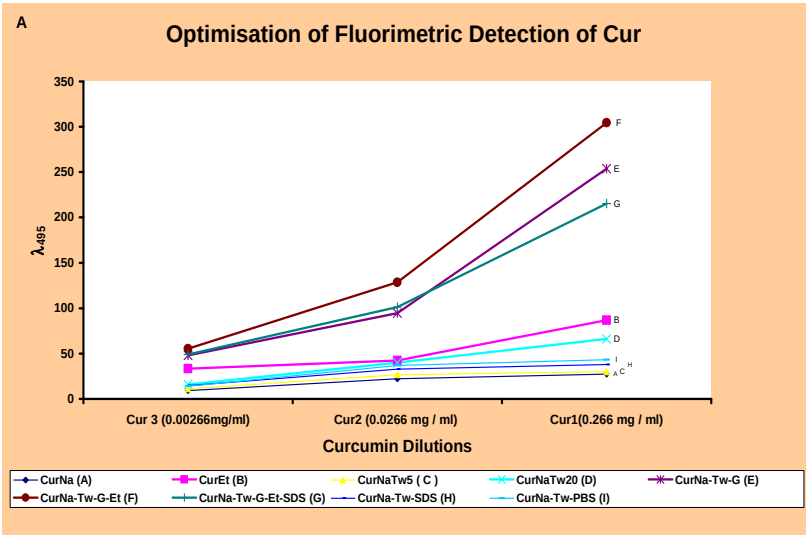

Figure 4.3. (A). *Optimisation of fluorescence enhancement by using combinations of different surfactants, ethanol, and GAA on three dilutions of CurNa (Series A to I = CurNa = Cur solution in PBS and NaOH; CurNaTw5 = CurNa + 5% Tween-20; CurNa-Tw-G = CurNa + Tween20 (20%) + GAA; CurNa-Tw-G-Et = CurNa + Tween20 (20%) + GAA + EtOH; CurNa-Tw-G-Et-SDS = CurNa + Tween20 (20%) + GAA + EtOH + SDS; CurNa-Tw-SDS = CurNa + Tween-20 + SDS; CurNa-Tw-PBS = CurNa + Tween-20 + PBS).*

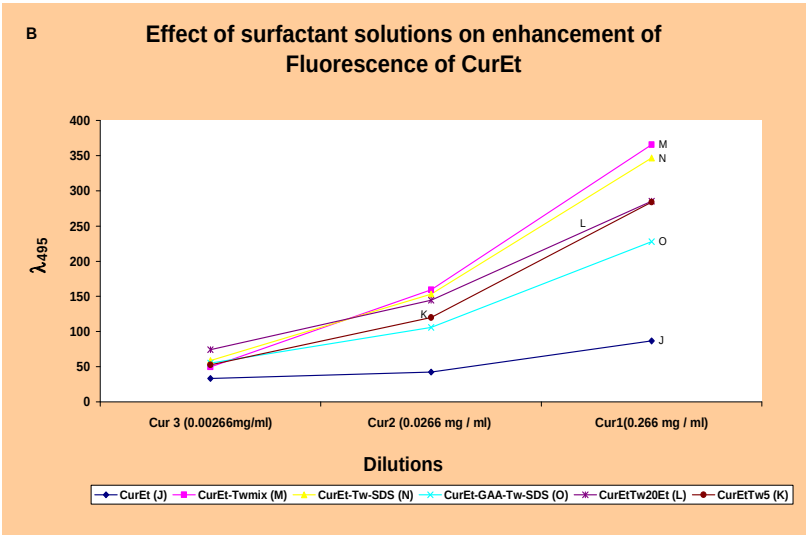

Figure 4.3. B. *The effect of surfactant solutions on the fluorescence of three different dilutions of CurEt (Cur prepared in absolute EtOH and diluted in 1% ethanol) (Series J to K = CurEt = Cur solution in EtOH; CurEt-Twmix = CurEt + Tween-20 (20%) + SDS; CurEt-GAA-Tw-SDS = CurEt + GAA + Tween-20 + SDS; CurEt-Tw20-Et = CurEt + Twee-20 + EtOH; CurEtTw5 = CurEt + Tween 20 (5%). The fluorescence emission values are shown on the Y-axis, and the Cur concentrations are shown on X-axis.*

Results: As shown in the Appendix R [table R4.2A, series (A) and (B)], and Fig 4.3B the fluorescence level of Cur in EtOH was higher than that of CurNa. The addition of Tween-20 (20%) [Series (D)], but not of Tween-20 (5%) [Series C)] Alone increased the fluorescence of Cur, and the fluorescence enhancement was more pronounced at higher concentration of Cur.

The addition of SDS to Tween-20 quenched the fluorescence enhanced by Tween-20 [series H]. When 20 µl of Tween-20 solution was made in GAA and EtOH (Tween-20 (20%): GAA: EtOH =

2:1:1), it enhanced the fluorescence to a greater extent (Fig 4.3B). When GAA was added to CurNA, it also enhanced the fluorescence in combination with Tween-20 and EtOH (Series E, F; Fig 4.3A). The addition of SDS to a mixture of Tween-20 and GAA enhanced the fluorescence only to some extent at lower concentration but there was quenching at higher concentrations (Series G; Fig 4.3A).

When the mixture of Tween-20 and SDS was added to CurEt, there was about 7 to 8 fold enhancement in the fluorescence (Series M and N; Fig 4.3B). SDS had a positive impact on the enhancement of fluorescence of CurEt by Tween-20. The addition of Tween-20 (20%) as well as Tween-20 (5%) also enhanced the fluorescence of CurEt (series K and L; Fig 4.3B).

Thus, from the Figs 4.3A and 4.3B as well as tables R4.2A and R4.2B, Appendix R, it was concluded that EtOH enhances the fluorescence of Cur. Tween-20 (20%) addition further enhances it. The addition of GAA to CurNa enhances its fluorescence. The addition of SDS enhances the fluorescence of CurNa at lower concentrations. (Series G; Fig 4.3A), but quenches at higher concentration. When mixed with Tween-20 (20%), it further enhances the fluorescence of CurEt. GAA and SDS should be used in optimum concentration, as their concentrations had a variable impact on the fluorescence of Cur. Based on the results of this assay, further modifications were required to optimize detection of CurNa in the CSF samples as will be explained below. GAA and SDS were used at a lower concentration for the detection of Cur in CSF.

4.4.5.3 Detection of Cur in CSF samples using fluorimetry.

CSF samples at each interval for the group of n = 6 rats were pooled, since individual volumes of CSF from a single rat at each sampling interval was not sufficient, to perform the assay. For the detection of Cur in CSF, the CSF samples from Cur R were pooled at six different time intervals (1, 2, 3, 4, 5, and 6) after the intranasal administration of CurNa. The first interval falls at approximately 1 h after the intranasal administration of Cur. For the control CSF samples, the CSF samples at three time points were used (1, 4 and 6), and the remaining CSF samples as well as samples at the other time intervals were used as control CSF (Ctrl CSF or CSFctrl) samples for the detection of VCP and tVCP in CSF. Three different concentrations of CurNa were used as a positive control. The detection limit tested for the fluorescence assay was found to be around 2.66 μg / ml (7.208 μM). Therefore, for the experimental assay, dilute solutions of Cur in the same range were used as positive controls. Briefly, 20 μl of 2 mg/ml stock solution of CurNa was diluted to 1 ml and 500 μl of this was diluted to 10 ml (Cur A = 5.556 μM), and the other 500 μl was diluted to 20 ml (Cur C = 2.778 μM). A and C were mixed (1:1) to give CurB (4.167 μM). 100 μl of each of these solutions was added to 96 well plate. 100 μl of PBS was used as a blank or negative control for Cur A, B and C. The volume of CSF from the pooled samples was 100 μl. To each of these wells, the following solutions were added:

1) 30 μl of EtOH 2) 10 μl of GAA 3) 50 μl of Tween-20 4) 10 μl of SDS. The order for the addition was from 1 to 4. There was no enhancement in fluorescence of Cur solutions used as positive controls as well as CSF samples used for testing. A possible explanation is that this level of Tween-20 was not optimum to form micelles of Cur. While developing the fluorescence assay, it was realised that EtOH

and Tween-20 act as fluorescence enhancers, so their proportions were increased, and a new fluorescence enhancer cocktail was prepared comprising of 2.5 ml of Tween-20 + 1 ml of EtOH, and 0.5 ml of GAA + 100 µl of SDS (Tween-20: EtOH:GAA:SDS = 25:10:5:1). 150 µl solution from each of wells of the 96 well plate was then transferred to a new 96 well plate kept on ice. 50 µl of this mixture was added to each well. The contents were mixed thoroughly by plate shaking the plate (kept on ice) for five min, and fluorescence was measured using different wavelengths. There was enhancement in the fluorescence at all the excitation wavelengths used from 420 to 425 nm as described in the previous section, but there was a shift in the λmax fluorescence values towards 484 nm in the Cur control samples. Therefore, although values at all the combinations of excitation and emission wavelengths were used initially for the analysis, only λ484 (emission wavelength) was considered for the results. The 50 µl of the mixture was also added to 150 µl of PBS used in the previous experiments, and these values were used as a blank. The negative controls as well as dilutions of Cur used in the current experiments were used in duplicate. Their λ484 values were later averaged to get the mean blank values. The mean blank values were subtracted from the mean fluorescence values for the positive and negative controls used in the experiments as well as the three CSF controls and six test samples to give corrected fluorescence values (CFV).

The three control CSF samples collected at different time intervals, without Cur showed some background fluorescence. In order to get the true fluorescence values (TFV) of CSF collected at different time points, the control CSF values were averaged to give average background fluorescence values (BFV), which was later deducted from CFVs of the CSF samples collected at different time interval. CFVs, BFVs, and TFVs were calculated at different combinations of excitation and emission wavelengths shown in table 4.2B below. The Cur dilutions were used with and without addition of the fluorescence enhancing mixture. The average fluorescence values of Cur dilutions without the addition of the mixture were subtracted from the average values obtained after the addition of the mixture to get the enhancement in the fluorescence of Cur by mixture (EFCur) at that particular dilution for a particular combination of wavelengths. These values (shown in Table 4.2A) were used to calculate the range of Cur concentrations in CSF samples tested, and are shown in the table 4.2 B below.

The degree of fluorescence enhancement in Cur solutions at different dilutions.

Sr	Concentration	EFCur 484	EFCur 490	EFCur 492	EFCur 495
Cur A	8.556 µg/ml	39.6966	40.679	28.6826	19.568
Cur B	4.167 µg/ml	35.1366	36.1276	17.132	16.6926
Cur C	2.778 µg/ml	7.329	6.209	10.336	1.343

Table 4.2A. *The dilutions of Cur (Cur A, B, and C) used in the experiment, and their EFcur values at the emission wavelengths 484, 490, 492, and 495.*

Detection of Cur in CSF by fluorimetry at emission wavelength 484 nm.

Sr	Samples	CFV484	BFV484	TFV484	Estimated Concentration Range (µg/ml) at 484 nm
1A	CSF Cur1	39.66166667	0.176833333	39.48483333	≤ 5.556
2A	CSF Cur2	7.325666667	0.176833333	7.148833333	≤ 2.778
3A	CSF Cur3	12.87966667	0.176833333	12.70283333	Between 2.778 and 4.167
4A	CSF Cur4	45.64066667	0.176833333	45.46383333	> 5.556
5A	CSF Cur5	2.888666667	0.176833333	2.711833333	<2.778
6A	CSF Cur6	28.47266667	0.176833333	28.29583333	Between 4.167 and 2.778

Table 4.2B. *Estimation of range of concentration of Cur in CSF samples (CFV, BFV, TFV at emission wavelength 484 are shown in columns 3, 4, and 5, respectively. Where: Sr represents serial numbers. The results at the other wavelengths are summarised in Appendix R (Table R4.3(B-D).*

Results: As shown in the table 4.2A, after the addition of the mixture of Tween-20, GAA, EtOH, and SDS, there was enhancement in the emission of wavelengths with the increase in the concentration of Cur at all the wavelengths. Therefore, from now onwards, this mixture will be referred to as a fluorescence enhancing mixture (FEMix) for simplification. The fluorescence emission maximum (Fem) was observed between 484 to 490 nm as compared to 495 nm in the case of the Cur dilutions used for the optimisation of the assay indicating a blue shift. A similar pattern was observed in the Fem of the CSF samples which were collected from Cur treated rats after the addition of FEMix. The order for BFV was BFV484 < BFV 492 < BFV495 < BFV490 indicating that the highest background or endogenous fluorescence levels in the control CSF samples is at 490 nm, and the lowest background fluorescence values at 484 nm. The pattern of Cur concentration in CSF in rats treated by intranasal administration of CurNa was similar at all the emission wavelengths used, although there was a variation in the concentration range at different wavelengths. The concentration was high at the first, fourth and sixth intervals (Table 4.2B).

4.4.6 Detection of VCP and tVCP in CSF using ELISA.

4.4.6.1 Optimisation of an ELISA method.

For the detection of VCP and tVCP in the cerebrospinal fluid, it was necessary to optimise the ELISA protocol. The aims were;

1) To determine the sensitivity of the technique.
2) To optimise the dilutions of primary and secondary antibodies used in the study and to check their binding with both VCP and tVCP.
3) To check the antibodies for cross reactivity against the CSF samples.
4) To increase the specificity with reduced background staining.

With these aims in mind, the following protocol was designed.

1) Preparation of solutions and reagents: 1 mg / ml (1μg/μl) solution of VCP and tVCP were prepared. These solutions were diluted to obtain 1, 0.1, 0.2, 0.5, 0.01, 0.02, 0.05 and 0.005 ng./μl, concentrations of VCP and 0.5, 0.05 and 0.005 ng./μl concentration of tVCP. The dilutions were made in 154 nM of autoclaved PBS (pH=7.2). Each plate was coated with 100 μl of each solution. To check the cross reactivity of the primary antibodies with the control CSF samples, 3 different CSF samples (100 μl each) were added to three different wells. The solution was kept at 4^{O}C for overnight incubation with agitation.

2) After overnight incubation (16 h), the coating solution was discarded, and any drops were removed by patting the plates on the filter paper. The wells were then washed 3 times with wash buffer (0.1 % Tween-20). The wells were cleaned, and again, the drops were treated with blocking buffer. As Tween-20 (0.5 %) with incubation for about 1 h was not able to reduce the background or non specific binding, 0.5 % BSA in 0.1 % Tween-20 was used as a binding buffer, and the plates were incubated for one and half hour with the binding buffer. 1% Tween-20 was found to reduce the sensitivity whereas 0.1 and 0.01 were found to increase the sensitivity as shown in a previous study (Halim et al. 2005). Therefore 0.1% concentration was used for dilution of BSA and for washing the wells, 0.1 % Tween-20 was used (3 X washes). After removing drops of the wash solution by gentle tapping on the filter paper, the plate wells were incubated with the primary antibodies [Rabbit-anti-VCP (R-Ig) and Chicken-anti-VCP (Ch-Ig)] at three different concentrations (1: 1000, 1: 2000, and 1:4000 in PBS with 0.1 % Tween-20) for about 4 h at RT. To one well at each of the above mentioned concentrations, no primary antibodies were added to check the cross reactivity of the secondary antibodies with VCP and tVCP. The wells were then washed with wash buffer and the secondary antibodies were added (1:10000) and incubated for about 2 h at room temperature. 100 μl TMB mix (TMB substrate and the substrate diluents mixed in 1:1 proportion just before addition) was added to each well. It was allowed to develop a blue colour for about 15-20 min, and 100 μl of 1 M phosphoric acid was added to the solution and it was mixed. The yellow coloured product (200 μl) was transferred to another 96 well plate, and the optical density was measured at 450 nm (OD_{450}).

4.4.6.1.1 Endogenous peroxidase activity and inhibition by VCP and tVCP.

The samples which were used for the ELISA assay were not discarded, but transferred to a 96 well plate and stored at -20^{O}C for further analysis. These samples were subjected to a peroxidase assay for measuring the inherent peroxidase activity of these samples. For this, 100 μl of TMB peroxidase substrate mix was added to 25 μl of VCPCSFin, tVCPCSFin, and VCPCSFdir at each interval. Alternatively, the remaining CSF samples at each time interval form each rat were mixed and, the CSF samples mixed in such a manner were further pooled from three different rats (R1 = rat 1 + rat 2 + rat 3; R2 = rat 4 + rat 5 + rat 6) to give two different sets of CSF samples for the estimation of VCP level in the individual rats. These samples were also analysed for the endogenous peroxidase activity. At the

same time, 20 µl of Ctrl CSF were added in triplicate to another ELISA plate. 5 µl of PBS, VCP (0.5 ng / µl), and tVCP (0.5 ng / µl) were added to the first, second, and third well of each of the time intervals as well as to R1 and R2. The plate was incubated at 30^{O}C for 30 min. After this, TMB peroxidase substrate (100 µl) was added to each well of the above two ELISA plates. After 10-15 min, the reaction was stopped using 75 µl of phosphoric acid, and the OD was recorded at 450 nm.

4.4.6.1.2 Quenching of peroxidase activity by 0.6% H_2O_2 and 2 % methanol.

Out of the 100 µl samples used for ELISA, 40 µl samples were transferred into another ELISA plate. The samples were incubated at 4^{O}C overnight. After the overnight incubation, the samples were discarded, and the wells were washed thrice with 0.1 % Tween-20 in PBS (wash buffer). After this, the plate was incubated with 200 µl of 0.6% (of 30%) H_2O_2 in 2% methanol for 10 min at RT. The plate was again washed thrice with wash buffer, and 100 µl of peroxidase substrate was added to each well. After 15 min, the ODs were analysed at 450 nm.

Results:

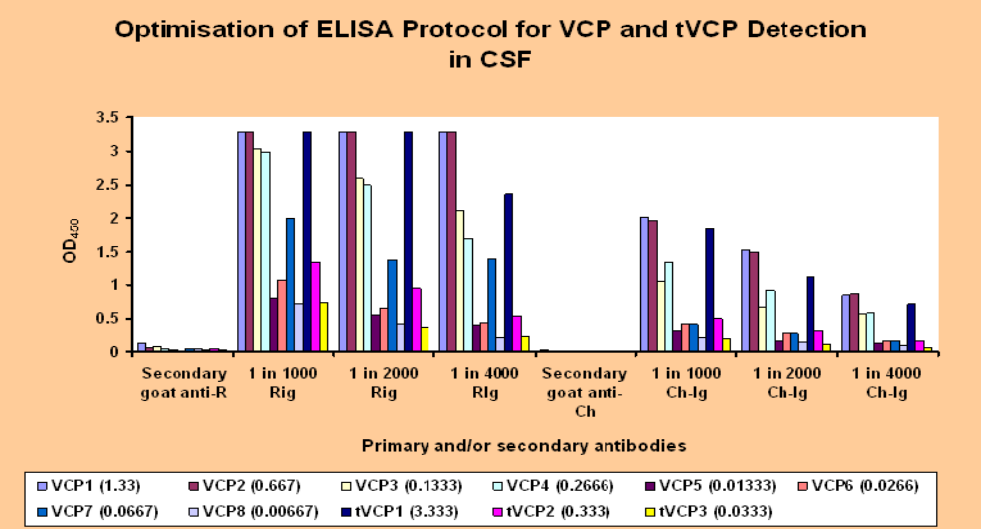

Figure 4.4. *OD_{450} values as an index of measurement of peroxidase activity (Y-axis) are plotted against 1:10000 dilutions of the secondary antibodies (goat-anti-R, and goat-anti-Ch) and the concentrations of R-Ig and Ch-Ig (1:1000; 1:2000, and 1:4000). VCP1 to VCP8 and tVCP1 to tVCP3shown in the legend represent different dilutions of VCP and tVCP (R = Rabbit, Ch = Chicken). Their concentrations (ng / µl) are shown in the parentheses of legends.*

Results: The OD_{450} at different concentrations, as shown in Fig 4.4 and Appendix R (Table R4.4), suggests that the primary antibodies add to VCP and tVCP in a concentration dependent manner. The OD_{450} is high at higher concentrations, and decrease with the decrease in the concentration of VCP and tVCP. Also, the primary antibodies add to VCP and tVCP in a manner depending on the concentration of the antibody. The OD_{450} is higher at 1:1000 dilution of the primary antibody, and the lowest at 1:4000

dilution. The R-Ig is more sensitive than that of Ch-Ig, but the sensitivity is attributed to several-fold higher concentrations of R-Ig used. The concentration below 0.00666 ng / µl can be detected using the primary antibodies at all the dilutions. There is non specific adsorption of the secondary antibody on VCP and tVCP to a very small extent and the adsorption can be directly correlated to the concentration of VCP and tVCP. At lower concentrations, the adsorption is negligible. There is some non-specific adsorption of both the primary antibodies on the control CSF samples (50 µl diluted to 100 µl) as well (not shown). In order to differentiate between it being non-specific adsorption or due to endogenous peroxidase activity in CSF, an assay was performed, in which peroxidase substrate was added to a few 20 µl control CSF samples from various rat brains. These samples showed peroxidase activity. Also, as shown in the SDS-PAGE analysis and subsequent western blot analysis, there was some non specific binding of the R-Ig to about 16 kDa and 18 kDa proteins in CSF samples collected from SNT R as well as VCP R (Fig 4.12).

After considering the problems encountered while optimising the protocol for the detection of VCP and tVCP using R-Ig CSF, a few modifications in the above protocol were made. 1) The R-Ig was selected as a primary antibody due to its high sensitivity. 2) The concentration of R-Ig was reduced to 1:3000 to keep the sensitivity intact and reduce the non-specific binding. 3) The time of incubation in block buffer was increased from 60-75 min to 120-140 min to further block the nonspecific binding sites. 4) 0.5% BSA in 0.1 % of Tween-20 was used as a blocking buffer to further reduce the non-specific binding and retain the sensitivity. 5) After the blocking step, the plates were washed thrice, and in order to quench peroxidase 0.6% of 30% H_2O_2 were mixed with 2% methanol in PBS (pH=7.2; 0.154 mM). 200 µl of this solution were added to each well for blocking the endogenous peroxidase. 6) The incubation time with the primary antibody was reduced by an hour and with that of the secondary antibody was reduced by half an hour. 7) The CSF samples at different time intervals were pooled from different rats from the control as well as treatment groups. In order to make the volume up to 100 µl, the samples from two different time intervals (0-1 h and 1-2 h 2-3 h and 3-4 h; 4-5 h and 5-6 h or 5-8 h) intervals were further pooled to give three different samples representing three different time intervals (0-2 h; 2-4 h, and 4-6 or 4-8 h). As discussed in the section 4.4.6.1.1, the remaining CSF samples at each time interval from each rat was mixed and, the CSF samples mixed in such a manner were further pooled from three different rats (R1 = rat 1 + rat 2 + rat 3; R2 = rat 4 + rat 5 + rat 6) to give two different sets of CSF samples for the estimation of VCP level in the individual rats. The pooling of the sample increased the sample size, and reduced the number of samples, thereby making the analysis a bit easier. Without pooling there would have been minimum of 36 CSF samples from each treatment group (6 rats X minimum 6 intervals) with small sample size. Analyzing all the samples at the same time, under similar conditions would have been very difficult from a practical point of view. This also might have resulted in large variations in measurements. In addition, VCP and tVCP are expected to reach the brain at a very low level, and therefore, it was necessary to use larger CSF volumes. The maximum volume of CSF that can be withdrawn from the rats is 40-60 µl from each rat at a particular time interval. In my experience the volume that can be collected at each time interval is highly variable. The

collection of CSF was also stopped after the first drop of blood appears in CSF. Taking into consideration all these factors, pooling the small volumes of CSF samples were thought to be necessary for the detection of VCP and tVCP.

Results:

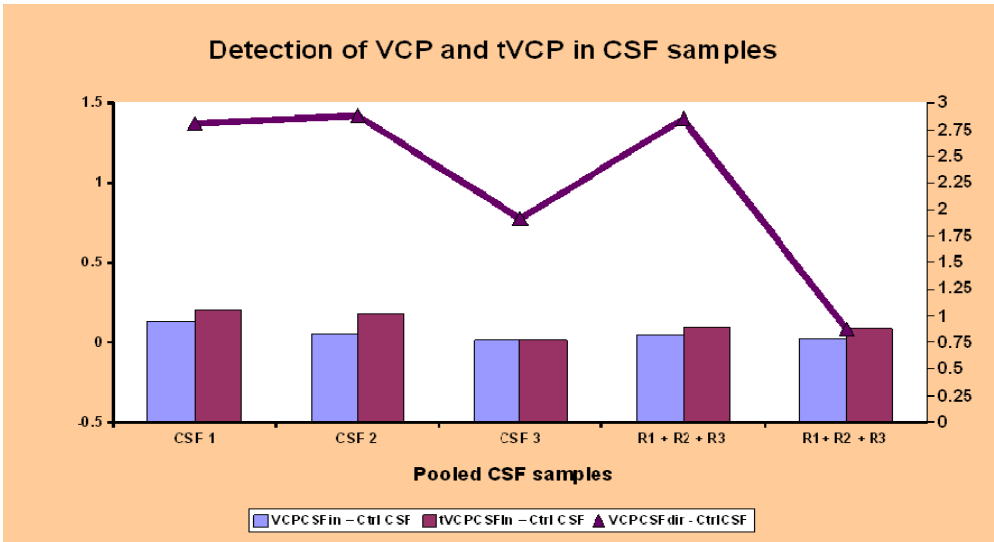

Figure 4.5. *OD_{450} values (Y axis) of VCPCSFin and tVCPCSFin of the pooled CSF samples at different time intervals(CSF1, CSF2, and CSf3) as well as from two sets of three rats each (R1+R2+R3 and R4 + R5 + R6) from each group (X axis). The secondary axis shows the OD_{450} values of VCPCSFdir (line graph). The primary and secondary axes values are shown by using different scales since the values of VCPCSFdir were of much higher scale than those of VCPCSFin and tVCPCSFin. The values shown in the graph are corrected OD_{450} obtained by subtracting OD_{450} values of Ctrl CSF samples at the same interval or same individual group sets as shown in the table R45A. and R4.5B of Appendix R..*

Results: OD_{450} for the detection of the VCP and tVCP in CSF samples after ELISA suggested that the OD_{450} of the treatment groups differs from that of control groups (Tables R4.5A and 4.5B of the Appendix R). For VCP R, the OD_{450} was high at the first interval, and decreased at the subsequent time intervals. At all intervals, the OD_{450} was higher than that of Ctrl CSF (Tables R4.5A and R4.5B of the Appendix R). Also for the individual rats, R1 and R2 of VCPCSFin were higher than that of the Ctrl CSF. The trend was similar for tVCPCSFin, but the difference between the OD_{450} at the first and second interval was higher than that of VCPCSFin at the same time intervals. For VCPCSFdir, the difference OD_{450} were several fold higher than that of the treatment groups at all the time intervals. For the first two intervals, as well as for R2, the OD_{450} were beyond the range of detection indicating that the concentrations were much higher during the first two intervals. When the OD_{450} values of the CSFctrl were subtracted from the OD_{450} values of the treatment groups, it was found that the difference was higher for tVCP R than that of VCP R, which suggested that tVCP was delivered to a greater extent than that of VCP (Fig 4.5, Table R4.5A, Appendix R).

When the difference in the OD_{450} was compared with the VCP, and tVCP dilutions which were

used as positive controls, and processed similar to the CSF samples at the same time under similar conditions in the same plate, it was found that the OD_{450} of the VCPCSFin, and tVCPCSFin was much lower than the final dilution of VCP and tVCP used as a positive control suggesting that the amount of VCP, and tVCP reaching the brain was less than 0.0005 ng / µl (Table R4.5B of Appendix R). The OD_{450} of positive control were a bit lower than that of VCPCSFdir suggesting that the amount of VCP was more than 0.5 ng/µl (R4.5A and R4.5B of Appendix R) after being administered directly into the left ventricle.

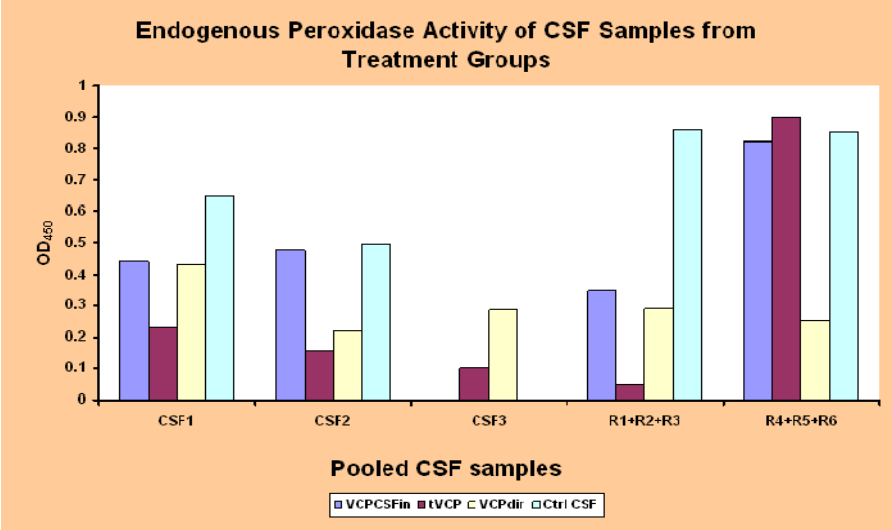

Figure 4.6. *OD_{450} indicating endogenous peroxidase activity (Y axis) of CSF samples at different time intervals(CSF1, CSF2, and CSF3) and two different sets of three rats each (R1 + R2 + R3 and R4+R5+R6) from the treatment groups (X axis).*

Results: The order of OD_{450} of CSF from different treatment groups was:

Ctrl CSF > VCPCSFin > VCPdir > tVCPCSFin. When tVCP, and VCP were added to CSFCtrl and OD_{450} were measured, OD_{450} of VCP treated CSFCtrl samples were less than the untreated samples (Fig 4.6). At the same concentration the OD_{450} of CSFCtrl samples treated with tVCP were also less than that of CSFCtrl samples, but greater than that of VCP treated CSFCtrl samples.

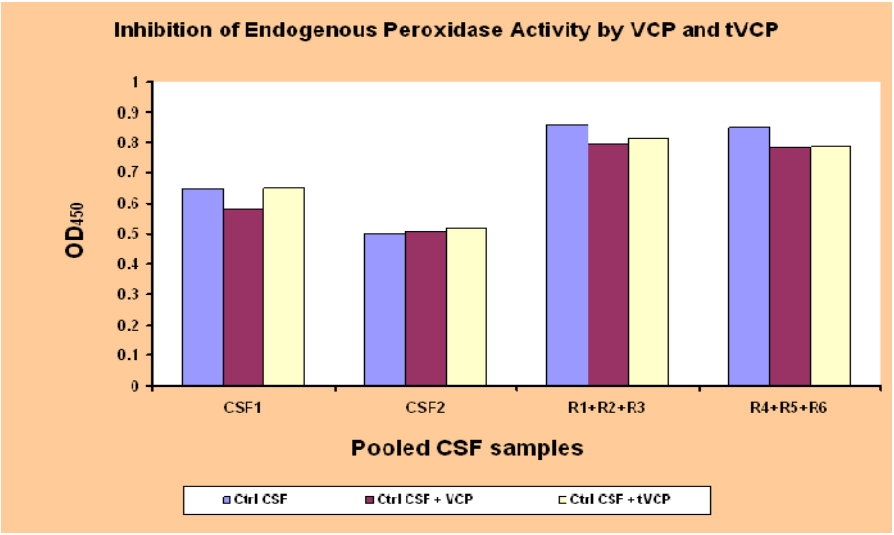

Figure 4.7. *OD_{450} values (Y axis) of pooled CSF samples at different time intervals (CSF1 and CSF2) and from two sets of three rats each (R1 + R2 + R3 and R4+R5+R6) from treatment groups (X axis)*

Results: The endogenous peroxidase activities of different treatment groups were lower than that of the Ctrl CSF ODs which suggested that VCP and tVCP reaching the brain might have suppressed the endogenous peroxidase activities (Fig 4.7, and table R4.6, Appendix R). When VCP and tVCP were incubated with the Ctrl CSF samples, they were found to reduce the OD_{450} values to some extent.

Quenching of endogenous peroxidases in CSF samples.

Intervals and rats	Negative Ctrl	VCP	VCPdlr	tVCP
Interval 1	0.005	0.004	0.004	0.002
Interval 2	0.007	0.003	0.001	0.001
Interval 3	0.006	0.003	0.001	0.002
Rats 1,2, and 3	0.005	0.005	0.001	0.003
Rats 4,5, and 6	0.004	0.003	0.002	0.003

Table 4.3. *OD_{450} of CSF samples subjected to peroxidase assay after treatment with hydrogen peroxide (0.6%) in 2% methanol solution in 0.154 mM PBS.*

Results: After the treatment with peroxidase in methanol, the OD_{450} was reduced almost to zero indicating complete blocking of inherent or endogenous peroxidase activity (Table 4.3).

4.4.7 Transcardial perfusion and processing of the brain tissue.

After the collection of CSF samples, the rats were deeply anesthetised, this time with sodium pentobarbitone, and they were perfused transcardially using 0.1 M PBS (pH = 7.2) followed by 4% paraformaldehyde, and their brains were collected and fixed in 4% paraformaldehyde solution. In order to further process the brain sections, they were cut into different parts (blocked) as shown in the fig 4.8 C below. While cutting, the sections were specifically checked for the appearance of the needle tract to confirm placement within lateral ventricle and hence appropriate delivery to intended target area (Fig 4.9) and the olfactory lobe (Fig 4.8 B).

Direct administration of VCP in the rat brain.

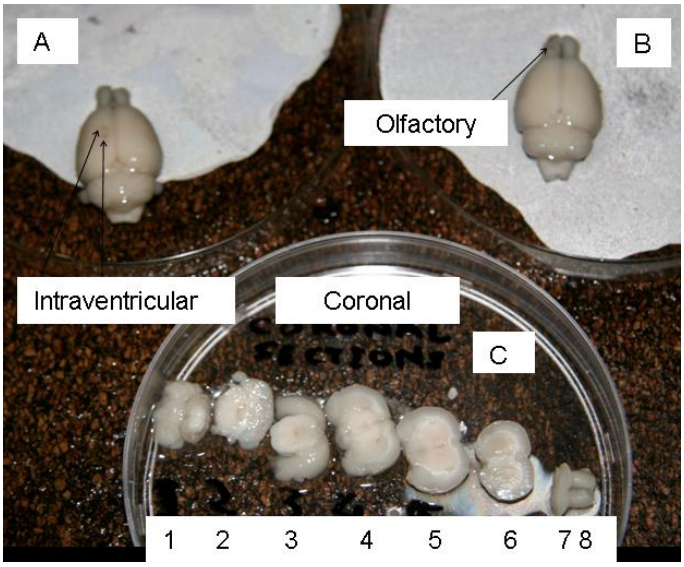

Figure 4.8. *The intraventricular administration into the rat brain is shown in brain A and direct administration of VCP into the olfactory lobe is shown in brain B. The fixed rat brain was divided into different parts which were numbered from 1 to 8 and later embedded into cassettes. The parts 7 and 8 which represent the olfactory lobes were used as a positive control for studying the pattern of distribution in the rats to which VCP was administered intranasally.*

Direct administration into the left lateral ventricle

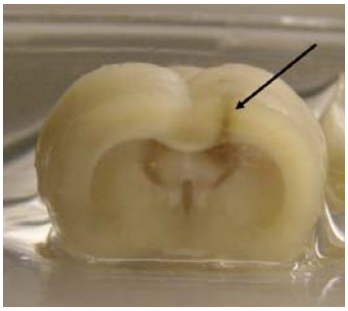

Figure 4.9. *The position of the needle (shown by an arrow) after being inserted stereotaxically into the rat brain A of Fig 4.8 for the direct administration of VCP into the left lateral ventricle of the rat brain*

Preparation of 4% paraformaldehyde solution: 4 g of paraformaldehyde (analytical grade: BDH chemicals) was dissolved in 0.10 M PBS (pH = 7.2) using sodium hydroxide pellets by heating to 60 ^{O}C to 70 ^{O}C and constant stirring. For 12 g of paraformaldehyde (300 ml solution) one big or two small pellets of NaOH were sufficient to dissolve paraformaldehyde. The transcardially perfused rat brains were further fixed in paraformaldehyde and cut into different parts and processed using the protocol mentioned in the table in the Appendix S (Table S3.1).

The brain sections were then embedded in wax blocks until the time they were used for the Immunohistochemical staining.

4.4.8 Immunocytochemical staining of various sections from VCP R, tVCP R, VCPdir and Negative controls.

4 μm thick coronal brain sections from different parts of the brain of VCP R, tVCP R, VCPdir and SNT R as shown in fig 4.8C were cut and placed on coated histopack glass slides. These sections were fixed on the slides by keeping them in oven at 42^{O}C for an hour. The sections were treated with xylol (2 X 10 min) for dewaxing, and rehydrated by keeping them in different alcohol concentrations [absolute (1 min X 3), 90% (1 min X 3), and 70 % (1 min X 3)]. After this, the sections were subjected to 2-3 % hydrogen peroxide in PBS or methanol (50 % to 100%). These sections were then treated with trypsin (0.05%) in calcium chloride solution for the antigen retrieval. Later, these sections were either treated with triton X 100 (0.03% for 10 min) or were directly blocked using goat serum (1 in 20) for 10 min. After draining off the goat serum, the sections were incubated with the primary antibody (Chicken-anti-VCP diluted to 1 in 150 or 3 μl / 500 μl) at RT for several hours (5 h) in a humidity controlled chamber or overnight at 4 ^{O}C. After 3 X washing with 0.05 % Tween-20 in PBS (wash buffer II), and rinsing (1 X) with PBS (0.1 M, pH = 7.2), the secondary antibody (Goat-anti-Chicken = 1 in 350 to 400) was added, and the sections were then incubated in a humidity chamber at RT for 1 h 30 min to 2h. The sections were then washed in wash buffer II, and rinsed with PBS (pH = 7.2; 0.1 M) and incubated with avidin (1:400 to 1:600; Dako) or streptavidin (1:400; Novacastro). DAB substrate (freshly prepared by mixing DAB with substrate diluent) was added, and the colour was allowed to develop for 15 min. The sections were then washed and treated with 5% copper sulphate solution for 3 min and counterstained with haematoxylin (30 s to 1 min), treated with Scott solution for 1 min and washed under tap water. After dehydration steps (70%, 90%, and absolute EtOH + Xylol), the sections were mounted using entellan, and digitally photographed at various magnifications of the objective.

Results:

Immunostaining of brain sections from VCPdir R.

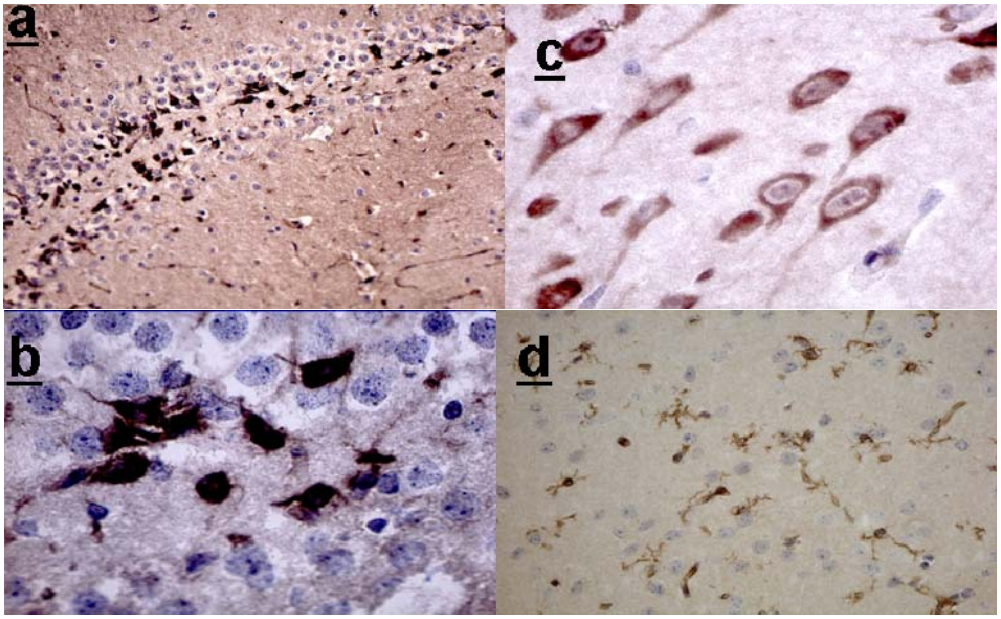

Figure 4.10. *The brain sections from the hippocampus of VCPdir R directly administered (a = staining of hippocampus (10x), b = 40x, c = 40x (neuronal), d (20x) the brain area 5 shown in Fig 4.7. Dark brown staining of the hippocampus or other brain regions against much lighter background indicative of positive staining*

Immunohistochemical staining of brain sections from VCP R and tVCP R.

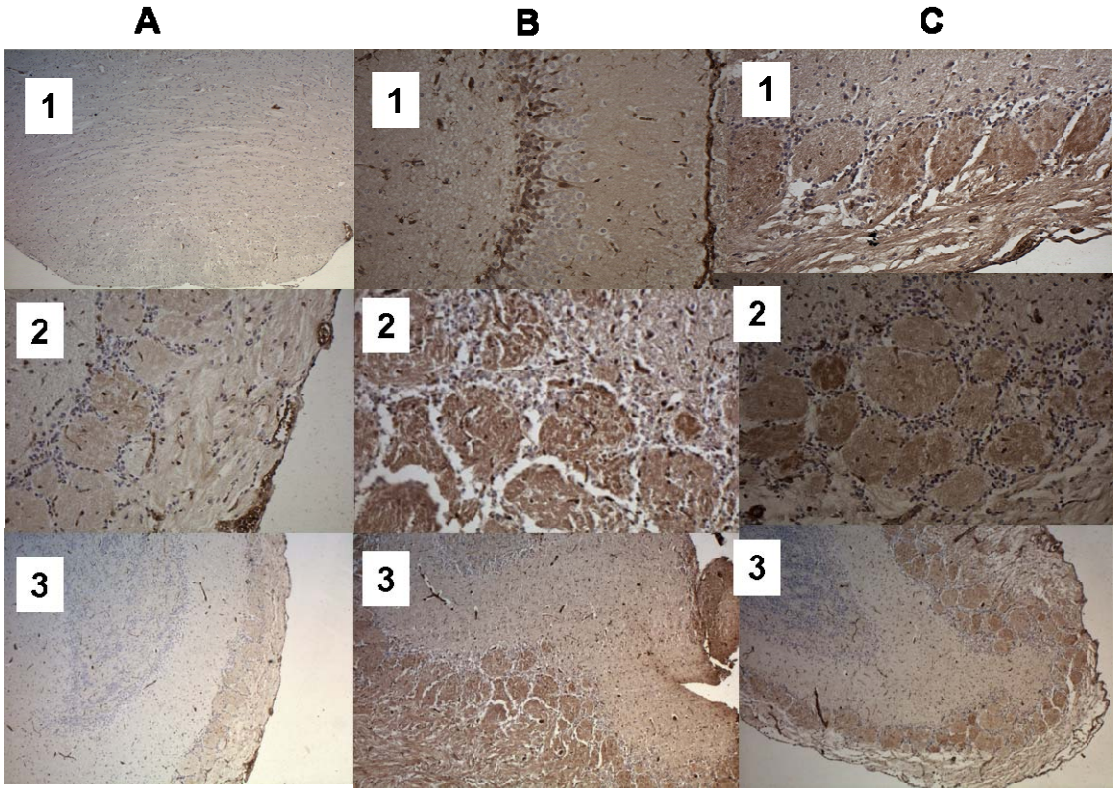

Figure 4.11. *Immunostaining of the area 7, 8 (see Fig 4.8 for the numbering of areas) of the brain sections from VCP R. Panel A (1, 2, and 3 represent (area 6 of Fig 4.8 [4x], olfactory lobe [40x), and [10x], respectively of SNTR. VCP dir (hippocampus = B 1 [10x]), B2, B3 and C1, C2, and C3 represent glomerular staining of the area 7, 8 or olfactory lobe in VCP treated rats at different magnifications (B2, C1, and C2 = 40x. B3 and C3 = 20x)*

Results: As shown in the Fig 4.10, the brain sections from the rats to which VCP was administered directly into the brain showed staining of the hippocampus [one rat] (4.10 a and b). The DAB staining of the hippocampal neurons (4.10 c) and other brain cells (4.10 d), probably astrocytes was also observed. When the brain sections from the rats to which VCP was administered intranasally were subjected to immunohistochemical analysis using DAB substrate, the staining of the glomerular cell layer of the rat olfactory bulb (B2, B3, C1-C3 [area 7 or 8] shown in Fig 4.11) [n = 6 rats; but only 3 rat brain sections which were randomly selected and section stained are shown here] was observed. A similar pattern of staining in the glomerular cell layer of the olfactory lobes of tVCP treated rats was observed. The rats to which VCP was administered directly into the olfactory lobe of the brain, also showed a similar pattern of staining of the glomerular cell layer, but these are not included here. The histological sections shown here (Fig 4.11) are representative of treatment groups.

4.4.9 Western blotting of CSF samples for the detection of VCP, and tVCP in the CSF samples.

Method.

15 µl of CSF samples collected from one rat of the VCP R group at different time points (1, 4 and 6 h intervals), and one sample from SNT R was subjected to SDS-PAGE analysis. The tVCP (15 µl crude supernatant before purification) expressed in the chapter 2 and rVCP standard (a positive control) were also subjected to western blotting. After the SDS-PAGE analysis, the proteins from the gel were transferred onto a nitrocellulose membrane, and the membrane was then treated with rabbit-anti-VCP antibody followed by a secondary anti-rabbit antibody labelled with HRP. After adding the HRP substrate, the blot was developed which was exposed to a thin film of X-ray. The film was later developed, dried and the photographed (Fig 4.12)

Western blot analysis of CSF samples, VCP, and tVCP.

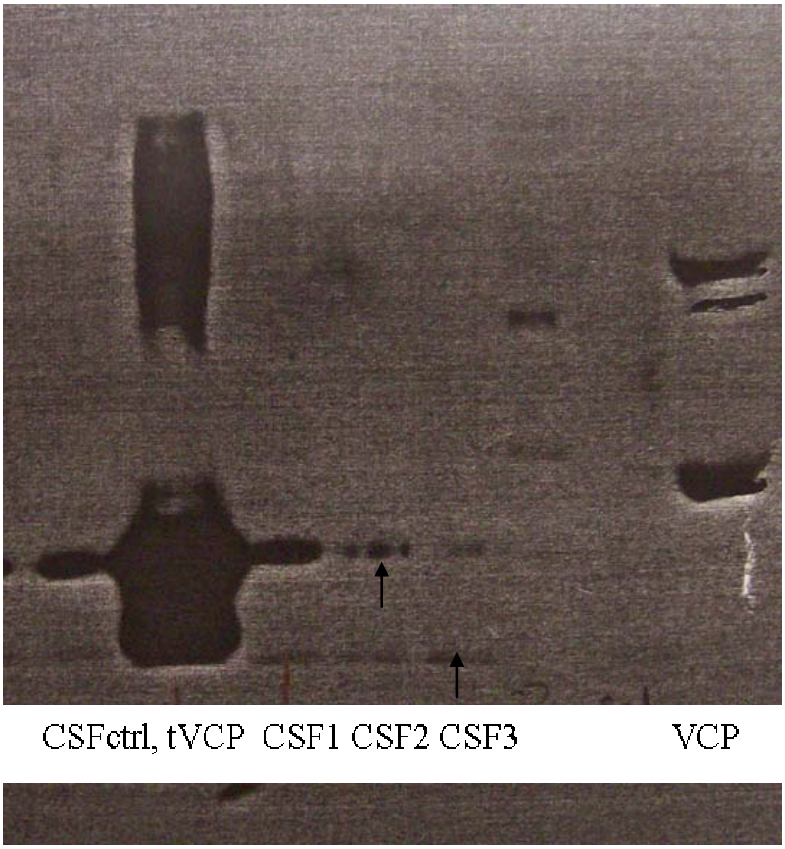

Figure 4.12. *The western blot analysis of the three CSF samples collected at different time intervals from VCP R (intervals 1, 4, and 6 = CSF1, 2, and 3, respectively; one control CSF sample (CSFctrl) and tVCP supernatant (chapter I), and VCP (+VE ctrl; the last lane). The order is as shown in the figure. The 15-16 kDa and 18-19 kDa non-specific bands are shown by black arrows.*

Results: The antibody showed binding to three proteins in the crude supernatant used for the detection of tVCP (lane 2, Fig 4.12). There was a band in the range of tVCP (18.8 kDa) suggesting the confirmation of expression of tVCP using *P. pastoris*. This also confirmed the binding of the primary antibodies to both VCP, and tVCP. There was no band in the range of VCP in the control CSF samples from SNT R (CSFctrl), as well as in the CSF samples from VCP R (CSF 1, 2, and 3). Two bands (one in the range of 15 to 16 kDa, and the other band in the range of 18-19 kDa) were observed in both the CSFctrl and VCPCSFin (VCP R) suggesting non specific binding by the primary antibody (R-Ig).

4.4.10. Summary of Results.

Sr	Experiment	Results	Conclusion
1	Colourimetric method of Cur detection (Fig 4.2).	CurNa and CurEt can be detected between 27.5 to 2.75 μM concentrations.	Method works better for higher concentrations of Cur, but the sensitivity of the assay decreases at lower concentrations of Cur.
2	Optimisation of Fluorimetric method for Cur Detection (Fig 4.3 A and B).	The fluorescence of Cur was enhanced many folds in the presence of Tween-20, EtOH, and GAA. The fluorescence values were higher for CurEt than that of CurNa at the same concentrations. The λmax was at 495. SDS further enhanced the fluorescence by Tween-20 in CurEt samples and quenched the fluorescence of CurNa samples to some extent.	The fluorimetric method to detect Cur appears to be optimal.
3	Fluorimetric detection of Cur in CSF samples (Table 4.2 A and B).	Cur was detected in μM range in CSF using this method, and the concentrations were higher at the first, fourth, and sixth intervals than at the other time intervals. The emission wavelength of 484 nm reduces background fluorescence, and specifically enhances Cur fluorescence.	Cur delivered intranasally detected in CSF in micromolar concentration. The three possible routes of uptake are: i. extraneuronal, ii. intraneuronal iii. systemic route.
4	Western blotting (Fig 4.12).	Two bands were detected both in CSFctrl and VCPCSFin samples. These bands were not in the range of VCP indicative of antibody cross reactivity with CSF.	VCP could not be detected in CSF samples using small volumes (15 μl).
5	Optimisation of an ELISA method for the detection of VCP and tVCP in CSF (Fig 4.4).	Anti-VCP R-Ig and Ch-Ig antibodies can be used to detect both VCP, and tVCP in CSF, and bind to VCP and tVCP in a concentration dependent manner. The primary antibody showed cross reactivity with Ctrl CSF. The secondary antibodies were adsorbed on VCP and tVCP to a negligible extent. The adsorption was minimal at lower concentrations.	With some modifications, the assay was used for the detection of VCP, and tVCP in CSF samples. The data support cross reactivity with CSF as shown in western blotting.
6	Detection of VCP, and tVCP in VCPCSFin, tVCPCSFin, and VCPCSFdir samples (Fig 4.5).	VCP and tVCP reaches the brain at a very low level after being delivered intranasally. VCP delivered in the brain and lateral ventricle directly could be detected in CSF even after 2.5 to 3 h after direct administration.	VCP and tVCP detection in CSF is indicative of uptake by olfactory mechanism.
7	Immunohistochemical detection of VCP, and tVCP after intranasal and direct administration (4.10 and 4.11).	VCP administered directly shows staining in the hippocampus and the olfactory lobe. There was background staining observed. VCP and tVCP delivered intranasally were detected in the glomerular cell layer of the olfactory lobe.	VCP and tVCP detection in the olfactory lobe is indicative of retention for several hours via either route. VCP administered directly in hippocampus was also detected after several hours (about 4-5 h).

Discussion.

After establishing the complement regulatory activity of Cur, VCP, and tVCP, these compounds were used in the current investigation to study their availability in the brain and CSF samples after being delivered intranasally. The aims were first to optimise a method for proper delivery of these compounds intranasally, optimisation of a method of collecting CSF samples at different time intervals, and development of sensitive, economic, and reliable techniques to detect these compounds in CSF and brain samples.

Generally, for distribution studies after intranasal administration, the rat is considered to be the best model. The collection of CSF is always challenging, and many methods are available with a varying degree of difficulty. The method optimised in the current investigation is suitable only for serial sample collections from the anaesthetised rats. This method has an advantage of simplicity, and requires only minimum use of stereotaxy for the positioning of the rat's head in order to gain access to the foramen magnum. The reference point used (the ridge of the cranium) was easy to locate using a blunt end of scalpel.

After collecting CSF and brain tissue, methods needed to be developed to detect these compounds in the brain, which were hypothesised to be delivered at a very low level.

Firstly, a method for the detection of Cur in CSF was required. As indicated in the fluorimetry methodology for the optimisation of cur detection using FEMix, there was a sudden rise in the level of fluorescence emission by Cur at different wavelengths, λmax for fluorescence emission (Fem) being 495 nm as shown in Fig 4.3A, 4.3B and tables 4.2RA, 4.2RB (Appendix R), and discussed in the results. These results also suggested that at lower concentrations of Cur, certain concentrations of EtOH, GAA, Tween-20 and SDS are critical for fluorescence enhancement, and under appropriate conditions the fluorescence could be enhanced up to 9 fold. With SDBS and CTAB, the enhancement in the fluorescence levels was shown to be several fold higher than this (Wang et al. 2006), but the assay shown here enhanced fluorescence to a detectable level. For optimal fluorescence enhancement protocol, Fem was found to be 495 nm.

Using this filter, when the fluorescence was recorded in the CSF samples, initially there was no pronounced difference observed in the fluorescence values of CSF from the control and the experimental rats. This could be because of the change in the volumes of sample and FEMix used. Initially, while optimising the assay, 30 µl of sample and 20 µl of FEMix were used. While analysing the CSF samples, the amount of CSF used was about 100 µl. Also, the optimum concentrations of Tween-20, GAA, and EtOH were essential for the optimum fluorescence. When the concentrations of these moieties were increased, a blue shift was observed in the λmax, and then there was enhancement in the fluorescence of CSF collected from Cur treated rats. Based on results of these optimisation tests, the filter was set to 495 nm while measuring the fluorescence levels in the initial samples and no change in the fluorescence levels was observed. This might be due to the blue shift in Fem to a lower wavelength (484 nm) which resulted in diminished fluorescence at 495 nm. Also as discussed earlier, the levels of Tween-20, SDS and GAA may not have been optimum with the net result of shifting the

emission wavelength to 484-490 nm. These two factors might have been responsible for the failure of the enhancement of the fluorescence while optimising the protocol. Once the protocol was optimised, and the emission wavelength was adjusted to 484-490 filter, Cur was detected in CSF.

As shown in Fig 4.3B, there was a correlation between the concentration and the fluorescence intensity of Cur after the addition of FEMix. It was higher at higher concentrations of Cur at all the wavelengths.

A similar fluorescence pattern was observed in the control samples. Although the fluorescence values were slightly higher at 490 nm than with 484 nm, and all the other wavelengths, BFV490 values were the highest in control CSF (Table R4.3B Appendix R) suggesting the highest fluorescence backgrounds at this wavelength. This high BFV may be due to the enhancement of the fluorescence of some of the compounds present in CSF. BFV484 values were the lowest suggesting lower background levels at this wavelength, and the fluorescence emission of CSF collected from the Cur R was also the highest at this wavelength. This trend was similar to Cur dilutions which were used as a positive control, suggesting the rise in the fluorescence levels of CSF samples was due to the presence of Cur in these samples. These findings thus confirm the presence of Cur in CSF. Although the pattern was similar at all the wavelengths, there was a variation in the concentration range of Cur determined at different wavelengths. This could be attributed to the difference in the BFV levels at different wavelengths. BFV was masked to a great extent at 484 nm, and the emission of fluorescence by Cur at the same concentration was higher than that of all the other wavelengths tested. Therefore, the fluorescence values at this wavelength were used for the determination of the concentration Cur.

Comparison of the concentration of Cur at different time points after intranasal administration suggested that the concentration was more at the first, fourth and the sixth time intervals (Table 4.2B). The variability in the levels of Cur in CSF could be attributed to the variable pattern of absorption of Cur in the brain after intranasal administration. Drugs administered via this route could be taken up intranasally via extraneuronal routes, intraneuronal routes, and also via the systemic circulation as discussed in the literature review (1.11.4 and 1.11.5). If the drug reaches the brain via extraneuronal route, it could be detected within minutes after being administered as observed with cocaine (Chow et al. 1999). Generally, small molecules are transferred to the brain via this route. The high peak during the first time point probably indicates the delivery of Cur via extraneuronal route as observed with cocaine (Chow et al. 1999). Cur might have been taken up into CSF via this route during the first hour after being administered intranasally. Cur being a polyhydroxy phenolic compound, it would be appropriate to compare its uptake into the CSF with that of dopamine, which although structurally not similar but shows the presence of dihydroxy phenolic groups, and is a small sized molecules like Cur. Dopamine was detected at a high concentration during the first four intervals (30 min to 4 h), and the peak concentration reached 4 h after intranasal administration (Dahlin et al. 2000, Dahlin et al. 2001). It was concluded that it could reach the brain via both the extraneuronal and intraneuronal routes. It is therefore possible that similar to dopamine, Cur might have taken up into the brain via both the extraneuronal and intraneuronal pathways. If the transport is neuronal, or via other mechanisms such as

adsorptive endocytosis, it may take several hours for the drug to reach the brain. WGA-HRP was detected 6 h after being administered intranasally and was delivered to the brain via adsorptive endocytosis (Broadwell and Ballin 1985). It is also known that the intranasally administered drugs may reach the systemic circulation. Dopamine was shown to be taken up into the systemic circulation after being administered intranasally (Dahlin et al. 2001). Cur is known to cross the BBB once it is delivered into the systemic circulation (Yang et al. 2005). Thus, Cur, in addition to the extraneuronal and intraneuronal routes might have also been first transported into CSF via systemic circulation. The possible transfer by more than one mechanism may be accounted for the variability in the absorption of Cur in the brain.

The next aim was to optimise a method to detect VCP and tVCP in CSF. An ELISA method for the detection of VCP, and tVCP was optimised (Fig 4.4). The initial optimization protocol showed that both the anti-VCP primary antibodies raised in rabbit and chicken used in the current investigation could be used to detect not only VCP, but also tVCP. While optimising the ELISA method, it was found that the secondary antibody showed some degree of adsorption on VCP in a concentration dependent manner, but the adsorption was negligible, especially at low concentration of VCP. However, the primary antibody showed some non-specific adsorption on the CSF samples.

The results support the western blot analysis data (Fig 4.12). Before optimising a method for detection of VCP and tVCP in CSF, attempts were made to detect VCP, and tVCP using western blot analysis. For this, 15 μl of CSF samples from control as well as experimental rats were subjected to western blot along with VCP and tVCP positive controls. The analysis did not reveal any band in the range of VCP, but a band in the range of approximately 15-16 kDa range and the other in the range of 19-20 kDa were observed (Fig 4.12). So, the primary antibodies used in the current investigation showed cross reactivity with 2 proteins from CSF. These proteins were observed in the range of 15 - 18 kDa. Oxyhaemoglobin, a protein in the same range has previously been shown to cross react with some other primary antibodies used to detect β-amyloid (Cutler et al. 1997). The 16 kDa protein detected in the CSF sample might be oxyhaemoglobin, because Oxyhaemoglobin shows some peroxidase activity and CSF samples in the current investigation also showed some endogenous peroxidase activity (Fig 4.6). CSF may contain some other proteins, and their cross reactivity with the primary antibody forms a part of future investigation.

It was also necessary to investigate whether the presence of any other factors might interfere with the actual assay. The serum samples often contain peroxidases, and CSF also contains some proteins but at lower level than that of serum samples. As the presence of peroxidases in the brain was not known, it was decided to check the inherent or endogenous peroxidase activity of CSF samples. When TMB, a peroxidase substrate was added to CSF samples, it showed some endogenous peroxidase activity. Consequently, in order to avoid the interference from peroxidases, 0.6% hydrogen peroxide in 2% methanol was used. It was shown that the endogenous peroxidase level of CSF samples was completely suppressed using this combination (Table 4.3), and therefore, in the actual experiment, the interference due to peroxidases was avoided. Using this standardised assay, it was shown that there was

a difference in the OD_{450} of the control CSF and CSF obtained from VCP and tVCP treated groups. This suggests that both VCP and tVCP could be detected in CSF.

It was also found that there was a difference in the endogenous peroxidases activity of the CSF samples from the control and treatment group (Fig 4.6). When VCP and tVCP were added to the CSF samples from the control groups, the endogenous peroxidase activity was masked to some extent by tVCP and to a relatively greater extent by VCP (Fig 4.7). This means that VCP is probably binding and inhibiting the endogenous peroxidases. As CSF samples were stored for long at $-20^{O}C$, during this time VCP may have blocked the activity of the compound responsible for the endogenous peroxidase activity. As the level of VCP in CSF samples of tVCP R and VCPdir R was more than that of VCP R, the endogenous peroxidase activity of CSF samples from these groups was low.

As discussed in the literature review and above, drugs delivered intranasally reach the brain by three routes, and if the drugs taking extraneuronal route could be detected in min after the intranasal administration. The high OD_{450} values in CSF during the first interval (0-2 h) after VCP administration suggested that these compounds reach the brain via extraneuronal route. VCP might have been delivered extraneuronally to SAS like HRP (Kristensson and Olsson 1971, Bannister and Dodson 1992, and Jansson 2004T). At later time points, the OD_{450} of the CSF samples from the treatment groups did not differ from the OD_{450} the control CSF which suggested clearance of these compounds from CSF at these time points. The compounds, however, were still detected eight hours after administration into the brain tissue suggesting distribution of these compounds continuing in the brain some time after commencing administration. These compounds showed OD_{450} much lower than the highest dilutions of the positive controls (0.0005 ng / μl). Based on the analysis of CSF samples, it was concluded that these compounds reach the brain at a very low level after intranasal delivery, and multiple administration are recommended rather than single administration before attaining therapeutic concentration. The immunohistochemistry study however suggested the uptake of VCP and tVCP in the olfactory glomerular area at a detectable level. The variation in the brain and CSF levels of these compounds might be attributed to the different routes taken by these proteins to reach the brain. As mentioned above, WGA-HRP was delivered to the brain 6 h after intranasal administration by adsorptive endoctytosis and no extracellular transport was observed (Broadwell and Balin 1985). It is therefore possible, that VCP and tVCP are taken up by more than one route into the brain. Further research needs to be done to establish the route taken by VCP and tVCP after being delivered intranasally.

It was also found that VCP administered directly into the brain can be detected in CSF. The level is very high during the first time interval and it is low during the last time interval that is 3-4 h after direct administration. Thus VCP delivered directly into the brain circulates in CSF for a relatively long period and slowly gets distributed in the brain. The ability to be retained in the tissue for long might have been responsible for its therapeutic utility even after a single dose of administration directly into the brain.

The immunohistochemical analysis of the brain sections shows that VCP administered directly into the hippocampus and the olfactory lobe indicates positively staining in those areas (Fig 4.10). After

direct administration, the immunological staining did not show staining of the other parts of the brain. Lack of staining elsewhere other than the restricted locus around the infection site may imply that VCP is unable to spread significantly. Additionally, this may also be dependent on size of injection. If it indeed is sparsely distributed, it may be masked by non-specific cross reactivity of the primary antibody with some unknown compounds. After intranasal administration, VCP and tVCP were detected only in the olfactory lobe (Fig 4.11). These proteins mainly showed localisation in the glomerular cell layer of the olfactory lobe. Proteins and drugs often localise in this part of the brain after intranasal administration. The cholera toxoid adjuvant has previously been shown to be localised specifically in this part of the brain after being delivered intranasally (van Ginkel et al. 2000). WGA-HRP was also detected in the olfactory lobe after being administered intranasally (Thorne et al.1995, Broadwell and Balin 1985). The localisation of VCP and tVCP administered intranasally in this part of the brain therefore has counterparts in so far as substances which include proteins similarly localise in this area of the brain.

Cur was detected in CSF in μM range in the current investigation at different time points, the first interval, the fourth and the last interval. The CSF samples in the current experiment were collected from the cisterna magna as this is in line with the usual practice of detecting the level of drugs in the brain after intranasal administration. Many other researchers have analysed CSF samples collected from the cisterna magna after CNS delivery (Dahlin et al. 2000, Dahlin 2001, Thorne et al. 2004). The cisterna magna produces CSF at a low level, but CSF produced in the ventricles or choroid plexus drains into the cisterna magna. Therefore, the CSF samples collected from the cisterna magna by cisternal puncture are indicative of distribution of the drug within CSF compartment. As Cur was found in the CSF samples collected at different time points, its delivery to the CSF compartments after being delivered intranasally was confirmed. Our objective to test whether Cur could be delivered to the CNS using this route of administration therefore was fulfilled. Cur may possibly gain access to the brain tissue from the CSF compartment, but in the current investigation, Cur samples were not detected in the frozen brain sections for a number of reasons.

The level of Cur in CSF was found to be very low, consequently its concentration in the brain was expected to be even lower. Unlike CSF samples, the paraformaldehyde fixed tissue shows autofluorescence in the range of emission by Cur (FITC filter range). Therefore, fluorescence of Cur will in all probability be masked due to this autofluorescence. Furthermore, the thickness of the tissue which is generally used for the fluorescence microscopic analysis ranges from 5-20 μ, which could further limit the detection of Cur in such a small sample size. Use of confocal microscopy which allows the use of relatively thicker sections with more sensitivity and reliability was beyond the scope of the thesis. Therefore, increasing the sensitivity of the fluorescence enhancer cocktail used in the study and its further application in detection of Cur levels in paraformaldehyde fixed frozen tissue needs to be further investigated and could form a part of a future project. Recently, uptake of Cur by lung cells was detected at picomolar concentration by confocal microscopy (Kunwar et al. 2006). Future attempts to detect Cur in the brain tissue using a similar confocal method with a special focus on more sensitive

fluorescence enhancers which could detect Cur at an extremely low concentration will need to be developed.

In conclusion, VCP administered directly into the brain could be detected 3-4 h after being directly administered. There is thus evidence for its uptake after sustained administration intranasally. Increased background stain masks degree of uptake to some extent and ways to reduce this need to be further explored. It could be detected in CSF samples by the ELISA method using TMB peroxidase substrate with measures to reduce endogenous peroxidase activity. Immunological detection of VCP in the brain is possible, but the non-specificity or cross reactivity of the primary antibody might be responsible for the background staining. VCP and tVCP delivered intranasally could be detected in CSF at a very low level using ELISA. These compounds are also taken up in the glomerular cell layer of the rat brain as revealed by the immunohistochemical analysis. Also, Cur delivered intranasally reaches the brain in micro molar concentrations. A simple method using Tween-20 in combination with ethanol and GAA developed in the current investigation could be used to enhance its fluorescence specifically at 484 nm without interference of background fluorescence in CSF samples. The method can be used to detect Cur in biological samples. These data suggest that VCP, tVCP, and Cur could be delivered to the brain using intranasal route of administration, but it seems likely that multiple doses will be required in order to attain therapeutic concentration.

Chapter 5.

Intracranial Administration of VCP, tVCP and Curcumin in MO/HU APPswe PS1δE9 Mice to Investigate the Effect on Associative Learning Using a Cheese Board Maze Model.

5.1 Introduction.

As shown in the previous chapters, VCP administered directly into the brain is retained in the CSF for several hours. It was also shown that it is detected in the hippocampus and olfactory area after being administered directly into these brain areas. Recently, from a behavioural perspective, intracranial administration of a single dose of VCP was also found to be beneficial in APPswe transgenic mice at an early age (Pillay et al. 2008). The current study is an extension of the previous research work aimed at studying the effectiveness of early administration of VCP in the possible prevention as well as treatment of the disease at a later age.

5.2 Objectives.

The main objective of the present investigation was to measure the effect of direct administration of VCP at an early age on the cognitive impairment in APPswe mice at a later age. The specific objectives were to investigate the effect of intracranial administration of VCP at an early age on;

1) Cued learning at a later age in APPswe PS1δE9 mice using ChBM
2) Spatial learning at a later age in APPswePS1δE9 mice using ChBM
1) The plaque pathology in APPswePS1dE9 mice using thioflavine S staining (qualitative analysis)

5.3 Materials.

Mo/Hu APPswe PS1δE9 transgenic mice (APPswe mice) supplied by Jackson laboratories. VCP was expressed in *P. pastoris* yeast expression system or highly pure endotoxin free VCP supplied by Inflamed, KY, USA). HEPES (Sigma), complete EDTA free protease inhibitor cocktail tablets (Roche). The transgenic mice used in this study were previously characterized for the presence of APPswe and PSEN1 transgenes. The same method mentioned in the chapter 6 was followed for the PCR characterisation of the transgenes, and the same primers were used for the detection of transgenes (Appendix P).

5.4 ChBM (Fig. 5.1) and description of the behavioural room.

The ChBM used in the current study consists of a circular wooden board, 80 cm in diameter, with 156 wells each of 1 cm in diameter and 1 cm deep. The wells were arranged in parallel rows in such a way that the distance between the nearest points of the two wells was approximately 2.5 cm. Three pictures composed of black and white geometric shapes, positioned at a distance of approximately 2 m from the centre of the maze at three different positions in the room served as extra-maze cues. The maze was elevated to a height of 72 cm from the ground.

Cheese Board Maze.

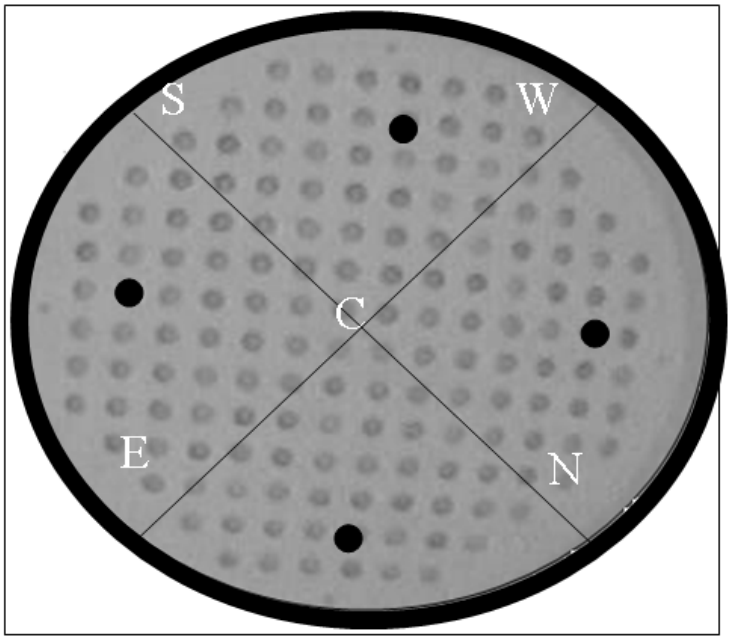

Figure 5.1 *Diagrammatic representation of a ChBM indicating positions of RF (Flagged wells baited with odourless food pellets shown by dark circles), and positions of mouse release points (S, E, N, W and C)*

5.5 Methods.

5.5.1 Grouping and intracranial administration.

The APPswePS1δE9 mice were divided into 3 treatment groups (n = 6). VCP was administered intracranially to a group of transgenic mice (5 µl of 1.7 µg/ml) on two occasions to group one, named as VCP treated group. Saline was administered to the second of group transgenic mice (ST). A group of transgenic mice with no treatment (Tg-only) was included as a sham control. VCP and saline injections occurred at 3 weeks and between 6 and 7 months of age. A group of non-transgenic mice (SNT) treated with saline was also included. For the intracranial administration, the mice were anaesthetized using standard i.p. dose of ketamine-xylazine mixture (1.2 ml of 90 mg/kg ketamine + 0.8 ml of 20 mg/kg of xylazine diluted to 10 ml using 0.9% saline). 5 µl of saline or VCP (1.7µg/ml) was administered intracranially by placing the needle in the parietal cortex area. The mice were continually monitored for ill effects after recovery from anaesthesia and regularly on the following few days.

5.5.2 Behavioural Methods.

1.*Mild food deprivation protocol for behavioural study* (Pillay et al. 2008):

The mice used in this study were subjected to a day-night cycle (12 h dark: 12 h light) with free access to standard food pellets and water and kept in a temperature controlled room of a standard animal house.

When mice reached an age of approximately two years, from the day before the pre-training task commenced they were subjected to a mild food deprivation protocol. Throughout the food deprivation protocol, mice were monitored for the weight loss, and due care was taken so as to not to allow the percentage weight loss to fall below a maximum of 15% of the original body weight. The odorless sugar pellets were put in mice cages (5 pellets / cage) one day before pre-training task to accustomize mice to the odorless pellets prior to the start of the experiment, so doing eliminating hyponeophagia. Otherwise mice were maintained on standard pellets throughout the study.

2. *ChBM paradigms* used in the current study with broad definitions: The ChBM is described as a dry land version of MWM (Kesner et al. 1991, Kesner et al. 1992) which is a relatively well known and thoroughly tested model for the assessment of spatial learning paradigm. It should be noted that although the names of the ChBM paradigms studied here appear similar to some of the MWM tasks, there is some differences in the learning patterns in these two models. Therefore, the definitions and/or concepts behind the various paradigms used in the current investigation are briefly summarized in this section. The behavioural tests and the protocols are also summarized in the table 5.1 just before the statistical analysis section.

a. *Pre-training:* Before Pre-training, the mice from different treatment groups were habituated (10 min) for ten days on ChBM with one pellet in each of the holes of the ChBM and no platform. Approximately 24 h after food deprivation, mice were subjected to a three day pre-training task. For this, four identical flags (as depicted in Fig. 5.1) were kept approximately at the centre of each of the four arbitrarily divided quadrants of the ChBM. For the pre-training, each mouse under trial was placed in the centre of the ChBM, and allowed to explore the maze for 5 min every day for three days at approximately the same time of the day. The extra-maze spatial cues (objects and pictures in the room) and position of the flags was kept the same throughout the pre-training task. The objective of the pre-training was that each mouse should learn to associate the flag with food (Reward flag = RF). This type of learning is referred to as associative learning. The number of odorless pellets consumed, as well as the number of times RFs were visited during the five minute period was recorded to compare the associative learning abilities of different the treatment groups.

b. *Cued- learning task:* The cued-learning task for ChBM can be defined as a type of associative learning. The mouse has to learn that the visible cue (i.e., the flag) on ChBM is associated with the reward pellets. The experiences reinforce one another and can be linked to enhancing the learning process. This test which essentially reflects associative learning abilities of different treatment groups is independent or less dependent on the hippocampus based spatial learning. The cued-learning task consisted of four sequential trials (duration each trial = 60 s, inter-trial interval = 20 min). For each trial, the mouse was released from a fixed position (South), and the flag was placed in a new position (random positions selected out of 5 locations, NE, SW, SE, NW and C). The flag was baited with 4 pellets during each trial. The mouse was required to visit the baited flag within 60 s, that is, it should find the 1st pellet hidden in the flagged well within 60 s. The mouse was permitted to consume the single pellet. If the mouse failed to locate the well

within this 60 s time frame, this was scored as a non-visit and it was then placed near RF for further 30 s. This training task also lasted for three consecutive days.

c. *Spatial acquisition task:* The three day spatial learning task was similar to the Cued-learning task; however the mice were released from a new position during each trial, the release point being selected out of five random release positions (N, W, E, S and C). This learning paradigm, although it involves associative learning like the previous paradigm, the release position changes frequently during each trial unlike the previous paradigm. During each trial, before searching for the flagged well baited with pellets, the mouse has to understand its spatial location using extra-maze cues and relative position to the flag and therefore quickly has to orient itself using these cues to locate the reward pellets in the stipulated 60 s. As the position of the flag changes during each trial, the task is comparable to the spatial working memory test in MWM, where the position of the escape platform in MWM is changed during each trial.

d. *Probe trial:* This was similar to the Cued-learning task with some modifications and was done on two consecutive days after the above mentioned learning paradigms were completed. While carrying out probe trials, flags were not baited with pellets in both trial one and trial four. It was designed so as to check whether the mouse under trial was not associating the odor (although pellets were deemed odorless) of the pellet, but rather associating the reward (pellets) with the flag. Only two probe trials were performed to avoid the so called "extinction effect" as observed with the repeated probe trials in MWM study (Vorhees and Williams 2006).

e. *Reverse probe trial:* This session was similar to the spatial-learning task with some modifications and was done on two consecutive days. While carrying out probe trials, flags were not baited with pellets in trial one and trial four. The reverse probe trial was designed to test whether the learning during spatial acquisition involved spatial and associative components of learning.

Summary of behavioural methods.

Test	Method	Days
Pre-training	Mice were allowed 5 min to investigate four flag positions on ChBM, each baited with pellets. The number of food pellets consumed and the number of times flags visited were recorded. Constant release position.	Three days (1x 5 min trial /day)
Cued Learning Task	Each mouse was allowed to find the reward flag (flag baited with pellets). The time taken to find the baited flag in four trials of 60 s each was recorded. The release point was always the same and the location of the platform changed randomly.	Three days (4 trials x 60 s / day)
Spatial Learning Task	Same as Cued trial, but four different randomized release points out of five positions (S, N, E, W and C).	Three days (4 trials x 60 s / day)
Probe Trials	Same as Cued trial, baited flag on trial 2 and 3, but no pellets on trial one (Probe one) and Trial Four (Probe 2).	Two days (4 trials x 60 s / day)
Reverse Probe Trials	Same as spatial trial, but no pellets in Trial one (Reverse Probe 1) and Trial four (Reverse probe 2).	Two days (4 trials x 60 s / day)

Table 5.1. *The behavioural test, method of behavioiural study and duration of each training task.*

5.5.3 Statistical analysis: This was done using STATISTICA software. ANOVA was used for the probe and reverse probe trials whereas repeated measures ANOVA (RMANOVA) was used for pre-training, Cued and spatial trials. The statistical analysis was done using more than one Post-Hoc analysis for better interpretation of the data, but the standard test Newman Keul's test for multiple comparisons is used to represent the level of significance between the treatment groups. The less stringent Duncan test was used to check the general trend of the differences between the treatment group in the cases where the stringent and standard post-hoc test such as Newman Keul's test for multiple comparison (NK) failed to show significant difference between the treatment groups. The same trend is followed throughout the behavioural study in subsequent chapters. The summary of statistical results is provided at the end of results section.

5.5.4 Thioflavine S staining.

After completion of the behavioural study, mice were deeply anesthetized, and just before the heart stopped pumping, they were transcardially perfused using HEPES buffer followed by freshly prepared 10% buffered formalin, and processed for paraffin-embedding. For thioflavine S staining, the protocol described by others (Yang et al. 2005) was followed with some minor modifications. Briefly, the following procedure was followed: Approximately 7 to 10 μ thick sections were deparaffinized by using xylol and rehydrated by treatment with absolute alcohol, 95 % and 70% alcohol prior to incubation with 0.3% Triton X-100 and 0.1 M PBS (pH 7.2) containing 3% BSA with 0.5% Tween 20 for 10 min each. The sections were then stained with 1% thioflavine S prepared in 40% ethanol for 10 min at room temperature and dipped for 1 min each in 70% ethanol, 95% ethanol, absolute ethanol followed by 95% ethanol, and 75% ethanol. Some of the sections were cryoprotected and frozen in Tissue-Tek O.C.T. compound instead of paraffin embedding, and thus were not dewaxed. These sections were directly subjected to thioflavine S staining after dipping them in 70% alcohol for ten minutes. After staining, fluorescent mounting medium (Mowiol-1994; Hoechst containing propyl-gallate [as an anti-fading agent], 0.2 M Tris + glycerol buffered at pH 8.5) was added, and the sections were then covered with a thin glass cover slip. All the sections were examined for the presence of plaques and photographed using Alexa-488 and Cy-3 optics, either singly or in combination of AxioVert fluorescence microscope at UCT. Only combined images are shown in Fig. 5.10.

5.6 Results.

The various treatment groups were subjected to behavioural paradigms discussed in the materials and methods sections and summarized in the Table 5.1. The results of different paradigms to which these mice were subjected are discussed in this section. Figures mentioned in each of the behavioural tasks discussed, summarizes the performance of each group and significance of the finding. P-values for all the results obtained are indicated using ANOVA tests. The post-hoc analysis using stringent Newman-Keul's (NK) multiple comparison test and less stringent Duncan (D) are also shown in the Summary of results section as well as in the Appendix R. These data are also presented graphically (error bars indicating +/- SEM) and

significant differences are indicated by asterisks. The color of the asterisk(s) matches with the color(s) of the bar representing mean values of a group whose value differs significantly.

5.6.1 Pre-training session.

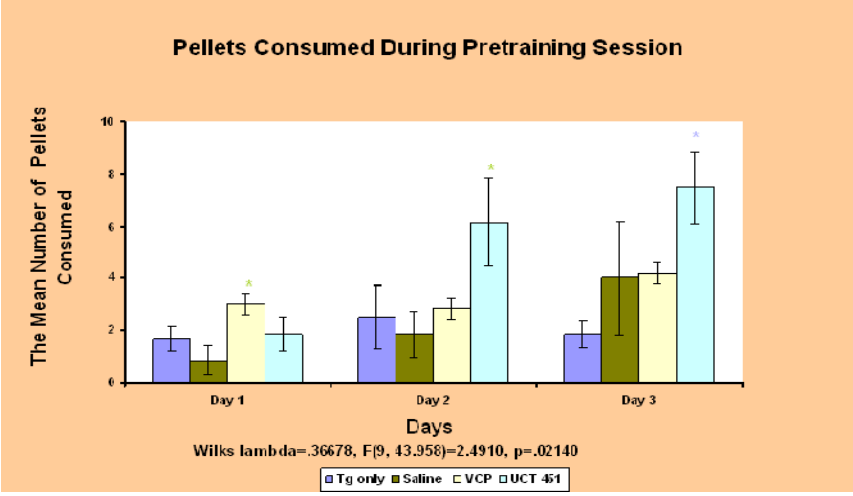

Figure 5.2. *The mean number of pellets consumed (Y axis) by various treatment groups (X axis). The level of significance of the difference between the treatment groups is shown by colour coded asterisks. The colour of the asterisk(s) matches with the colour(s) of the bar(s) being compared.*

Results: RMANAOVA revealed a significant difference in the mean number of pellets consumed by the treatment groups during 3 days of pre-training session. VCP treated group on day one (NK), and SNT group on day two (D) differ significantly from ST mice in the mean number of pellets consumed by them (Fig. 5.2). There was no significant difference between the mean number of pellets consumed by various treatment groups on day three of pre-training task (NK). However, less stringent D test revealed a significant difference between SNT and Tg only groups in the mean number of pellets consumed by them on the final day of pre-training session (R5.1B, Appendix R).

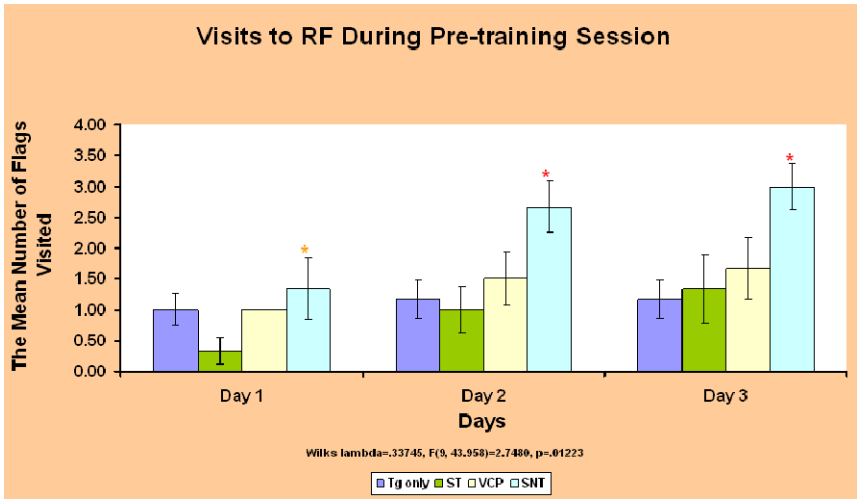

Figure 5.3. *The mean number of visits to flags (Y axis) by different treatment groups (X axis) during pre-training session of ChBM.*

Results: The analysis of the mean number of visits to RF by various treatment groups using RMANOVA/ANOVA test show that there is a significant difference in the mean number of visits to RFs during pre-training session (Fig 5.3). Further post-hoc analysis using NK suggested that the mean number of visits to RFs by SNT group revealed that there was no significant difference between the mean number of visits to RFs by various transgenic treatment groups (ST, VCP and Tg-only) during the pre-training task . The SNT group showed more visits to RFs than all the transgenic groups on day two and three of the pre-training task (NK/D). SNT mice also showed a significant difference from ST group (D) on day one of pre-training session, but there was no difference between SNT and VCP treated mice on the day one of pre-training session (Table R 5.2B, Appendix R).

5.6.2 Cued-trial session.

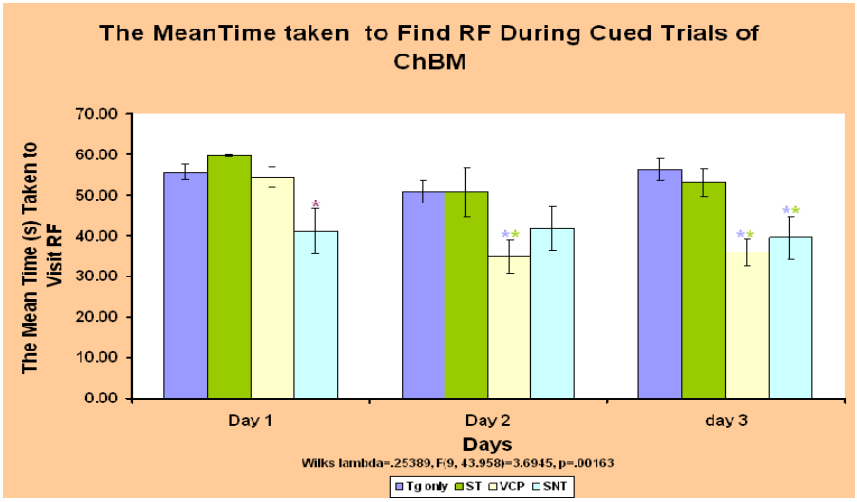

Figure 5.4. *The mean time taken to visit RF (Y axis) by the treatment groups (X axis) during cued trial task of ChBM. The level of significance is shown by colour coded asterisks. The colour of the asterisk matches with the colour of the bar being compared. The red coloured asterisk indicates difference from all the treatment groups*

Results: As evidenced from P-values from RMANOVA, and shown in summary of results (Section 5.6.7) and Fig 5.4, the difference in time taken by treatment groups to visit the RF was highly significant (P = 0.00163). The post-hoc analysis using NK (and D) suggested that SNT mice took significantly less time to visit the RF on day one than that of the other groups. There was no difference in the mean time taken by the treatment groups to visit the RF on day two as revealed by NK, however, on day three, VCP treated mice and SNT mice took significantly less time to visit the RF than all other transgenic control groups (Table R5.3B, Appendix R) Inspection of the D test results also lead to a similar conclusion, and suggests that the time taken by the VCP treated group on day two was significantly less than that of ST and Tg only groups.

5.6.3 Spatial Trials.

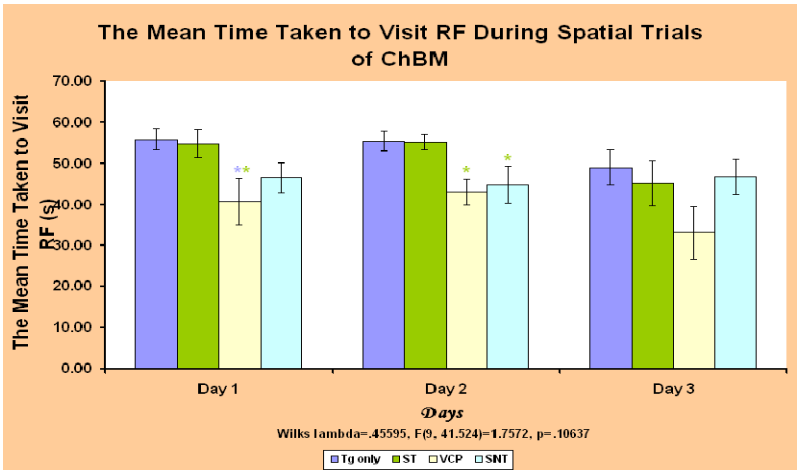

Figure 5.5. *The comparison of the mean time taken (Y axis) by different treatment groups (X axis) to visit flags during the spatial-learning task of ChBM. Significant differences are indicated by asterisks. The colour of the asterisk(s) matches with the colour(s) of the bar(s) being compared*

Results: There was no significant difference between the treatment groups in the time taken to visit the RF as suggested by P-value of RMANOVA (Summary of results [5.6.7] and Fig 5.5). The post-hoc analysis using NK lead to similar observation, however, less stringent test (D) suggested that VCP treated mice on day one and day two as well as SNT group on day two took significantly less time than that of the transgenic control groups (Table R5.4B, Appendix R). On day three, however, the treatment groups did not differ from each other in time to find the RF as suggested both by NK and D tests.

5.6.4: Probe Trials.

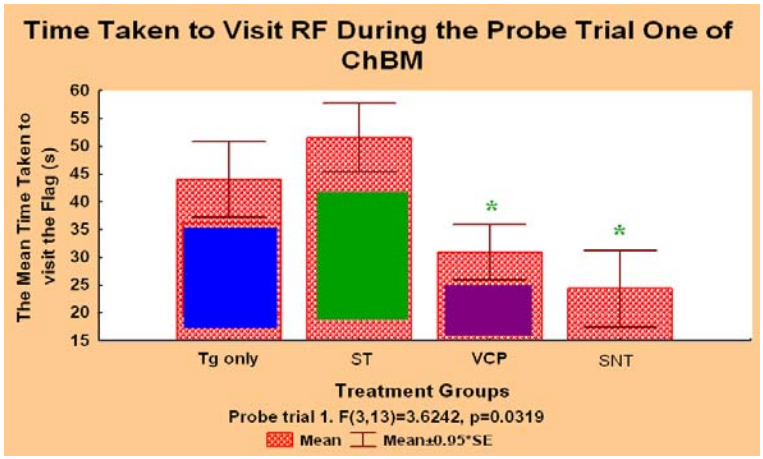

Figure 5.6. *The mean time taken to visit RF (Y axis) by the various treatment groups (X axis) during probe trial one.*

Probe trial one: The analysis of the probe trial results using ANOVA revealed that SNT mice took significantly less time than that of all other treatment groups to visit the RF during probe trial one (NK; Fig 5.6). The less stringent post-hoc analysis (D) also indicated that the mean time taken by the treated group is significantly less than that of the ST group (Fig 5.6, Table R5.5B).

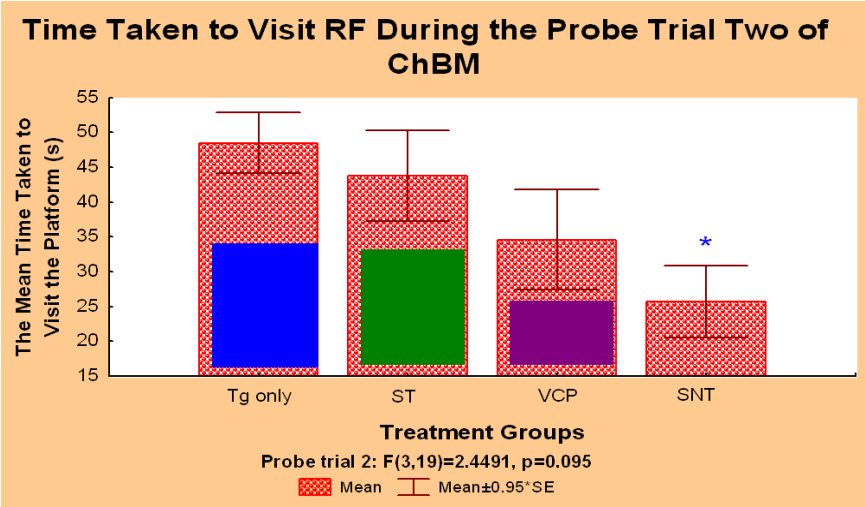

Figure 5.7. *The mean time taken (Y axis) by various treatment groups(X axis) to visit RF during the probe trial two of ChBM.*

Probe trial two. No significant differences for the different treatment groups are revealed by ANOVA for the probe trial two. Post-hoc analysis using NK also revealed no difference amongst the treatment groups. However, the less stringent statistical analysis revealed a significant difference between SNT and Tg only groups. VCP took less time to find RF than the transgenic controls, but the effect was not significant (Fig 5.7).

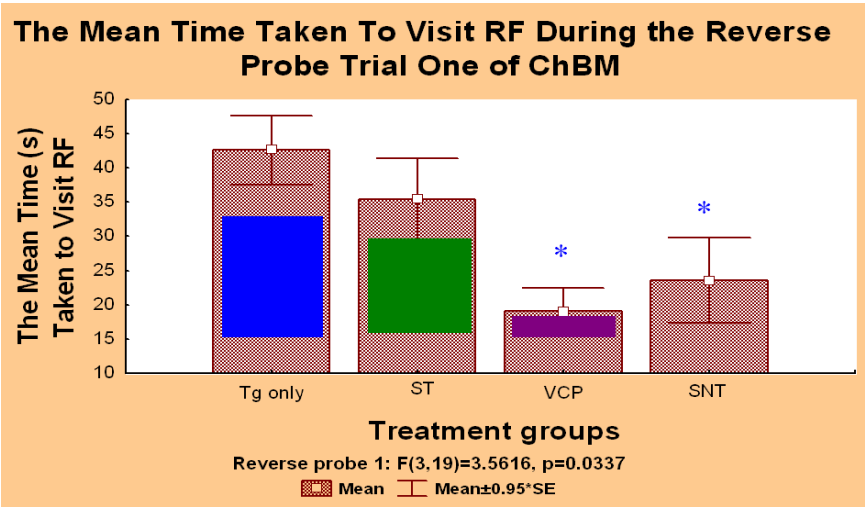

Figure 5.8. The *comparison of the mean time taken by different treatment groups to visit flags during the reverse probe trial one.*

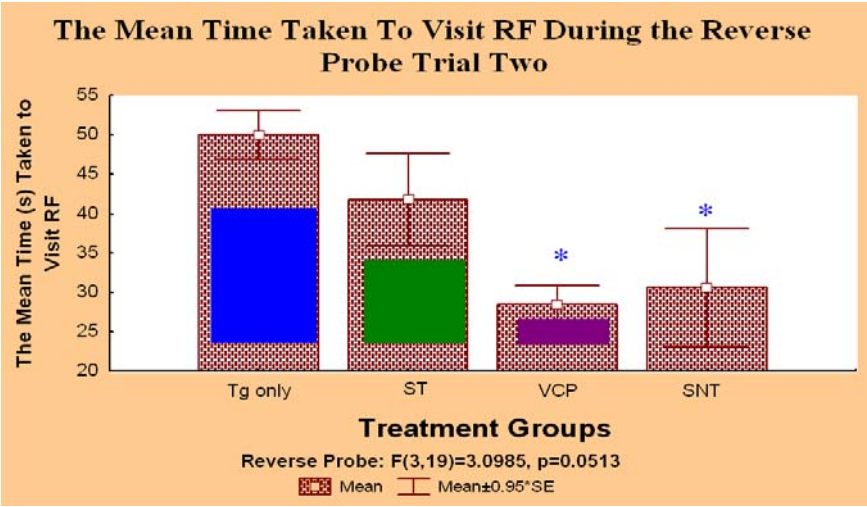

Figure 5.9. *The comparison of the mean time taken(Y axis) by various treatment groups(X axis) to visit RF during reverse probe trial two.*

5.6.5 Reverse probe trials (one and two). As suggested by p values (Section 5.6.7, Appendix R [table R5.7A] and Fig. 5.8), during this trial, the treatment groups differed significantly in the mean time taken by them to visit the RF. Further post-hoc analysis using less stringent D test revealed that VCP treated mice and SNT mice took significantly less time to locate the RF than that of the other groups, however, NK test showed that only VCP treated group took less time than that of the Tg-only mice.

As can be seen by the P-value (Section 5.6.7, Appendix R [R5.8B], and Fig. 5.9), the treatment groups do not differ significantly from each other in their ability to find the RF during this trial. While the NK test led to the same conclusion, the less stringent D test revealed that both VCP treated and SNT mice took significantly less time to visit the flag than that of the other transgenic control groups.

5.6.6 Thioflavine S staining of mice brain sections

Thioflavine S staining

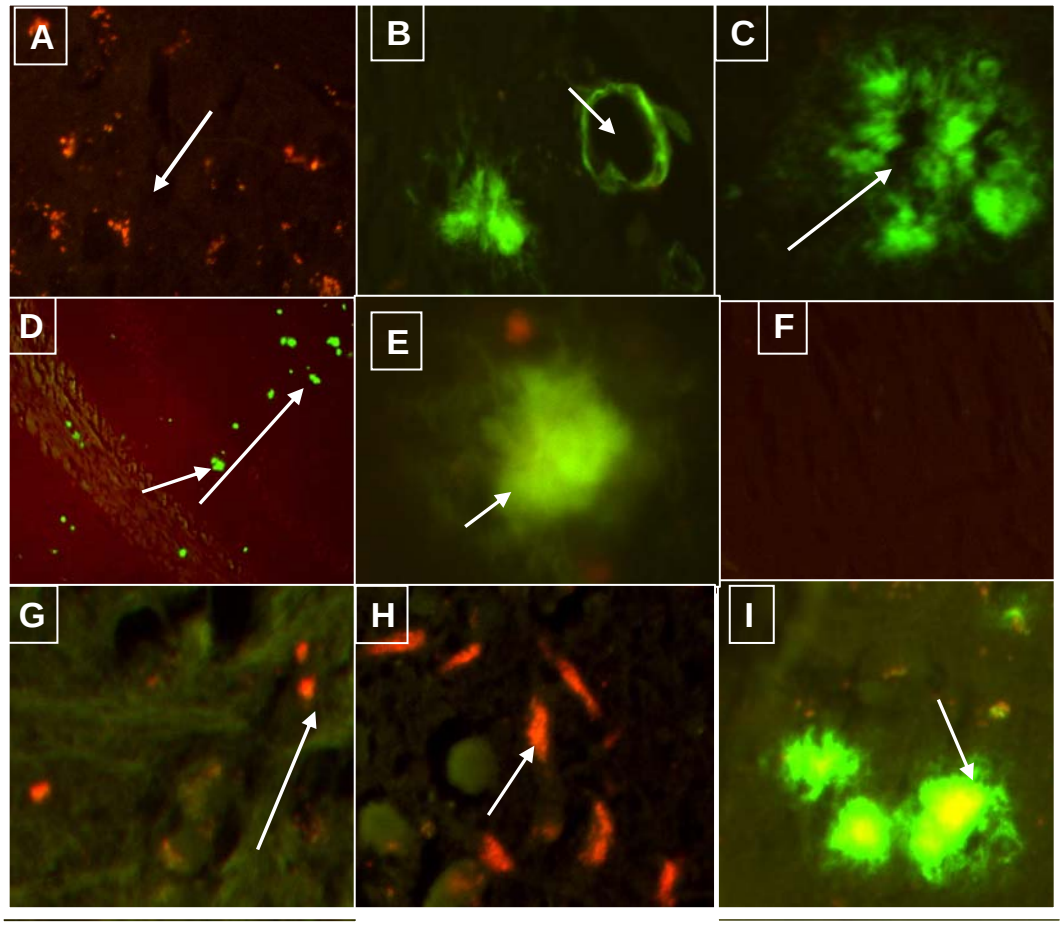

Figure 5.10. *The emission spectras using Alexa-488 (green fluorescence) and cy-3 (red fluorescence) filters of AxioVert fluorescence microscope were combined to obtain the images shown in this Figure. Image (a) is a representative view of frontal cortex in ST group. Images (b)–(e) representative views of Tg-only group, where images (b) and (d) show fluorescent staining (apple green color) in cortical sections indicating scattered plaques and an example of an amyloid containing section showing green fluorescent solid amyloid plaques. Image (e) is an example of the olfactory cortex.. Image (f): representative view of cortex in SNT group. No fluorescent (green and red) staining observed in this SNT group. Images (g) and (h) are representative images from two individual VCP treated transgenic mice brain sections showing red fluorescent structures but no green fluorescent plaques. Image (i): image of cortical area obtained from a representative section of a VCP-treated transgenic mouse brain showing the presence of green fluorescent plaques blood vessel.*

Thioflavine S staining.

Thioflavine S staining patterns of different brain region sections from the treatment groups subjected to Alexa-488 and Cy3 filters of the fluorescence microscope are shown in the Fig 5.10. As indicated in the Fig. 10 legend, the images shown are a combination of green and red fluorescence emitted by thioflavine S stained plaques/structures. As shown in image of the Fig 5.10, using high magnification.

(40 x) revealed no significant apple green fluorescence in one ST mouse. However, there is red fluorescence observed in various parts of the brain, especially in the cortex as shown here. Thioflavine S staining of the sections from various parts of the brain sections obtained from Tg only group reveals apple green fluorescent labeled plaques as shown in the panels b and c (40 x). These samples also showed red fluorescence with the Cy-3 filter. The image of a thioflavine S stained blood vessel and typical solid amyloid plaque emitting apple green fluorescence is shown in Fig. b and c (Tg only), respectively. Using low magnification (10 x) of thioflavine S labeled cortical brain sections reveal numerous solid plaques throughout the cerebral cortex, as shown by solid green fluorescent structures in d (Tg only), Fig 5.10. The magnification of the solid plaque at 100 x is shown in e as a bright apple green fluorescent body. Neither green nor red fluorescence was observed at 40 x magnification of the brain sections procured from the SNT mice and as shown in f. The brain sections from two different VCP treated mice (images g and h) showed red fluorescent structures in the cortical areas but no green fluorescence. The brain section from three of the mice treated with VCP showed green fluorescence similar to transgenic controls. The typical green fluorescent plaques in one of the brain sections in the cortical area of a VCP treated mouse is shown in image (i) of Fig. 5.10. The few brain sections and examples shown here qualitative assessment of VCP treatment are represantative for the various groups of mice.

5.6.7 Summary of Results.

Sr. No.	Trial	Parameters	ANOVA/ RMANOVA	Post-Hoc analysis (NK/D)	Conclusion
1	Pellets consumed during pre-training session. (Fig 5.2)	Day one	p*=0.0214	VCP*>ST	SNT groups performed better than other groups during pre-training session. On the commencement of the trial, VCP treated mice performed better than the transgenic control ST and the overall difference in the levels of significance values between VCP and SNT was less than the transgenic controls indicating better performance of VCP group.
		Day two		SNT*>ST(D)	
		Day three		SNT*> Tg-only (D)	
2	Visits to RF during pre-training (Fig 5.3)	Day one	p*= 0.01223	SNT*>ST(D)	
		Day two		SNT>All other groups (NK)	
		Day three		SNT>All other groups (NK)	
3	Cued Trials (Fig 5.4)	Day one	p*= 0.00163	SNT>All other groups (NK/D))	Impairment in cued learning task. VCP treatment of transgenic mice improves spatial learning.
		Day two		VCP and SNT*> ST and Tgonly (D)	
		Day three		VCP and SNT >ST and Tg only (NK/D)	
4	Spatial Trials (Fig 5.5)	Day one	p= 0.10828	VCP*>ST and Tg only (D)	Slight impairment on the initial days of spatial learning. VCP treatment improves the same.
		Day two		VCP*>ST(NK) SNT*>ST (NK)	
		Day three		No* (NK)	
5	Probe trials (Figs 5.6 and 5.7)	One (Avg of two trials) (Day one and Day two)	p*=0.0319	SNT>ST (NK) VCP and SNT*>ST (D)	Better performance during probe trial by VCP treated mice than the transgenic controls during the probe trial one.
		Two (Avg of two trials (Day one and day two)	p=0.0950	No* (NK) VCP and SNT*ST (D)	
6	Reverse probe trials (Figs 5.8 and 5.9)	One (Avg of two trials) (Day one and Day two)	p*=0.0337	VCP>Tg only (NK) VCP and SNT*>Tg only (D)	Better performance by VCP treated mice than the transgenic controls during the reverse probe trial one. No difference between the treatment groups during the reverse probe trial two.
		Two (Avg of two trials) (Day one and Day two)	p*=0.0513	No* (NK) VCP and SNT*>Tg only (D)	
D =Duncan test, NK = Neumann-Keul's multiple comparison, RMANOVA = repeated measures ANOVA					

5.7 Discussion.

In the current investigation, VCP was tested for its therapeutic effectiveness in the treatment of AD using APPswe transgenic mouse model. APPswe double transgenic mice used in the study represent a familial form of AD due to expression of APPswe and PSEN1A genes. Previous studies with VCP suggested beneficial roles of VCP in rodent models of CNS disorders (Reynolds 2003; Reynolds 2004; Hicks 2002; Pillay 2005; Pillay 2006T, Pillay 2007). The current study was carried out to determine the effectiveness of intracranially administered VCP at an early age in contributing to the improvement of AD associated cognitive decline at a later age. The results of the various learning paradigms and cognitive behavior testing by use of ChBM suggest improvement in the cognitive decline in 2 to 2.3 year old mice by intracranial VCP treatment at an early age.

On commencement of the pre-training task, VCP treated transgenic mice showed better performance on the than that of the transgenic counterparts as indicated by a greater number of pellets consumed by this group compared to their transgenic counterpart (ST) on the first day of pre-training session (Fig 5.2). This indicates a better learning ability of the VCP treated groups compared to the other two groups during the initial days of pre-training session. However, there was no significant difference in the mean number of visits to RF by the transgenic treatment groups (Fig. 5.3) although the trend in mean values of VCP is on higher side than that of the ST groups on all the three days. It is thus concluded that VCP tends to improve the performance of mice during the pre-training session. As anticipated, the SNT group, however, performed better than all the transgenic treatment groups during the pre-training session.

During the cued-learning task of ChBM, the VCP and SNT groups took significantly less time (Summary of results table [5.6.7]) to visit the RF compared to that of the transgenic controls on days two and three. On the first day of cued learning there was no difference between VCP treated groups and the transgenic controls (ST and Tg only), however VCP treated group showed gradual improvement of their performance on days two and three which was significantly better than that of the transgenic counterparts. This gradual increase in their performance could be attributed to improved cognitive abilities compared to that of the Tg-only and ST groups.

The cued-learning paradigm used on the ChBM differs somewhat from the cued-learning task in the MWM context. Although ChBM is considered a dry-land version of MWM (Kesner et 1991, Kesner et al.1992), it is necessary to differentiate the cued-learning trial in ChBM from that of MWM. In MWM, this task is performed to study whether the observed difference in the performance of the treatment groups is due to impairment of the visual system. The cued-learning in ChBM is an associative learning task. As the release position is the same and only the position of the flags changes during each trial, it is difficult for the mouse to locate the reward based only on extra-maze cues. The mouse learns to associate the flag with the reward rather than relying solely upon the spatial cues. Although there is to some degree, a spatial component involved, the mouse under test has to associate the reward object (flag) with the reward (odorless sugar pellets) in order to obtain the reward. Thus, from the significant results ($P = 0.00163$

ANOVA) of cued-learning trials and subsequent post-hoc analysis, there is a clear indication that intracranial administration of VCP at an early age improves associative learning in 2 to 2.3 year old APPswe transgenic mice.

The probe trial was designed to study the reference memory of the cued learning task. This trial was done to ensure that the observed improvement in cued-learning was not associated with the ability of mice to smell the pellets (although odorless pellets were used), and that mice were really able to get the reward solely on the basis of their ability to locate the RF.

The better performance of VCP treated mice during the probe-trial compared to that of the transgenic controls suggests improvement of reference memory by VCP and is also indicative of the observed improvement in the cued-learning task, as well as being a true reflection of the associative learning.

The spatial learning task in ChBM however shows some degree of similarity with that of MWM. However, the spatial acquisition task designed in the current ChBM model is not solely spatial, but involves some degree of non-hippocampal associative learning as well.

The treatment with VCP does not improve the spatial learning to the extent that it improves cued-learning as shown by the results with the spatial learning trial tasks as well as reverse probe trials (ANOVA/ RMANOVA and NK), however, the less stringent post-hoc test suggests a similar trend to that of cued-learning with VCP where SNT mice performed better than that of the transgenic controls (Table R5.3B, Appendix R). The NK test reveals better performance of VCP treated group than that of ST.

The brains of the various treatment groups were qualitatively examined by means of thioflavine S fluorescence detection. Thioflavine S staining detects amyloid plaques, indicated by apple green fluorescence in the Tg-only group as shown in Fig 5.10. The location of the plaques in the groups is predominantly in the cerebral cortical area as shown in D of Fig. 5.10.

There is also an evidence of thioflavine S staining of the blood vessels (B of Fig 5.10), an observation recorded as well by other researchers (Backsai et al. 2001) or discussed in many reviews (Fan et al. 2007; Selkoe 2001). The plaques were classified as solid (C, and E of Fig 5.10) and can be described as type-I amyloid plaques with dense core (as apposed to diffuse plaques) as observed and described by others (Bussiere et al. 2004). However, an unusual type of staining pattern (not described in the literature to the best of my knowledge) was observed in various parts of the brains of one of the mice from ST group subjected to thioflavine S staining. There are red fluorescence emitting structures scattered throughout the cortex as observed in Cy-3 filter (A, Fig 5.10). However, in SNT mice (F, Fig 5.10), there was neither red nor apple green fluorescence observed in these brain sections.

Three out of five of the VCP treated mice showed a pattern of thioflavine S staining similar to that of ST mice, whereas two out of five VCP treated mice showed no green fluorescent plaques and only red fluorescent structures similar to one of the mouse brain section from ST group. The apparent number of plaques as well as the amyloid staining pattern showed variation amongst the mice from the VCP treated

group. However, it is noteworthy that two out of five transgenic mice treated with VCP showed absence of green fluorescent plaques. The possibility of inadequate intracranial administration and/or slight variation of the site of injection of VCP may account for this variable pattern of staining observed in these mice. The outcome of the current investigation suggests that VCP improved associative learning in APPswe mice is most probably by virtue of its ability to regulate the inappropriately activated complement system. The effect of VCP on plaque pathophysiology however needs to be further explored. It would be informative to study VCP's ability to reduce the plaque burden in APPswe transgenic mice, as suggested by the preliminary qualitative data, by use of more precise morphometric and stereological analysis of plaque burden.

In the current study VCP improved associative learning which probably involves the hippocampus to a minimal extent. The hippocampus, the most important part of the brain associated with spatial learning, is involved in paired-associative learning only when the stimulus is dependent on spatial cues, and it may not play a significant role in associative learning tasks with lesser degree of involvement of spatial learning (Gilbert and Kesner 2002). This differential involvement of the hippocampus in these two different learning paradigms and the possibility of delivery of VCP to the hippocampus at a concentration below therapeutic level could be attributed to the minimal or insignificant improvement in spatial learning mediated by VCP as observed in the current investigation.

The outcome of the current investigation suggests that VCP improved associative learning in APPswe mice most probably by virtue of its ability to regulate the inappropriately activated complement system. As observed in this investigation, administration of VCP at an early age in APPswe mice prevents cognitive decline in old APPswe mice. Therefore, VCP may be useful in the prevention and treatment of amyloid associated brain disorders such as AD and HAD. The findings can be correlated to the distribution study in the previous chapter, where VCP was distributed throughout the CSF and detected in CSF several hours after its administration. It could thus be concluded that after direct administration, VCP is either retained in the brain for a long time and/or produces long term changes in the hippocampus at synaptic level to modulate the CNS response. It could thus be used as a model to develop complement based neuroprotective agents. In order to further increase its therapeutic value, it is proposed to deliver VCP to the brain via intranasal administration since this is less invasive route.

AD and HAD are complex disorders of the brain and not only cognition, but other behaviours are also affected. So, VCP, its analogue tVCP and Cur after being delivered to the CNS via non-invasive routes, need to be tested for the modulation of other behaviours such as anxiety and exploration. The effect on cognition should be tested using more than one model as each model test different aspects of learning and memory. In the subsequent chapters, VCP will be administered intranasally and the effect of VCP in modulating anxiety, spatial learning, working memory, and other forms of associative learning will be examined.

In conclusion, VCP treated APPswePS1δE9 mice show improvement in associative learning in APPswe transgenic mice probably due to VCP's complement regulatory activity and other biological roles discussed in the literature review. VCP therefore potentially be used in the treatment of neuroinflammatory and possible prevention of these types of disorders. Consequently, its therapeutic effectiveness after being administered by a non-invasive route such intranasal administration, as discussed in the previous chapters will be the subject of investigation in the next series of studies. The modulation of behaviour by VCP, tVCP and Cur will also be further explored using more than one behavioural model.

Chapter 6.

To Investigate the Effect of Intranasally Administered VCP, tVCP, and Curcumin on Anxiety and Exploratory Behaviour in MO/HU APPswe PS1δE9 Mice.

6.1 Introduction.

In AD, mutations in amyloid precursor protein (APP) and presenilin (PSEN1) gene results in deposition of amyloid plaques in the brains of AD patients, particularly in the cortex and hippocampus. Amyloid deposition triggers the proinflammatory mediators and there is a general decline in overall brain function due to widespread neuroinflammation in AD. The symptoms rapidly develop with the progression of the disease. The most common behavioural function affected in AD is cognition which results in dementia as the hippocampus and other brain areas are affected. There is a growing body of evidence that dementia is associated with anxiety and considerable work is being done in this direction from the last few years. The clinical features associated with various types of dementias including AD, and anxiety symptoms associated with them are thoroughly reviewed in a recent review (Seignourel et al. 2008). The types of anxiety associated with various stages of these disorders are also discussed in this review. No or minimal correlation between the anxiety and severe or terminal forms of dementia in AD was observed, but anxiety is found to be associated with an early stage of the disease. Similar changes in anxiety and / or abnormal exploratory behaviour are shown in animal studies using transgenic mouse models for AD (Lalonde et al. 2004, Puolivali et al. 2002, Savonenko et al. 2003).

Anxiety and exploration are opposing behavioural states. Anxiety reflects inhibitory state of mind whereas exploratory behaviour reflects disinhibitory state of mind. Increase in anxiety is associated with the decline in exploratory behaviour and vice versa. It has previously been reported that these two behaviours are affected in transgenic mice models, but the results vary considerably according to strain, age, and the model used for the study. No changes in the anxiety levels were observed in APPswe mice (Arendash et al. 2001). The level of anxiety in these animals was increased according to one report (Puolivali et al. 2002), whereas in 7 months and 12 months mice of the strain, there was an elevation in the exploratory behaviour and reduction in the anxiety in APPswePS1δE9 mice (Lalonde et al. 2004). Apart from the strain and age differences, variation in the methodology and the laboratory conditions, e.g., the changes in temperature of the behavioural room affects the anxiety and exploration behaviour in rodents (Martinez et al. 2007).

The data shown in the previous chapter suggest improvement in the cognitive impairment in APPswe transgenic mice by intracranially administered VCP using the ChBM model (Chapter 5 and Pillay et al. 2008). ChBM is an open circular field / arena elevated to a certain height similar to EPM. Therefore, it was also necessary to study the effect of VCP on anxiety behaviour in these mice to find out whether VCP improves cognitive deficit solely on the basis of modulation of cognition or through its ability to control anxiety / exploratory behaviour. Exploratory behaviour is related to anxiety and is an indirect measure of anxiety (Ohl 2003). Anxiety gradually affects exploration and anxiolytic compounds reduce the inhibition of exploration (Ohl 2003, Crawley et al. 1980, Handley and Mithani 1984, Pellow et al. 1985). Anxiety also represents cognitively driven behavioural inhibition in goal directed behaviour (Ohl et al. 2002, Ohl 2003, Ohl et al. 2003). The emotional memory and cognition are related to anxiety and exploration. Hence, it is appropriate to study the modulation of these behaviours by VCP and Cur.

In order to distinguish between anxiety and exploratory behaviour of various treatment groups, the EPM was used in this study, the reason being its suitability and its widespread use as a model to test these behaviours. The EPM model represents an unconditioned form of anxiety which can be assumed to be equivalent to generalised anxiety in human beings (Ohl 2003). Also, the model allows direct comparison of the anxiety and exploratory type behaviours.

The objectives of the present investigation were therefore as follows.

6.2 Objectives.

1. To measure the anxiety and exploratory behaviour of APPswe mice.
2. To test whether these behaviours are modulated by VCP, tVCP and Cur administered via the intranasal route.

6.3 Materials.

Highly pure VCP and tVCP (Chapter 2), Cur (Sigma; solution: Appendix S), complete EDTA-free protease inhibitor cocktail tablets were from Roche Diagnostics (provided in *EASYpack),* Taq-DNA-polymerase (Taqpol; 5 U/µl), 10X reaction buffer, $MgCl_2$ (25 mM), dNTP mix (10 mM) from Peq-Lab, Germany (supplied by Optima Scientific Co., SA). Proteinase-K (Roche Diagnostics, Gmbh, Germany), PCR primers (Appendix P) and templates (Integrated DNA technologies, USA; www.jax.org). Kb bench top DNA ladder, Promega, USA), gel loading pipette tips for intranasal administration (Eppendorf; long, flexible with circular orifice), thermoregulatory pad, EPM for mouse (Part No. ENV 560, MED associates inc. P.O. Box 2089, Georgia, VT 05468), web surveillance camera for video recording, Ethovision 3.1 (Noldus) HEPES (Sigma), Mo/Hu APPswe PS1δE9 transgenic mice (APPswe mice; either sex) supplied by Jackson laboratories.

6.4 Methods.

6.4.1 Housing and the Mice Strains.

The stock mice (Mo/Hu APPswe PS1δE9) were housed in RAF, FHS, UCT with ambient air, temperature, and free access to water and food pellets. All the animals were maintained under a 12 h light and dark cycle. The male mice and females were group housed in separate cages. The mice were bred at the RAF The mice were free from all the known pathogens. The serum collected from representative mice (No CB2; BioDoc No 17500) were sent to Laboratory for Biomedical Diagnostics-BioDoc (Laor fur biomedizinische Diagnostik), Hannover, Germany, and were screened at 1:20 dilutions by Indirect Immunofluorescence for all the known pathogens including *Toxoplasma gondii*, SV5 and Rotaviruses. The protocols were approved by Animal Ethics Committee (AEC), FHS, SA (Ref: 04 / 030 and amendments).

6.4.2 Genotyping of mice.

Since the mice used in this study had not been characterized for the presence of APPswe and PSEN1 genes, it was considered necessary to confirm the genotyping.

Characterization of APPswe transgenic mice: The mice tails (transgenic and non-transgenic) were digested using proteinase-K lysis buffer (PK lysis buffer) and were characterized for the presence of APPswe (350 bp), PSEN1A (608 bp) and PSEN1B or MPP genes (750 bp) by PCR and subsequent Agarose gel electrophoresis (0.7 % gel) using TBE buffer. The method described by Jackson laboratories (www.jax.org) was followed for isolation of DNA as well as PCR analysis and the PCR products were separated by agarose gel electrophoresis (Refer Appendix P for the Primers, Genotyping and PCR analysis).

6.4.3 Grouping.

One year old transgenic mice were divided into five groups (n=6, except for tVCP = 4 as two mice died before starting the behavioural study). Saline treated transgenics (ST), rVCP treated (VCP), tVCP treated (tVCP), Cur treated (Cur T) and saline treated non-transgenic mice (SNT).

6.4.4 Dosing schedule and the Intranasal Administration.

Cur solution was prepared as mentioned in the Appendix S. VCP, and tVCP were highly pure and free of endotoxin (Chapter 2).

For intranasal adminstration, mice were anaesthetised with 0.2 ml of ketamine-xyalzine mixture (*1.2 ml of 100 mg/kg ketamine and 0.8 ml of 20 mg/kg xylazine mixed and diluted to 10 ml normal saline*) injected intraperitoneally (i.p.). Once the mice were surgically anaesthetized, they were maintained with their backs on heating pads. A thermister probe maintained the pad at 37^{O}C. The compounds under study (rVCP, tVCP, Cur and saline) were then administered intranasally using Eppendorf gel loading pipette tips (sterile). The mice were allowed to remain on the heating pads on their backs for about 45 min. Once they started recovering from the anaesthesia (moving tails and / or formation of drops of urine), they were returned to the respective cages for full recovery. The multiple dosing regimen was used prior to EPM study as shown in Appendix F (Fig F1.3). The volume (10 – 14 μl), was adjusted depending upon the final dilutions of VCP and tVCP to give 10-14 μg / mouse during the first 8 days of intranasal administration, after which the dosing was increased to 36 μg to 42 μg/mouse from the day 8 and onwards. The dosing was repeated and carried out at regular time intervals for 26 days prior to the EPM study. The final dosing was done a day before (16h to 18h) EPM study. The dosing regimen was as shown in the figure shown in Appendix F (Fig F1.3). The multiple dosing regimen was adopted to follow for the following reasons:

The distribution study suggested that VCP and tVCP administered intranasally reaches the olfactory lobe of the brain, and enters the glomerular cells of the brain as shown by immunostaining (Chapter 3). The VCP and tVCP were detected in the CSF at low level. In order to attain therapeutic concentration, it is considered necessary to administer multiple doses of VCP. It has previously been shown that VCP was

taken up in a mixed mast/endothelial cell culture (Reynolds et al. 2000), and shown to bind to heparin (Smith et al. 2000, Smith et al. 2003, Murthy et al. 2001) as well as to the complement components using Q-sense or SPR (Chapter 3, Smith et al. 2003). As discussed in the review of literature, the complement components are elevated in AD and are associated with the elevated levels of amyloid proteins. Thus, it was considered that intranasally administered VCP may bind to the elevated complement components and HSPGs in the brain and be retained in the brain tissue for a period of time. Consequently, to effect optimal binding it is considered necessary to administer multiple doses of VCP to attain comparable levels of VCP delivered directly to the brain. The same protocol was followed for the controls, Cur and tVCP for appropriate comparison.

Dosing regimens and safety data regarding multiple intranasal doses of VCP and tVCP are not reported in the literature. Therefore, initially, the doses of VCP and tVCP were randomly selected and kept low. The mice were monitored for any signs of discomfort. As no noticeable signs of discomfort were observed in the treatment groups, the doses were increased to 36 to 42 μg/ mouse from 8th day and onwards. Cur is reported to be safe in the literature, and therefore, its dose was elevated to between 50 to 70 μg/ mouse throughout the study. Cur was found to reach CSF at much higher level than VCP and tVCP after being administered intranasally (Chapter 4). However, it was found to be thousand fold less potent than VCP in inhibiting the complement system. Accordingly, in order to get a comparable effect, it was administered at higher concentration than that of VCP, and tVCP. However, after administration of the first dose in the first mouse, due to some signs of discomfort, the saturated solution of Cur (10 mg / ml) was diluted to 5 mg/ml, then administering approximately 50 to 70 μg of Cur per mouse.

6.4.5 Elevated plus maze (EPM) set up and protocol.

EPM, as the name implies consists of two enclosed arms and two open arms forming a plus sign elevated to a specified height (Fig 6.1). The EPM used in the study consisted of five zones. The two open arms and two enclosed arms forming four zones, separated from each other by a central zone. The length (11.75”), arm width (2”) and the height of elevation (21.25”) were the same for both the open as well as enclosed arms, except the enclosed arm was closed from three sides (wall height 6”. The central zone was 2” X 2”. As the mice used for the study were black coloured, the EPM was coated with white bench coat to provide the contrasting background to capture the data required for analysis by use of EthoVison basics 3.1 software supplied by Noldus.

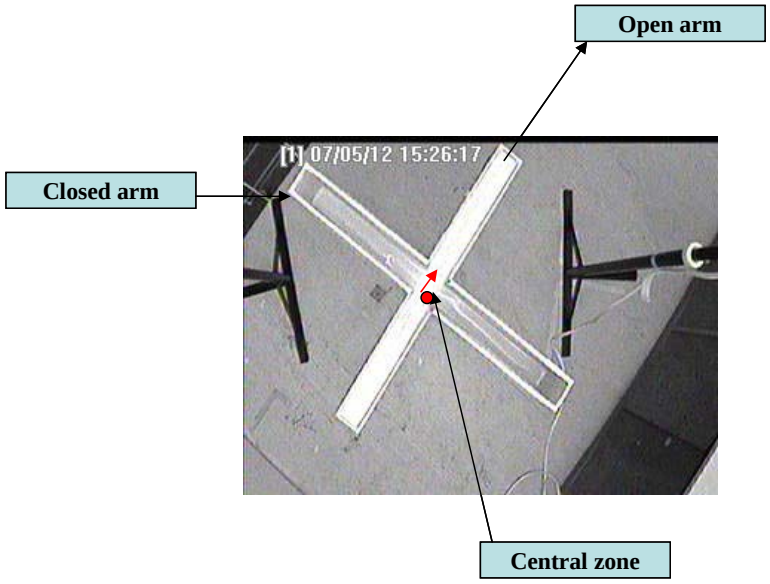

Figure 6.1. *EPM showing open and enclosed arms and the central zone. The red arrow indicates the start position of the mouse under trial with an arrow showing the direction of the head facing in the direction of one of the open arms.*

Set up of the room: The experimental room was separated from the data capturing room by a partition. The rooms were temperature controlled. Fluorescent tubes were positioned as a direct source of light and were placed above the web surveillance camera. In order to avoid reflections, the light source was covered by a white cloth with matt finish. The room was balanced with regard to the enclosed versus open arms with the open arms equidistant from the camera stand as shown in Fig 6.1. All the arms were equidistant from the web surveillance camera stand.

Protocol: The mice were housed in the adjacent room in order to get acquainted with the surrounding environment. Five to ten minutes before starting the experiment, the mice were kept in the experimental room. Once the mouse was taken out of the cage, it was placed in the central zone of the EPM within 10 seconds. The mouse was held by its tail and placed in the central zone in such a way that it was facing the open arm with its fore and hind limbs in the centre *(shown by red arrow in the* Fig 6.1. The observer then left the experimental room.

After each trial, all the arm surfaces were wiped off using a paper napkin immersed in 10% isopropyl alcohol, and sufficient time was allowed for the isopropyl alcohol to evaporate. Each mouse was allowed to explore the maze for five minutes. The time spent in the open and enclosed arms, arm entries in both the arms were noted. The mouse was considered to have entered the arm only when it had placed all its four paws in that arm. The arm entries were counted manually and double checked with ethovision 3.1 software. In order to study the open arm end exploration, the open arms were divided into zones, and the frequency in end zones was noted. The video data for some of the mice from tVCP treated groups and Cur

treated groups was lost probably due to data storage 'bug'. The results excluding these mice as well as manually recorded behaviours are shown. The number of mice used for the analysis is mentioned in the figure legends / results only if it differed from that indicated in the original grouping section. Each mouse was exposed for the test for just one trial of five minutes. Since the second exposure may result in decay effect, only one trial is recommended for the assessment of anxiety and exploration (Bertoglio and Carobrez 2002, Walf and Frye 2007).

6.5 Results.

6.5.1 Genotyping.

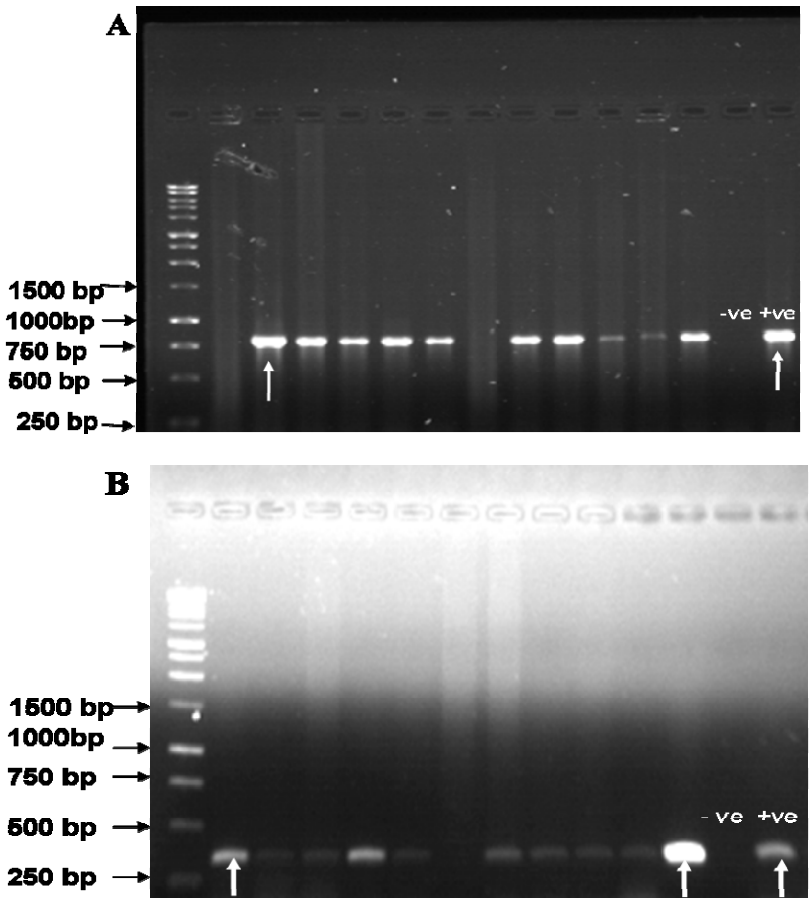

Figure 6.2. *Agarose gel (0.7 %) showing PCR products of the genomic DNA extracted from APPswePS1δE9 mice tails. A. The 750 bp band indicating the presence of PSENb [mouse prion promoterprotein (MPP)] transgenes (white arrow).* ***B.*** *350 bp band indicating the presence of APP transgenes (white arrow).*

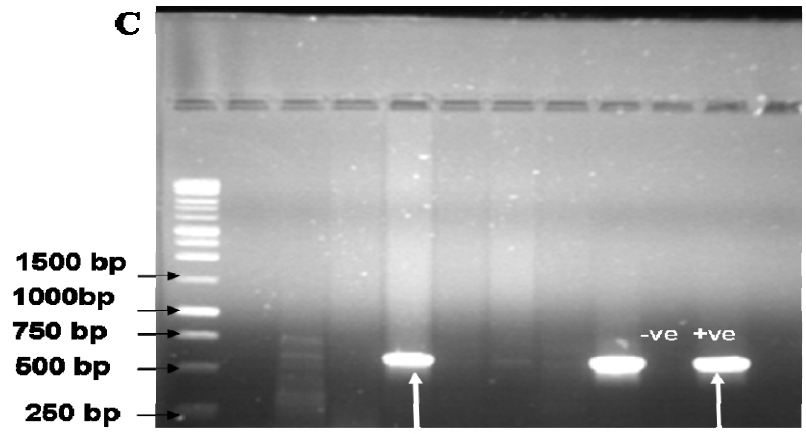

Figure 6.2. ***C. 608*** *bp band in 0.7% gel indicating the presence of PSENA transgenes (white arrow**).** *-ve and + ve indicate negative and positive controls, respectively.*

6.5.2 EPM Study.

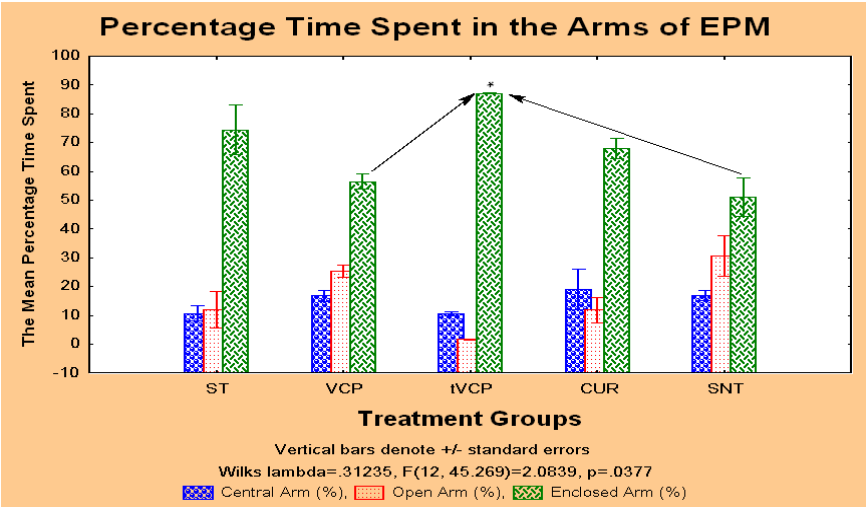

Figure 6.3. *The mean percentage time spent (Y-axis) by the treatment groups (X-axis) on various arms of EPM is shown in this figure. The significant difference between the treatment groups is shown by an asterisk above the bar graph, and the treatment groups whose value differs from the bar bearing the asterisk are shown by arrows.*

Results: Although ST mice spent relatively more time in the enclosed arms than the remaining three groups, there was no statistically significant difference between ST and all the treatment groups in the mean time spent in the central, open and enclosed arms of EPM (NK). The tVCP treated mice differed significantly from the VCP and SNT groups in the mean percentage time spent by them in the enclosed arms of EPM as shown in Fig 6.3 (NK). tVCP mice also spent less time in the open arm of EPM than that of the SNT group as shown by the NK test. The less stringent Duncan test revealed a significant difference between SNT and ST mice, as well as VCP and tVCP groups in the mean percentage time spent in the

enclosed arms of EPM (Table R6.1B, Appendix R). The data shown in this figure represents mean values from six mice for VCP, ST and SNT groups. As there was a problem with the video tracking system, the data for 2 tVCP treated mice and 2 Cur treated mice was lost. Thus n = 4 for Cur and 2 for tVCP group for this result.

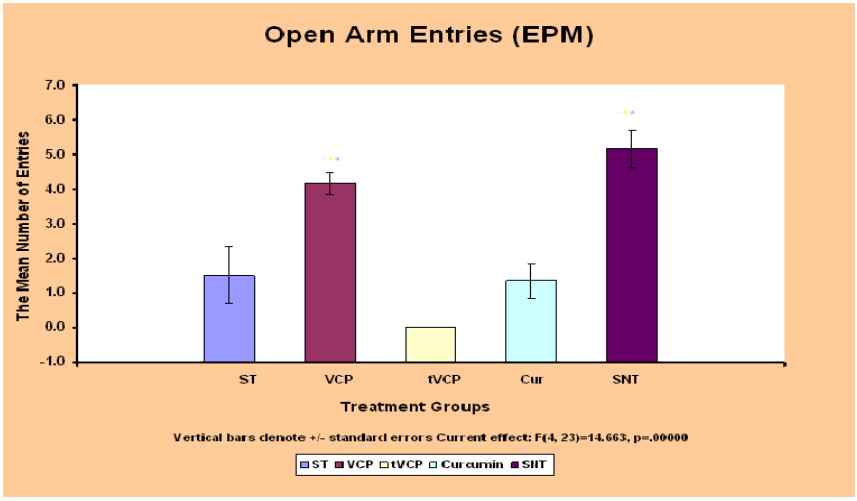

Figure 6.4. *The mean entries by the treatment groups in the open arms of EPM are shown by coloured bars and the level of statistical significance between the different treatment groups by colour coded asterisks. The colour matches with the bar graph being compared.*

Results: As shown in the Fig 6.4, and revealed by NK, the mean number of entries into the open arm of an EPM by VCP and SNT groups differ significantly from tVCP, ST and Cur groups. These two groups showed more open arm entries than that of all the other treatment groups. None of the mice from tVCP group visited an open arm. The p values calculated using NK revealed that SNT groups performed better than all the treatment groups followed by VCP treated group. Although, the performance of the mice from tVCP group appeared to be poorer than that of ST group, the difference was not significant.

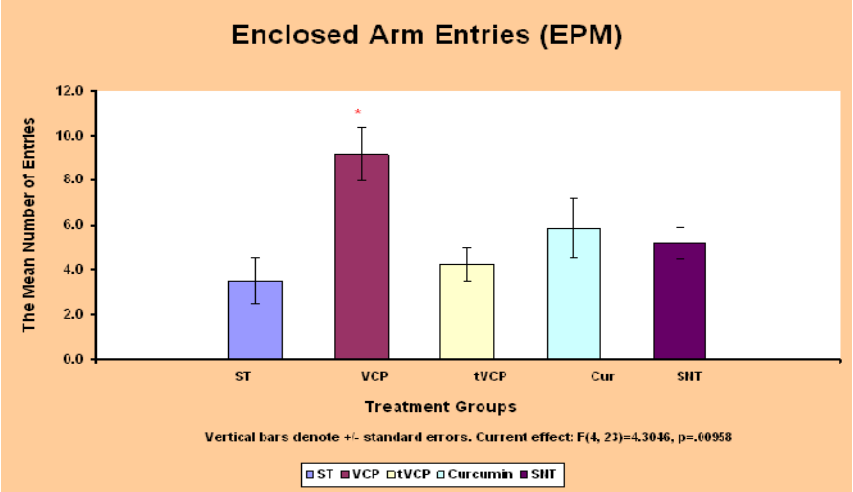

Figure 6.5. *The coloured bars represent the mean number of entries into the enclosed arms of EPM. The red asterisk represents significant difference to all the treatment groups*

Results: The mean number of entries in the enclosed arms by VCP treated group was significantly greater than that of all the treatment groups. The mean number of entries by all the other treatment groups did not differ significantly from each other by NK test (Fig 6.5, Table R6.3B, Appendix R).

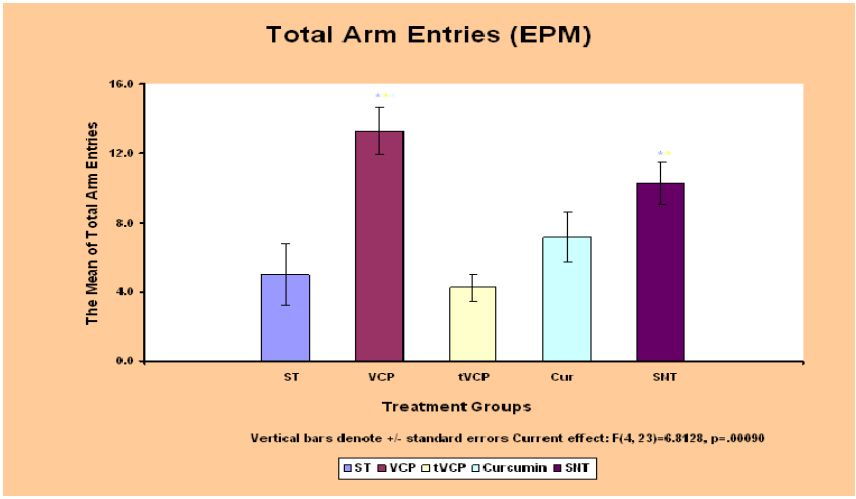

Figure 6.6. *The mean of the total number of entries into the enclosed and open arms of EPM by the treatment groups are shown by coloured bars. The colour coded asterisks are used to show the level of significance. The colour matches with the bar graph being compared*

Results: The mean of the total number of entries by VCP treated group is significantly higher than all the treatment groups except for SNT group. The mean of the total number of entries by SNT in both the enclosed and open arms is greater than that of ST and tVCP groups, but it did not differ from Cur and VCP treated groups (Fig 6.6, Table R6.4B, Appendix R).

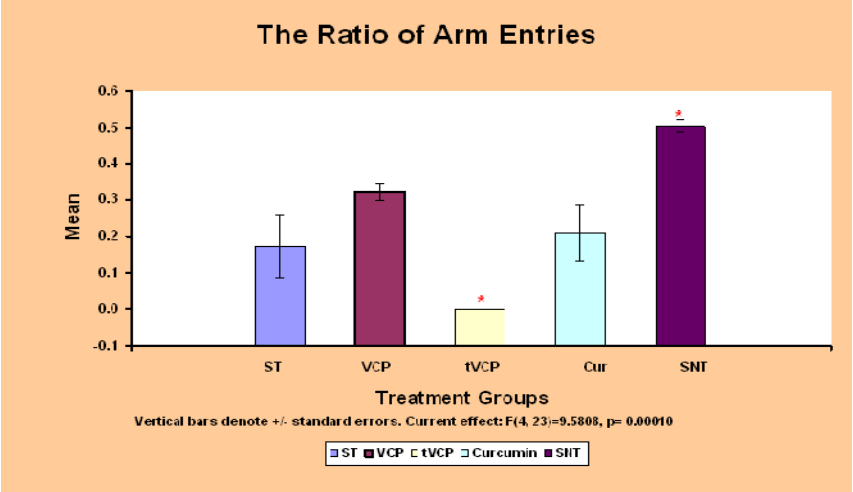

Figure 6.7. *The mean values of the ratio of the open arm entries to the total arm entries for the treatment groups are shown using coloured bars. The red coloured asterisks above tVCP and SNT bars indicate that the ratio for these two groups differs significantly from all the treatment groups.*

Results: The mean values of the ratio of the open arm entries to the total arm entries represented in Fig 6.7 and the post hoc analysis using NK (Table R6.5B, Appendix R) shows statistically significant difference between SNT, tVCP and all the other treatment groups, the mean value of the ratio being the highest for SNT, and the lowest for tVCP group.

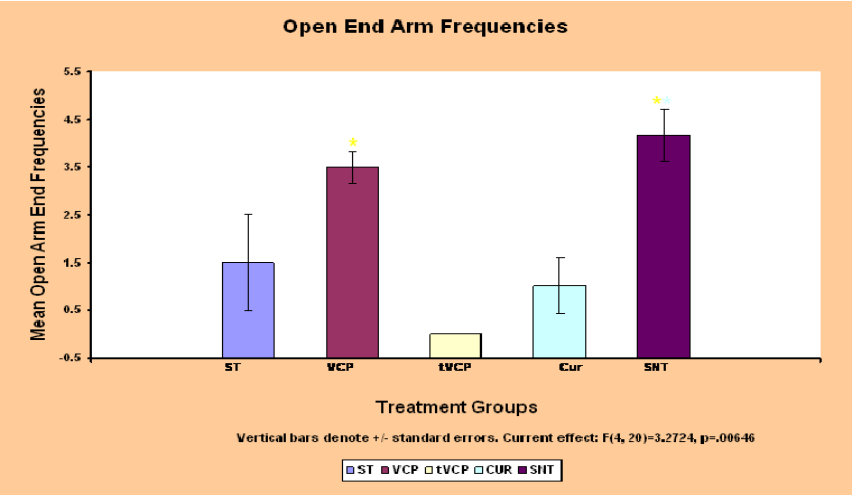

Figure 6.8. *The mean values of the open arm end frequencies of the treatment groups are shown as coloured bars and the coloured coded asterisk represent the level of significance. The colour of the asterisk matches with the bar graph being compared.*

Results: One way ANOVA revealed a significant difference between the treatment groups in the mean open end arm frequencies by them. As shown in the Fig 6.8, the difference in the mean number of

frequencies of the ST, and SNT groups was not significant. However, post hoc analysis using NK revealed better open arm end exploration by VCP and SNT than that of tVCP as shown by the open arm end frequency analysis. NK also revealed a significant difference between SNT and Cur groups. The less stringent Duncan test revealed the difference between SNT and all the other treatment groups except for VCP (Table R6.6B, Appendix R).

6.5.3 Summary of Results.

Experiment		**Results**		**Conclusion**
Genotyping of APPswe PS1δE9 mice (Fig 6.2)		**MPP (750 bp), APP (350 bp), and PSEN1A (608 bp) were amplified by PCR of the DNA extracted from APPswePS1δE9 mice. SNT mice showed the presence of MPP gene, but APP and PSEN1A were absent.**		**The APPswePS1δE9 strain confirmed.**
Screening of mice serum for pathogens.		**The mice were pathogen free.**		
Sr	**Experiment**	**ANOVA/ RMANOAVA**	**Post Hoc (NK and/ or D)**	**General Conclusion**
2	**The mean % time spent (Open/Central/Enclosed) (Fig 6.3)**	**P*=0.0377**	**VCP* and SNT* > tVCP [Enclosed (NK)]. SNT*>tVCP [Open (D)] Others = No***	**Mice from ST groups are more anxious and show less exploration than the SNT group. Intranasal VCP treatment improves exploration and inhibitory tendencies in APPswePS1δE9 mice. Intranasal administration of tVCP decreases exploration and increases anxiety.**
3	**The mean mumber of entries (Open Arms) (Fig 6.4)**	**p*<0.000009**	**VCP* and SNT* > ST, Cur, tVCP**	
4	**The mean number of entries (Enclosed Arms) (Fig 6.5)**	**p* = 0.00958**	**VCP*> SNT, tVCP, ST, Cur**	
5	**The mean number of total arm entries (Fig 6.6)**	**p*=0.00090**	**SNT*>ST and tVCP VCP*>ST**	
6	**The mean of the ratio of the open arm entries to the total arm entries (Fig 6.7)**	**p*=0.00010**	**SNT* > ST, VCP, tVCP, Cur (The highest mean ratio) tVCP*< ST, VCP, SNT, Cur (The lowest mean ratio)**	
7	**The mean open end arm frequencies (Fig 6.8)**	**p*=0.00646**	**SNT and VCP* >tVCP (NK), SNT* >Cur (NK) SNT*> all tg groups except for VCP**	
No* = No significant difference, * = siginificant difference, p = significance value, D = Duncan test, NK = Neumann Keul's multiple comparison test; RMANOA = Repeated measures ANOVA; tg = transgenic treatment groups				

Discussion.

The EPM is a robust tool employed to study the anxiety and exploratory behaviour in rodents. In the current investigation, the five min test protocol has revealed significant information regarding the effect of VCP, tVCP and Cur on the exploratory behaviour and anxiety in APPswe transgenic mice. In previous studies, APPswe mice showed exploratory behaviour on EPM, with greater open arm/total arm ratio (i.e. relative time spent in open) as compared to the non transgenic counterparts (Lalonde et al. 2004). In this study, contradictory results are evident. RMANOVA suggested a significant difference in the mean percentage time spent by the various treatment groups in open, enclosed or central arms of EPM. The NK test revealed no significant difference between ST and SNT groups as well as between the ST and the transgenic treatment groups (NK; Fig. 6.3, Table R 6.1B, Appendix R). The less stringent Duncan test suggested a better exploratory performance by VCP and SNT groups compared to tVCP, and ST groups, respectively. However, there was statistically significant difference between the treatments groups in the mean number of entries into the open arms, enclosed arms as well as total number of entries in both the arms. The Post hoc analysis (NK) revealed a significant difference between the ST and SNT groups in the mean number of open arms entries. The mean number of open arm entries shown by VCP treated group was significantly greater than that of ST, Cur, and tVCP transgenic mice (Fig. 6.4). However, the mean of the total number of entries into the enclosed arm of EPM by VCP treated mice was statistically significantly higher than all the other treatment groups, including SNT. Therefore, the ratio of the number of open arm entries to the total number of arm entries was calculated. It was found that the ratio was the highest for SNT group, the lowest for tVCP group, and the other groups showed intermediate scores. The post hoc analysis using NK revealed that the ratio was significantly higher for all the other groups compared to tVCP treated mice (Fig 6.7). For SNT mice it was significantly higher than all the transgenic groups. When P values of the post hoc analysis using NK for different groups were compared to study the level of significance between SNT and the other treatment groups, the following order was observed: SNT and tVCP (0.000150) > SNT and ST (0.002927) > SNT and Cur (0.004451) > VCP and SNT (0.037360). This means that the difference between tVCP and SNT was very highly significant, between SNT and ST (and Cur) was highly significant and the level of significance was relatively low for the difference between SNT and VCP groups. This suggests that ST mice are more anxious than SNT mice. tVCP is found to have inhibitory effect on exploration in APPswe mice, whereas VCP could be working in an anxiolytic manner, since it increased the exploratory behaviour in APPswe mice as shown by the highest mean total number of arm entries (Fig 6.6). Also the mean number of entries into the open arm shown by VCP group was more than that of ST, tVCP and Cur groups (Fig 6.4). The mean of the ratio of open to total arm entries was also higher for VCP than the other transgenic mice. The observed exploratory behaviour in VCP treated mice could be attributed to an anxiolytic type of activity, because exploratory behaviour can be regarded as an indirect measure of anxiety. The higher the anxiety, lower the exploration. When the results of the EPM analysis was extended to study the exploration

of end of open arms (i.e.10 cm area towards the extreme end of the open arms of the maze), ANOVA revealed a significant difference between the treatment groups. Further post-hoc analysis (NK and/or Duncan) revealed a significant difference between the arm end exploration by VCP and SNT group compared to the tVCP group, but these groups did not differ from the other treatment groups. This suggest that tVCP, a truncated version of VCP not only failed to attenuate the anxiety in APPswe mice, but appeared to generate anxiogenic activity. The observed differences between the opposite actions could be attributed to their structural differences. The lack of module one in the structure of tVCP is responsible for its low level of complement regulatory activity, as shown in the previous chapters. The activation of the complement system in AD might be related to the elevated or high levels of generalised anxiety in these animals. VCP, by virtue of its ability to regulate complement activation, controls neuroinflammation and this may explain the modulation of anxiety and exploratory behaviour by VCP. VCP has not as yet been tested for its anxiolytic activities in non transgenic mice or rats. It might have pharmacological actions on the GABA receptors like other anxiolytics, which needs to be further investigated. Thus it will be important to find out whether its anxiolytic action is specific in APPswe transgenic mice or if it works as a general anxiolytic. One important outcome of this investigation is that all the four modules are essential for the anxiolytic effect of VCP, the property prerequisite for the complement regulation by VCP. Cur did not show any effect, one possibility being that it was not delivered to the brain in sufficient amount to exert the neurobehavioural effects.

It is important to address the difference between our results with the anxiety and exploratory behaviour of APPswePS1dE9 mice and that of Lalonde et.al.(2004) using the same strain, and of nearly the same age. The difference could mainly be attributed to the variation in the apparatus. In their study, Lalonde et al. have used an EPM with 10 cm X 10 cm (4" X 4") central area as well as the length of the arm being 70 cm (28"), and width of the arm being 10 cm (4"). The maze used by them was almost double the size of the maze used in the current study. An EPM of standard size recommended for mice was used for the current investigation. The 10 cm X 10 cm central area and 10 cm arm width might not have induced significant anxiety in mice in the study by Lalonde et al., whereas the standard 5 cm width in the current study was sufficient to be anxiogenic. Also, prior to the EPM study, their mice were exposed to open field and other models which might have contributed to the variation in the results.

Our results match with that of Savonenko et al (2003) who has also reported elevated anxiety in APPswe mice (single mutation), and with that by Puolivali et al. (2002) where APPswe and PS1 double transgenic mice were used although the strain was different, but the transgenes were the same (APPswe and PS1) as in this study.

Recent findings in clinical studies of AD and other demented individuals showed association between anxiety and dementia (Ohl 2003). It has also been shown that there was an elevation in the level of brain enkephalin in transgenic mice expressing APP (Meilandt et al. 2008). Recently, it was found that direct administration of enkephalin agonists into the CEA region of amygdala decrease the open arm entries

whereas under similar circumstances, the enkephalin antagonists increase the open entries in EPM (Wilson and Junor 2008). VCP treatment has also resulted increased open arm entries by APPswePS1δE9 mice used in the current investigation. It would be informative to investigate whether VCP has antagonistic activity against enkephalin receptors in the brain.

The above study possibly adds new dimension to the neuropharmacological activity of VCP. Previously, it has been shown that four modules of VCP are essential for its *in-vitro* biological activity (Smith et al. 2003). This can be correlated with the current *in-vivo* findings. Moreover, in the current study the modulation of behaviour by VCP was observed after intranasal delivery of VCP, further expanding its use as a potential neuropharmacotherapeutic agent of clinical significance by administration using a non-invasive route.

The inhibitory activity on behaviour shown by tVCP needs further attention, although the number of mice was only four, all of them have shown a similar pattern of behaviour. In many psychiatric disorders, disinhibitory behaviour is symptomatic, and tVCP might play an important role in such disorders with disinhibitory tendencies through its inhibitory actions.

VCP with four modules intact appears to act as an anxiolytic, whereas just deleting one module from its structure results in its truncated version (tVCP) with a possible disinhibitory effect on the exploratory behaviour in APPswe mice. The structural difference makes them unique in their neuropharmacological profile. The neurobehavioural modulation by VCP and tVCP after multiple intranasal administrations needs to be further explored for their potential use pharmacologically in non transgenic mice and rats as well as in transgenic mice using T-Maze, open field and other models to study exploratory behaviour. This will give more information regarding their neuropharmacological profile.

Chapter 7.

To Investigate the Effect of Intranasally Administered VCP, tVCP, and Curcumin on Spatial Learning, Spatial Reversal Learning and Spatial Working Memory in MO/HU APPswe PS1δE9 Mice.

7.1 Introduction.

APPsweePS1dE9 mice used in the current investigation showed anxiogenic tendencies and deficit in the exploratory behaviour, and intranasally administered VCP was found to improve the observed behavioural deficit. Previous research also suggests that these mice at the age of six months (Pillay et al. 2008) and at the age of two years show a deficit in the spatial learning, cued learning and associative learning (Chapter 5). In these studies direct administration of VCP was found to be beneficial in correcting the behavioural deficit.

Similar studies by others have shown that cognitive deficit is observed in transgenic mice from the age of 6 to 18 months of age (Middei et al. 2006, Savonenko et al. 2005, Good and Hale 2007, Reiserer et al. 2007). These studies were carried out either in single transgenic mouse models such as transgenic mouse model with APP transgene (Tg2576) as well as in double transgenic mouse models such as APPsweePS1δE9.

The most common model used to assess cognitive deficit in these studies is Morris Water Maze (MWM). Using this model, it has previously been shown that these transgenic mice show deficits in spatial learning (Liu et al. 2002).

Since this whole study is based on APPsweePS1δE9 mice, this strain was used to test the therapeutic effectiveness of various treatments in correcting the cognitive deficits in these mice aged 11-15 months. As discussed in the previous chapters, these double transgenic mice express the mouse/human chimeric amyloid precursor protein and mutant human presenillin directed to CNS neurons (Jackson data sheet). These mutations are associated with early-onset AD. The amyloid protein is deposited from the age of 6-7 months. It has also been shown that these transgenic mice show elevated levels of complement components (Matsuoka et al. 2001). Therefore these mice represent a highly suitable model for AD, HAD, other amyloidopathies and disorders such as HAD which are also associated with amyloid deposition and subsequent activation of the complement components leading to neurodegeneration, and are thus ideal models for testing the effectiveness of various substances.

The complement system, as discussed in the literature review, plays a damaging role in AD and HAD. VCP has previously been shown to be effective in preventing the *in-vitro* complement activation by amyloid protein (Daly and Kotwal 1998). VCP was also found to be effective in preventing and treating the cognitive deficit associated with these mice (Pillay et al. 2008, Chapter 5). VCP and tVCP has also been shown to improve spatial learning and memory in a rat head injury model (Pillay et al. 2005, Hicks et al. 2002). However, VCP has thus far not been tested for its effectiveness in spatial learning in these mice. In most previous studies, the therapeutic effectiveness of VCP are reported in terms of its *in-vitro* complement regulatory activity. Similarly, in most of the studies modulation of behaviour by VCP in rodent models of CNS disorders has not been compared with its structural analogue, tVCP. In a recent study, tVCP which does not inhibit the complement system at moderate concentration (Smith et al. 2003) has been shown to be effective in the treatment of TBI (Hicks et al. 2002). The improvement in TBI and other rodent models therefore could be attributed to heparin binding by VCP in addition to its complement regulatory activity. Cur, which has been shown to inhibit

the up-regulated complement activation (refer to Chapter 2 and 3), was also found to reduce plaque formation in a mouse model of AD by other researchers and improve cognitive deficit (Yang et al. 2005). In the later study, Cur was found to be effective in micromolar concentration in correcting behavioural deficits in these mice, but it was administered orally. The effects of multiple doses of VCP, tVCP or Cur delivered via intranasal route on various behaviours in rodent models of CNS disorders have not as yet been reported in the literature.

7.2 Objectives.

The specific objectives of the current investigation are to investigate the effect of multiple doses of intranasally administered VCP, tVCP and Cur in APPswePS1dE9 mice in modulation of;

1) Spatial learning, using the spatial learning paradigm (Sp L P).
2) Reference memory of Sp L P using probe trials.
3) Spatial reversal learning using spatial reversal paradigm (Sp R P).
4) Reference memory of Sp R P using reverse probe trial session.
5) Spatial working memory, using spatial working memory paradigm (Sp W P).

7.3 Materials.

APPswePS1δE9 mice (genotyped and grouped in the chapter 6), MWM, VCP, tVCP and Cur (Prepared and used in chapter II and VI) video monitoring system, EthoVision supplied by Noldus.

7.4 MWM set up: It consists of a circular tank filled with water. Typically, the diameter of the tank varies from 1 m to 2 m, and for the current experiment it was 176 cm. The height of the tank was 63 cm. The tank was painted in white using acrylic white paint (matt finish) on the inside. It was mounted on a stand raised 45 cm from the floor to assist with the drainage, and was divided into four cardinal points, south (S = Researcher's position), North (N = Opposite), East (E = right), and West (W). Thus, there were four quadrants, South-West (SW), South-East (SE), North-East (NE) and North-West (NW). Appropriate measures were taken to avoid the intra-maze clues.

The Escape Platform: A circular platform (5.5 cm diameter and 32.5 cm height) was used as an escape platform. The surface of the platform was covered with transparent plastic adhesive and it was roughened using sandpaper in order to provide proper grip for the mouse, to assist in mounting the platform.

The position of the platform: The platform was placed in one of the four quadrants of the MWM depending upon the trial (spatial acquisition or reversal trial) in such a way that the distance between the centre of the platform from and the wall was about 32 cm.

Water in the Maze: The maze was filled with water up to the height of 33.5 cm, that is, one cm above the circular platform. The later was made opaque by adding 400 g of non-toxic white tempera paint (matt finish to avoid reflections of light) pre-dissolved in 1 L of water to avoid the formation of lumps

in the water. The temperature of the water was maintained to 22-24^{O}C by heating for about two and half to three hours before starting the experiment. The temperature of the room was maintained at 25-26^{O}C.

Lighting: Four incandescent fluorescent light globes (20 W) were fixed on aluminium angles placed at the four corners of the tank. They were used as indirect diffuse sources of light. It was necessary to use the indirect source of light to avoid the reflection of overhead light on the water surface while, analysis using Ethovision 3.1 (Supplied by Noldus).

Testing rooms: The experimental room (where MWM was located) was separate from the data capturing room/drying room. In the experimental room, three extra-maze clues were placed on the wall within 2 m from the centre of the pool. Three pictures (A4 size) were used as extra maze visual cues. They were placed in such a way as to make 70 to 90 degree angle with the centre of the pool. The black, white and blue coloured strips, triangle or circles were pasted on A4 paper (pink) as the rodents can distinguish the colour in blue-green spectra and not the red spectra. There were air conditioner (AC) and the camera (Sony Handycam) above the tank. The camera was about 2 m above the water level (167cm above the surface of the tank). Two wide angles (Sony; 1:0.6 and 1:0.5 reduction, respectively of the original size) were used to get the view of the entire MWM.

The holding cages were organized at two places. 1) In the experimental room, mice were housed 30 min prior to the experiment. 2) In the data capturing room (or drying room), the cages were kept for drying the mice during the intertrial interval. The inter-trial interval was approximately 20-25 m, and in order to avoid hypothermia the mice were kept under warming lamps.

The Video Capturing System and Data Analysis: The sony handycam was connected to WinFast TV USB deluxe-II, TV tuner by Leadtek for capturing the video images of the behaviour of the mice in the MWM. The configurations used for capturing the video were adjusted to meet the requirements of the EthoVISION 3.1 (basic) software for analyzing the data (PAL with MPEG-I format).

7.5 Methods.

7.5.1 Genotyping and Grouping: The same treatment groups used in chapter 6 were used for the current study.

7.5.2 Dosing Schedule and the Intranasal Administration: The same protocol as discussed in chapter 6 was followed. However, the dosing intervals were increased from 2-3 days prior to the start of MWM study to 7 to 11 days during MWM study. The dosing was done a day before the commencement of the and on the last day of the learning paradigm. For the working memory paradigm, the dosing was done on the 7th day of the training session, as the protocol lasted for 11 days. Refer chapter 6 and Appendix F (Fig F1.3) for the diagram for the dosing pattern and dosages.

7.5.3Housing and the Mice Strains: The mice were housed in the departmental animal research facility with controlled ambient air, temperature, and free access to water and the food pellets. The automatic light switch on-off system was used to provide 12 h light and dark cycle. The males and females were housed in separate cages. As indicated above cages were brought to the experimental room allowing 30 min for acclimization to new environment.

7.5.4 Habituation: The mice were allowed to swim in water for one minute for two consecutive days to test their ability to swim in the tank, and acquainte them with the water maze while monitoring their behaviour.

7.5.5 Spatial learning paradigm (Sp L P) of MWM.

The submerged platform was kept in NW quadrant (Fig 7.1A below) close to the cardinal point W. The three release positions selected were S, NE and N (Shown as red ellipses in the Fig 7.1A). In order to carry out the training session, the mice from various groups (ST, VCP, tVCP, and SNT) were released from these release positions with their heads facing towards the wall, and were allowed to locate the platform. Except for the first day, each training session consisted of three training trials. If the mice did not reach the platform within 75 s during each trial, they were guided to the platform. In either case, they were allowed to remain on the platform for 15 s.

On the first day, only two trials were conducted, and consecutively for the next six days, three trials were conducted per mouse with the release positions as mentioned in the table 7.1 below.

MWM set up and release positions.

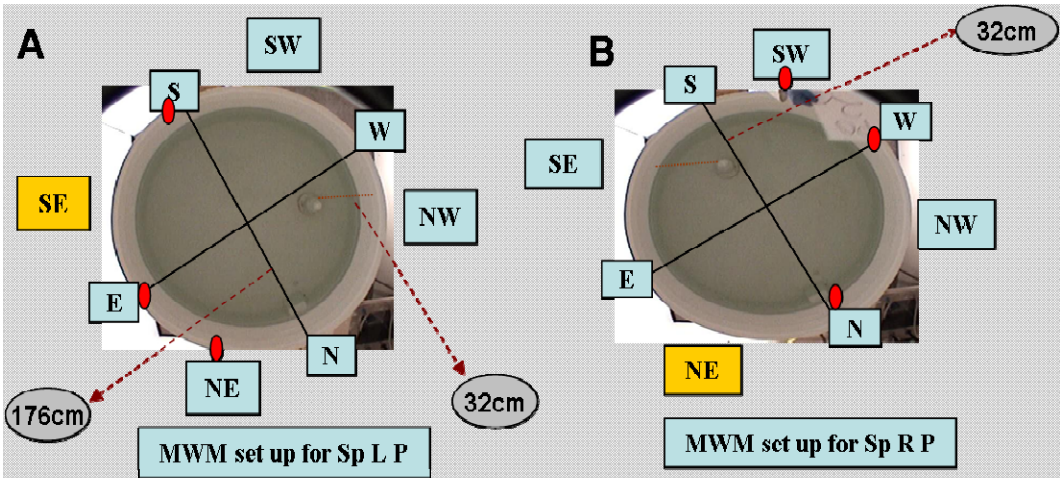

Figure 7.1. *The diagrammatic representation of MWM set up for Sp L P (A) and Sp R P (B) with the dimensions of the tank, arbitrary quadrants, release positions (shown by red ellipses), and position of the platform. The release positions during the probe and reverse probe trials conducted after SP L P and Sp R P, respectively are also shown (the golden yellow rectangles; SE for probe trial [A] and NE for reverse probe trial [B]). The platform was removed from the tank for probe and reverse probe trials.*

The release positions of mice during Sp L P and Sp R P.

Days	Trial one		Trial two		Trial three	
	Sp L P	**Sp R P**	**Sp L P**	**Sp R P**	**Sp L P**	**Sp R P**
1	S	N	E	W	…	…
2	E	W	S	SW	NE	N
3	S	SW	NE	N	E	W
4	NE	SW	E	W	S	N
5	NE	W	E	N	S	SW
6	NE	N	E	SW	S	W
7	E	SW	S	N	E	W

Table 7.1. *The patterns of release positions of mice from different treatment groups subjected to three trials (columns 2, 3, and 4) for seven days (column 1) of Sp L P and Sp R P*

7.5.6 Probe trial.

In order to test the effect on long term reference memory, only one probe trial session was conducted for four days after the last training session of the spatial acquisition. The time interval was kept long to study the effect on the reference memory independent of the last training session (Vorhees and Williams 2006). To avoid the extinction effect, only one probe trial was performed. For the probe trial, the mice under test were allowed to swim in the pool for about 60 s with no platform in the tank. After sixty seconds, mice were removed from the tank, dried and then returned to the cages. The release position used for the probe trial session was different from all the three positions used for the spatial trials (SE; Fig 7.1A).

7.5.7 Spatial reversal paradigm (Sp R P).

The protocol for Sp R P was the same as that of Sp L P, except for the position of the platform and the release positions. The platform was moved to the SE quadrant close to the cardinal point S, and the release positions were changed to SW, W and N (red ellipses; Fig 7.1B). The spatial reversal was carried out for seven days (Seven sessions; each session = Three trials except for the day one when two trials were given; one trial for 75S , and the release positions for seven days were as mentioned in table 7.1.

7.5.8 Reverse Probe Trial.

This was done in a manner similar to that of the probe trial, but the platform was kept in NE quadrant (Fig 7.1B).

7.5.9 Spatial Working Memory Paradigm (Sp W P).

For Sp W P, the protocol mentioned in the Nature protocol (Vorhees and Williams 2006) was followed. In this paradigm, the position of the platform (goal) is changed everyday unlike Sp L P and Sp R P (Table 2). In this study, the Sp W P lasted for 11 days in order to match the days with Sp L P and Sp R P (7 days + probe / reverse probe after 4 days = 11 days). The Sp W P consists of one sample trial (the first trial conducted) and one or more test trials (also referred as match to sample trials) conducted after the sample trial. In the current study, one sample trial was followed by two test trials. For the sample trial, the position of the platform as well as release position was changed randomly everyday but it was the same for the sample and the test trials carried out on the same day (Table 7.2). The percentage reduction in the mean average escape latencies during the test trials was used as a parameter to assess the effect on the working memory of the different treatment group. As the position of the platform changes everyday, this trial measures the effect of various treatments on the working memory.

The release and platform positions during 11 days of Sp W P.

Day	Platform position (goal)	Release Position
1	SE	N
2	NE	S
3	Between NW and N	W
4	Between NW and W	E
5	Between SE and S	NW
6	Between NW and W	SE
7	NE	NW
8	Between NW and N	S
9	Between NW to W	E
10	SE	N
11	N	SW

Table 7.2. *The release positions and locations of the platform (Goal) during Sp W P of MWM for one sample trial and subsequent test trials (two). S = South, N = North, W = west, E = East, NW = North-West, NE = North East, SE = south East, SW = South west*

7.5.10 Behavioural assessment and the data analysis.

The data captured using the Win-Fast video capturing system was then analyzed using EthoVision 3.1 supplied by Noldus. The mice from different treatment groups were monitored for standard behavioural parameters such as the mean average escape latency, the mean average time spent near the platform proximity, the time spent in the central zone, thigmotaxis (time spent in the peripheral zone), and velocity during these trials. The behavioral data for all the days was recorded digitally and scored manually. For Sp L P and Sp R P, day 1, 2 and 7 were selected. For Sp W P, days 1, 5 and 7 were

selected for the analysis using Ethovision 3.1. The probe and reverse probe trials were analyzed using EthoVision 3.1 only as no manual recording was possible. While carrying out the analysis, it was found that some of the mice showed unusual behaviours not reported in the literature. This behaviour was termed "Kissperi" since it involved the movement of the head of mouse with respect to side of tank as if the mouse was "kissing" the periphery. The concept behind the "Kissperi behaviour" and its broad definition is included in the Table below and also discussed later in the discussion. This behaviour was noticed only after Sp L P and thus was recorded during the probe trial and further study. The information regarding various behaviours recorded during various paradigms and broad definitions is reported in the Table 3. Repeated measures ANOVA or ANOVA was used for the statistical analyses. The level of significance between the treatment groups was analyzed using more than one post hoc test, but for consistency with the other behavioural studies the standard Newman-Keul's multiple comparison test (NK) used by the other researchers for the MWM study (Bourque et al. 2008). In a few cases, the Duncan's post-hoc test was also used, if the NK test failed to show any significance. In some of the cases, where it was necessary, the within group difference was also analyzed.

The MWM test paradigm and broad definition of the behaviour tested.

Sr	MWM Paradigm	Behavior Tested	Behavior Defination and parameter analysis
1	Sp L P, Sp R P	The mean average escape latency	The average values of time taken by mouse under trial to find out the platform in two trials on the first day, and three trials on subsequent days. The mean of these average values was calculated and used for the statistical analysis. It provides information regarding the cognitive ability of mice tested. This behaviour was recorded manually for all the seven days and using Ethovision for three days (1, 2, and 7).
2	Sp L P, Sp Rp, Probe trial, Reverse probe trial	The mean average percentage time spent in the central zone	MWM was divided into two arbitrary zones. The central zone of approx 156 cm in diameter, and the peripheral zone of approx 10 cm wide area between the periphery and the border of the central zone. This parameter gives information regarding the central dwelling tendencies and "thigmotaxis" which is defined as the tendency of mice to remain confined to the periphery of MWM instead of exploring the centre to find the escape (submerged platform). The mean of the average of the values from different trials was calculated as mentioned in the above column. For the probe and reverse probe trials, the means alone were calculated as only one trial was performed.
3	Sp L P, Sp R P, Probe trial, Reverse probe trial	The mean average percentage time spent in the nearest platform proximity	A circle of about 25 cm diameter was drawn around the centre of the platform. As the platform was 32 cm away from the periphery of the MWM (no platform during probe and reverse probe), the circle was drawn in such a way that its border was at least 15 cm away from the periphery of MWM to avoid the inaccurate measurements due to thigmotaxis. The mean values for the statistical comparison were calculated from the average percentage values. For the probe and reverse probe trials, the mean values were calculated as these trial sessions comprise of only one trail. There was no platform during the probe and reverse probe trial. So for the probe and reverse probe trials, the area equivalent to the diameter of the platform was selected at the same position where the platforms were located during Sp L P (Probe platform proximity) and Sp R P (Reverse probe platform proximity), and the percentage dwelling time in these areas was recorded as the mean percent time spent in the probe and reverse probe platform proximities for the probe and revrese probe trials, respectively.

Sr	MWM Paradigm	Behavior Tested	Behavior Defination and parameter analysis
4	Sp L P, Sp R P	The mean average escape latency	The average values of time taken by mouse under trial to find platform location in two trials on the first day, and three trials on subsequent days. The mean of these average values was calculated and used for the statistical analysis. It provides information regarding the cognitive ability of mice tested. This behaviour was recorded manually for all the seven days and using Ethovision for three days (1, 2, and 7).
5	Sp L P, Sp Rp, Probe trial, Reverse probe trial	The mean average percentage time spent in the central zone	MWM was divided into two arbitrary zones. The central zone of approx 156 cm in diameter, and the peripheral zone of approx 10 cm wide area between the periphery and the border of the central zone. This parameter was used differentiate thigmotaxis behaviour as explained in the series 2.The mean of the average of the values from different trials was calculated as mentioned in the above column. For the probe and reverse probe trials, the means alone were calculated as only one trial was performed.
6	Sp L P, Sp R P, Probe trial, Reverse probe trial	The mean average percentage time spent in the nearest platform proximity	A circle of about 25 cm diameter was drawn around the centre of the platform. As the platform was 32 cm away from the periphery of the MWM (no platform during probe and reverse probe), the circle was drawn in such a way that its border was at least 15 cm away from the periphery of MWM to avoid the inaccurate measurements due to thigmotaxis. The mean values for the statistical comparison were calculated from the average percentage values. For the probe and reverse probe trials, the mean values were calculated as these trial sessions comprise of only one trail. There was no platform during the probe and reverse probe trial. So for the probe and reverse probe trials, the area equivalent to the diameter of the platform was selected at the same position where the platforms were located during Sp L P (Probe platform proximity) and Sp R P (Reverse probe platform proximity), and the percentage dwelling time in these areas was recorded as the mean percent time spent in the probe and reverse probe platform proximities for the probe and revrese probe trials, respectively.

Table 7.3. *The Table showing MWM paradigm, Behaviour tested and Behavioural definition and parameter analysis of the behaviour tested. Sr = serial number.*

7.6 Results.

7.6.1 Sp L P.

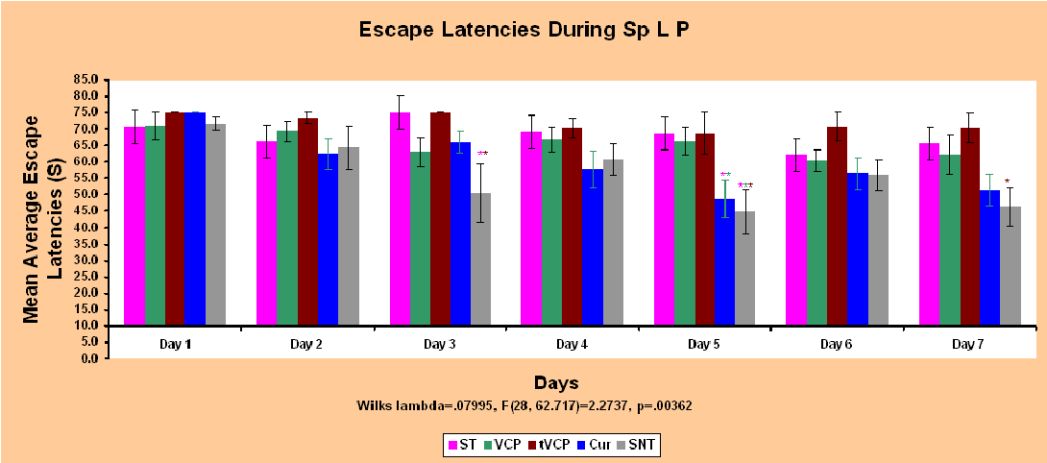

Figure 7.2. *comparison of the mean average escape latency (s; Y-axis) of the treatment groups on daily trials (Days 1-7; X-axis) of Sp L P. On day one, the mean values were calculated from the average of two trials and from days two to seven, the mean values were calculated from the average of three trials per day. The between group significant difference is shown by colour coded asterisk(s). The colour of the asterisk(s) match(es) with the bar of the group(s) being compared.*

Results: As shown in Fig 7.2, the mean average escape latencies of all the treatment groups did not differ significantly on days one and two of Sp L P. On the day 3, there is a significant difference between the mean escape latencies of SNT and ST groups as well as SNT and tVCP groups (Fig 7.2 and Table R7.1C, Appendix R). On day 5, the mean escape latencies of Cur and SNT groups are significantly lower than that of the VCP and tVCP treated mice. In addition, the SNT group is significantly different from tVCP group on day 5 and day 7. The within group analysis suggests that the combined mean average escape latencies of all the treatment groups on days five, six and seven are significantly less than that on the day one (Table R7.1D, Appendix R).

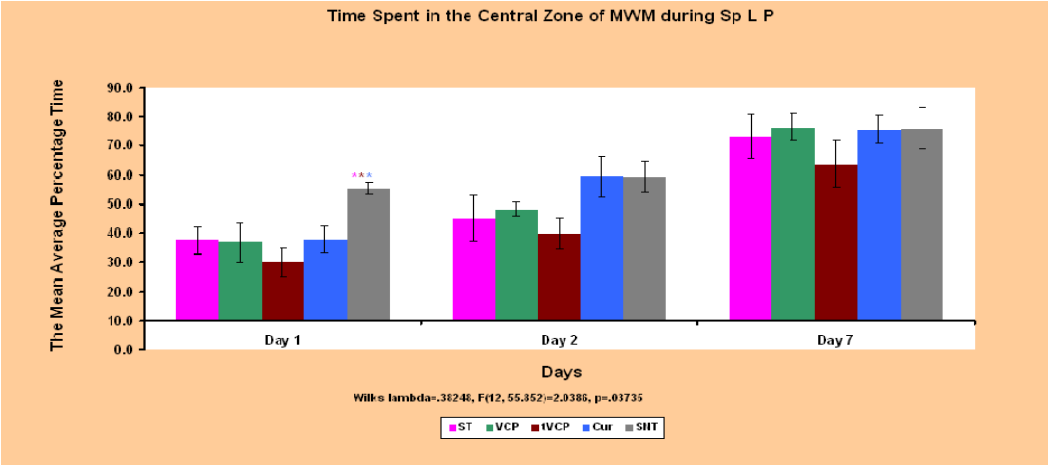

Figure 7.3. *The mean average percentage time (Y- axis) spent in the central zone of MWM by the treatment groups on Days 1, 2, and 7 (X axis) of Sp L P. The significant difference in the mean percentage time spent by the treatment groups is shown by the colour coded asterisk(s). The colour of the asterisk(s) match (es) with the bar of the group(s) being compared*

Results: The mean percentage time spent in the central zone by the mice from SNT group significantly differs from that of ST, tVCP, and Cur group. The exception is the VCP treated group on the day one of MWM Sp L P (Fig 7.3 and Table R7.2B, Appendix R). The within group analysis suggested that there was a significant difference in the combined mean percentage time spent in the central zone by the treatment groups on day one two and seven (Table R7.2C, Appendix R).

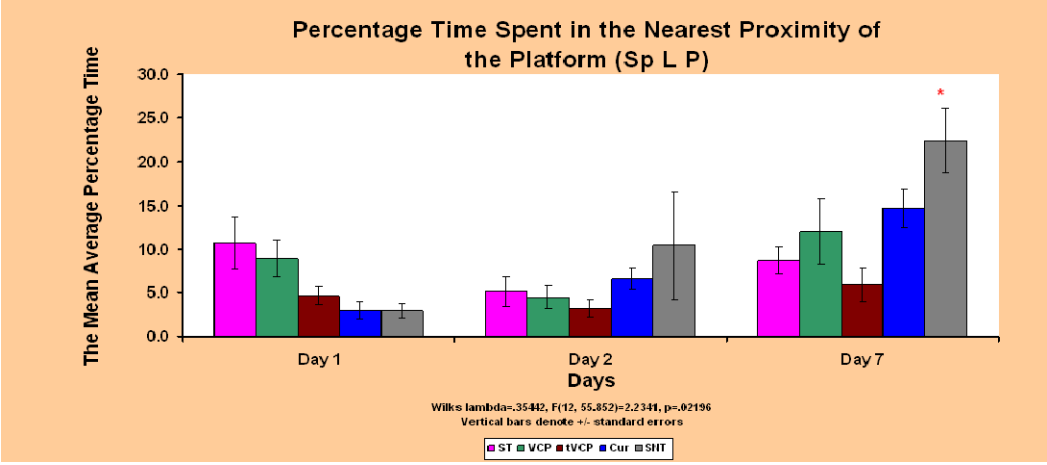

Figure 7.4. *The mean average percentage time spent in the zone of the nearest proximity by the treatment groups (Y axis) in the nearest platform proximity on the days one, two and seven of MWM Sp L P. The red asterisk on the SNT bar indicates that the mean average time spent by SNT group is significantly different from all the treatment groups on the day seven.*

Results: There was no difference in the mean average percentage time spent by the treatment groups in the nearest proximity of the platform on days one and two. However, on day seven, the mean average time spent by the SNT group was significantly higher than that of all the treatment groups (Fig 7.4 and

Table R7.3B, Appendix R). The within group analysis suggested that the mean average time spent by the SNT groups on day seven was significantly higher than that on days one and two. It also suggested that the combined average percentage values were significantly higher on days 2 and 7 compared to that on the day 1 (Table R7.3B, Appendix R).

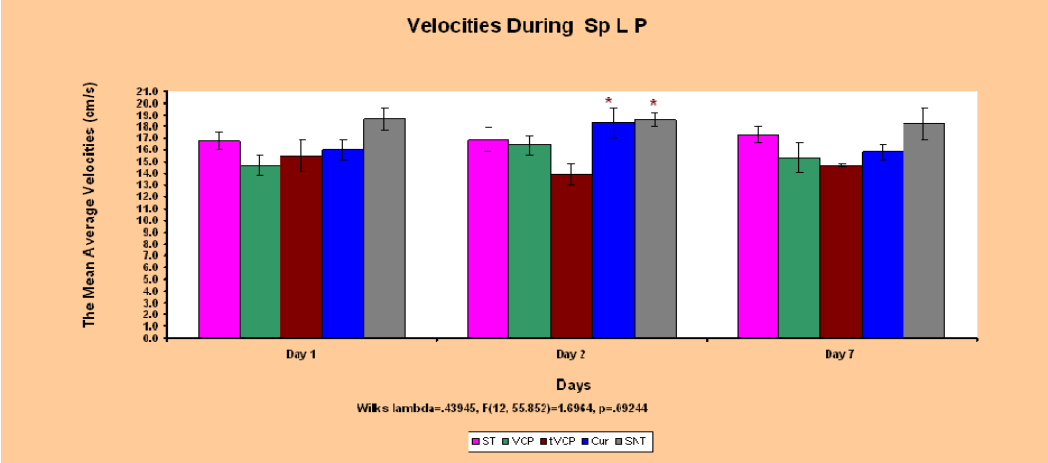

Figure 7.5. *The mean average velocity per trial of the treatment groups (Y axis) on days one, two and seven of MWM Sp L P (X axis). Significant difference between the treatment groups is shown by the colour coded asterisks, where the colour of the asterisk(s) represents the colour of the bar(s) being compared.*

Results: There was no significant difference in the mean average velocities of the treatment groups on days 1 and 7. However, on day 2, the mean average velocities of the SNT and Cur were significantly higher than that of tVCP group (Fig 7.5 and Table R7.4B).

7.6.2 Probe trial.

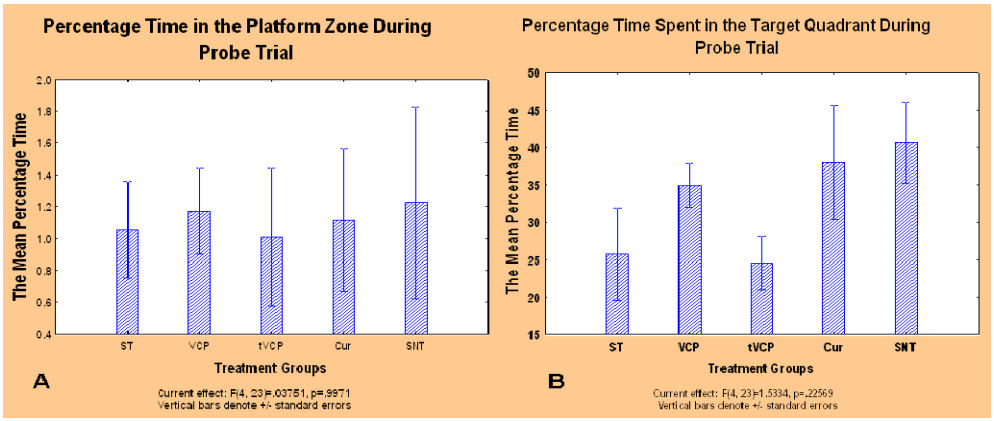

Figure 7.6. *The mean percentage time (Y axis) spent by the treatment groups (X axis) in the Platform Proximity (Fig A) target quadrant (Fig B) where the platform was originally located during Sp L P of MWM during the probe trial session of MWM.*

Results: There was no significant difference in the mean percentage time spent by the treatment groups in the close proximity zone and the target quadrant of MWM, where the platform was originally located (Fig 7.6 and Table R7.5A and B, Appendix R).

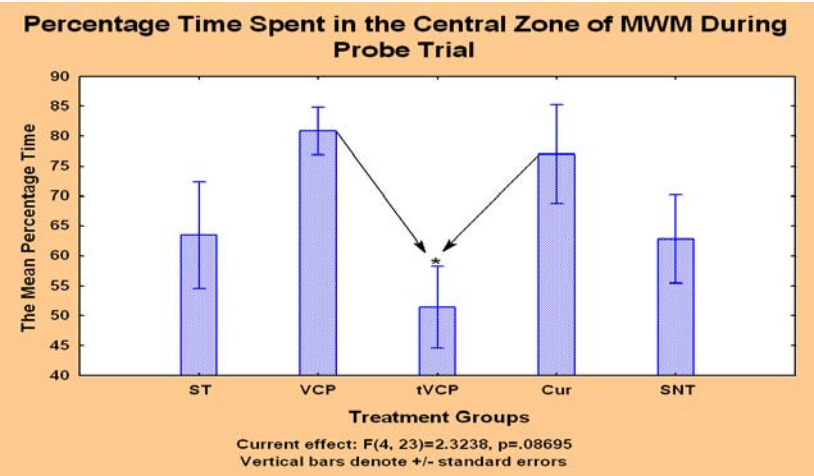

Figure 7.7. *The mean percentage time spent (Y axis) by the treatment groups (X axis) in the central zone of MWM during the probe trial session of MWM Sp L P. The bar bearing asterisk differs significantly from the bars indicated by the black arrows*

Results: There was no significant difference in the mean percentage time spent by the treatment groups in the central area of MWM as revealed by NK. However, Duncan's test revealed a significant difference between VCP and tVCP treated mice (Fig 7.7 and Table R7.6B, Appendix R).

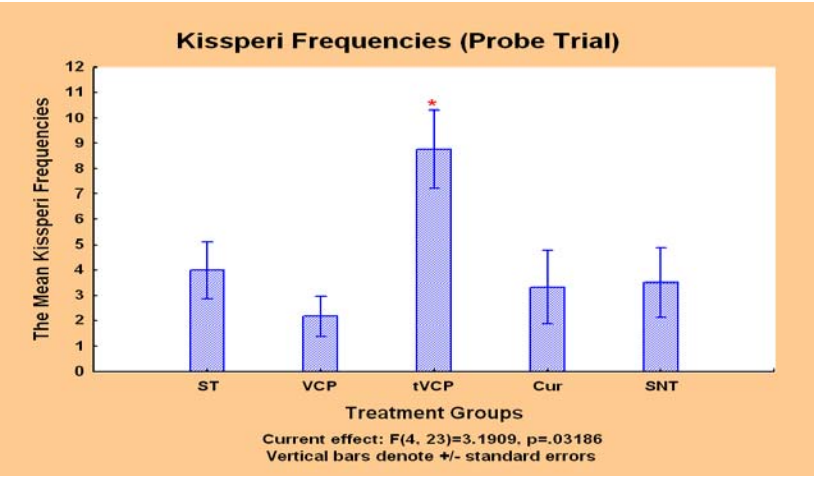

Figure 7.8. *The mean kissperi frequencies (Y- axis) shown by the treatment groups (X- axis) during the probe trial session of MWM. The red asterisk bearing bar differs significantly from all the other treatment groups*

Results: The statistical analysis using ANOVA revealed a significant difference between tVCP and all the other treatment groups in the mean kissperi frequencies by this group during the probe trial session of MWM (Fig 7.9 and Table R7.7B, Appendix R).

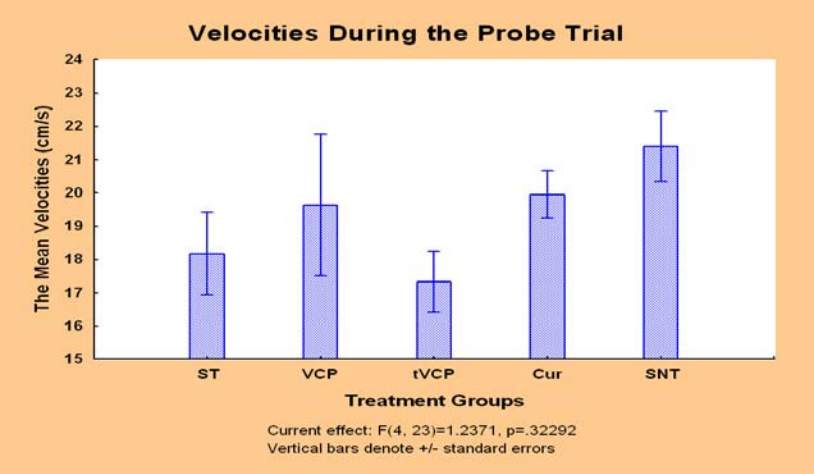

Figure 7.9. *The mean velocities (Y axis) of the treatment groups (X axis) during the probe trial session of MWM.*

Results: There were no significant differences between the treatment groups in their mean velocities during the probe trial session of MWM, measured during the probe trial session (Fig 7.9)

7.6.3 Sp R P

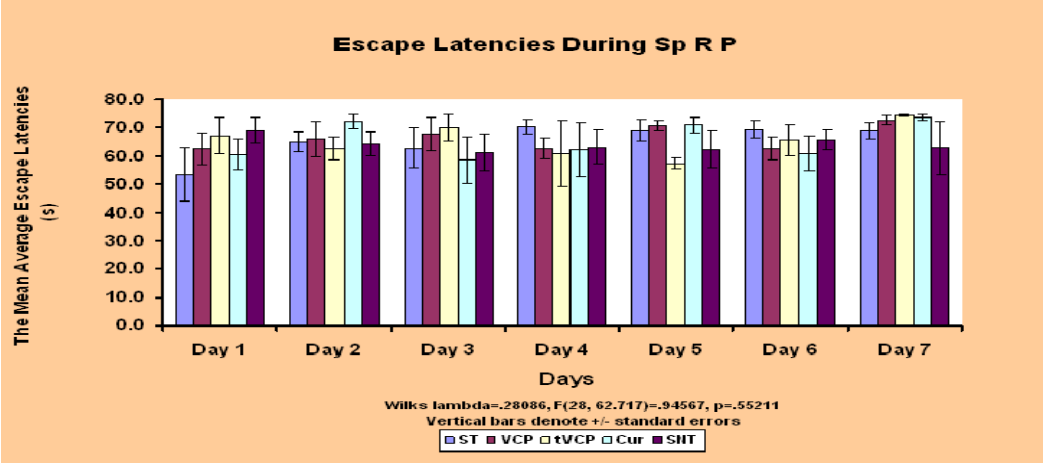

Figure 7.10. *The mean average escape latencies of the treatment groups (Y axis) during seven days (X axis) of MWM Sp R P.*

Results: There are no significant differences in the mean average escape latencies of the treatment groups during MWM Sp R P as suggested by repeated measures ANOVA (Fig 7.10). The post hoc analysis using NK revealed no significant difference within the treatment groups in their mean escape latencies.

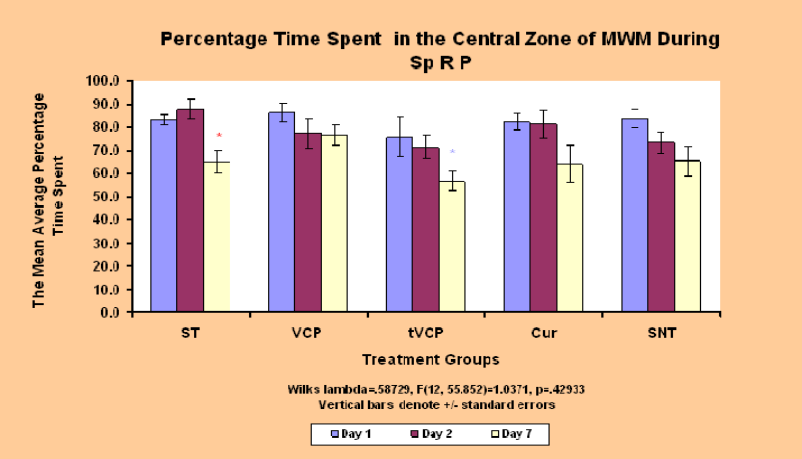

Figure 7.11. *The mean average percentage time spent in the central zone of MWM (Y axis) by the treatment groups (X axis). The significance of the within group difference on different days is shown by colour coded asterisk(s). the mean average percentage of time spent in the central zone by the treatment groups on days 1, 2, and 7 are shown by The colour of the asterisk(s) matches with the colour of the bar representing the mean average percentage time taken by the same group, but on a different day.*

Results: There was no significant difference between the treatment groups on days one, two and seven of Sp R P as revealed by repeated measures ANOVA and NK. However, within group analyses suggest that there was a significant drop in the overall mean average percentage time spent by the treatment groups in the central zone on day 7 (Table R7.10B, Appendix R). Also, tVCP and ST groups spent significantly less time in the central zone of MWM on the seventh day of Sp R P ($p^* = 0.030422$ for ST [between day 2 and day7] and 0.049727 for tVCP [between day 1 and day 7].

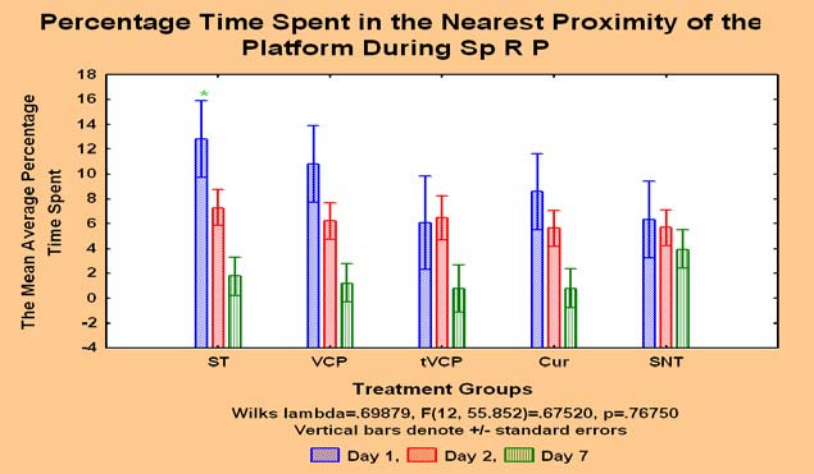

Figure 7.12. *The mean average percentage time (Y axis) spent by the treatment groups (X axis) in the nearest proximity of the platform during Sp R P of MWM. The level of significance of difference within the treatment group is shown by the colour coded asterisk(s). The colour of the asterisk(s) matches with the colour of the bar representing the mean escape latency of the same treatment group, compared to a different day of Sp R P.*

Results: There was no significant difference between the treatment groups in the mean average percentage time spent by them in the nearest proximity of the platform during Sp R P as revealed by repeated measures ANOVA (Fig. 7.12). However, the within group analysis of the pooled data revealed a drop in the overall mean average percentage time spent by all the treatment groups in the nearest proximity of the platform on the second and seventh day (Table R7.11B, Appendix R). In the case of ST group, there was a significant drop in the mean average percentage time spent by these mice in the nearest proximity of the platform on day seven (Fig 7.12 and Table R7.11C, Appendix R).

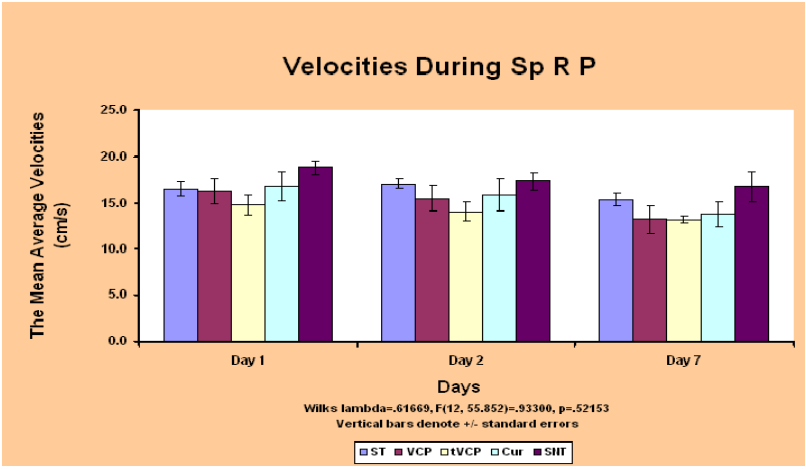

Figure 7.13. *The mean average velocities (Y axis) of the mice from various treatment groups on days one, two and seven (X axis) of Sp R P of MWM.*

Results: The repeated measures ANOVA showed no significant difference in the mean average velocities of the treatment groups on the first, second and seventh day of Sp R P of MWM (Fig 7.13)

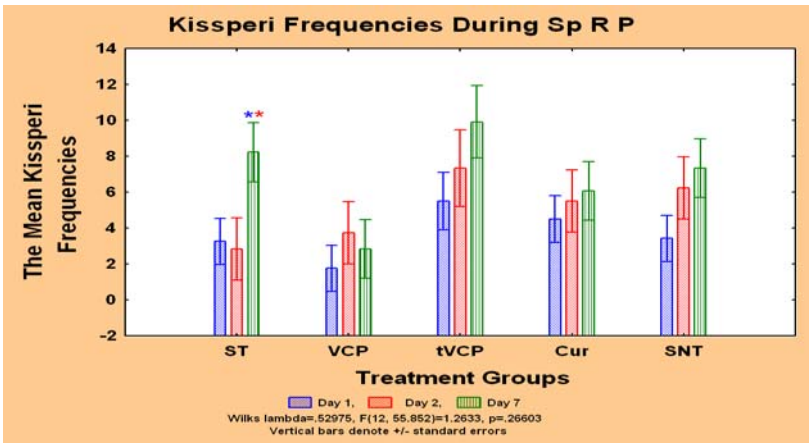

Figure 7. 14. *The mean average kissperi frequencies (Y-axis) of the treatment groups (X-axis) on the first, second and seventh days of SP R P of MWM.*

Results: There was no significant difference between (and within) the treatment groups in the mean average kissperi frequencies shown by them on days one, two and seven of Sp R P as revealed by repeated measures ANOVA and NK (Fig 7.14). However, the overall mean kissperi frequencies of the treatment groups on days 2 and 7 was significantly higher than that of the mean kissperi frequencies shown by them on day 1 of Sp R P (Table R7.13B, Appendix R). The overall increase in the mean kissperi frequencies on days 2 and 7 was almost linear in all the groups (not shown). The post-hoc analysis using Duncan test also revealed that the kissperi frequencies on the 7th day of the ST group were significantly higher than days 1 and 2 (Table R7.13C, Appendix R).

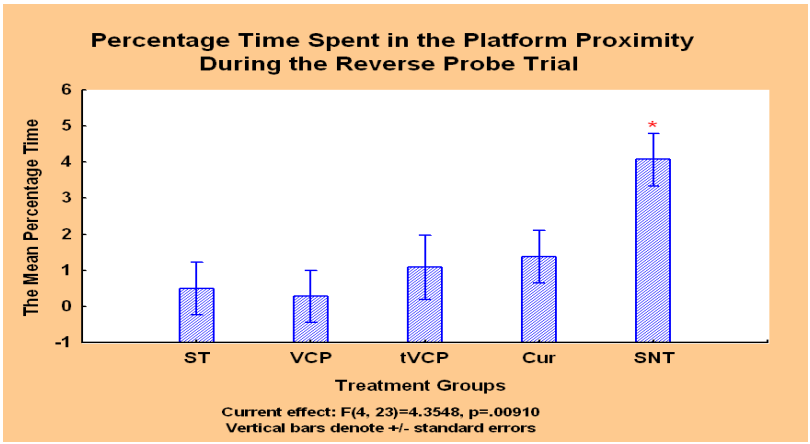

Figure 7. 15. *The mean percentage time (Y axis) spent by the treatment groups (X axis) in the platform proximity (the position of the platform during Sp R P of MWM). The red asterisk shows significant difference from all the treatment groups.*

Results: As shown in the Fig 7.15 the mean percentage time spent by the SNT group in the platform proximity was significantly higher compared to the other treatment groups (Table R7.14B, Appendix R).

7.6.4 Reverse Probe Trial.

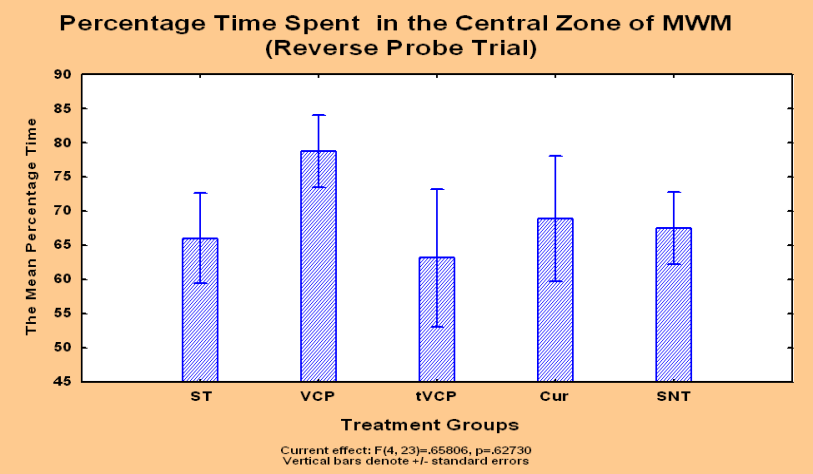

Figure 7.16. *The mean percentage time spent (Y axis) by the treatment groups (X axis) in the central zone of MWM*

Results: There was no significant difference in the mean percentage time spent by the treatment groups in the central zone (Fig 7.16)

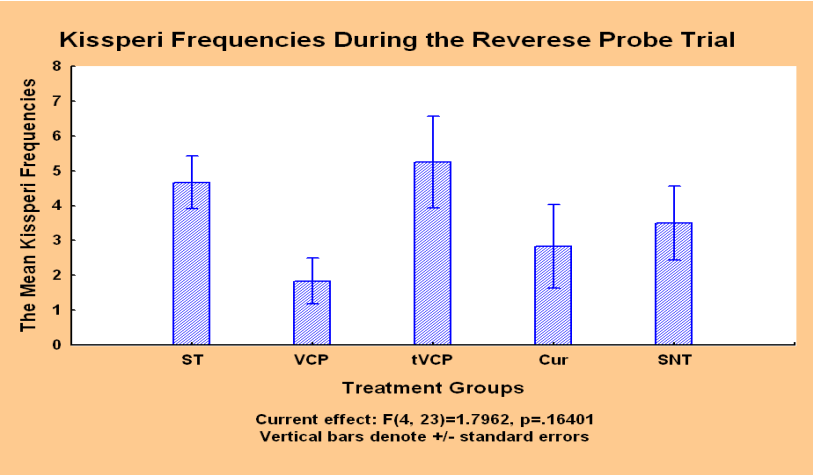

Figure 7.17. *The mean kissperi frequencies of the treatment groups during the reverse probe trial session of MWM.*

Results: There was no significant difference between the treatment groups in the mean kissperi frequencies shown by them during the reverse probe trial session of MWM.

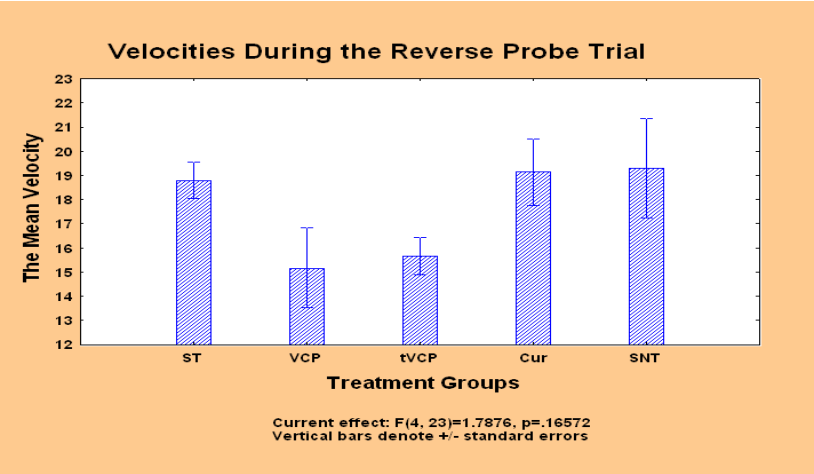

Figure 7.18. *The mean velocities of the treatment groups during the reverse probe trial session of MWM*

Results: There was no significant difference between the treatment groups in their mean velocities during the reverse probe trial session of MWM.

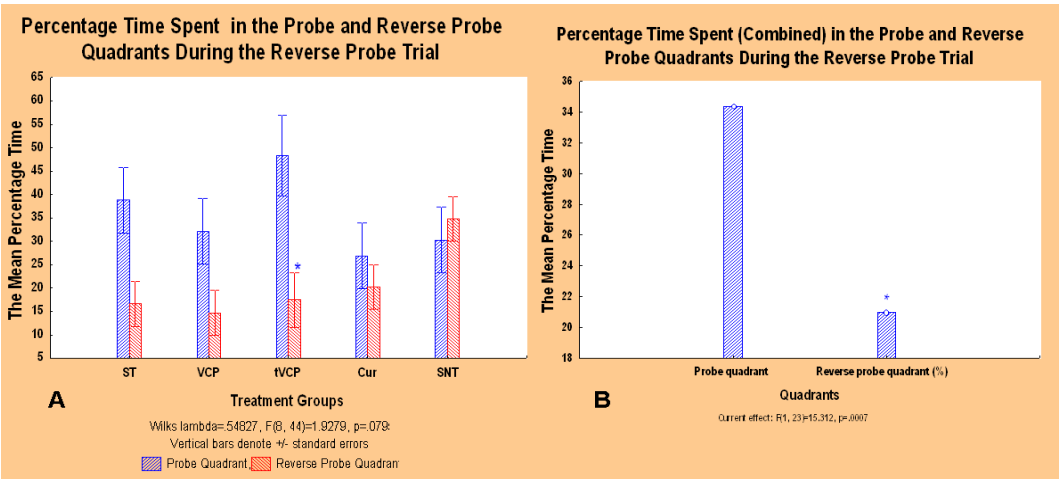

Figure 7.19.A. *The mean percentage time spent by the treatment groups in the probe and reverse probe quadrants during the reverse probe trial session of MWM.* **B.** *The comparison of the combined mean values of the percentage time spent by all the treatment groups during the probe with that of the reverse probe trial.*

Results: There was no significant difference between the treatment groups in the mean percentage time spent by them in the probe and reverse probe quadrants during the reverse probe trial session (Fig 7.19 A). However, within group analysis using repeated measures ANOVA and subsequent post-hoc analysis (NK) revealed a significant difference in the mean time spent by tVCP groups in the probe quadrant compared to that of the reverse probe trial session quadrant ($p = 0.021231$; Table R7.18B, Appendix R).

Also, the combined mean values of the percentage time spent by all the treatment groups in the probe quadrant was significantly higher than the combined mean values of the percentage time spent by these treatment groups in the reverse probe quadrant (Fig 7.19B, Table R7.18C, Appendix R).

7.6.5 Mean Path Shapes During probe and reverse probe trial.

Path Shapes and Final Positions of Mice at the End of the Probe and Reverse Probe Trials.

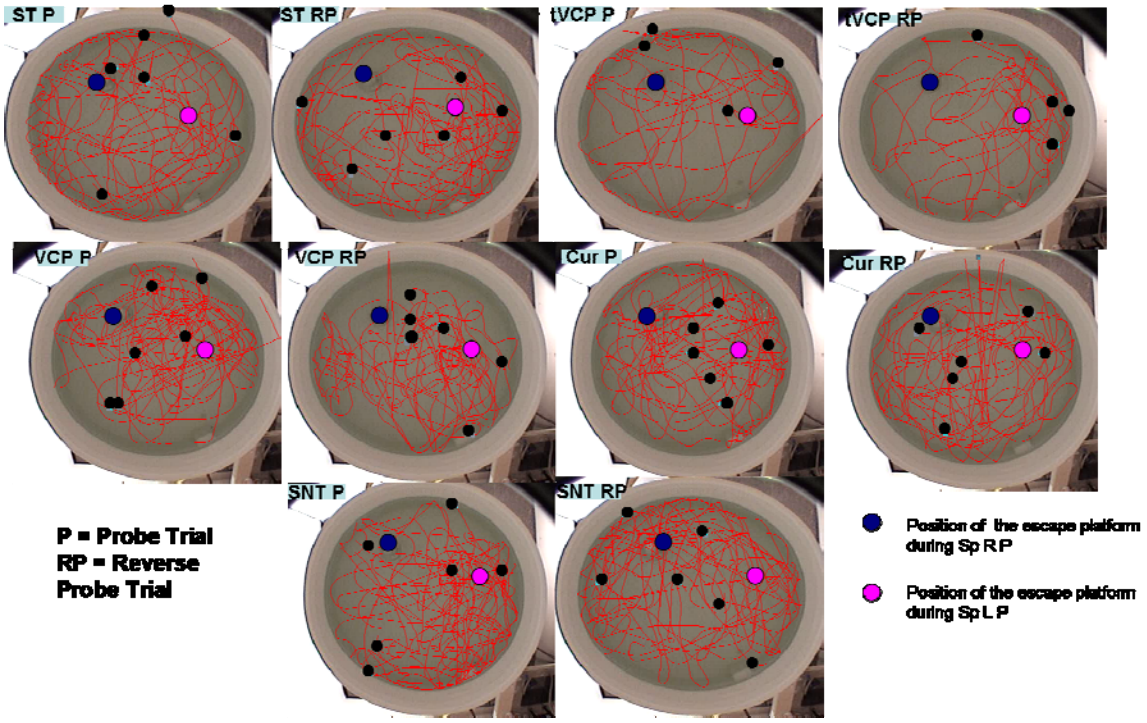

Figure 7.20. *Examples of the mean path shapes of the treatment groups during the probe and reverse probe trials. The black dots indicate the final positions of individual mice within the treatment group at the end of the trial. The positions of the escape platform during Sp L P and the Sp R P are shown by blue and pink circle, respectively. For the discussion of the results, the term "probe platform position" refers to the position of the platform during the Sp L P and "reverse platform position" refers to the position of the platform during Sp R P.*

Results: As shown in the Fig 7.20, the mean path shape (indicated by the red lines) for each treatment group was typical and varied from the other treatment groups during both the probe and reverse probe trials. Inspection of the path shape for each treatment group during the probe trial was similar to that during the reverse probe trial.

The density of the path shape of ST group in the central and peripheral zones suggested equal exploration of these zones by these mice during the probe and reverse probe trials. The final position of mice from the ST groups during the probe trial session and reverse probe trial session (as shown by black dots) was closer to the periphery than the centre, although one or two of them were dwelling in the close proximity of the position of the probe or reverse probe platforms. These mice also spent

considerable time in the proximity of the probe quadrant (ST P of Fig 7.20). The mean path shape of this group, however, was denser in the proximity of the probe quadrant than in the reverse probe quadrant (ST RP of Fig 7.20) during the reverse probe trial session.

The VCP treated mice showed central tendencies as shown by the density of the path shape during the probe (VCP P of Fig 7.20) and reverse probe trial sessions (VCP RP of Fig 7.20). Even during the reverse probe trial, the path shape of the mice from this group was denser in the proximity of the probe platform than in the proximity of the reverse probe platform.

The path shape for the mice from tVCP group was denser at the periphery during both the probe and reverse probe trials (tVCP P and tVCP RP). These mice spent more time in the proximity of the probe platform even during the reverse probe trial session as suggested by the dense path in the proximity of the probe platform and the final position of these mice indicated by black dots near the probe platform.

The path shape for the mice from Cur group showed almost equal density near the proximity of both the probe and reverse probe platforms during the probe and reverse probe trials (Cur P and Cur RP of Fig 7.20), although it is somewhat denser in the proximity of the probe platform during the reverse probe trial session. The mean path shapes of the mice from this group during both the trials suggested that these mice explored the periphery to a greater extent than that of the VCP treated mice.

The mice from SNT group showed a denser path in the proximity of the probe platform during the probe trial session (SNT P of Fig 7.20) and almost equally dense path shapes in the probe and reverse probe platform proximity. These mice showed denser central path shape than that of ST or tVCP group, but the peripheral path shape was denser than that of VCP group. The path shape for this group was denser in the reverse platform proximity during the reverse probe trial session than that of the other treatment groups.

7.6.6 Sp W P.

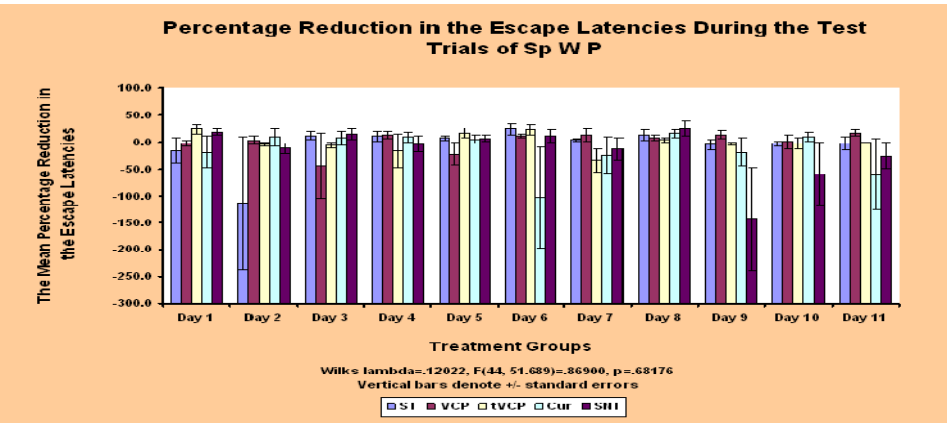

Figure 7.21. *The mean percentage reduction in the average matching escape latencies(Y axis) of the treatment groups during the test trials conducted over a period of 11 days (WMD1 to WMD11) during Sp W P of MWM. The Y axis crosses the X axis at -300. The negative values of the mean percentage reduction indicate increase in the mean escape latencies during the test trials.*

Results: The mean escape latencies during the test trials of Sp W P were expected to decrease from the escape latencies during the sample trial. However, there was no reduction in the mean percentage of the average escape latencies during the test trials of MWM Sp W P. The negative values of percentage reduction (See section 7.5.9 for the calculation of the mean percentage reduction values) in the treatment groups during the trials, in fact, suggest increase in the mean average matching escape latencies during the test trials of MWM Sp W P. This indicated that all the treatment groups were not able to learn the task during Sp W P.

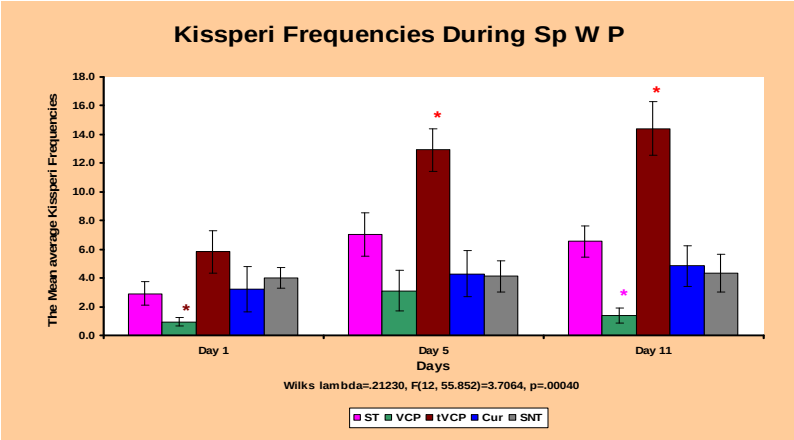

Figure 7.22. *The mean kissperi frequencies(Y axis) of the treatment groups on the first, fifth and eleventh (the last) day of Sp W P (X axis). Significant difference between the treatment groups is shown by the colour coded asterisks, where the colour of the asterisk(s) represents the colour of the bar(s) being compared. The red asterisk(s) represent a significant difference from all the treatment groups on the same day of testing*

Results: As shown in the Fig 7.22 (Table R7.20B, Appendix R), there is a significant difference in the mean average kissperi frequencies by VCP and tVCP treated groups on the first day of Sp W P of MWM. On the fifth and eleventh day, tVCP treated mice differed significantly from all the other treatment groups in the mean kissperi frequencies by them (Fig 7.22 and Table R 7.20B, Appendix R). On the eleventh day, the mean average kissperi frequencies by ST group were significantly more than that of the VCP treated group (Fig 7.22 and Table R 7.20B, Appendix R).

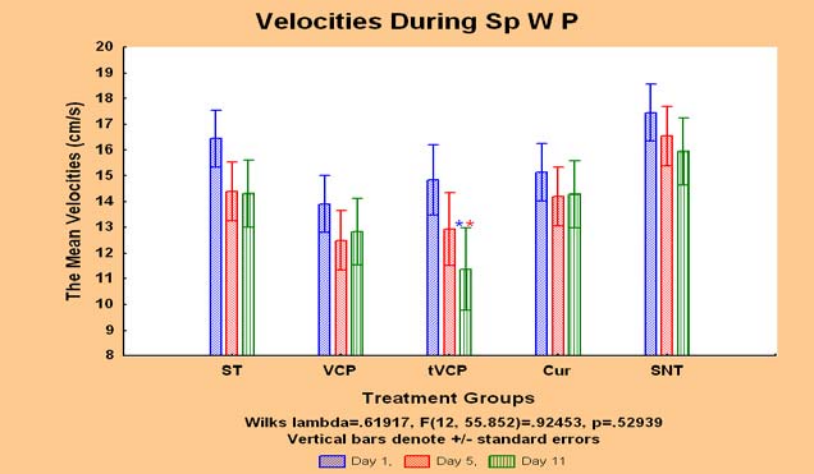

Figure 7.23. *The mean average velocities (Y axis) of the treatment groups on the first, fifth and eleventh day of Sp W P of MWM (X axis).*

Results: There was no significant difference in the mean velocities of the treatment groups on the days one, five and eleven of Sp W P of MWM. The within group analysis suggested that in the case of tVCP treated mice, there was a significant drop in the mean average velocity on the eleventh day of Sp W P ($p = 0.008208$; NK). There was overall reduction (Significant; NK) in the mean velocities of all the treatment groups on days five and eleven (Table R7.21B, Appendix R).

7.6.7 Summary of Results.

Sr	Experiment	ANOVA/ RMANOVA	Post-Hoc (NK/D)	Conclusion
1	Escape Latency during Sp L P (Fig 7.2)	p = 0.00362*	Day 3 = SNT* > ST and tVCP (NK)	Impairment of cognitive function in ST. No improvement with intranasally administered VCP and tVCP. Slight improvement with intranasal Cur treatment.
			Day 2 = SNT*> ST, VCP, tVCP (NK) Cur* > ST and tVCP (NK)	
			Day 7 – SNT > tVCP	
2	Time spent in the central zone (Fig 7.3)	p = 0.03735*	SNT*>ST, tVCP, and Cur (NK; Day one)	Intranasal VCP treatment improves exploration of he centre on day 1
3	Time spent in the nearest platform proximity (Fig 7.4)	p=0.02196*	SNT* > ST, VCP, tVCP, Cur	Impairment of Sp L P in APPswe mice, and failure of the intranasal treatment to correct the same
4	Mean velocities during Sp L P (Fig 7.5)	p=0.09244	SNT* and Cur* > tVCP only on day two	There was no difference within the treatment groups in their mean velocities. On day two of Sp L P, the mean velocitiy of the tVCP treated group was lower than that of SNT and Cur.
5	Mean % time spent in the probe proximity (Fig 7.6A)	p=0.9971	No*	No difference in the spatial reference memory amongst the treatment groups
6	Mean % time spent in the target quadrant (Fig 7.6B) (Probe trial)	p=0.22569	No*	No difference in the spatial reference memory amongst the treatment groups
7	Mean % time spent in the central zone during probe trial (Fig 7.7)	p=0.08695	tVCP*<VCP and Cur (NK)	Decreased exploration of the central zone and increased thigmotaxis by intranasal tVCP administration. Intranasal VCP and Cur showed improvement in the central tendencies, and reduced thigmotaxis.
8	Mean Kissperi frequencies during probe trial (Fig 7.8)	p=0.03186*	tVCP*>ST, VCP, Cur, SNT	tVCP group showed elevated collisions with tank wall - May be behavioural index of anxiety.
9	Mean velocities during Probe trial (Fig 7.9)	p=0.32292	No*	No difference in the locomotor activities of the treatment groups
10	Mean escape latencies during Sp R P (Fig 7.10)	p=0.55211	No*	The treatment groups as well as controls did not learn to locate the platform
11	Mean time spent in the central zone during SP R P (Fig 7.11)	p=0.42933	ST* day 7 < ST day 1 tVCP day 7 < tVCP day 2	No significant difference between groups. Within groups difference between tVCP and ST groups. Overall reduction in the exploration of the central zone by the groups

Sr	Experiment	ANOVA/ RMANOVA	Post-Hoc (NK/D)	Conclusion
12	Mean % time in the nearest platform proximity (Fig 7.12)	p=0.7675	No* between group STday 1 > Day 2 and Day 7	No difference between the treatment groups. Within group analysis showed a significant reduction in the time spent in the nearest proximity on days 2 and 7 particularly in ST group
13	Mean velocities during Sp R P (Fig 7.13)	p=0.52153	No*	No difference in the locomotor activities of the treatment groups during Sp R P
14	Mean kissperi frequencies during Sp R P (Fig 7.14)	p=0.26603	No* between group ST day 7 > days 1 and 2	No difference between the treatment groups. Within group analysis suggested an overall increase in the Kissperi frequencies of the treatment groups. St groups showed increased kissperi frequencies on the day 7
15	Mean % time in the platform proximity during reverse probe trial (Fig 7.15)	p=0.0091	SNT*>ST, VCP, tVCP, and Cur	The SNT groups spent more time in the nearest platfrom proximity than all the other treatment groups indicating better reference memory of this group than all the other groups
16	Mean % time spent in the central zone during the reverse probe trial (Fig 7.16)	p=0.6275	No*	All the groups showed similar central tendencies
17	Mean kissperi frequencies during the reverse probe trial (Fig 7.17)	p=0.16401	No*	No difference between the treatment groups in the mean kissperi frequencies by them
18	Mean velocities during the reverse probe trial (Fig 7.18)	p=0.16572	No*	No difference in the locomotor activities of the treatment groups
19	Mean % time spent in probe and reverse probe quadrants during the reverse probe trial (7.19 A and B)	p=0.07959	No* between group tVCP probe*>tVCP reverse probe	Overall trend: Spent less time in the reverse probe quadrant than the probe quadrant even during reverse probe trial. tVCP group spent less time in the reverse probe quadrant
20	Mean path shapes during probe (P) and reverse probe (RP) trials (Fig 7.20)	Subjective analyses		ST P and RP = peripheral dense VCP P and RP = dense in the centre tVCP P and RP – dense in the periphery Cur / SNT P and RP = equal density in the central and peripheral zones

21	The mean percentage eduction in mean escape latencies during Sp W P (Fig 7.21)	p=0.68176	No*	No reduction in the % escape latencies. Negative values indicate percentage increase in the mean escape latencies
22	The mean kissperi frequencies during Sp W P (Fig 7.22)	p*=0.00040	Day 1: VCP*<tVCP Day 5: tVCP>ST, VCP, Cur< and SNT Day 11: VCP*<ST, tVCP, Cur, and SNT	Intranasal administration significantly reduced kissperi frequencies in APPswe mice, whereas tVCP administration increased the same.
23	Mean velocities during the reverse probe trial (Fig 7.23)	p=0.52939	No*between group tVCP day 11*<days 1 and 5	No effect of various treatments on the locomor activity. No difference in the mean velocities of the treatment groups. tVCP (within group: reduction on day 1 and 5)
NK = Newman Keul's multiple comparison test; D = Duncan test; * = Significant difference; p = level of significance				

7.7 Discussion.

The present study demonstrates impairment in spatial learning in 12 to 13 month old APPswePS1δE9 mice as compared to the age matched non-transgenic control mice. It has been established that greater the ratio of the platform to the tank, the greater the difficulty of the task (Williams et al. 2004, Mactutus and Booze 1994, Vorhees and Williams 2006). MWM apparatus used in the current study has increased the difficulty of the task due to increased ratio of the platform to maze. The diameter of the platform in the current investigation is 5.5 cm whereas the diameter of the water tank is 176 cm. The standard size of the tank recommended by Vorhees and Williams (2006) is 122 cm for mice, but the tanks up to 200 cm have been successfully employed for screening mice (human APP transgenic mice) for their spatial learning abilities (Galvan et al. 2006). Even with these dimensions of the tank in the current investigation, the mice from different treatment groups were able to learn the task of locating the hidden platform. However, the reduction in the mean escape latencies was not as sharp as expected even though the mice were given 75 s during each trial to locate the platform instead of the usual 60 s, and the SP L P was carried out for 7 days instead of regular 5 days mentioned in the nature protocol (Vorhees and Williams 2006).

As shown in the Fig 7.2, (Table R7.1C), there is a significantly higher mean average escape latencies of the ST compared to the SNT group on days 3 and 5. The difference between the SNT and ST group was not significant on the final day of the training (NK), which suggests that due to slow rate of learning of ST mice, there was only a slight drop in the mean average escape latencies in this group on the final day. Intranasally administered Cur showed some improvement as seen from the significantly reduced mean average escape latency on day five of this group, however the effect was not persistent on the other days. The VCP (Avg. mean escape latency on day eight = 62 s) treated mice performed slightly better than ST mice (Avg. mean escape latency on day eight = 65 s), but the difference in the mean escape latencies of this treatment group never reached significance. On the day 5, the SNT mice performed better than that of VCP treated mice, but otherwise the differences in the mean escape latencies of these treatment groups are not significant. Intranasal administration of tVCP to mice resulted in poor performance by them in Sp L P. On the day 7, there was a significant difference between tVCP and SNT mice (Fig 7.2, Table R7.1C Appendix), highlighting the difference in spatial learning of the treatment group. The combined mean average escape latencies of all the treatment groups showed a significant drop in the mean escape latencies on the days 5, 6 and 7 (Table R7.1D Appendix), meaning that all the groups of mice learnt the position of the platform.

When the mice were analyzed for the time spent in the central zone, it was found that the SNT group spent more time than that of all the other groups on day 1 with the exception of the VCP treated group (Fig 7.3 and Table R7.2B, Appendix R). This indirectly suggested that except for VCP group, all the other treatment groups spent more time in the peripheral zone (thigmotaxis) rather than showing central tendencies on day 1. However, on days 2 and seven, there was no significant difference in the mean percentage time spent by all the treatment groups in the centre of MWM. The combined mean average

percentage time spent by mice from all the treatment groups in the central zone showed a significant drop in the time spent by the treatment groups in the central zone on days 2 and 7 (Table R7.2C, Appendix R) suggesting a reduction in the overall thigmotaxic behaviour by them. This could be interpreted that they might have learnt with time that the escape was in the centre.

When the mice from all the treatment groups were analyzed for the mean percentage time spent in the nearest proximity of the platform, it was found that the SNT group spent more time in the zone nearest to the platform on day 7 than all the other treatment groups. The difference between SNT and all the treatment groups was highly significant on day seven (Fig 7.4 and Table R7.3B, Appendix R). This shows that only SNT mice learnt precisely the position of the platform and spent more time in the nearest proximity of the platform than that of all the other treatment groups. All the treatment groups, especially SNT group spent more time in the nearest proximity of the platform on the last day of the training session (Table R7.3B, Appendix R).

There was no difference in the mean average velocities of the treatment groups on days one and seven (Fig 7.5), but on day two, the mean average velocity of Cur and SNT group was more than that of tVCP group (Fig 7.5 and Table R7.4B, Appendix R). This suggests that tVCP might be affecting locomotor activity. However, it was observed that these mice showed some passive or floating behaviour on this day. There was no difference in the average velocity on the other days which suggests that the drop in the velocity could be attributed to the passive or floating behaviour of one or two mice in this group on that day and therefore not due to a variation in the motor behaviour per se.

When the probe trials were conducted to study the effect on the reference memories of these treatment groups, it was found that all the treatment groups spent nearly the same time in the probe platform proximity as well as in the target quadrant (Fig 7.6A and B, respectively) suggesting intact reference memory in all the treatment groups. However, when the significance was determined by the less stringent Duncan test rather than NK (Fig 7.7 and Table R7.6B) it was found that tVCP treated mice spent significantly less time in the central zone than that of Cur and VCP treated mice. This suggests thigmotaxic behaviour to some extent in these mice.

When the tVCP treated mice were analyzed for the kissperi frequencies during the probe trial, they showed significantly higher kissperi frequencies than that of all the other treatment groups (Fig 7.8 and Table R7.7B, Appendix R). The mice from tVCP group also show less central tendencies during the probe trial session of Sp L P as discussed previously. tVCP was also found to increase anxiogenic tendencies and reduce exploration in APPswePS1δE9 mice on EPM as shown in the previous chapter (Chapter 6). This anxiogenic tendency of tVCP treated mice could account for the reduced central tendency and increased kissperi frequencies of this group. There was no platform during the probe trial session. Increased kissperi by intranasal treatment of tVCP during probe trial may be an indicator of helplessness since they were not able to find the platform. When compared with the other treatment groups these tVCP treated mice showed significantly higher mean kissperi frequencies than all the other treatment groups. Thus the "kissperi frequency" parameter considered in this chapter could

be attributed to the anxiety status and may be used as an index of helplessness in mice. This interesting behaviour needs to be further explored.

There was no significant difference in the mean velocities of the treatment groups during the probe trial session (Fig 7.9).

As shown in Fig 7.10, there was no significant difference in learning the relocated position of the platform in all the treatment groups during Sp R P, as reflected by the unaltered mean escape latencies. This suggests that the mice did not learn the spatial reversal task.

When the mice from all the treatment groups were analyzed for the mean average percentage time spent by them in the central zone of MWM on days one, two and seven of Sp R P, the mice from ST and tVCP groups show a significant decrease in the central tendencies suggesting increased thigmotaxic behaviour by these groups on the day 7 of Sp R P (Fig 7.11).

When the treatment groups were analyzed for the time spent by them in the zone nearest to the platform, there was no difference between the treatment groups. There was a significant reduction in the overall mean percentage time spent by the respective treatment groups in the nearest proximity to the platform (Fig 7.12 and Table R7.11B, Appendix R) indicating the overall reduction in the ability of all the treatment groups to relocate the new position of the platform during the 7 day period of Sp R P. The within group analysis suggested a significant drop in the mean percentage time spent by ST groups in the nearest proximity of the platform on day 7 of the spatial learning from that of day 1 (Fig 7.12 and Table R7.11C, Appendix R). This suggested diminished ability of ST mice to relocate the changed position of the platform during Sp R P.

There was no significant difference in the mean average velocities of the treatment groups on days one, two and seven of MWM (Fig 7.13). None of the treatments therefore appeared to affect swimming ability.

When mice were analyzed for the kissperi frequencies, there was no significant difference between the treatment groups (Fig 7.14). However, when the average kissperi frequencies of all the treatment groups were combined, and this combined value was compared to the mean combined kissperi frequencies of all the treatment groups on days two and seven of Sp R P, there was significant increase in the overall kissperi frequencies by all the treatment groups (Table R7.13B Appendix R). Although the bar graph of VCP group for the mean average kissperi frequencies was always lower than that of other groups in general and tVCP group in particular due to overall increase in the kissperi frequencies in all the treatment groups, this effect was not significant.

For the reverse probe trial session analysis, when the mice were analyzed for the mean percentage time spent by them in the nearest proximity to the platform in the reverse probe trial (i.e. the area where the platform was located during Sp R P), it was found that the SNT mice spent significantly more time in this zone than that of all the other treatment groups (Fig 7.15 and Table 7.14B, Appendix R). The mean percentage time spent by the other treatment groups was from 0 to 2 percent whereas it was in the range of 4 to 5 % in the case of SNT group suggesting strong reference memory for the position of the platform during Sp R P of MWM compared to the other treatment groups. This suggests that there was

impairment in the spatial reference memory (for the spatial reversal learning) in APPswePS1δE9 mice used in the current study, and multiple intranasal doses of VCP as well as Cur failed to correct the deficit.

When the mice from all the treatment groups were analyzed for the mean percentage time spent by them in the central zone (Fig 7.16), kissperi (Fig 7.17) and mean velocities (Fig 7.18) for the reverse probe trial, there was no difference between the treatment groups.

It was suggested by Vorhees and Williams (2006) in their review on MWM in nature protocol that mice find it difficult to relocate the changed position of the platform during Sp R P and the mice preferentially choose the original position of the platform during Sp L P. In order to test whether the mice from the various treatment groups used in the current study preferred the original position of the platform during Sp L P of MWM, the mean percentage time spent by them in the probe quadrant and reverse probe quadrants were compared. As shown in the Fig 7.19 A, the mean percentage time spent by the treatment groups did not differ from each other. However, as shown in the Fig 7.19 A, all the treatment groups tend to spend more time in the probe quadrant rather than in the reverse probe quadrant , but the difference was significant only in the case of tVCP group. Comparison of the overall combined mean percentage time spent by the treatment groups in the probe and reverse probe quadrant suggested that the overall time spent by the treatment group in the probe quadrant was significantly higher than the time spent by them in the reverse probe quadrant ($p \leq 0.0007$; Fig 7.19B). This strongly suggests that all the treatment groups had intact reference memory for the position of the platform during Sp L P. Due to the strong reference memory for the platform position during Sp L P, they are not able to relocate the new position of the platform during Sp R P. However, all the treatment groups spent more time in the probe quadrant during the reverse probe trial session. This inability of the mice to relocate the platform position during Sp R P was also observed by Vorhees and Williams (2006).

When the mean path shapes of these mice were further analysed as shown in Fig 7.20 and discussed in the results section, it was found that ST mice showed mixed tendencies (i.e. Central + peripheral), tVCP group had shown peripheral tendencies whereas VCP treated group show central tendencies. The Cur and SNT groups also displayed a mixture of central and peripheral tendencies. SNT mice however showed dense path shape in the proximity of the platform during both the probe and reverse probe trials suggesting intact spatial reference memory and the ability to learn to locate the platforms during both Sp L P and Sp R P. The increased exploration of the central zone of VCP treated group during Sp R P could be attributed to the less anxiety in this treatment group. This behaviour complements the exploratory behaviour shown by the mice from this group on the EPM (Chapter 6).

When the groups of mice were further studied for the effect of the treatment on their working memory, they were not able to learn the task, since there was no significant reduction in the mean escape latencies during the test trials of Sp W P (Fig 7.21). In fact, there was increase in the overall mean escape latencies during the test session. The mice from all the treatment groups were not able to learn the task probably because the position of the platform changed during this paradigm. This may be accounted for on the basis of difficulty of the task, where the already difficult task has been

made even more complex as explained above. The mean velocity values of all the treatment groups did not differ from each other significantly during this trial (Fig 7.23).

When the mice were analyzed for the kissperi frequencies on the days 1, 5 and 11 of Sp W P trials, there is a significant difference in the mean average kissperi frequencies of VCP and tVCP groups on these three days of Sp W P. No significant difference between tVCP and the other treatment groups was found on the day one of SP W P, but on days 5 and 11 (Fig 7.22), these mice showed more kissperi frequencies than all the other treatment groups (Fig 7.22 and Table R 7.20B, Appendix R). This increase in the kissperi frequencies could be explained on the basis of the combined effects of anxiety and learned helplessness as discussed previously. The relocation of the platform on each consecutive day of Sp W P probably adds to the already difficult level of the task of locating the non-existant escape platform. The tVCP treatment elevates anxiety as shown in EPM study (Chapter 6). This high level of anxiety may be attributed to the higher kissperi frequencies by this group. On the last day of Sp W P, the kissperi frequencies of VCP treated mice were significantly lower than that of ST group. The mice from the VCP treated group showed central tendencies. Also, they showed less anxiety and more exploratory tendencies in the EPM study (Chapter 6). This could be the underlying reason for the lower kissperi frequencies shown by them throughout the study, and especially during Sp W P. The mean average velocity appears to be high on the first day of Sp W M of MWM and decreases on the subsequent days although the within and between group differences were not significant. However the overall decrease in the combined mean average velocity of all the treatment groups was observed on the days five and eleven of Sp W P (Table R 7.21B, Appendix R). This may be attributed to the "learned helplessness" by them as they learn that the platform is difficult to locate, and thus stop trying to locate the platform and perhaps conserve their energy, in the knowledge that the platform is difficult to find.

In conclusion, the APPswePS1δE9 mice show poor MWM performance as compared to the age matched non transgenic mice. Intranasally administered VCP was not able to improve the cognitive deficit in these mice, but it increased the central exploration by these mice in MWM throughout the study, and reduced anxiety in these VCP treated mice as shown by the reduced mean average kissperi frequencies and increased exploration of the central zone of MWM. The intranasal treatment of VCP was not effective in improving the ability of the mice to locate the platform probably because of the difficulty of the task. This is in contrast to previous studies, where direct administration of VCP and tVCP was found to improve the MWM performance in rodent model of TBI. Another possible explanation is that VCP was not delivered to the hippocampus at therapeutic concentration, and thus failed to improve the hippocampus dependent Sp L P. Since, VCP was shown to be taken in the olfactory glomerulor cell layer in the previous chapter, it is therefore necessary to design a behavioural model which requires use of the olfactory lobes to accomplish the task instead of using visual spatial cues to test the efficacy of VCP. Intranasally delivered Cur was able to improve the performance in Sp L P to a limited extent (only on day five), but the effect was not persistent and did not show any improvement in Sp R P. tVCP showed poor MWM performance in all the paradigms probably due to high level of anxiety in tVCP treated mice. One could argue that the behavioural difference between

VCP and tVCP could possibly be attributed to the structural differences between them and that VCP is also able to regulate the complement system, where tVCP fails to do so. The parameter "mean kissperi frequency" discussed in this chapter could be used as an important measure to explain the MWM behaviour of mice with high level of anxiety. This newly defined behaviour, reported for the first time here merits further exploration.

Chapter 8.

Intranasal Administration of VCP, tVCP and Curcumin in MO/HU APPswe PS1δE9 Mice to Investigate the Effect on Paired Associative Learning Using a Novel Cheese Board Maze Model.

8.1 Introduction.

It has been reported that the six months old APPswe mice performed less well in locating the baited flags than their non-transgenic counterparts using the ChBM paradigm (Pillay et al. 2008). In the same study using 6 months old mice, it was found that administration of VCP directly into the parietal cortex of these mice showed improvement in the ChBM performance. Further exploration of this work discussed in the chapter 5 of the thesis showed that an early administration of VCP (at 3 weeks and 6 months of age) improves associative learning in these mice in the ChBM paradigm. In the same chapter it was also concluded that there was a significant difference between ST and SNT groups, in cued learning trials compared to that of the Sp L P, and that VCP improves performance. The next objective was to study the therapeutic effectiveness of intranasally delivered VCP on learning and memory in the transgenic mice and compare the effect of VCP to that of tVCP and Cur. However, as discussed in the chapter 6, there was a difference in the spatial learning abilities of the ST and SNT groups. VCP treatment tended to improve the exploration of the central zone of MWM as suggested by mean path shapes during the probe and reverse probe trials, but the effect on the spatial learning was not statistically significant, probably because MWM is based on the spatial learning which requires hippocampus (Barnes et al. 1988, Jarrard et al. 1993). As discussed in Chapter 3, VCP delivered intranasally could be detected in the glomerular cells of the olfactory lobes, and not in the hippocampus. It was therefore necessary to test the effect of intranasally administered VCP on a task which involves the olfactory lobes.

The ChBM behavioural results of mice treated with VCP as discussed in the chapter 5 have shown that cued-learning and spatial memory rather than spatial learning is affected in aged APPswe mice. VCP treated mice show improvement in cued learning in these mice. Although VCP, tVCP and Cur were administered intranasally in this study, and these compounds, delivered via this route, were detected in the glomerular cell layer of the olfactory lobe, in none of the models used in the current study was the olfactory related task used. It is well known that this part of the brain is affected at an early age in AD patients. It is also reported that transgenic APPswe Fischer344 AD rats show deficit in the spatial dependent social transmission food preference (STFP) paradigm which requires odour-odour association to get the food reward (Ruiz-Opazo et al. 2004). The APPswe transgenic mice also show impairment in object discrimination tasks (Ewers et al. 2006). Thus, data from the animal studies (Ruiz-Opazo 2004, Ewers et al. 2006, Good and Hale 2007, Good et al. 2007) as well as human studies suggests that many forms of learning including hippocampus dependent spatial and associative learning are affected in AD.

Most of the routinely used animal models for cognitive assessment focus on one particular aspect of learning and memory, e.g. MWM is extensively used for spatial learning (Vorhees and Williams 2006); contextual fear conditioning related to fornix damage associate fearful response with place (Phillips and LeDoux 1994), whereas some learning paradigms associate odour with the reward (Alvarez et al. 2002), and some others are based on location of objects (Good and Hale 2007). Learning in human being as well as in rodents is a complex phenomenon which involves the use and/or

association of more than one cue or factor. Therefore, in the current investigation, it was decided to develop a model using ChBM which requires association of more than one cue to find out whether there is a difference in associative (or association) learning between APPswe mice and their age matched non transgenic controls and modulation of the same by multiple doses of VCP, tVCP and Cur.

8.2 Objectives.

In the line with the overall aim of investigating the effects of VCP, tVCP and Cur on different forms of learning, the objectives of the chapter were:

1) Comparison of the paired associative learning abilities of ST and SNT mice using a novel paired associative learning cheese board maze model (PAL-ChBM), and modulation of the same by VCP, tVCP and Cur treatment.

2) Investigation of the effect of VCP, tVCP, and Cur on various paired associations using probe trials.

8.3 Materials.

VCP and tVCP expressed in *P. pastoris* yeast expression system (Chapter 2), and rendered free of endotoxin. These were diluted in phosphate buffered saline (PBS). Cur (Sigma) solution was freshly prepared prior to intranasal administration by dissolving as mentioned in the Appendix S. All other materials such as thioflavine S, HEPES etc were the same as in Chapter 5. The mice used in the study were already genotyped in the Chapter 6.

8.4 ChBM and description of the behavioural room.

The ChBM used in the current study consists of a circular wooden board, 80 cm in diameter, with 156 wells each of 1 cm in diameter and 1 cm deep. The wells were arranged in parallel rows in such a way that the distance between the nearest points of the two wells is approximately 2.5 cm. As the transgenic mice used in the study were black, the board was painted in white with matt finish to provide the contrast while analysing the data. Three pictures composed of black and white geometric shapes, positioned at a distance of approximately 2 m from the centre of the maze at three different positions in the room served as extra-maze cues. The maze was elevated to a height of 72 cm from the base of a 175 cm circular tank in which it was placed for logistical reason. The edge of the maze from all the sides was approximately 75 cm away from the periphery of the circular tank.

8.5 Methods.

8.5.1 Grouping.

The same transgenic mice groups that were previously used in the MWM study were used in this study, i.e., ST, VCP treated, Cur and tVCP treated, and (SNT). The number of mice used was six per group except for the tVCP group (n=4, and = 3 during the probe trials, as one mouse died just before the

commencement of the probe trials). Even though only four (or three in some of the probe trials) mice were in this group, they were included in the statistical analysis because of the consistent results shown by them, and there were no spare transgenic mice of the same age treated in a similar manner that were available.

8.5.2 Dosing.

After the MWM study was over, one day before the commencement of pre-training session, VCP, tVCP, and Cur were administered intranasally to the respective treatment groups. For the dosing regimen refer to chapter 6 (section 6.4.4) and chapter 7 (section 7.5.2). The time intervals for dosing are as shown in the Appendix F (Fig F1.3).

8.5.3 Paired-association learning (PAL).

This task which involves spatial-object-odour associative learning to find the reward was defined as PAL- ChBM. Before commencing the 8 day PAL-ChBM paradigm, the mice were subjected to a mild food-deprivation protocol, habituation, and a pre-training session of three days. When mice reached an age of approximately 13 and half months, from the day before the habituation commenced they were subjected to the mild food deprivation protocol. The protocol and conditions for the food deprival were similar to that described in the chapter 5 and followed by others (Pillay et al. 2008). Five sugar pellets were introduced into the cages of these mice to familiarize them with pellets and to avoid behaviours such as hyponeophagia. The mice were also monitored for the percentage weight loss, allowing not more than 10-15% of their body weight loss.

8.5.4 Habituation.

As discussed in the Chapter 6, the anxiety and exploratory profile in APPswe mice is different from VCP and SNT treated mice. The elevated anxiety or reduced exploration as observed in these mice in EPM could be attributed to neophobia and it was necessary to habituate the mice prior to the start of the experiment. In an attempt to further reduce the effect of neophobia and anxiety in these mice, the ChBM was kept at the centre of the MWM tank. Mice were familiar with the room environment and thus habituated to the room environment.

For habituation on ChBM, the mice from various treatment groups were allowed to explore the ChBM baited with one pellet per well as mentioned in the Chapter 5. However, as there were five groups, the time of habituation was reduced to 150 s and also the habituation lasted for 3 days instead of 10 days. In the current study, the mice were familiar with the room environment, unlike the mice in the Chapter 5, and therefore three days were considered to be sufficient for the habituation phase. The mice used for the ChBM study in the chapter 5 were habituated for 10 days as they were never exposed to the behavioural room prior to the experiment.

8.5.5 Pre-training before PAL-ChBM.

The pre-training was similar to the ChBM pre-training paradigm used in chapter 5 but with some modifications. In PAL-ChBM, it was decided to use two different types of flagpoles (A = a flagpole bearing one flag and B = a flagpole bearing three flags) as two different objects. For the purpose of discussion, these flagpoles are referred as flags A and B throughout the text. The arrangement of flags A and B for PAL-ChBM task is shown in the Fig 8.1. For the pre-training session the same flags A and B shown in Fig 8.1 were used, but the number of flags and their arrangement was different (not shown). The pre-training task in before PAL-ChBM is similar to the pre-training session before ChBM study (Chapter 5, section 5.5.2 A). Briefly, instead of using 4 similar flags (4 X A) used during the pre-training session of ChBM, 6 flags (3 X A + 3 X B) were randomly placed at the centre of the ChBM for the pre-training session. The mouse under trial was placed at the centre of the ChBM, and was allowed to explore the ChBM during the pre-training session for 4 min 15 s (255 s). The time of the trial was adjusted to finish pre-training of all the treatment groups during day time. During each trial, either flags A or flags B were baited with sugar pellets. For three mice in each group (2 for tVCP), flags A were baited with pellets, whereas for the remaining three mice (two mice for tVCP group) flags B were baited with pellets. The flags placed in the wells baited with pellets are termed reward flags (RFs). The time required by the mouse under test to find the RF was recorded as latency to find out the RF. The number of visits to the RFs as well as pellets consumed during pre-training session was also recorded. The other behaviours such as measurement of faecal boli were also monitored.

8.5.6 PAL-ChBM paradigm.

The model requires that the mouse under test searches for the reward by using the extra-maze spatial cues as well as intra-maze object cues (Flags A ad B) and association of an odour when in close proximity to the flag associated with the reward cue. For this task, ChBM was modified as shown in the Fig 8.1 below. Briefly, the ChBM was arbitrarily divided into four quadrants. Two different flags (A and B) indicated wells flavoured either with cumin (Flag A) or cinnamon (Flag B) were kept at a distance of 52 cm from each other in opposite quadrants as shown in the Fig 8.1 were at-least 1.5 m from the centre of ChBM. For flavouring the well indicated by the flags, either cinnamon or cumin powder was mixed with a small amount of press stick (approximately quarter to half of a tea spoon of powder / 6g of press stick). A small ball of flavoured press-stick was inserted into the flagged well. The extra-maze cues (black and white shapes). A was RF for three mice, whereas for the remaining three mice RF was B. The various treatment groups under test were subjected to 8 days PAL-ChBM protocol, and three probe trial sessions (Type I, Type II and Type III). The protocol is summarised in the table 8.1.

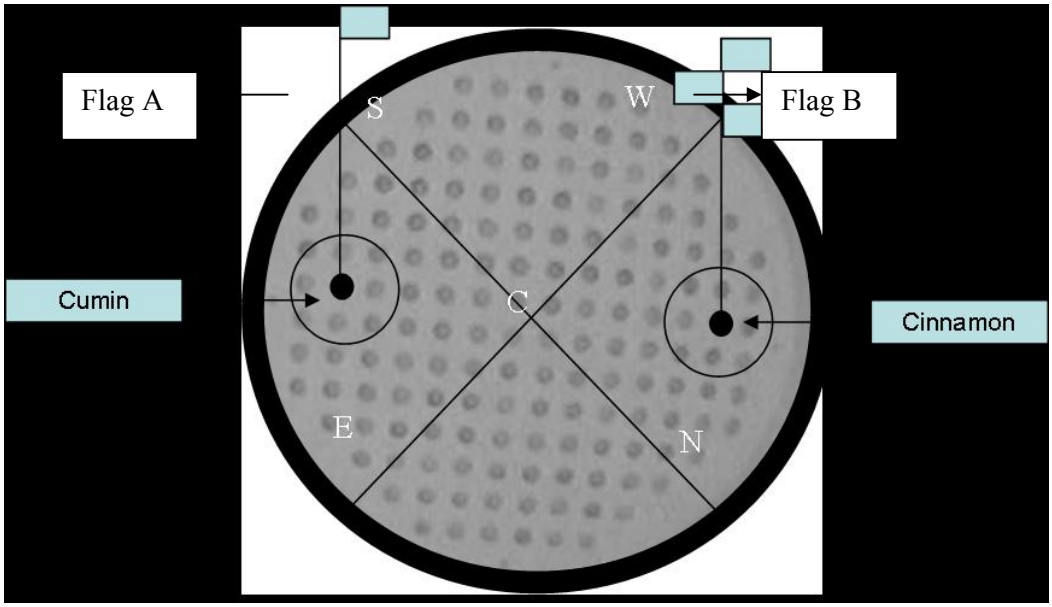

Figure 8.1. *Diagrammatic representation of ChBM indicating positions of RFs A and B (Flagged wells baited with odourless food pellets shown by dark circles), and positions of mouse release points (S, E, N, W and C) to test for PAL.*

Behavioural test and testing protocol for PAL-ChBM

Sr	Test	Protocol	Duration
1	PAL	Only one of the odour wells was baited with reward (sugar pellets). For each trial, a mouse was released from different release points (Fig 8.1) and allowed 60 s to visit the correct flag or the reward flag (RF). The mouse was considered to have visited RF only if it consumes a pellet hidden in the flagged well. The total number of visits to RF on test days and average time taken to visit RF was used as an index of learning.	60 s X 4 trials / day for eight days
2	Probe Trial Type I (Odour-Spatial)	No flags were used. The mouse has to find the pellets based on odour and spatial cues. For half of the mice in each group Cumin, and for the rest of them, Cinnamon was associated with reward.	2 trials/day + 2 regular trials for two days
3	Probe Trial Type II (Flags-Odour)	The ChBM was surrounded by a curtain (approx 90 cm from the centre of ChBM) to hide the extra-maze cues. The mouse under trial has to locate RF using flags and odour cues.	2 trials/day + 2 regular trials for two days
4	Probe Trial Type III (Odour only)	Probe Trial Type Three: The ChBM is surrounded by a curtain, but no flags used. Mouse under trial has to locate the well which was previously indicated by the RF using odour cues only.	2 trials/day + 2 regular trials for two days

Table 8.1. *Outline of the behavioral test, testing protocol and duration of each training session (Sr = Serial number).*

8.5.7 Thioflavine S staining. At the end of the study, the mice were subjected to transcardial perfusion and the brain sections were subjected to thioflavine S staining as mentioned in the Chapter 5 (section 5.5.4).

8.5.8 Data recording and analysis.

The behavioral data was analysed using Ethovision 3.1 supplied by Noldus. For the analysis, the ChBM was divided arbitrarily into 4 zones. Two zones were flagged zones (meaning zone comprising flags), and two zones were non-flagged zones. The Flagged zones were also divided into various proximity zones. Repeated measures ANOVA and post-hoc analysis using Newman-Keuls and/or Duncan's test were used for the statistical analysis. The graphs plotted (MS Office Excel or Statistica) are least square (LS) means ± SEM values. The significance levels are indicated by colour coded asterisks. The colour matches with the bar graph being compared. Red asterisks indicate significant difference to all treatment groups.

8.6 Results.

8.6.1 Pre-training session.

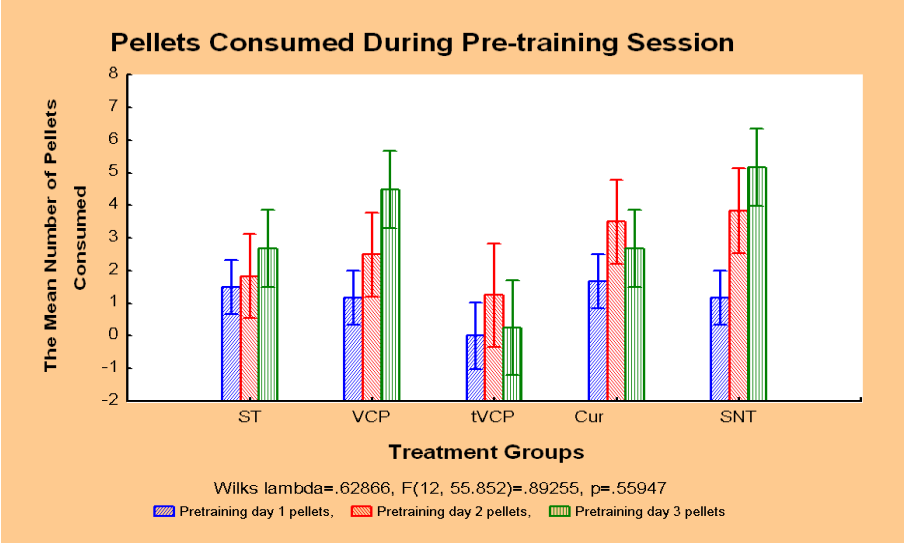

Figure 8.2. *The mean number of pellets consumed (Y axis) by the treatment groups during the period of three days of the pre-training session.*

Results: There was no difference in the mean number of pellets consumed by the treatment groups during pre-training session as shown in the Fig 8.2, the NK test also revealed no difference between the treatment groups in the mean number of pellets consumed by them during the pre-training session. The less stringent Duncan test revealed a significant difference in the mean pellets consumed by the SNT and tVCP group on day three of the pre-training session (Appendix R [Table 8.1B]).

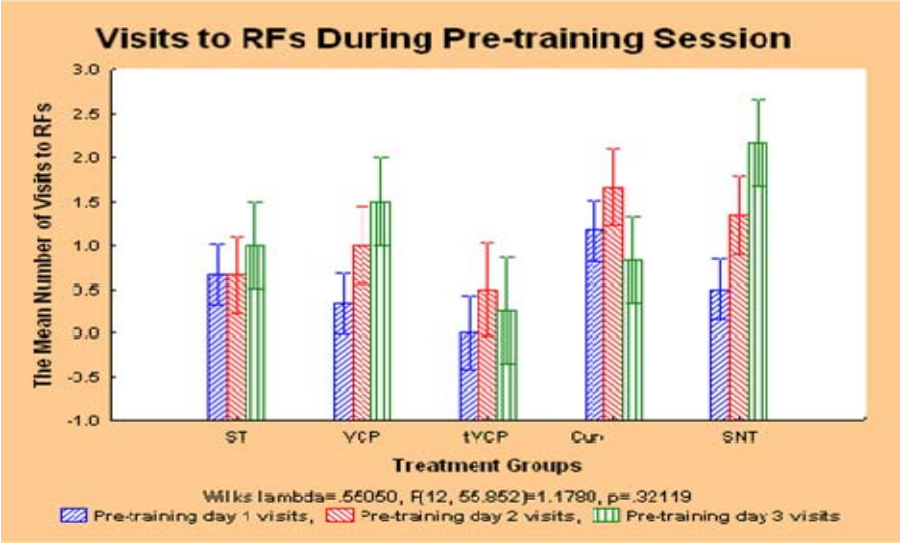

Figure 8. 3. *The mean number of visits to RFs (Y axis) by various treatment groups (X axis) during pre-training session of ChBM-PAL paradigm.*

Results: There was no difference in the mean number of visits to RFs by the treatment groups (Fig 8.3). Although the difference was not significant, the mean number of visits within the treatment groups ST, SNT and VCP increased on day two and three showing a trend in the increased mean number of pellets consumed. In tVCP and Cur treated groups, the mean number of visits to RFs are more on the second day than that of the first and the third day, but the difference was not significant.

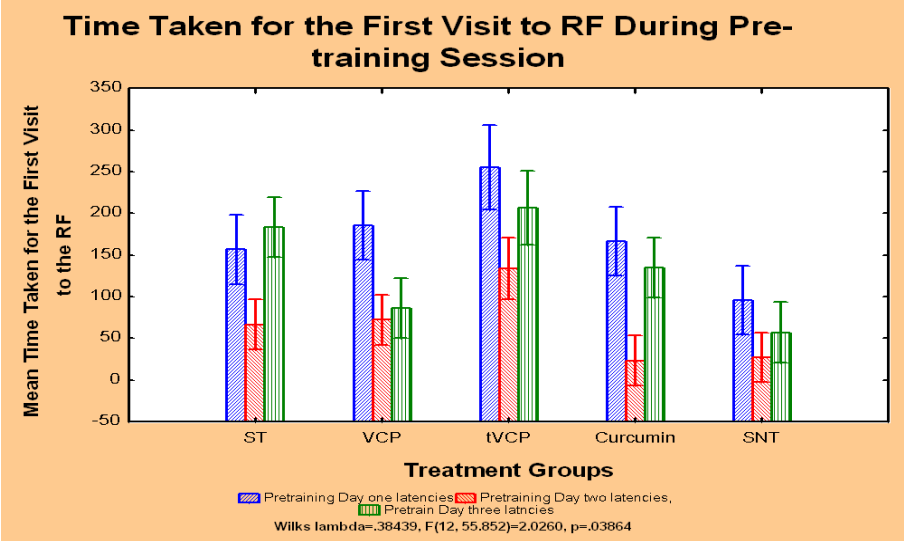

Figure 8.4. *The mean time* taken (Y axis) by the treatment groups (X axis) for their first visit to a RF during pre-training session

Results: Repeated measures ANOVA revealed a significant difference between the treatment groups in the mean time taken by them for their first visit to a RF (Fig 8.4). However, post Hoc analysis using NK revealed no difference between the treatment groups. Less stringent Duncan test however revealed a significant difference only between SNT and tVCP group on day one. On the day two, the mean time taken by Cur and SNT groups to visit the first flag was significantly less than that of the tVCP group. On the final day of the pre-training session, the mean time taken by the tVCP treated group to visit the first RF was significantly more than all the other treatment groups except for Cur group (results not

shown. Refer to summary of results table (Section 8.6.6) and the Appendix R (Table R8.3B) for the significance values and / or significant differences between the treatment groups.

8.6.2 PAL-ChBM.

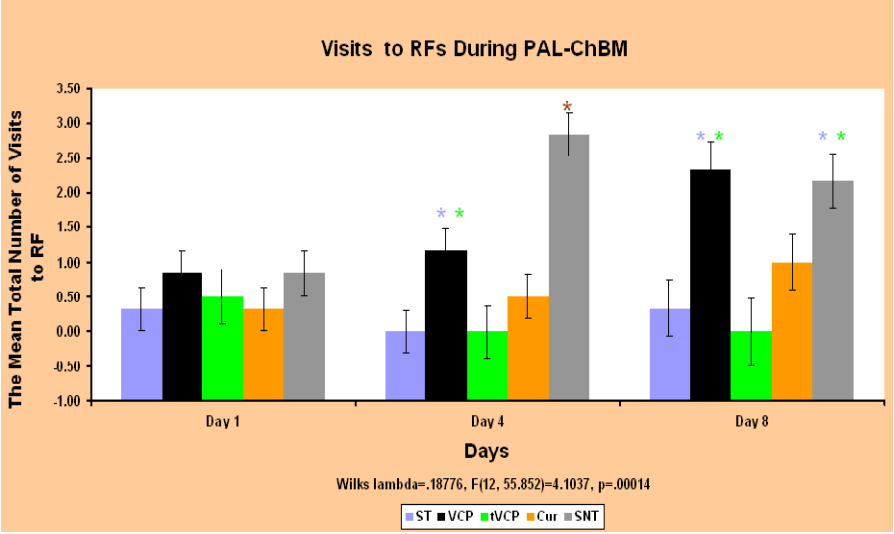

Figure 8.5. *The mean total number of visits (4 trials) to RFs by the treatment groups during PAL-ChBM*

Results: There was no difference in the mean total number of visits to RF on day one of PAL-ChBM paradigm (Fig 8.5). On day four, the mean number of visits by the VCP treated group was more than that of ST and tVCP groups, whereas SNT group visited RFs a greater number of times than all the treatment groups. On day eight, the mean number of visits to RF by VCP and SNT mice was significantly more than that of tVCP and ST groups (Table R8.4B, Appendix R).

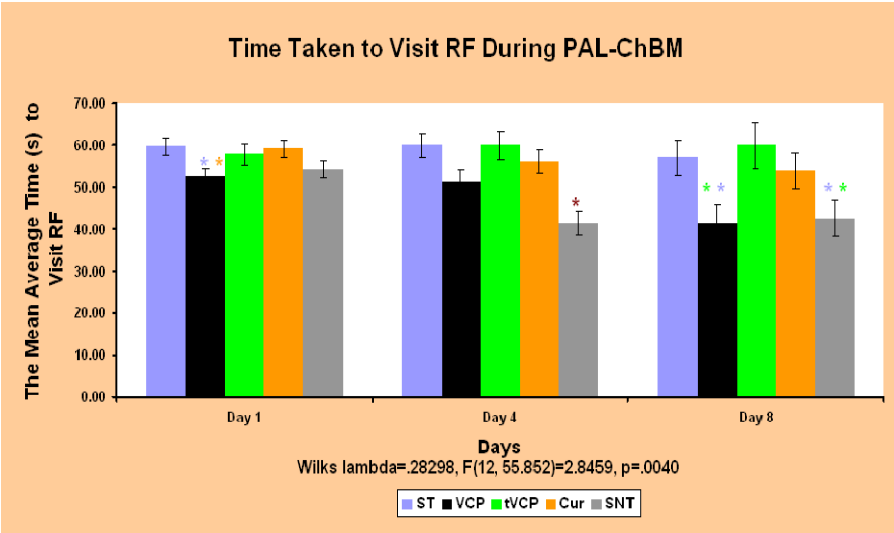

Figure 8.6. *The mean (average time of 4 trials) time taken by the treatment groups to visit RF during PAL-ChBM task on days one, four and eight.*

Results: The mean average time taken by VCP and SNT mice was significantly less than that of tVCP and ST groups on day eight of PAL-ChBM (Fig 8.6, Table R8.5B, Appendix R). All the treatment groups took significantly more time to visit RF than that of SNT as revealed by the mean average time

analysis on day four. On day one, the mean average time taken by VCP treated mice to visit RF was less than that of Cur and ST groups.

8.6.3 Probe Trials.

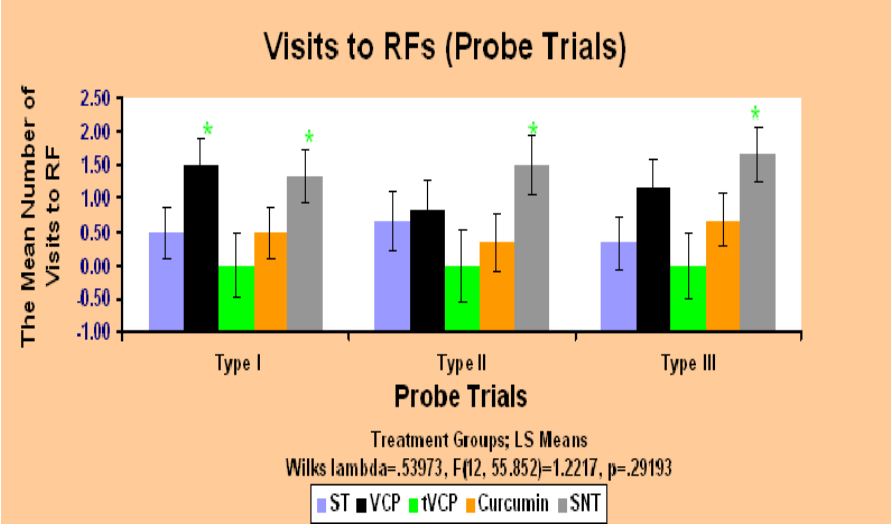

Figure 8.7. *Comparison of the mean number of visits (Y axis) by various treatment groups (X axis) during Probe Trials Type I, II, and III.*

Results: Repeated measures ANOVA did not reveal any significant difference between the treatment groups (Fig 8.7). However, post hoc analysis using Duncan test revealed significant difference between VCP and tVCP treated groups during the probe type I session, and SNT mice performed better than that of tVCP treated mice during all the three probe trial sessions (R8.6B, Appendix R)

8.6.4 Path shape analysis.

Path Shapes on Day One.

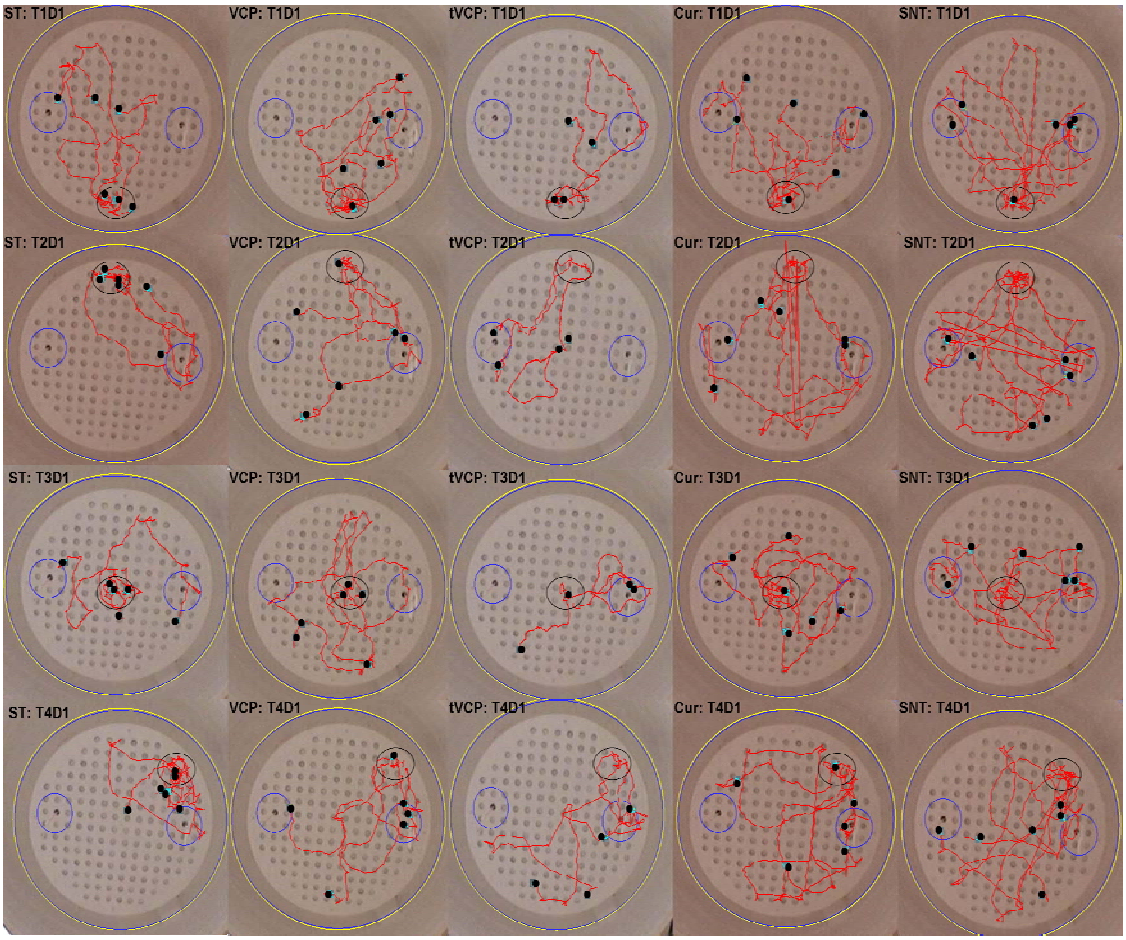

Figure 8.8. *The mean path shapes taken by various treatment groups during four trials (T1, T2, T3, and T4) on Day 1 (D1) of ChBM-PAL task (black ellipse = release positions, black dots = final position of individual mice, blue circles = flag position, red lines = average path shape. (Note: Position of individual mice is shown by black dots. The path shapes were captured using Ethovision 3.1 (Noldus).*

Path Shapes on Day Eight.

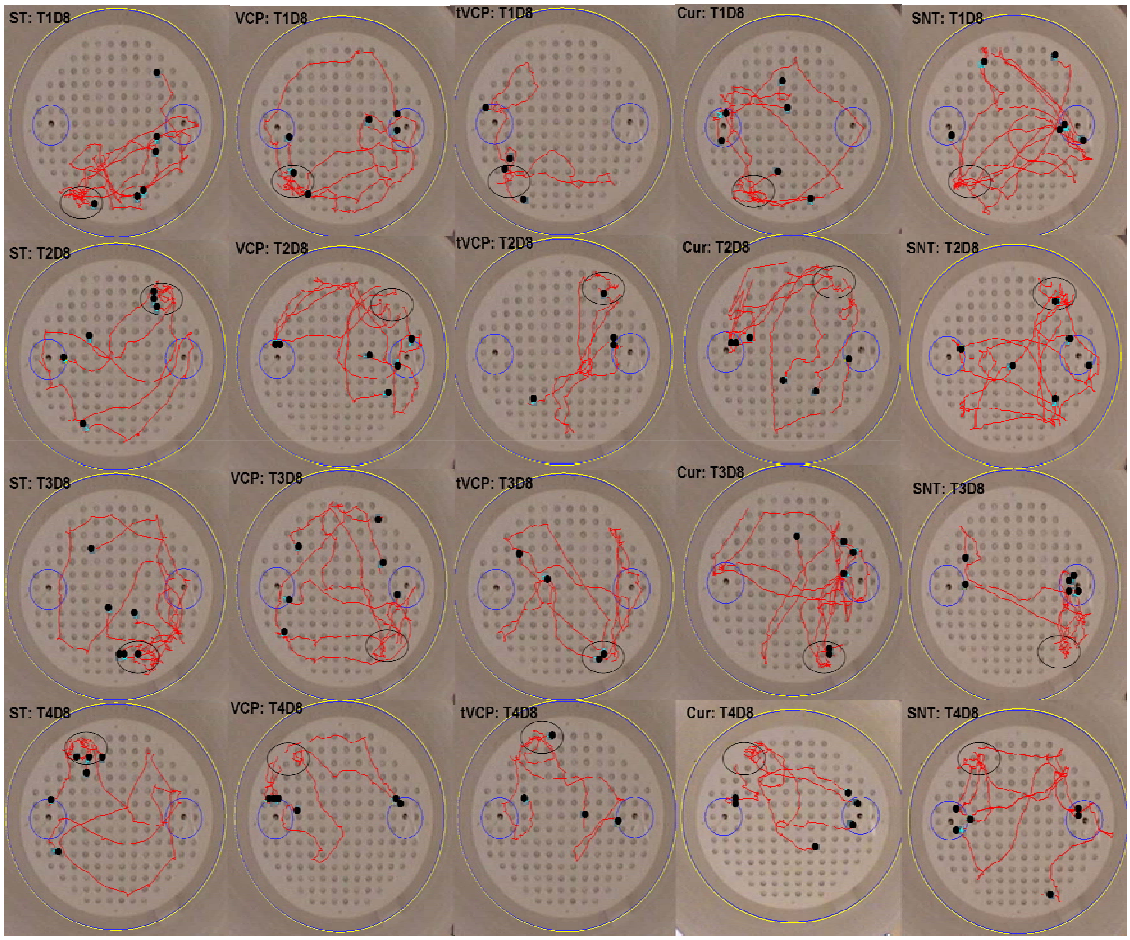

Figure 8.9. *The mean path shapes taken by various treatment groups during four trials (T1, T2, T3, and T4) on Day 8 (D8) of ChBM-PAL task (black ellipses = release positions, black dots =final position of individual mice, blue circles = flag position, red lines =average path shapes*

Results: Comparison of the mean path density as an index of time spent near RP taken by various treatment groups during four trials (T1 to T4) on day one (Fig 8.8) and day eight (Fig 8.9) revealed that the mice from ST group spent more time near the release positions (RPs) on day one and day eight during all the four trials as shown by more dense red average path shapes near the RPs (i.e. black circles) than in other area of the ChBM. These mice were not moving far from the RPs, and were visiting the flag nearest to the release position irrespective of it being RF or NRF. VCP treated mice spent less time at the release positions and explored the maze on day one and day eight as is evident form the path shapes taken by them on ChBM. On day 8 (Fig 8.9) they spent more time in the proximity of flags (mostly RF). The mice from tVCP group on the first as well as on the last day showed variable response. They spent more time either at the release positions (esp. day eight) or near the non RF. The mice from Cur group explored the maze well on both days although they spent more time near the

release positions on day one (Fig 8.8), but explored the maze quite well on the day eight and spent more time in the near proximity of the flags, but the frequency of the exploration didn't convert into a visit as most of them did not eat pellets from the odour matched RF. SNT mice explored the maze quite well on the day one and day eight, but spent more time near the release position on day one and spent more time in the proximity of RFs on day eight. The frequent exploration of the RF was converted into a visit in most of them as they consume the pellets from the well indicated by RF. Details regarding the mean path shapes, path density, release positions, and conclusion are shown in the summary of results section.

8.6.5 Thioflavine S staining.

Thioflavine S stained brain sections.

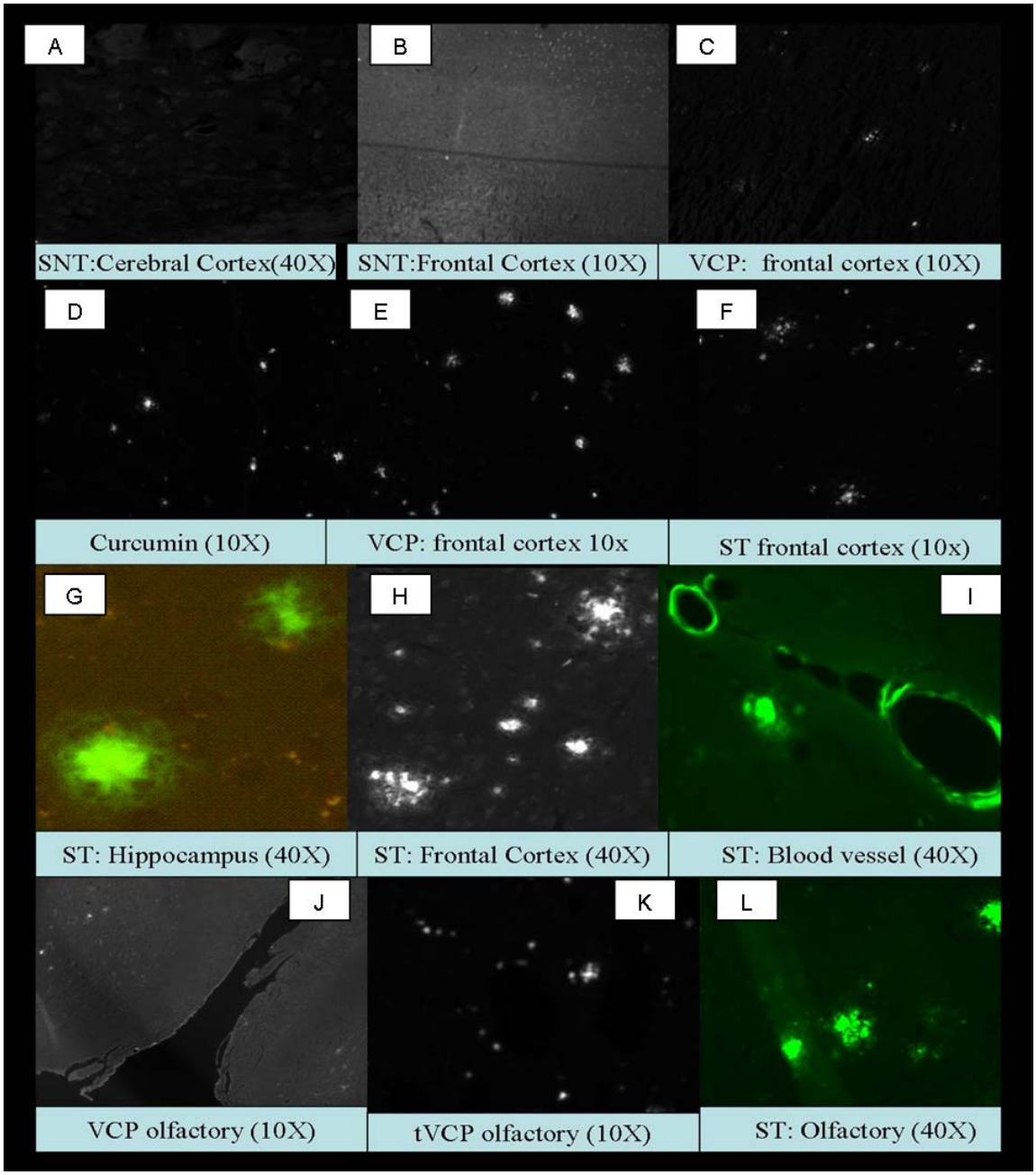

Figure 8.10. Examples of *thioflavine S stained brain sections from different parts of the brain from ST, VCP, tVCP, and SNT treatment groups (at 10x or 40x; colored or black and white)*

Results: None of the mice from SNT group showed thioflavine S staining (A and B). The mice from ST group showed staining of the frontal cortex (F), hippocampus (G), cerebral cortex (H), blood vessels (I), as well as the olfactory lobes (L). The transgenic mice from the other treatment groups also showed a similar pattern of staining in different parts of the brain, although it appeared relatively less intense in some of the VCP treated mice brain sections (C and J).

8.6.6 Summary of Results.

Sr. No	Session / Trial	Parameters	ANOVA/ RMANOVA	Post-Hoc analysis (NK / Duncan (D)	Conclusion
1	Pre-training session (Fig 8.2 to 8.4)	Mean Pellets Consumed	0.63866 (RMA)	No* (NK) VCP and SNT*>tVCP [(day 3 (D)]	Tendency to learn to associate cues with reward. No difference between the treatment groups. However, SNT and VCP showed better trend in pre-training task than the other groups, especially tVCP. Cur also performed slightly better than tVCP group.
		Mean Visits to the RF	0.5505 (RMA)	No* SNT>tVCP (day 3)	
		Mean Time for the First Visit to the RF	0.038439* (RMA)	NK = No* SNT*<tVCP [(day 1 (D)] SNT and Cur*< tVCP [(day 2 (D)] SNT*<ST and tVCP [Day 3 (D)] VCP*<tVCP [Day 3 (D)]	
2	PAL-ChBM Mean Total number of Visits to RFs (Fig 8.5)		0.00014***	No (Day one) NK	Impairment in PAL in ST. No impairment in SNT. Intranasal VCP treatment improves PAL-ChBM.
				VCP*>ST and tVCP (Day 4) SNT* > all (Day 4) NK	
				VCP* and SNT*> ST and tVCP (Day 8) NK	
3	PAL-ChBM (Fig 8.6)	Mean Avg Time to Visit RFs	0.00408** (RMA)	VCP*> Cur / tVCP (NK; Day 1)	Impairment in PAL in ST. No impairment in SNT. Intranasal VCP treatment improves PAL-ChBM.
				SNT*> all (NK; Day 4)	
				SNT* and VCP* > Cur / ST (NK)	
4	Probe type I (Odour-Spatial) (Fig 8.7)	Mean number of Visits to RFs	0.29193 (RMANOVA)	VCP* and SNT* > tVCP (D) NK = No*	SNT used all the cues effectively, and performs slightly better than the other other groups. ST, Cur and tVCP requires object cues as well. VCP group could associate Odour and spatial cues with reward. tVCP performed more poorly than all the groups, but differed significantly from SNT. Trend for VCP group to perform slightly better than tVCP group (to some extent better than ST, Cur).
	Probe Type II (Odour-Flags) (Fig 8.7)	Mean number of Visits to RFs		SNT* > tVCP (D) NK = No*	
	Probe Type III (Odour only) (Fig 8.7)	Mean number of Visits to RFs		SNT* > tVCP (D) NK = No*	

5	The mean Path Shapes, density and release positions (RP) on DAY ONE.			
	Mean Path Densities, Shapes, and the final positions of mice at the end of the trial (Near RP or flags) of Mice from Treatment Groups on Day One of PAL ChBM (Fig 8.8)	Treatment Groups	Observation	Conclusion
		ST (n=6)	Density: Dense near RP in all the trials. Shape: short, leading to the nearest flag or centered around RP. RP: More mice at RP. Flags: 1 mouse during each trial.	Less Exploration. More Anxiety.
		VCP (n=6)	Density: Dense near RP. Equal spread near flags and rest of the ChBM Shape: leading towards both the flags, and in 2 trials centered around RP, and throughout the maze. RP: Only one mouse near RP except for the trial three. Flags: 2 to 3 mice near flags except for trial three.	Better Exploration compared to the ST group. Less Anxiety than the ST group.
		tVCP (n=4)	Density: More dense in the proximity of RP, but explored flags and rest of the maze Shape: leading towards the flag nearest to RP, centered around RP, and to some extent in the rest of the maze. RP: No or 2 mice at RP Flags: 1 to 2 mice near flags except for trial one.	Better exploration and less anxiety than the ST group.
		Cur (n =6)	Density: More dense in the proximity of RP, but equal spread near flags and rest of the maze Shape: leading towards both the flags, in the proximity of RP, centered around RP, and to some extent in the rest of the maze. RP: No or 1 mouse at RP Flags: at least mouse near each flag.	Better exploration and less anxiety than the ST group.
		SNT (n=6)	Density: Equal spread in the proximity of RP, near flags and rest of the maze Shape: leading towards both the flags, in the proximity of RP, centered around RP, and to some extent in the rest of the maze. RP: No mouse at RP in T2-T4 (T1 =1) Flags: at least 2 mice near each flag.	Better exploration and less anxiety than all the transgenic treatment groups and ST in particular. Better ability to associate the reward with the RPs than all the other treatment groups.

6	The mean Path Shapes, density and release positions (RP) on DAY EIGHT			
	Mean Path Densities, Shapes, and the final positions of mice at the end of the trial (Near RP or flags) of Mice from Treatment Groups on the Day Eight of PAL-ChBM (Fig 8.9)	ST	Density: Dense near RP in all the trials, but equal spread near both the flags except for the trial one Shape: short, leading to the nearest flag (both flags in a few cases) or centered around RP. RP: 3-4 mice at RP. Flags: 1 or no mouse near flags.	Less Exploration. Mice still anxious. Could not associate the RF with reward.
		VCP	Density: less dense at RP. Equal spread near flags and rest of the maze Shape: leading towards both the flags. RP: No mouse near RP except for the trial one (2 mice). Flags: 3 to 6 mice near flags. 1 to 2 mice near each flag (RF).	Better Exploration than ST. Less Anxiety than ST. Better association of RF with reward (sugar pellets) than the ST group.
		tVCP	Density: More dense in the proximity of RP, but explored flags and rest of the maze Shape: leading towards the flag nearest to RP, centered around RP, and to some extent in the rest of the maze. RP: 1 to 3 mice near RP Flags: 1 to 2 mice near flags except for trial three.	Better exploration and less anxiety compared to the ST group. No improvement in the associative learning.
		Cur	Density: Less dense in the proximity of RP, but equal spread near flags and rest of the maze Shape: leading towards both the flags, and the rest of the maze. RP: No mouse at RP Flags: at least 2 mice near each flag (mostly NRF).	Better exploration and less anxiety than the ST group. Learn to locate the flag, but could not associate reward with RF suggesting no improvement in associative learning.
		SNT	Density: Less dense at RP, equal spread near flags and rest of the maze Shape: leading towards both the flags, and to some extent in the rest of the maze. RP: No mouse at RP except for the trial two (1 mouse) Flags: 3 to 6 mice near each flag. At least 2 mice near each flag.	Better exploration and less anxiety than all the other groups, except for VCP. Intact ability to associate reward with the RF.
7	Thioflavine S staining (Fig 8.10)	There was staining of the plaques in the cerebral cortex, hippocampus, and olfactory area. Pattern was similar in the treatment groups and ST. No thioflavine staining in SNT group.		Impairment of cognition in ST could be attributed to the plaques. VCP, improves cognition, probably through its ability to prevent plaque mediated neuroinflammatory events rather than inhibiting plaque formation.
NRF = Non reward flag; RF = Reward Flags; Cues = flags, odour and spatial;				

8.7 Discussion.

Associative learning or paired-associative tasks in rodents is not a new concept. The object-odour pairing or odour-place associative learning models have been used in the past (Gibb et al. 2006, Gilbert and Kessner 2002) for the assessment of cognitive behaviour in rodents. In these studies, cinnamon and/or cumin were paired either with an object or place. Using the same concept of the paired associative learning, a new model was developed and employed in the current investigation which requires paired association with odour-spatial-object cues (RF) in order to find the reward. The ChBM was similar to the one used by others (Gilbert and Kessner 2002, Pillay et al. 2008). As the modified ChBM protocols were based on the concept of paired-associative learning (PAL), it was named as PAL-ChBM.

This newly developed PAL-ChBM was successfully employed in the current investigation to study the paired associative learning ability in APPswe PS1δE9 mice, transgenic treatment groups, and SNT groups. For this study, initially mice were habituated. During habituation, ST mice spent more time exploring the area in the proximity of the release positions. The exploration behavioral strategies differed in various treatment groups as evident the current investigation. The mice from VCP, tVCP, Cur and SNT group showed good exploration strategy on the day three of habituation as shown by similar central and peripheral exploration tendencies by these mice.

When these mice were subjected to a pre-training session of three days, these mice did not differ significantly in the number of pellets consumed by them (Fig 8.2), number of visits to RFs (Fig 8.3), and the time taken by them for their first visit to a RF (Fig 8.4). The graphs, however, suggest that on the final days of the pre-training session, the performance of VCP treated and SNT groups improved compared to other treatment groups than that of the other treatment groups, but the difference was not statistically significant as per NK test. However, Duncan test revealed a significant difference between SNT and tVCP groups in the mean time taken by them for their first visit to a RF.

During the PAL-ChBM task, the mean number of visits by different treatment groups on day four and eight (Fig 8.5), and the time taken by these mice to visit RF (Fig 8.6), revealed a better performance of SNT mice compared to all the treatment groups. The effect was prominent on day four of the testing. On day eight, VCP treated mice also showed a similar performance on PAL-ChMB task. Their performance was better than that of tVCP and ST groups. The results suggest that there is impairment in the paired-associative learning abilities of APPswe PS1δE9 mice as compared to age matched non transgenic controls. These data are in parallel with some other studies (Gruart et al. 2008) where they have shown impairment in associative learning in these mice. VCP was able to significantly improve the observed deficit. The effect of VCP administration was better than that of tVCP. As discussed in previous chapters, tVCP is structurally related to VCP, but lacks one module. The number of tVCP mice during this trial was less than the minimum required number for the statistical analysis (n=6) as some of the mice in this group died before the behavioural trials commenced. However, the four remaining mice showed a similar behavioural trend, this being the reason why they were included in the study. Marked variation in the behavior of VCP and tVCP treated transgenic mice could be attributed to the lack of module one in the structure of tVCP. As discussed in the previous chapters, as

well as shown by others (Smith et al. 2003), all the four modules of VCP contribute to its unique biological profile. As VCP is a better inhibitor of complement than that of tVCP, the observed improvement in the PAL-ChBM task by VCP could be attributed to its complement regulatory activity.

When probe trials were conducted to study the effect of various paired-associations (Table 8.1 and Fig 8.7) there was no significant difference between the treatment groups. This suggested that all the three cues, spatial, object (flag) as well as odour played an important role in learning by SNT treated groups. There was probably mild cognitive decline in ST mice, which could be attributed to its poor performance in the PAL-ChBM task.

When, mean path shapes of different treatment groups were examined (Fig 8.8 and 8.9; series 5 and 6 of the summary of results [table]) on day one and day eight, it was found that ST mice spent more time near the release positions compared to that of the SNT group on the 1st and 8th day. VCP treated mice, on the other hand, spent less time near the release positions during all the four trials on the 1st and 8th day (Fig. 8.8 and 8.9). This suggests that better exploratory behaviour by VCP treated mice may underlie their better performance during the PAL-ChBM task. tVCP and Cur showed better a better exploration profile on day eight than that of the day one on examination as shown by the mean path shapes executed by these groups (Fig 8.8 and 8.9). However, the mean number of visits to RF and the mean time taken by these groups to visit RF (Fig 8.5 and 8.6) did not differ significantly from the ST group.

When the brain sections from different treatment groups were stained with thioflavine S, it was found that all the transgenic mice showed a pattern of staining similar to ST group. The apparent intensity of plaques in the olfactory lobe of one of the VCP treated mice was less than that of ST as well as tVCP mouse. However, this observation needs to be replicated in a number of sections before any conclusions can be made. The olfactory lobes in mice are tiny. They were lost during processing from most of the brain sections, and the analysis of only one of the brain section is insufficient for proper conclusion. There was marked angiopathy that is staining of blood vessels in the brain sections from all the transgenic mice. This is similar to findings in AD patients (Oshima et al. 2008, Axer et al. 2008).

It is reported that thioflavine S stained plaques are associated with dementia and activate the complement system via C1q (Afagh et al. 1996). The presence of thioflavine S stained plaques in the current study, and the improved performance in VCP treated mice could thus be attributed to the complement inhibition by VCP.

The treatment groups showed a pattern of thioflavine S staining similar to that of the ST groups. None of the brain sections from SNT group showed thioflavine S staining. In a very few mice from all the treatment groups, however the plaques were not detectable as indicated by thioflvine S. Several reasons could be attributed for the observed variation in the pattern of thioflavine S staining in these groups. The possible contamination of paraformaldehyde solution used for processing with formic acid which hinders thioflavine S staining, inability of thioflavine S to detect the diffused plaques, and variation in the individual plaque burden in the transgenic mice could be attributed to this. If the plaque burden is very less due to variation in the individual mice as observed by, the autofluorescence of the

paraformaldehyde processed brain tissue might have also have masked the fluorescence by these small plaques. Different types of plaques are observed in AD patients (Griffin et al. 1995, Afagh et al. 1996, Thal et al. 2008). The neuritic plaques indicative of β-sheet confirmation can be detected by thioflavine S staining. The thioflavine S or even congo red cannot detect certain type of plaques with no β-sheet confirmation (Afagh et al. 1996).

In APPswe PS1δE9 mice both diffuse plaques and amyloid plaques are observed, and deposition of plaques is an age dependent phenomenon with plaque number and size increasing with age (Gracia-Alloza et al. 2006). However, it was found that 10 month old mice showed less plaque burden than the 8 month old mice, and this was attributed to inter-animal variability (Gracia-Alloza et al. 2006). Due to individual variation in amyloid burden, a very few mice from the treatment group might have developed the diffuse plaques, but the burden of fibrillar plaques in the mice used in the current investigation might have been too low, and masked by the autofluorescence of the paraffin embedded sections. Hence thioflavine-S staining method used in the current investigation might not have been able to detect the plaques in those cases with a very low burden. As discussed the β-amyloid immunopositive diffuse plaques are thioflavine S negative and cannot be detected using thioflavine S (Afagh et al. 1996). The variability in the thioflavine S staining in the VCP, tVCP and Cur treated groups may also be attributed to the variability in the absorption of these drugs after being administered intranasally.

Cur is also known to bind the plaques and reduce the plaque burden in mice (Yang et al. 2005). However, the current study was qualitative, and the preliminary qualitative data clearly point the way for morphometric and stereological analysis of these brain sections to further explore the effect of VCP, and Cur on the number and size of plaque formation.

In conclusion, this type of paired associative task using ChBM has been shown to be a useful paradigm for testing for behavioural deficits in a mouse model of AD. It may well be applicable to other rodent models of neurodegenerative disorders. Multiple intranasal doses of VCP have been shown to be effective in PAL and therefore could be effective in the treatment of AD mouse models. The improved performance of mice treated with VCP could be attributed to its ability to regulate the amyloid activated complement pathways. Since the brain tissue could be harvested in these mice, what was needed to be confirmed *a priori* is the presence of plaques in the APPswe mice used in this study, and the absence of plaques in SNT mice is indeed the case and confirmed in the immunofluorescent study of mouse brains shown in Fig 8.10. The results obtained from the VCP treated transgenic mice demand an in depth quantitative investigation on the effects of plaque burden.

Chapter 9.
General Discussion.

Since its discovery by Alois Alzheimer in the last century, AD is a somewhat mysterious disease affecting more than 14 million people all over the world. The whole world celebrated the centenary of AD in 2006, but the solution to this neurodegenerative disorder is still a far cry from reality. The rapidly emerging streams of scientific research only add to the already complex picture of the pathogenesis of AD (Daly and Kotwal 1998). Another disorder in the past century affecting millions of the world population is AIDS, which also leads to neurological complications and HAD as discussed in the literature review. These two disorders are equally damaging to society. Every year billions of dollars are being spent in the treatment of patients suffering from dementia (Kalaria et al. 2008, AD facts and figures 2008) and in the development of effective preventive and treatment strategies. However, all the attempts to control the primary factors in the aetiology of these disorders such as development of a vaccine against AD have failed (Karkos et al. 2004). HAART used to treat HIV-1, results in the increased levels of complement and may cause peripheral neuropathy (Spear et al 1999, Datta and Rapoport 2002). These two disorders pose a great challenge for the drug development marked by their complex aetiology. Identification of key targets in their pathogenesis is therefore of central importance for their control, prevention and treatment.

Although there are dissimilarities in the pathogenesis of AD and HAD, the aetiological features such as amyloid, tau, APOE4, and HSPG are common to them (Minagar et al. 2004, Shapshack et al. 2006, Shapshack et al. 2008). Microglial activation, induction of cyclooxygenases, oxidative stress, and neuroinflammation mediated by pro-inflammatory mediators is also evident in both. As discussed in the literature review, proinflammatory mediators, mainly the complement system is activated in these two disorders and plays a devastating role (Fonesca et al. 2004, Yasojima et al. 1999, Huber et al. 2006, Bruder 2003). HIV-1, a smart and treacherous trader in death, is not only able to evade the attack by complement components, but effectively uses the complement components for its own cause. HIV may use complement opsonins to infect cells (Stoiber et al. 2005). Not only this, but HAART therapy which is effective in treating AIDS is also known to activate the complement system, and thereby causes neurological symptoms (Spear et al. 1999, Datta and Rapoport 2002). The neurons in the brain are highly susceptible to the complement components as they express a very low level of complement components.

Despite all these facts and figures, currently there is no complement regulatory agent available on the market to treat these neuroinflammatory disorders (Makrides 1998). Although eculizumab, a complement regulatory monoclonal antibody against complement anaphylotoxins, is currently under development for the treatment of other disorders (Charneski and Patel 2008, Kaplan 2002), it has never been tested for its effectiveness in the treatment of neuroinflammatory disorders of the brain. It is

therefore evident that there is an urgent need for the development of complement regulatory agents which can be combined with other agents to control the neuroinflammation associated with these disorders.

VCP, a viral protein mimics the human complement regulatory molecules (McKenzie et al. 1992). It is known to regulate both pathways of complement activation (Kotwal and Moss 1988, Kotwal et al. 1990, McKenzie et al. 1992). It was also found to be effective in the treatment of rodent models of CNS disorders such as TBI (Hicks et al. 2002), SCI (Reynolds et al. 2003, Reynolds et al. 2004), mild and severe head injury (Pillay et al 2005, Pillay et al. 2007), and more recently in an AD rodent model (Pillay et al. 2008). Pillay et al. (2008) directly administered VCP into the brains of mice at an early age, and VCP administered in this manner was found to be effective at an early stage of AD in APPswePS1δE9 mice. This further supports the beneficial role of complement regulatory molecules such as VCP in the treatment of neuroinflammatory disorders. VCP can therefore be used as a basic model for the development of other complement regulatory molecules.

However, the therapeutic effectiveness of this potential wonder drug is hampered by its molecular weight. Because of its large size, it was surmised that it would not cross BBB. Therefore, one of the main objectives of this investigation was to deliver VCP to the brain using various routes. Alternatively, development of small sized complement regulatory molecules was also thought to be an effective approach. For this reason Cur, an active ingredient of turmeric widely used in Ayurveda (Indian system of Medicine) was selected. Cur has previously been known to be an effective anti-inflammatory compound with well established roles in controlling pro-inflammatory mediators (Aggarwal 2008). It is known to dissolve plaques in AD mouse model (Yang et al. 2005). However, its effect on the complement system was not studied, although it was structurally related to RA, Qur, and other polyhydroxy phenolic compounds with known complement regulatory activities (Fig A1, Appendix). When Cur was tested for its ability to regulate activation of the complement system using a normal haemolysis assay, the attempts to establish its effectiveness on the complement system failed, since it absorbed in the same range as RBCs. Therefore, a simple modification of the assay was done (Fig 2.1, Chapter 2), and using this assay, Cur was shown to inhibit the complement system with greater efficacy than RA (Chapter 2). However as shown in this study, all these compounds were found to be a thousand fold less active than that of VCP (Fig 2.7B). Another compound, tVCP, a structural analogue of VCP with one module less, was found to inhibit the complement system at only moderate level (25%; Fig 2.5). Cur was further shown to inhibit zymosan activated AP at relatively higher concentration (Fig 2.10). The complement regulatory activity of Cur on both AP and CP of complement activation has thus firmly been established by these data.

C3 and C3b are central to the activation of AP and CP and found to be involved in the aetiology of AD and HAD. Thus, it was necessary to investigate the effects of these aforementioned compounds on C3 and C3b. VCP is known to bind C3b. However, it has previously not been tested for its ability to bind to C3. tVCP was used as a control for VCP-C3/VCP-C3b binding, and BSA, a compound with known ability to bind Cur was used as a positive control for Cur-C3/Cur-C3b binding. For this

comparative investigation, QCM-D, a relatively new technology developed in Sweden was used (Chapter 3). The sensitivity and rapidity of this technology offers an advantage of online monitoring, rapidity without losing specificity, and gives extra information regarding the binding (D factor; Rigid vs. reversible binding). Using this technology, it was found that VCP, Cur and tVCP were able to bind to C3 and C3b (Fig 3.4 to 3.7). However, VCP showed stronger affinity to C3 and C3b than the other two. Cur showed stronger affinity to both C3 and C3b than for BSA. It was therefore concluded that these compounds regulate both the CP and AP via their ability to bind to C3 and C3b. The stronger affinity of VCP for both C3 and C3b than the other two can be accounted for in terms of its better *in-vitro* complement regulatory profile observed in chapter 2. Thus, a new dimension in the biological activity of Cur and VCP has now been documented. The complement regulatory activity of Cur and its mode of action on C3 and C3b have thus been established. VCP was also shown to bind C3. tVCP was shown bind to C3 and C3b, but with less affinity than that of VCP as shown by the others (Smith et al. 2003).

After establishing the complement regulatory activity of Cur, and the interaction of Cur, VCP and tVCP with C3 and C3b, the next challenge was to deliver these compounds to the brain to be therapeutically effective in the treatment of neuroinflammatory disorders. Cur is known to cross BBB, but its oral bioavailability is poor. Also, in the current investigation, it was used as its sodium salt (as it was dissolved with the aid of NaOH). Due to increased polarity, it was presumed that it would not cross BBB which is impermeable to water soluble compounds. The intranasal route offers a great advantage in that it is a non-invasive route to administer high molecular weight and polar compounds that may be taken up and made available to the nervous tissue. Many high molecular weight proteins, peptides (Gozes 2001, Thorne and Frey 2001, Liu et al. 2001) and small sized compounds (Sakane et al. 1991, Westin et al. 2005, Kaya et al. 2008) have been delivered to the brain via this route. When VCP, tVCP, and Cur were administered intranasally to the rat, VCP and tVCP were detected in CSF as well as in the glomerular cell layer of the olfactory lobe (Fig 4.11). The amount of VCP and tVCP detected in the brain using ELISA was low (Chapter 4). However, these compounds were also detected in the olfactory lobe of the brain. Mucosal adjuvant cholera toxin (CT) delivered intranasally reached the brain and was detected in the olfactory glomerular cell layer similar to VCP and tVCP, and was retained there at detectable level for more than six days (van Ginkel et al. 2000). This latter compound reaches the brain via retrograde transport. Whether VCP and tVCP reach the olfactory lobe via this route needs to be further investigated.

In order to detect Cur in the CSF, it was necessary to develop a method sensitive enough to be able to detect Cur at a very low concentration. A colourimetric method developed in the current investigation proved to be less sensitive, however a method based on the enhancement of fluorescence of Cur was able to detect Cur in CSF at μM concentration (Chapter 4). The olfactory lobes are very tiny, and without having a sensitive method in hand to detect Cur in the brain tissue, it would have been impossible to detect it in minute level in the tiny olfactory lobes. The formaldehyde fixed and paraffin embedded brain tissue also poses a problem of auto fluorescence in the range of Cur emission. More

sensitive confocal microscopy based methods to detect fluorescent labelling of Cur in the brain tissue embedded in paraffin to get more information regarding its uptake in the brain tissue forms a part of future research work.

VCP, although delivered intracranially in the previous studies using rodent models of CNS disorders, its bioavailability in CSF and distribution in various parts of the brain had not been previously reported. In order to detect the fate of VCP and tVCP in the brain tissue as well as in the CSF, it was necessary to have the presence of VCP in the tissue or CSF confirmed so that a positive control can be visualized using immunohistochemistry (brain sections) or ELISA (CSF). When VCP was directly administered into the left ventricle, it was detected in CSF collected from the cisterna magna between 1-3 h after the administration at nanogram levels. This indicated that VCP is retained in the CSF for a relatively long period probably due to its ability to bind some proteins in the CSF. After being administered stereotaxically into the hippocampus, it was also detected in the hippocampus. The detection of VCP and tVCP in CSF and brain several hours after being delivered either intracranially or intranasally into the brain also confirms the stability of VCP in the body fluids. It was previously detected in the serum even 8 h after being administered into the systemic circulation (Jha et al. 2003).

After establishing the delivery and confirming the distribution of VCP, tVCP and Cur in the brain and CSF, it was necessary to complement studies that have demonstrated their therapeutic effectiveness in neuroinflammatory disorders. In a study by Pillay et al. (2008) where they showed the therapeutic effectiveness of VCP administered directly into the brain of APPswePS1δE9 mice, a further study was required to demonstrate the therapeutic effectiveness of VCP in the treatment of AD at a later age in these transgenic mice. It was therefore necessary to investigate whether direct VCP treatment is effective in the prevention of the disease at a later age. It was argued that this would further substantiate the use of VCP in the treatment of neuroinflammatory disorders. Direct administration was also necessary for proper comparison of the effectiveness of the intranasally administered VCP. Therefore, as discussed in the chapter 5, VCP was administered twice directly into the brains APPswePS1δE9 mice at an early age (3 weeks and 6 months). The same VCP treated transgenic mice were subjected to a similar ChBM model used by Pillay and colleagues (2008), and the same protocols were followed. However, before carrying out the behavioural testings, these mice were allowed to age to between 24-27 months. When these mice were subjected to the ChBM model, VCP was found to be effective in the prevention and treatment of cognitive impairment. In the current study VCP was found to improve paired associative learning. Further investigation of the plaque pathology using thioflavine S revealed that the apparent number of plaques as well as the amyloid staining pattern showed quite a bit of variation amongst the mice from the VCP treated group. Three VCP treated transgenic mice showed angiopathy (staining of blood vessels), and plaques similar to the transgenic controls. However, in two of VCP treated transgenic mice, red fluorescent structures are observed amongst the green fluorescent plaques. Such findings have not been as yet reported in the literature. Clearly these studies need to be extended for further detailed investigation of alterations in plaque burden, but being fully cognizant of the fact that maintaining mice for over 2 and half years is both an onerous task and costly.

Since in this aged transgenic mouse model, the therapeutic effectiveness of directly administered VCP was established, it was considered appropriate to investigate the effectiveness of a less invasive route for the administration of VCP. As discussed above, VCP, tVCP and Cur administered intranasally reach the CNS at a low level (Chapter 4). Therefore multiple sequential doses of VCP, tVCP and Cur were administered to appropriate groups of mice. Their therapeutic effectiveness in modulation of behaviour of APPswe mice was tested using EPM and MWM. The EPM study revealed a significant difference in the anxiety and exploration profile of ST and SNT mice. Intranasal VCP treatment was found to improve the anxiety and exploration whereas tVCP treatment resulted in inhibitory tendencies and decrease in the exploratory behaviour in the transgenic mice used in the current investigation (Chapter 6). When these treatment groups were tested for their behaviour in Sp L P in MWM, there was impairment in the ability of ST mice to learn the task (Chapter 7). Intranasally administered VCP and tVCP were not able to improve the performance of mice in Sp L P. It could be argued that delivery to the hippocampus occurred at sub therapeutic levels. The intranasal Cur treatment improved Sp L P on day 5, but the effect was not persistent. The mice from all the treatment groups did not learn Sp R P or Sp W P. The large size of the tank may have been a contributing factor since this may have increased the level of difficulty of the task. Mice to which VCP was administered intranasally showed central tendencies and lower kissperi frequencies as opposed to the peripheral tendencies and increased kissperi frequencies in tVCP treated and to some extent in ST mice. Increased kissperi frequencies could be attributed to a behavioural manifestation of helplessness when the mice were unable to locate the submerged platform.

VCP was detected by immunohistochemical means in the olfactory lobes of the rat brain after being administered intranasally (Chapter 4). Since the localization of VCP within the olfactory lobe may potentiate olfactory related behaviour, it was decided to investigate the effect of VCP on the olfactory related task in mice. As shown in chapter 5, direct administration of VCP was found to improve associative learning where mice had to rely upon pairing of object-spatial cues to get the reward (sugar pellets).The same model was modified to design PAL-ChBM task which was based on the ability of mice to differentiate between RF and NRF by associating the flag-odour-spatial cues with the reward. When the various treatment groups were subjected to this task, it was found that the ST group performed more poorly than the SNT group. Intranasally administered VCP was able to improve the PAL-ChBM task in the transgenic mice. VCP was able to improve this task probably because the task does not rely completely upon the hippocampus to locate RF as opposed to Sp L P of MWM which requires the use of only spatial cues.

The current investigation adds a further dimension to the neuropharmacological profile of VCP. These behavioural findings suggest that VCP, tVCP and Cur could be delivered to the brain using the non-invasive nasal route. VCP was found to be significantly better than the other two in improving PAL in APPswePS1δE9 mice (Chapter 8). In the earlier study, VCP was found to improve the exploration and reduce the anxiety in these mice (Chapter 6). The path shapes in the PAL-ChBM (Fig 8.8 and 8.9) suggest that VCP might have improved the PAL-ChBM performance through its ability to improve

exploration. Intranasal tVCP treatment failed to improve PAL probably due to an increase in the anxiety and inhibitory tendencies in these mice. As discussed in the literature review, VCP and tVCP are known to bind HSPGs which play an important role in neuroinflammation associated with amyloid plaques (O'Callaghan et al. 2008). HSPGs are also implicated in various conditions such as neuroinflammation, amyloid formation and angiogenesis. The necessity to consider implications of HSPGs in many neuroinflammatory disorders is highlighted in a recent review by Lindahl (2007). However, as VCP, but not tVCP was found to be effective in the current investigation, it could be concluded that complement might be involved to a greater extent than HSPGs in mediating neuroinflammation in the mouse model used in the current investigation. VCP was found to be better than tVCP due to its ability to regulate the activated complement components. This supports the previous *in-vitro* findings where VCP was found to inhibit Aβ activated complement system (Daly and Kotwal 1998).

As discussed previously VCP and tVCP were detected in CSF at a very low level (Chapter 4), but still they were found to significantly modulate the behaviour of APPswePS1dE9 mice (Chapter 6 to 8). This suggests the therapeutic utility of multiple sequential regimens of intranasal administration as employed in the current investigation. Even though VCP was detected at a low level in CSF, it was found in the olfactory lobes of the rat brain as detected by means of immunohistochemistry. Although it has been suggested that VCP might have been retained in the brain tissue similar to other proteins such as CT (van Ginkel et al. 2000)**, i**t is also possible that VCP might have been taken up into the brain by more than one mechanism, when it was administered intranasally. The distribution study in rats lasted up to 8 h, after which rats were killed**.** Also during this period, the rats were maintained on light anesthesia to avoid discomfort and stress during CSF withdrawal. It is known that anesthesia delays the absorption via this route (Hussain et al.1997, Sakane et al. 1995). The rats were anaesthetized for a long period as opposed to mice which were anaesthetized just for 20 min, and were maintained on the multiple intranasal dosing for months. This variation must be taken into account while comparing the results of the distribution study to the behavioural study in mice. The results of the current study clearly indicate that further research is needed to understand the mechanism of uptake of VCP and tVCP into the brain for the purpose of further optimizing the dosing regimen. Some large molecular weight proteins WGA-HRP (almost twice the size of VCP) have been reported to reach the brain 48 h after being administered intranasally. They were shown to reach the brain via the trigeminal pathways. In order to design an appropriate dosing regimen, it will be necessary to further investigate whether VCP and tVCP are also transported to the brain via these mechanisms.

In addition to this, attempts should also be made in future studies to increase the bioavailability of VCP and tVCP via intranasal route in order to reduce the number of doses required for a therapeutic effect. The simplest approach may be to develop a pH balanced formulation of VCP. The reduction of pH to 4.5 to 5 is known to improve the intranasal delivery of some proteins and other molecules via this route (Constantino et al. 2005, Loftus et al. 2006). The coupling with polyethyleneimine (PEI) also increased the nasal uptake of some of the proteins into the brain (Loftus et al. 2006).

Cur has previously been shown to be effective in the improvement of spatial learning in APPswePS1dE9 mice (Yang et al. 2005). It was also shown to improve gp120 (HIV envelope protein) induced spatial deficit in a mouse model (Bao et al. 2008). However, in the current mode although it showed improvement in the spatial learning on the fifth day of Sp L P, it failed to do so persistently. Intranasal treatment of Cur also failed to improve PAL in the ChBM model. A possible reason could be the delivery of Cur to the brain at sub therapeutic level after being administered intranasally. The possible variability in absorption after being delivered intranasally should also be considered. Therefore, future attempts should also be aimed at increasing the bioavailability of Cur in the CNS.

The preliminary qualitative findings concerning the differential pattern of thioflavine S staining observed in VCP (direct/intranasal), tVCP and Cur treated aged mouse brain sections need to be further explored using morphometric and stereological approaches to analyze the changes in the plaque burden.

In addition to the core findings, this investigation has also lead to development of a number of small techniques and assays which have been crucial to the final outcome of the study and/or may form a part of the future research work. The modified haemolysis assay, blind technique for CSF withdrawal, possible non-specific binding of the primary antibodies to 15-16 and 18-19 kDa proteins in CSF, standardization of ELISA methodology for VCP and tVCP detection by masking endogenous peroxidase, possibility of inhibition of endogenous peroxidases by VCP, colourimetric and fluorimetric detection of Cur all as discussed above did not form the major focus of the current investigation, but has had a great impact on the key findings.

In summary and conclusion, the current investigation expands the view of Cur's anti-inflammatory role since Cur was found to regulate the complement activation through its ability to regulate both the CP and AP of complement. The QCM-D technology employed in the current investigation revealed the binding of Cur to C3 and C3b, the complement components central to the activation of both the CP and AP. VCP, and to a lesser extent, tVCP was also shown to bind to C3 and C3b. In the literature, there are no reports of VCP, (as well as tVCP and Cur) binding to C3 with stronger affinity than to C3b. Perhaps binding of these compounds to C3, thereby preventing its conversion into its active form, could be the basis of their complement regulatory action. VCP administered directly was found to be retained in the brain tissue and CSF for several hours. Direct administration of VCP at an early age was shown to improve associative learning at an old age in the mouse model of AD. Intranasally administered VCP, tVCP were detected at low level in CSF and the brain. Cur administered intranasally was also detected in μM concentration in CSF using the FEM technique developed in the current investigation. Intranasally administered Cur also showed some improvement in Sp L P, but the effect was not persistent. Multiple sequential administration of VCP via the intranasal route might improve exploratory behaviour and anxiety associated with AD, and behaviour not previously described, namely, "kissperi". VCP was also shown to improve PAL in the novel PAL-ChBM model. The results of the investigation strongly suggests the therapeutic utility of large sized (VCP) and small sized polar complement regulatory molecules (Cur) in the treatment of neuroinflammatory disorders such as AD and HAD employing multiple dosing regimens via intranasal

administration. There is no single behavioural model covering all the aetiological factors involved in these disorders. Therefore, these compounds need to be tested for their effectiveness by using more than one behavioural model covering different factors involved. The gp120 based model used by Bao and colleagues (2008) would be of great help in this regard. Development of formulations for intranasal administration to enhance bioavailability of these compounds presents a challenge in future research work in this field.

Finally, in overview of this study and the multilevel approach adopted, the importance of extending the molecular information to the whole organism is emphasized. I believe this goes a long way to increasing the understanding between molecular biology and whole animal physiology and systems biology. Consequently this thesis is in line with Staub's (2002) philosophy concerning the explosion of molecular biology outpacing advances in clinical medicine due to basic sciences "limited ability to translate its findings to the complexity of the complete organism". Hopefully the contributions made by this study will complement the trend towards an increased understanding of molecular biology in the context of the whole animal.

Appendix F.

Figure F1.1. Structures of Qur, RA, and Cur.

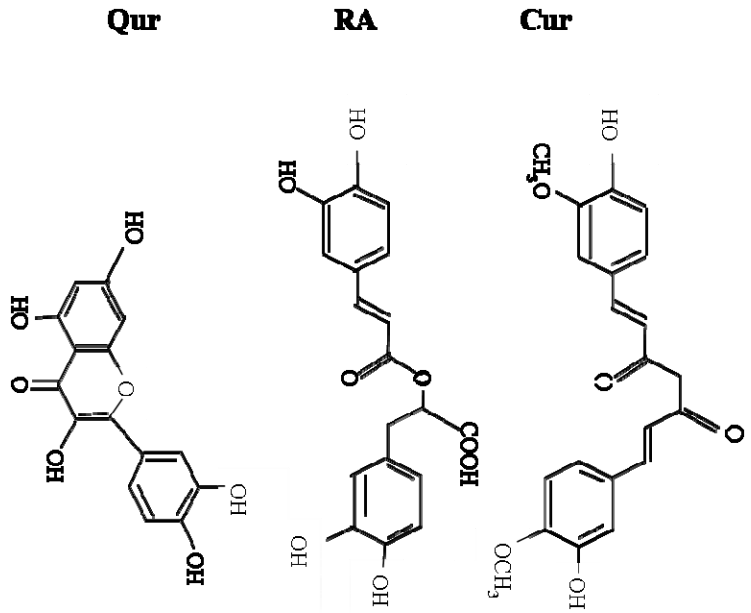

Qur, RA, and Cur are polyhydroxy phenolic compounds (Structures Modified from Sigma website)

Figure F 1.2. Map of pPIC9 vector with VCP or tVCP inserts.

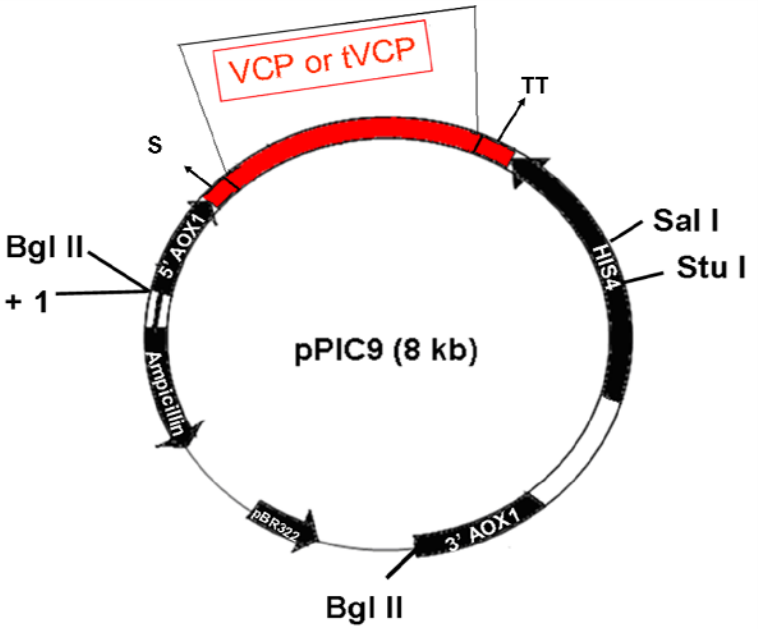

Expression vector pPIC9 showing cloned VCP and tVCP genes expressing VCP, and tVCP, respectively. tVCP corresponds to amplified fragments of genomic DNA from vaccinia virus encoding amino acids 18-262 of VCP. S = a-secretary signal of 5'-AOX gene. AOX1= alcohol oxidase - 1 gene S = α factor secretion signal, TT = 3'AOX1 transcription termination).

Figure F 1.3. Dosing regimen for the intranasal administration of VCP, tVCP and Cur for the behavioral study.

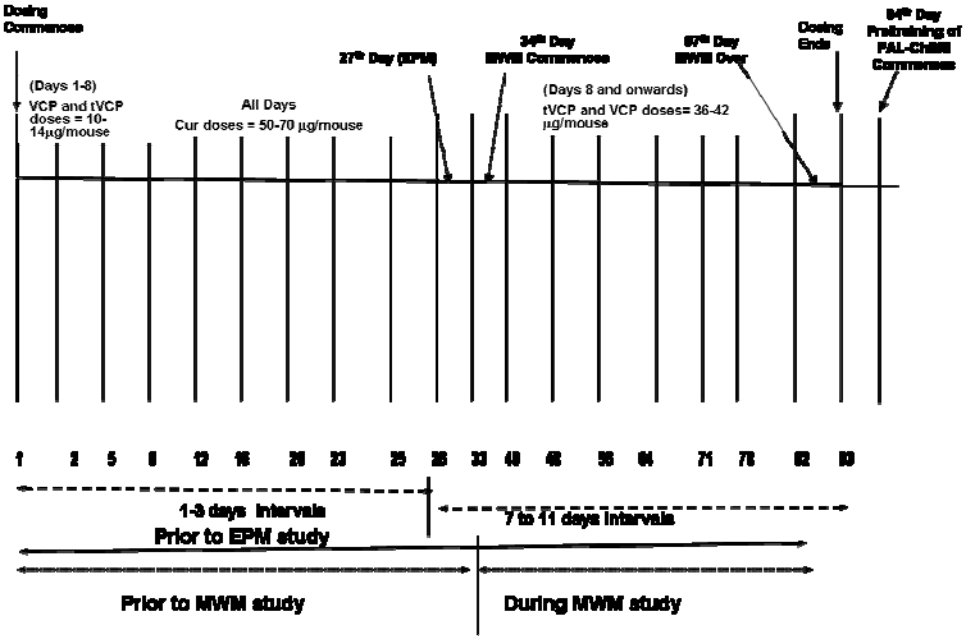

Appendix P.

P.1. Primers used for PCR cycling.

Primers were made according to JAX® Mice Data Sheet. They were ordered from Integrated DNA Technologies, Inc., 1710, Commercial Park, Coral Ville, Iowa, 52241, (319) 626-8400. [Note: A = sense / forward, B = antisense / reverse; mouse prion promoter (MPP)].

MPP

A) GK1: 5' CCT CTT TGT GAC TAT GTG GAC TGA TGT CGG 3' (Properties: Tm (50mM NaCl) = 61.5 ^{O}C; MW = 9,235.0; [(OD_{260} = 5.9) = 21.3 nMoles = 0.20 μg])

B) GK2: 5' GTG GAT AAAC CCC TCC CCC AGC CTA GAC C 3' (Properties: Tm (50mM NaCl) = 66.6 ^{O}C; MW = 8439.5; [(OD_{260} = 4.2) = 16.46 nMoles = 0.14 μg])

PSEN1A

A) GK3: 5' AAT AGA GAA CGG CAG GAG CA 3' (Properties: Tm (50mM NaCl) = 56.0 ^{O}C; MW = 6233.1; [(OD_{260} = 4.1) = 16.46 nMoles = 0.12 μg])

B) GK4: 5' GCC ATG AGG GCA CTA ATC AT 3' (Properties: Tm (50mM NaCl) = 55.0 ^{O}C; MW = 6126.0; [(OD_{260} = 5.1) = 16.83 nMoles = 0.10 μg])

APPswe

A) GK5: 5' GAC TGA CCA CTC GAC CAG GTT CTG 3' (Properties: Tm (50mM NaCl) = 60.9^{O}C; MW = 7313.8; [(OD_{260} = 5.9) = 26.37 nMoles = 0.19 μg])

B) GK6: CTT GTA AGT TGG ATT CTC ATA TCC G 3' (Properties: Tm (50mM NaCl) = 53.4^{O}C; MW = 7638.0; [(OD_{260} = 5.6) = 23.73 nMoles = 0.18 μg])

P.2. Genotyping of APPswe transgenic mice.

Table P.1.1 Composition of PK-lysis buffer.

Sr.	Contents (final Conce.)	Stock	500 ml	50 ml
1	100 mM NaCl	25 M	20 ml	2
2	100mM TrisCl (pH = 8)	1 M	5 ml	0.5
3	25 mM EDTA (pH = 8)	250 mM	50 ml	5
4	0.5% SDS	20%	12.5 ml	1.25
5	ddH_2O	(Upto)	500 ml	50 ml

P.2.1. Protocol for DNA extraction from mice tails (Jackson datasheet) and PCR analysis.

1. The tails were cut and transferred to separate 2 ml eppendorf tubes containing 500 µl of PK lysis buffer prepared by the method shown in the table. To this mixture, 12 µl of proteinase-K was added and the mixture was kept at 55^{o}C in a water bath for overnight digestion.
2. The eppendorf tubes were then spun at 13,200 rpm for 15-25 minutes.
3. The supernatants were then carefully added to the new eppendorf tubes containing 500 ml of isopropanol and the tubes were inverted10-20 X until a visible precipitate was formed. 400 ml of super -saturated solution of sodium chloride was added if there was no formation of precipitate. It was then subjected to 13,200 rpm for 20 sec (sometimes 10 min) to form the pellet. The supernatant so formed was discarded. One ml of 75 % ethanol was then added to the pellet and the pellet was resuspened by vortexing.
4. It was then spun for 5 minutes at 13,200 rpm and the supernatant was removed. The pellet was dried for at least an hour to allow complete evaporation of ethanol. The pellet was then resuspended in 200 µl of TE and it was incubated at 55^{O}C until DNA dissolves (sometimes overnight).
5. These DNA samples were then stored in TE at -20 and subjected to PCR analysis.
6. For the PCR analysis, the reaction mixtures composition and PCR cycling conditions were as mentioned in the table P6.2 below. The PCR products were analysed using 0.7% agarose gel as shown in the chapter 6 (Section 6.5.1, Fig 6.2).

Table P.1.2. PCR cycling conditions and composition of reaction mixture for genotyping.

PCR Reaction mix for APPswe, PSEN1A and MPP

Sr	APPswe	PSEN1	MPP
1	ddH2O make upto 20 µl of volume	ddH2O make upto 20 µl of volume	ddH2O make upto 20 µl of volume
2	10X PCR buffer (1X) / 2.5 µl	10X PCR buffer (1X) / 2.5 µl	10X PCR buffer (1X) / 2.5 µl
3	25 mM MgCl2 (2 mM) / 1.6 µ1	25 mM MgCl2 (2 mM) / 1.6 µ1	25 mM MgCl2 (2 mM) / 1.6 µ1
4	40 mM dNTP (0.2 mM) / 0.5 µ1	40 mM dNTP (0.2 mM) / 0.5 µ1	40 mM dNTP (0.2 mM) / 0.5 µ1
5	20 µ M Gk5 (1 µ M)	20 µ M Gk3(1 µ M)	20 µ M Gk1 (1 µ M)
6	20 µ M Gk6 (1 µ M)	20 µ M Gk4 (1 µ M)	20 µ M Gk2 (1 µ M)
7	5 µ / µ1 Taq Pol (0.016 µ / µ I)	5 µ / µ1 Taq Pol (0.016 µ / µ I)	5 µ / µ1 Taq Pol (0.016 µ / µ I)
8	DNA 2 µ1	DNA 2 µ1	DNA 2 µ1

PCR Cycling conditions for APPswe, PSEN1A, and MPP

Step	Temperature (°C)	Time	
1	94	3 min	
2	94	30 sec	
3	69 (Appswe); 67 (PSEN1A), 70 (MPP)	1 min	
4	72	1 min	Repeat steps 2-4, 35 cycles
5	72	2 min	
6	10		

Appendix R.

Appendix for results (R)

Chapter 2.

Table R2.1. Determination of IC50 value of VCP.

Log of Concentration	0.8417	1.1427	1.443
percentage inhibition	20.21	48.49	100

Table R2.2. Determination of IC50 value of Cur, RA, and Qur (CP).

Compounds	Concentration (μM)				
	80	160	320	640	800
RA	35.155	44.913	47.785	48.6933	54.4233
Cur	15.883	23.8253	28.25	70.56	35.8
Qur	30.463	26.428	51.1683	77.21	55.5933

Table R2.3. Mean values for complement inhibition by Cur, RA, and Cur (Modified haemolysis assay results and Post-Hoc analysis).

	Concentration	RA-Mean	RA Std.Err.	Qur Mean	Qur Std.Err.	Cur Mean	Cur Std.Err.
1	80microM	42.18750	1.562500	29.68750		14.25781	2.148438
2	160microM	44.92188	2.174908	26.43229	2.728168	23.82813	0.596690
3	320microM	47.78646	6.218726	51.17188	9.966680	28.25521	1.722494
4	640microM	48.69792	2.033919	77.21354	1.501636	70.57292	6.348240
5	800microM	54.42708	1.535134	53.77604	6.541592	35.80729	3.568279

Newman-Keuls test; variable RA. Approximate Probabilities for Post Hoc Tests Error: Between MS = 60.089, df = 10.000

RA	Concentration	{1} - 35.156	{2} - 44.922	{3} - 47.786	{4} - 48.698	{5} - 54.427
1	80microM		0.154045	0.163777	0.205745	0.073296
2	160microM	0.154045		0.660659	0.825130	0.471626
3	320microM	0.163777	0.660659		0.888499	0.564769
4	640microM	0.205745	0.825130	0.888499		0.386841
5	800microM	0.073296	0.471626	0.564769	0.386841	

Newman-Keuls test; variable Qur Approximate Probabilities for Post Hoc Tests Error: Between MS = 91.461, df = 10.000

Qur	Concentration	{1} - 30.469	{2} - 26.432	{3} - 51.172	{4} - 77.214	{5} - 53.776
1	80microM		0.616615	0.024418	0.000806	0.033655
2	160microM	0.616615		0.024932	0.000628	0.024832
3	320microM	0.024418	0.024932		0.019011	0.745785
4	640microM	0.000806	0.000628	0.019011		0.013469
5	800microM	0.033655	0.024832	0.745785	0.013469	

Newman-Keuls test; variable Cur Approximate Probabilities for Post Hoc Tests Error: Between MS = 36.326, df = 10.000

Cur	Concentration	{1} - 16.986	{2} - 23.929	{3} - 28.256	{4} - 70.573	{5} - 35.807
1	80microM		0.137775	0.072562	0.000177	0.010811
2	160microM	0.137775		0.389662	0.000209	0.082447
3	320microM	0.072562	0.389662		0.000207	0.156053
4	640microM	0.000177	0.000209	0.000207		0.000209
5	800microM	0.010811	0.082447	0.156053	0.000209	

Table R2.4. Inhibition of zymosan mediated complement activation by Cur.

Concentrations (μM)	160 μM	320 μM	640 μM	960 μM	1280 μM
Log of Concentrations	2.2041	2.5051	2.8061	2.9822	3.1072
Percentage inhibition	10.89	26.694	56.707	65.074	50.87

Chapter 3.

R3.1. Study of binding of VCP, tVCP, Cur to C3 on polystyrene surface.

Sr.	AMs	dD_{30avg}/dF_{30avg}	dD_{finavg}/dF_{finavg}	dF_{30avg}	$dF_{fin\ avg}$	$dF_{ML\ fin}$	mass (ng/cm2)	No of molecules adsorbed (X10 13
1	VCP-C3ps	0.0322	0.0517	-2.8840	-7.3670	-5.1569	30.4257	0.6362
2	VCPps	0.0134	0.0141	-23.5536	-24.7846	-17.3492	102.3600	2.1403
3	tVCPps	0.0162	0.0137	-36.0126	-36.4495	-24.8147	146.4064	4.6697
4	VCPhops	0.0314	0.0340	-149.6925	-140.8610	-98.6957	581.7146	12.1695
5	tVCPhops	0.0157	0.0124	-33.3560	-35.9400	-25.1580	148.4322	4.7546
6	C3ps	0.0105	0.0105	-161.7505	-177.9675	-124.5913	735.0664	2.3298
7	BSAps	0.0175	0.0157	-21.6825	-22.0225	-15.4158	90.9529	0.8055
8	C3-VCPps	0.0107	0.0099	-163.4400	-162.2495	-113.5747	670.0904	2.1238
9	C3- tVCPps	0.0110	0.0110	-135.4285	-142.2435	-99.5705	587.4557	1.8520
10	C3-VCPhops	0.0006	0.0002	-70.0776	-72.4925	-50.7448	299.3940	0.9489
11	C3-tVCPhops	0.0092	0.0094	-153.1900	-159.2420	-111.4694	657.5595	2.0546
12	Cur-C3ps	0.0555	0.0545	-57.3115	-57.9605	-40.5834	239.5008	391.5073
13	Cur-BSAps	0.1832	0.1744	-49.0945	-48.6835	-34.0785	201.0629	328.6736

(Note: For tables R3.1 to R3.4 the dF_{MLfin} indicate the corrected $dF_{fin\ avg}$ values for water bound to the protein molecules. These values were used to calculate the mass deposited using Sauerbrey correlation (ng/cm^2) as well as number of molecules adsorbed on the surface using Avogadro's number shown in (2 (e) in Section 3.7.3 of chapter 3.)

Table R3.2. Binding of VCP, tVCP, Cur to C3b on PS.

Sr. No	AMs	dD_{30avg}/dF_{30avg}	dD_{finavg}/dF_{finavg}	dF_{30avg}	$dF_{fin\ avg}$	$dF_{ML\ fin}$	mass (ng/cm2)	No of molecules adsorbed
1	VCPps	0.0126	0.0119	-34.0770	-35.1820	-24.63	145.3	3.0382 X 10^{13}
2	tVCPps	0.0171	0.0161	-31.3325	-29.7455	-20.82	122.85	3.9361 X 10^{13}
3	Cur-C3bps	0.0110	0.0106	-122.9140	-119.2650	-83.49	492.56	1.6479
4	BSAps	0.0175	0.0157	-21.6825	-22.0225	-15.42	90.95	0.8055 X 10^{13}
5	C3b-VCPps	0.0280	0.0284	-67.6700	-61.0320	-42.72	252.06	0.8433 X 10^{13}
6	C3b-tVCPps	0.0273	0.0273	-24.8000	-23.2770	-16.29	96.13	0.3216 X 10^{13}
7	Cur-C3bps	0.1466	0.1327	-30.7095	-35.4205	-24.79	146.29	239.1320 X 10^{13}
8	Cur-BSAps	0.1832	0.1744	-49.0945	-48.6835	-34.08	201.06	328.6736 X 10^{13}

Table R3.3. Binding of VCP, tVCP, Cur to C3 on gold surface.

Sr No.	AMs	dD_{30avg}/dF_{30avg}	dD_{finavg}/dF_{finavg}	dF_{30avg}	dF_{30avg}	$dF_{ML\ fin}$	mass (ng/cm2)	No of molecules adsorbed
1	VCPg	0.0271	0.0237	-48.5860	-49.0975	-34.3683	202.7727	4.2399×10^{13}
2	tVCPg	0.0295	0.0277	-42.7095	-41.5920	-29.1144	171.7750	5.5023×10^{13}
3	C3g	0.0054	0.0036	-174.7740	-175.3005	-122.71	723.99	2.2947×10^{13}
4	BSAg	0.0116	0.0116	-44.9475	-45.7410	-32.02	188.91	1.6730×10^{13}
5	C3-VCPg	0.0049	0.0042	-135.657	-142.5205	-99.7644	588.6097	1.8656×10^{13}
6	C3 -tVCPg	0.0084	0.0073	-135.6040	-143.4175	-100.39	592.31	1.8773×10^{13}
7	Cur-C3g	0.0404	0.0404	-70.0185	-70.0330	-49.02	289.24	472.8090
8	Cur-BSAg	0.1293	0.1303	-62.3875	-61.8640	-43.3	255.5	417.6582×10^{13}

Table R3.4. Binding of VCP, tVCP, Cur to C3b on gold surface.

Sr. No.	AMs	dD_{30avg}/dF_{30avg}	dD_{finavg}/dF_{finavg}	dF_{30avg}	$\Delta F_{fin}avg$	$dF_{ML\ fin}$	mass (ng/cm2)	No of molecules adsorbed
1	VCPg	0.0278	0.0281	-47.2935	-44.8505	-31.4	185.23	3.87×10^{13}
2	tVCPg	0.0201	0.0194	-46.0470	-43.5350	-30.47	179.8	5.76×10^{13}
3	C3bg	0.0059	0.0036	-160.9125	-158.1050	-110.67	652.97	2.18×10^{13}
4	BSAg	0.0116	0.0116	-44.9475	-45.7410	-32.02	188.91	1.67×10^{13}
5	C3b-VCPg	0.0117	0.0114	-39.4440	-36.7970	-25.76	151.97	0.51×10^{13}
6	C3b-tVCPg	0.0331	0.0339	-12.5950	-12.2850	-8.6	50.74	0.17×10^{13}
7	Cur-C3bg	0.0626	0.0608	-23.9390	-24.7895	-17.35	102.38	167.36×10^{13}
8	Cur-BSAg	0.1293	0.1303	-62.3875	-61.8640	-43.3	255.5	417.66×10^{13}

Table R3.5. The ratio of binding of the number of molecules of AM1 to AM2.

AM1: AM2 (Surface)	Ratio
VCP : C3 (PS)	12.8182273645166 : 1
C3 : VCP (PS)	2.51868256478683 :1
C3 : VCP (PS)	3.66216341723047 : 1
Cur : C3 (PS)	168.040172435555 :1
Cur : BSA (PS)	408.052698966526 : 1
VCP : C3b (PS)	3.60282310918862 : 1
tVCP : C3b (PS)	12.2351394262805 : 1
Cur : C3b (PS)	145.11300893302 : 1
VCP : C3 (Gold)	1.95473251028807 : 1
tVCP : C3 (Gold)	2.93091624697867 : 1
Cur : C3 (Gold)	206.046548508057 : 1
Cur : BSA (Gold)	249.651064473919 : 1
VCP : C3b (Gold)	7.6178934424002 : 1
tVCP : C3b (Gold)	33.9295456316733 : 1
Cur : C3b (Gold)	100.037583453644 : 1

The ratio of binding of the number of molecules of one adsorbing moiety adsorbed on the gold or polystyrene surface (AM1) to the second moiety (AM2) interacting with the first one. These values are approximate and thus not discussed in the results of the chapter 3.

Chapter 4.

Table R4.1. Colourimetric detection of Cur.

Sr	Cur concentrations	OD_{550nm}
1	27.145 mM	3.298
2	2.7145 mM	0.434
3	271.45 µM	0.00743
4	27.145 µM	0.0063
5	2.7145 µM	-0.001
6	271.45 nM	0.002
7	27.145 nM	-0.0035
9	271.45 pM	-0.005
10	27.145 pM	-0.002
11	2.7145 pM	-0.0033

Table R4. 2A. Fluorimetric detection of Cur.

Addition of surfactants / solutions	Abbreviations		Cur 3 (0.00258mg/ml)	Cur2 (0.0258 mg / ml)	Cur1 (0.258 mg / ml)
CurNa	CurNa	(A)	9.388	22.942	27.4625
CurEt	CurEt	(B)	33.374	42.188	86.748
Tween-20 (6%) + CurNa	CurNaTw6	(C)	10.994	28.6215	29.799
Tween-20 (20%) CurNa	CurNaTw20	(D)	16.0645	40.087	66.076
Tween-20-GAA + CurNa	CurNa-Tw-G	(E)	47.921	94.6175	253.9475
Tween-20 + GAA + EtOH + CurNa	CurNa-Tw-G-Et	(F)	55.439	128.5235	304.554
Tween-20-GAA-EtOH-SDS to CurNa	CurNa-Tw-G-Et-SDS	(G)	48.0955	101.198	215.4295
CurNa + Tween-mix Tween-20 + SDS)	CurNa-Tw-SDS	(H)	14.7135	32.668	37.928
CurNa +Tween-20 + PBS	CurNa-Tw-PBS	(I)	13.9785	38.662	43.213

Table R4.2B. Effect of surfactant solution on enhancement of fluorescence of CurEt.

Surfactant / Mix	Abbreviations	(series)	Cur 3 (0.00268mg/ml)	Cur2 (0.0268 mg / ml)	Cur1(0.268 mg / ml)
CurEt	CurEt	(J)	88.374	42.188	86.748
CurEtOH + Tween-mix (10 ml Tween-20 + 10 ml SDS)	CurEt-Twmix	(M)	49.8005	169.0976	365.553
CurEtOH + Tween-20 + 10 ml SDS)	CurEt-Tw-SDS	(N)	58.7155	152.9845	348.7025
CurEtOH + Tween-mix Tween-20 + SDS)	CurEt-GAA-Tw-SDS	(O)	54.9725	105.975	227.6165
Tween-20 (20%) + CurEt	CurEtTw20Et	(L)	74.441	144.249	286.3125
Tween-20 (5%) CurEt	CurEtTw5	(K)	52.5755	119.8925	253.728

Table R4.3. Detection of Cur in CSF by fluorimetry.

B

Sr	Samples	CFV490	BFV490	TFV490	Estimated Concentration Range (µg/ml) at 490 nm
1B	CSF Cur1	37.1106	10.33316667	26.77733333	Between 4.167 and 2.778
2B	CSF Cur2	8.5025	10.33316667	-1.830666667	<2.778
3B	CSF Cur3	14.9095	10.33316667	4.576333333	<2.778
4B	CSF Cur4	42.3315	10.33316667	31.99833333	Between 4.167 and 2.778
5B	CSF Cur5	8.3675	10.33316667	-1.965666667	<2.778
6B	CSF Cur6	23.9415	10.33316667	13.60833333	Between 4.167 and 2.778

C

Sr	Samples	CFV492	BFV492	TFV492	Estimated Concentration Range (µg/ml) at 492 nm
1C	CSF Cur1	35.378	5.39766667	29.98033333	>5.556
2C	CSF Cur2	7.47	5.39766667	2.072333333	<2.778
3C	CSF Cur3	15.663	5.39766667	10.26533333	>2.778
4C	CSF Cur4	41.77	5.39766667	36.37233333	>5.556
5C	CSF Cur5	2.424	5.39766667	-2.973666667	<2.778
6C	CSF Cur6	27.359	5.39766667	21.96133333	Between 4.167 and 5.556

D

Sr	Samples	CFV495	BFV495	TFV495	Estimated Concentration Range (µg/ml) at 495nm
1D	CSF Cur1	26.08	6.903333	19.17667	>5.556
2D	CSF Cur2	10.152	6.903333	3.248667	Between 4.167 and 2.778
3D	CSF Cur3	16.207	6.903333	9.303667	Between 4.167 and 2.778
4D	CSF Cur4	23.634	6.903333	16.73067	Between 4.167 and 5.556
5D	CSF Cur5	1.669	6.903333	-5.23433	<2.778
6D	CSF Cur6	19.293	6.903333	12.38967	Between 4.167 and 2.778

***Table* R4.3.** *Estimation of range of concentration of Cur in CSF samples (CFV, BFV, TFV at emission wavelengths 484 (See Chapter 4 results 4.2 B) 490 (B), 492 (C), and 495 (D) are shown in columns 3, 4, and 5. Sr represents serial numbers. Letters A, B, C, and D are used to show the serial numbers of CSF samples from Cur treated groups at emission wavelengths 484, 490, 492, and 495, respectively. CSF Cur1 to CSFCur6 shown in column 2 denote pooled CSF samples collected from six Cur treated rats at six different time points after the intranasal administration.*

Table R4.4. Optimisation of ELISA protocol for the detection of VCP and tVCP in CSF.

	VCP1	VCP2	VCP3	VCP4	VCP5	VCP6	VCP7	VCP8	tVCP1	tVCP2	tVCP3
	1.33	0.667	0.1333	0.2666	0.01333	0.0266	0.0666	0.0066	3.333	0.333	0.0333
No primary	0.138	0.062	0.09	0.043	0.028	0.022	0.054	0.047	0.031	0.044	0.03
1 in 1000 Rig	3.299	3.299	3.048	2.997	0.805	1.071	2.004	0.707	3.299	1.345	0.728
1 in 2000 Rig	3.299	3.299	2.598	2.495	0.548	0.642	1.371	0.402	3.299	0.946	0.352
1 in 4000 RIg	3.299	3.299	2.132	1.694	0.385	0.419	1.401	0.228	2.355	0.526	0.244
No primary Pre bled serum	0.035	0.022	0.018	0.018	0.017	0.014	0.014	0.017	0.025	0.021	0.019
1 in 1000 Ch-Ig	2.014	1.968	1.054	1.337	0.304	0.406	0.406	0.227	1.847	0.499	0.21
1 in 2000 Ch-Ig	1.534	1.494	0.669	0.925	0.166	0.271	0.271	0.151	1.114	0.306	0.118
1 in 4000 Ch-Ig	0.852	0.863	0.569	0.571	0.135	0.176	0.176	0.097	0.708	0.176	0.07

OD_{450} of VCP and tVCP at different concentrations after the addition of primary antibodies (R-Ig and Ch-Ig) at different concentrations (1:1000, 1:2000, and 1:4000), or without addition of the primary antibodies.

Table R4.5A. Detection of VCP and tVCP in CSF samples (OD_{450} values after ELISA).

A	Pooled samples	CSF std	VCP CSF1a	tVCP CSF1a	VCP CSF std	VCP CSF1a – CSF std	tVCP CSF1a – CSF std	VCP CSF std – CSF std
	CSF 1	0.419	0.554	0.622	>3.229	0.135	0.203	>3.229 – 0.419
	CSF 2	0.347	0.402	0.524	>3.229	0.055	0.177	>3.229 – 0.347
	CSF3	0.482	0.496	0.493	2.395	0.014	0.011	1.913
	R1	0.377	0.428	0.468	>3.229	0.051	0.091	>3.229 – 0.377
	R2	0.313	0.35	0.408	1.204	0.037	0.095	0.891

Table R4.5B. OD_{450} values of VCP and tVCP controls at different concentrations (ELISA).

B	Concentration (ng/µl)	VCPctrl (+)	tVCP ctrl (+)
	0.5	2.671	3.13
	0.05	2.701	1.151
	0.005	1.486	1.198
	0.002	0.827	0.872
	0.001	0.703	0.825
	0.0005	0.769	0.765

Table 5: A. *OD_{450} after HRP assay of ELISA analysis of pooled CSF samples from VCPdir R, tVCP R and VCP R(Interval 1, 2, and 3 = pooled CSF samples at three different time points; R1 and R2 = samples pooled from a group of three rats from the each group except for VCPdir. For VCPdir R1 = R2 = two rats each. CSFctrl = CSF from SNT R, VCPCSFin and tVCPCSFin = CSF collected from VCP R and tVCPR after the intranasal administration; VCPCSFdir = CSF collected after direct administration of VCP into the brain. The OD_{450} of CSFctrl were substracted from the OD_{450} of the treatment groups, and are shown in the columns 6, 7, and 8. B. OD_{450} of positive controls (VCP, and tVCP shown) at different dilutions.*

Table R4.6. Endogenous peroxidase activity of CSF samples and effect of VCP and tVCP on peroxidases.

CSF samples	CSF ctrl	CSF ctrl + VCP (5 µl / 25 µl)	CSF ctrl + (5 µl / 25 µl)	VCPCSFin	tVCP	VCPdir
CSF1	0.649	0.579	0.65	0.44	0.23	0.428
CSF2	0.498	0.504	0.515	0.473	0.155	0.217
CSF3	NA	NA	NA	0.016	0.103	0.286
R1+R2+R3	0.859	0.795	0.813	0.348	0.046	0.29
R4+R5+R6	0.851	0.782	0.788	0.822	0.899	0.249

TableR4.6. The OD_{450} after the peroxidise assay to measure the peroxidise activity of CSF samples from the different treatment groups. Some of the samples were not subjected to analysis, and are shown by NA.

Chapter 5.

Table R 5.1A. Pellets consumed during pre-training session (Mean and SEM).

Mean values	Tg-only	ST	VCP	SNT
Day 1	1.666667	0.833333	3.000000	1.833333
Day 2	2.500000	1.833333	2.833333	6.166667
Day 3	1.833333	4.000000	4.166667	7.500000
SEM values				
Day 1	0.494413	0.542627	0.447214	0.854047
Day 2	1.231530	0.872417	0.833333	1.701307
Day 3	0.542627	2.221111	1.869343	1.384437

Table R 5.1B. Post-hoc analysis for the pellets consumed during pre-training session.

Newman-Keuls test; Day 1 pellets

Sr	Groups	{1} - 1.6667	{2} - .83333	{3} - 3.0000	{4} - 1.8333
1	Tg-only		0.288346	0.213479	0.829593
2	ST	0.288346		0.046347	0.406655
3	VCP	0.213479	0.046347		0.142433
4	SNT	0.829593	0.406655	0.142433	

Duncan test; Day 2 pellets

Sr	Groups	{1} - 2.5000	{2} - 1.8333	{3} - 2.8333	{4} - 6.1667
1	Tg only		0.701337	0.847782	0.054956
2	Saline	0.701337		0.588053	0.029351
3	VCP	0.847782	0.588053		0.065943
4	UCT 451	0.054956	0.029351	0.065943	

Duncan test; Day 3 pellets

Sr	Groups	{1} - 1.8333	{2} - 4.0000	{3} - 4.1667	{4} - 7.5000
1	Tg only		0.358881	0.350631	0.033922
2	Saline	0.358881		0.943204	0.165902
3	VCP	0.350631	0.943204		0.164016
4	UCT 451	0.033922	0.165902	0.164016	

Table R5.2A. Visits to RF during pre-training session.

Mean values			
Treatment Groups	Day 1	Day 2	Day 3
Tg-only	1.000000	1.166667	1.166667
ST	0.333333	1.000000	1.333333
VCP	1.000000	1.500000	1.666667
SNT	1.333333	2.666667	3.000000
SEM values			
Treatment Groups	Day 1	Day 2	Day 3
Tg-only	0.258199	0.307318	0.307318
ST	0.210819	0.365148	0.557773
VCP	0.000000	0.428174	0.494413
SNT	0.494413	0.421637	0.365148

Table R5.2B. Post-hoc analysis for the visits to RF during pre-training session.

Newman-Keuls test; Day 1 visits to RF

Sr	Treatment Groups	{1} - 1.0000	{2} - .33333	{3} - 1.0000	{4} - 1.3333
1	Tg only		0.276673	1.000000	0.438635
2	Saline	0.276673		0.129681	0.115424
3	VCP	1.000000	0.129681		0.713042
4	SNT	0.438635	0.115424	0.713042	

Newman-Keuls test; Day 2 visits to RF

Sr	Treatment Groups	{1} - 1.1667	{2} - 1.0000	{3} - 1.5000	{4} - 2.6667
1	Tg only		0.762040	0.546084	0.030868
2	Saline	0.762040		0.633478	0.028389
3	VCP	0.546084	0.633478		0.044098
4	SNT	0.030868	0.028389	0.044098	

Newman-Keuls test; Day 2 visits to RF

sr	Treatment Groups	{1} - 1.1667	{2} - 1.3333	{3} - 1.6667	{4} - 3.0000
1	Tg only		0.792843	0.708024	0.038270
2	Saline	0.792843		0.600291	0.038146
3	VCP	0.708024	0.600291		0.045862
4	SNT	0.038270	0.038146	0.045862	

Duncan test; Day1 visits to RF

Sr	Treatment Groups	{1} - 1.0000	{2} - .33333	{3} - 1.0000	{4} - 1.3333
1	Tg only		0.149514	1.000000	0.438635
2	Saline	0.149514		0.129681	0.040058
3	VCP	1.000000	0.129681		0.464315
4	SNT	0.438635	0.040058	0.464315	

Table R5.3A. Time taken to find the RF during Cued trials (Mean and SEM).

Mean values			
Treatment Groups	Day 1	Day 2	Day 3
Tg only	55.79167	50.91667	58.37500
Saline	59.79167	50.83333	53.25000
VCP	54.50000	34.75000	35.83333
SNT	41.12500	41.91667	39.45833
SEM values			
Treatment Groups	Day 1	Day 2	Day 3
Tg only	1.894601	2.760334	2.694840
Saline	0.209309	8.095391	3.439356
VCP	2.509160	4.068974	3.289412
SNT	5.628332	5.440943	5.409178

Table R5.3B. Post-hoc analysis for the time taken to find the RF during Cued trials.

Newman-Keuls test; Avg time cued trial day 1

Sr	Treatment Groups	{1} - 55.792	{2} - 59.792	{3} - 54.500	{4} - 41.125
1	Tg only		0.390461	0.779773	0.011547
2	ST	0.390461		0.488918	0.003006
3	VCP	0.779773	0.488918		0.008321
4	SNT	0.011547	0.003006	0.008321	

Newman-Keuls test; Avg time cued trial day 3

Sr	Treatment Groups	{1} - 56.375	{2} - 53.250	{3} - 35.833	{4} - 39.458
1	Tg only		0.571379	0.006001	0.014485
2	Saline	0.571379		0.011841	0.019605
3	VCP	0.006001	0.011841		0.512045
4	SNT	0.014485	0.019605	0.512045	

Duncan test; Cued trial day 2

Sr	Treatment Groups	{1} - 50.917	{2} - 50.833	{3} - 34.750	{4} - 41.917
1	Tg only		0.990367	0.038001	0.220810
2	Saline	0.990367		0.033961	0.200865
3	VCP	0.038001	0.033961		0.300407
4	SNT	0.220810	0.200865	0.300407	

Table R5.4A. Time taken to visit RF (Spatial trials).

Mean			
Treatment Groups	Day 1	Day 2	Day 3
Tg only	55.85000	55.45000	49.00000
Saline	54.79167	55.16667	45.08333
VCP	40.66667	43.04167	33.04167
SNT	46.50000	44.75000	46.75000
SEM			
Treatment Groups	Day 1	Day 2	Day 3
Tg only	2.628688	2.466526	4.272733
Saline	3.490115	1.950071	5.392381
VCP	5.683920	3.169133	6.546124
SNT	3.614784	4.465609	4.329846

Table R5.4B. Post-hoc analysis for the time taken to visit RF (Spatial trials).

Duncan test; Spatial trials day 1

Sr	Treatment Groups	{1} - 55.850	{2} - 54.792	{3} - 40.667	{4} - 46.500
1	Tg only		0.858742	0.026544	0.146738
2	Saline	0.858742		0.032988	0.173478
3	VCP	0.026544	0.032988		0.332245
4	SNT	0.146738	0.173478	0.332245	

Duncan test; Spatial trials day 2

Sr	Treatment Groups	{1} - 55.450	{2} - 55.167	{3} - 43.042	{4} - 44.750
1	Tg only		0.951327	0.020753	0.037904
2	Saline	0.951327		0.020233	0.034613
3	VCP	0.020753	0.020233		0.712997
4	SNT	0.037904	0.034613	0.712997	

Table R5.5A. Time taken to visit RF (Probe trial 1).

Sr	Treatment Groups	Probe 1 Avg - Mean	Probe 1 Avg - SEM
1	Tg only	44.00000	7.111610
2	ST	51.58333	6.535055
3	VCP	30.91667	5.270067
4	SNT	24.33333	7.291167

Table R5.5B. Post-hoc analysis for the time taken to visit RF (Probe trial 1).

Newman-Keuls test; Probe Trial 1

Sr	Treatment Groups	{1} - 44.000	{2} - 51.583	{3} - 30.917	{4} - 24.333
1	Tg only		0.426349	0.176890	0.114702
2	Saline	0.426349		0.094099	0.040041
3	VCP	0.176890	0.094099		0.488936
4	SNT	0.114702	0.040041	0.488936	

Duncan test; Probe Trial 1

Sr	Treatment Groups	{1} - 44.000	{2} - 51.583	{3} - 30.917	{4} - 24.333
1	Tg only		0.426349	0.176890	0.059097
2	Saline	0.426349		0.048194	0.013529
3	VCP	0.176890	0.048194		0.488936
4	SNT	0.059097	0.013529	0.488936	

(Note: saline refers to ST)

Table R5.6A. Time taken to visit RF (Probe trial 2).

Sr	Treatment Groups	Probe 2 Avg - Mean	Probe 2 Avg - SEM
1	Tg only	48.50000	4.546977
2	Saline	43.75000	6.879620
3	VCP	34.58333	7.619511
4	SNT	25.66667	5.472152

Table R5.6B. Time taken to visit RF (Reverse probe trial 1).

Sr	Treatment Groups	Reverse Probe trial 1 Mean	Reverse Probe trial 1 SEM
1	Tg-only	42.60000	5.297169
2	ST	35.41667	6.273511
3	VCP	19.08333	3.608824
4	SNT	23.58333	6.575734

Table R5.7A. Post hoc for the time taken to visit RF (Reverse probe trial 1).

Newman-Keuls test; Reverse probe trial 1

sr	Treatment Groups	{1} - 42.600	{2} - 35.417	{3} - 19.083	{4} - 23.583
1	Tg-only		0.377648	0.037158	0.067154
2	ST	0.377648		0.126516	0.153125
3	VCP	0.037158	0.126516		0.578060
4	SNT	0.067154	0.153125	0.578060	

Duncan test; Reverse probe trial 1

Sr	Treatment Groups	{1} - 42.600	{2} - 35.417	{3} - 19.083	{4} - 23.583
1	Tg-only		0.377648	0.012542	0.034160
2	ST	0.377648		0.065396	0.153125
3	VCP	0.012542	0.065396		0.578060
4	SNT	0.034160	0.153125	0.578060	

Table R5.8A. Time taken to visit RF (Reverse probe trial 2).

Treatment Groups	Rverse probe 2 - Mean	Rverse probe 2 - SEM
Tg only	50.00000	3.240370
ST	41.75000	6.155959
VCP	28.41667	2.573638
SNT	30.58333	7.886081

Table R5.8B. Post-hoc analysis for the time taken to visit RF (Reverse probe trial two).

Newman-Keuls test; Reverse Probe Trial 2

Sr	Treatment Groups	{1} - 50.000	{2} - 41.750	{3} - 28.417	{4} - 30.583
1	Tg only		0.311201	0.059852	0.060056
2	ST	0.311201		0.237782	0.175231
3	VCP	0.059852	0.237782		0.787676
4	SNT	0.060056	0.175231	0.787676	

Duncan test; Reverse Probe Trial 2

	Var1	{1} - 50.000	{2} - 41.750	{3} - 28.417	{4} - 30.583
1	Tg only		0.311201	0.020363	0.030493
2	ST	0.311201		0.126949	0.175231
3	VCP	0.020363	0.126949		0.787676
4	SNT	0.030493	0.175231	0.787676	

Chapter 6.

Table R 6.1A. Percentage time spent in the arms of EPM.

Sr	Treatment Groups	Control Arm (%) - Mean	Control Arm (%) - SEM	Open Arm (%) - Mean	Open Arm (%) - SEM	Closed Arm (%) - Mean	Closed Arm (%) - SEM
1	ST	18.75667	2.498014	12.01167	6.167649	74.34333	8.505197
2	VCP	18.83167	2.003265	25.43500	2.087696	55.51000	2.531195
3	tVCP	18.53000	0.600000	1.73000	0.286006	97.00000	0.208000
4	CUR	19.08250	7.156302	11.91750	4.414077	68.07250	3.475296
5	SNT	16.96500	1.660375	30.79667	7.087634	51.03833	6.659105

Table R 6.1B. Post-hoc analysis of the percentage time spent in the arms of EPM.

Newman-Keuls test; (Percentage time spent in the open arms of EPM)

Sr	Treatment Groups	{1} - 12.012	{2} - 26.436	{3} - 1.7360	{4} - 11.918	{5} - 30.767
1	ST		0.148837	0.494961	0.991793	0.116139
2	VCP	0.148837		0.068036	0.306095	0.557830
3	tVCP	0.494961	0.068036		0.267819	0.030194
4	CUR	0.991793	0.306095	0.267819		0.184943
5	SNT	0.116139	0.557830	0.030194	0.184943	

Newman-Keuls test; variable Enclosed Arm (%)

Sr	Treatment Groups	{1} - 74.343	{2} - 56.510	{3} - 87.070	{4} - 68.073	{5} - 51.098
1	ST		0.208299	0.223323	0.542464	0.133374
2	VCP	0.208299		0.032479	0.286948	0.598678
3	tVCP	0.223323	0.032479		0.171926	0.015909
4	Cur	0.542464	0.286948	0.171926		0.238713
5	SNT	0.133374	0.598678	0.015909	0.238713	

Duncan test; variable enclosed Arm (%)

Sr	Treatment Groups	{1} - 74.343	{2} - 56.510	{3} - 87.070	{4} - 68.073	{5} - 51.098
1	ST		0.110224	0.223323	0.542464	0.046595
2	VCP	0.110224		0.010946	0.286948	0.598678
3	tVCP	0.223323	0.010946		0.090014	0.004001
4	Cur	0.542464	0.286948	0.090014		0.127482
5	SNT	0.046595	0.598678	0.004001	0.127482	

Table R 6.2A. Open arm entries (Mean and SEM).

Sr	Treatment groups	Mean Open arm entries	SEM
1	ST	1.500000	0.806226
2	VCP	4.166667	0.307318
3	tVCP	0.000000	
4	Cur	1.333333	0.494413
5	SNT	5.166667	0.542627

Table R 6.2B. Post-hoc analysis for the open arm entries.

Sr	Treatment groups	Mean Open arm entries	SEM
1	ST	1.500000	0.806226
2	VCP	4.166667	0.307318
3	tVCP	0.000000	
4	Cur	1.333333	0.494413
5	SNT	5.166667	0.542627

Table R 6.3A. Enclosed arm entries (Mean and SEM).

Sr	Treatment Groups	Mean Enclosed Arm Entries	SEM
1	ST	3.500000	1.024695
2	VCP	9.166667	1.194897
3	tVCP	4.250000	0.750000
4	Cur	5.833333	1.327069
5	SNT	5.166667	0.703167

Table R 6.3B. Post-hoc analysis for the enclosed arm entries (NK).

Sr	Treatment Groups	{1} - 3.5000	{2} - 9.1667	{3} - 4.2500	{4} - 5.8333	{5} - 5.1667
1	ST		0.009872	0.630879	0.445153	0.534382
2	VCP	0.009872		0.019757	0.041170	0.041186
3	tVCP	0.630979	0.019757		0.567130	0.557609
4	Cur	0.445153	0.041170	0.567130		0.669237
5	SNT	0.534382	0.041186	0.557609	0.669237	

Table R 6.4A. Total arm entries.

Sr	Treatment Groups	Mean Total Arm Entries	SEM
1	ST	5.00000	1.751190
2	VCP	13.33333	1.382429
3	tVCP	4.25000	0.750000
4	Cur	7.16667	1.492574
5	SNT	10.33333	1.201850

Table R 6.4B. Post-hoc analysis for the total arm entries.

Sr	Treatment Groups	{1} - 5.0000	{2} - 13.333	{3} - 4.2500	{4} - 7.1667	{5} - 10.333
1	ST		0.002750	0.719283	0.304019	0.041963
2	VCP	0.002750		0.001838	0.017269	0.159012
3	tVCP	0.719283	0.001838		0.349727	0.033638
4	Cur	0.304019	0.017269	0.349727		0.138062
5	SNT	0.041963	0.159012	0.033638	0.138062	

Table R 6.5A. The ratio of arm entries.

Sr	Treatment Groups	Mean ratio (open arm entries/totalarm entries)	SEM
1	ST	0.172222	0.086245
2	VCP	0.321283	0.023054
3	tVCP	0.000000	
4	Cur	0.208333	0.077381
5	SNT	0.503704	0.016581

Table R 6.5B. Post-hoc analysis for the ratio of arm entries.

Sr	Treatment Groups	{1} - .17222	{2} - .32126	{3} - 0.0000	{4} - .20833	{5} - .50370
1	ST		0.189881	0.048249	0.665826	0.002927
2	VCP	0.189881		0.003910	0.184418	0.037360
3	tVCP	0.048249	0.003910		0.047971	0.000150
4	Cur	0.665826	0.184418	0.047971		0.004451
5	SNT	0.002927	0.037360	0.000150	0.004451	

Table R 6.6A. Open end arm frequencies.

Sr	Treatment Groups	Open arm end frequencies -Mean	SEM
1	ST	1.500000	1.024695
2	VCP	3.500000	0.341565
3	tVCP	0.000000	
4	CUR	1.000000	0.577350
5	SNT	4.166667	0.542627

Table R 6.6B. Post-hoc analysis for the open end arm frequencies.

Newman-Keuls test; variable Open end arm frequencies

Sr	Treatment Groups	{1} - 1.5000	{2} - 3.5000	{3} - 0.0000	{4} - 1.0000	{5} - 4.1667
1	ST		0.090779	0.392949	0.661019	0.069226
2	VCP	0.090779		0.026800	0.091959	0.559522
3	tVCP	0.392949	0.026800		0.384105	0.011441
4	Cur	0.661019	0.091959	0.384105		0.049023
5	SNT	0.069226	0.559522	0.011441	0.049023	

Duncan test; variable Open end arm frequencies

Sr	Treatment Groups	{1} - 1.5000	{2} - 3.5000	{3} - 0.0000	{4} - 1.0000	{5} - 4.1667
1	ST		0.090779	0.220865	0.661019	0.035234
2	VCP	0.090779		0.008946	0.047088	0.559522
3	tVCP	0.220865	0.008946		0.384105	0.002873
4	CUR	0.661019	0.047088	0.384105		0.016616
5	SNT	0.035234	0.559522	0.002873	0.016616	

Appendix R
Chapter 7.

Table R7.1A. The Mean average escape latencies during Sp L P.

	ST	VCP	tVCP	Cur	SNT
Day 1	70.55167	70.93583	75.00000	74.98917	71.74250
Day 2	66.38222	69.33722	73.50500	62.61222	64.49944
Day 3	75.00000	63.11111	75.00000	66.05556	50.50000
Day 4	69.22222	67.00000	70.33333	58.00000	60.77778
Day 5	68.72222	66.44444	68.75000	48.72222	44.72222
Day 6	62.39889	60.44389	70.74167	56.51111	55.99944
Day 7	65.77111	62.37500	70.47417	51.48889	46.38778

Table R7.1B. SEM for the mean average escape latencies during Sp L P.

	ST	VCP	tVCP	Cur	SNT
STD1	4.448333	4.064167	0	0.010833	2.091807
STD2	3.889498	3.037291	1.495000	4.570701	6.460404
STD3	0.00000	4.528647	0.00000	3.284550	8.913473
STD4	3.608289	3.801559	2.748737	5.576405	4.831737
STD5	3.128621	4.222222	6.250000	5.840102	6.845067
STD6	5.612303	3.269123	4.258333	4.863341	4.733513
STD7	3.750607	6.052552	4.379302	4.769449	5.899796

Table R7.1 C Post-Hoc Analysis for the Mean.

(Newman-Keuls test; Day 3 Sp L P)					
ST		0.380558	1.000000	0.448731	0.020383
VCP	0.380558		0.252271	0.689657	0.096659
tVCP	1.000000	0.252271		0.231609	0.013306
Cur	0.448731	0.689657	0.231609		0.104358
SNT	0.020383	0.096659	0.013306	0.104358	
(Newman-Keuls test; Day 5 Sp L P)					
ST		0.770360	0.997258	**0.041409**	**0.023571**
VCP	0.770360		0.952057	**0.031029**	**0.025527**
tVCP	0.997258	0.952057		**0.071067**	**0.035393**
Cur	0.041409	**0.031029**	**0.071067**		0.608845
SNT	**0.023571**	**0.025527**	**0.035393**	**0.608845**	
(Newman-Keuls test; Day 7 Sp L P)					
ST		0.652736	0.534001	0.156370	0.070406
VCP	0.652736		0.531132	0.157415	0.102449
tVCP	0.534001	0.531132		0.078450	0.027352
Cur	0.156370	0.157415	0.078450		0.500289
SNT	0.070406	0.102449	**0.027352**	0.500289	

Table R7.1 D. The within group analysis.

Newman-Keuls test; (MWM Spatial learning 7 days) Overall Within Group Analysis							
STD 1		0.066702	0.051524	**0.056157**	**0.000151**	**0.001034**	**0.000138**
STD 2	0.066702		0.618382	0.768639	0.070597	0.174170	0.075479
STD 3	0.051524	0.618382		0.846934	0.152924	0.272423	0.179455
STD 4	0.056157	0.768639	0.846934		0.136566	0.178149	0.185178
STD 5	**0.000151**	0.070597	0.152924	0.136566		0.574902	0.920352
STD 6	**0.001034**	0.174170	0.272423	0.178149	0.574902		0.786191
STD 7	**0.000138**	0.075479	0.179455	0.185178	0.920352	0.786191	

Table R7.2A. Time spent in the central zone of MWM during Sp L P.

	Mean values				
	ST	VCP	tVCP	Cur	SNT
Day 1	37.62500	36.79333	29.98000	37.81000	55.51917
Day 2	45.08833	48.31889	39.84917	59.41611	59.27333
Day 7	73.19667	76.46056	63.69750	75.68222	75.88778
	SEM values				
	ST	VCP	tVCP	Cur	SNT
Day 1	4.612053	6.578153	5.038282	4.544665	2.014209
Day 2	7.909395	2.436735	5.420832	6.934116	5.356068
Day 7	7.633896	4.743977	8.016662	4.875653	7.099730

Table R7.2B. Post-hoc analysis for the time spent in the central zone of MWM during Sp L P (Between Group).

Newman-Keuls test; Time Spent Central Zone (Sp L P)					
ST		0.905149	0.518561	0.978932	**0.041390**
VCP	0.905149		0.333496	0.988183	0.055829
tVCP	0.518561	0.333496		0.671978	**0.009433**
Cur	0.978932	0.988183	0.671978		**0.017328**
SNT	**0.041390**	0.055829	**0.009433**	**0.017328**	

Table R7.2C. Post-hoc analysis for the time spent in the central zone of MWM during Sp L P (Overall Groups on days 1, 2 and 7).

Newman-Keuls test; variable: The mean average percentage time spent in the central zone during Sp L P (Overall groups)			
STD1 central		0.006391	0.000128
STD2 Central	0.006391		0.000119
STD7 Central	0.000128	0.000119	

Table R 7.3A. Percentage time spent in the nearest proximity of the platform (Sp L P).

Mean	ST	VCP	tVCP	Cur	SNT
Day 1	10.61333	8.90250	4.66750	2.94000	2.94000
Day 2	5.11944	4.48222	3.22583	6.57333	10.40778
Day 7	8.65556	11.97167	5.89667	14.89556	22.47667
SEM	ST	VCP	tVCP	Cur	SNT
Day 1	2.966499	2.101104	0.976451	0.995186	0.784396
Day 2	1.679627	1.277575	1.003821	1.228007	6.170895
Day 7	1.552197	3.803272	1.887873	2.247657	3.627028

Table R 7.3B. Post-hoc analysis for the percentage time spent in the nearest proximity of the platform (Sp L P).

Newman-Keuls test; variable: Day 7 Sp L P (Percentage time in the nearest proximity)						
	Treatment Groups	{1} - 8.6556	{2} - 11.972	{3} - 5.8967	{4} - 14.896	{5} - 22.477
1	ST		0.435692	0.515790	0.335169	**0.015222**
2	VCP	0.435692		0.331142	0.521081	**0.049101**
3	tVCP	0.515790	0.331142		0.181233	**0.005099**
4	Cur	0.335169	0.521081	0.181233		**0.075544**
5	SNT	**0.015222**	**0.049101**	**0.005099**	**0.075544**	

Newman-Keuls test; Within group anlaysis (Only data related to SNT is shown)			
SNT Day 1 Proximity		0.710686	**0.001159**
SNT Day 2 Proximity	0.710686		**0.029040**
SNT Day 7 Proximity	**0.001159**	**0.029040**	

Table R 7.4A.Velocities during Sp L P.

Mean	ST	VCP	tVCP	Cur	SNT
Day 1	16.77917	14.68917	15.52000	15.99083	18.62000
Day 2	16.85278	16.38611	13.90917	18.30667	18.52056
Day 7	17.24000	15.30500	14.68583	15.79833	18.18722

SEM	ST	VCP	tVCP	Cur	SNT
Day 1	0.761995	0.901698	1.356993	0.856547	0.926114
Day 2	1.000047	0.776245	0.883483	1.281876	0.608444
Day 7	0.684077	1.257010	0.101173	0.662378	1.365549

Table R7.4B. Post-hoc analsysis for the velocities during Sp L P.

Newman-Keuls test; Day 2 Sp L P Velocity						
	Treatment Groups	{1} - 16.853	{2} - 16.386	{3} - 13.909	{4} - 18.307	{5} - 18.521
1	ST		0.736722	0.102354	0.299973	0.455859
2	VCP	0.736722		0.083987	0.356942	0.421673
3	tVCP	0.102354	0.083987		0.019080	0.020479
4	Cur	0.299973	0.356942	0.019080		0.577468
5	SNT	0.455859	0.421673	0.020479	0.577468	

Table R7.5A. Percentage time in the platform zone during probe trial.

Sr	Treatment Groups	Proximity platform (%) - Mean	Proximity platform (%) - SEM
1	ST	1.056667	0.304211
2	VCP	1.171667	0.270190
3	tVCP	1.007500	0.433135
4	Cur	1.113333	0.446084
5	SNT	1.225000	0.601995

Table R7.5B. Percentage time in the platform zone during probe trial.

Sr	Treatment Groups	Target Quadrant (%) - Mean	Target Quadrant (%) - SEM
1	ST	25.75167	6.209403
2	VCP	34.94833	2.964069
3	tVCP	24.58000	3.550998
4	Cur	38.01667	7.845950
5	SNT	40.69167	5.438496

Table R7.6A. Percentage time in the central zone during probe trial.

	Treatment Groups	Central (%) - Mean	Central (%) - Std.Err.
1	ST	63.48833	8.905754
2	VCP	80.88000	3.933366
3	tVCP	51.39750	6.823022
4	Cur	77.03333	8.256841
5	SNT	62.82167	7.419249

Table R7.6B. Post-hoc analysis for the percentage time in the central zone during probe trial (Duncan test).

	Treatment Groups	{1} - 63.488	{2} - 80.880	{3} - 51.397	{4} - 77.033	{5} - 62.822
1	ST		0.134994	0.294364	0.215763	0.950652
2	VCP	0.134994		0.018919	0.721080	0.132782
3	tVCP	0.294364	0.018919		0.035720	0.294148
4	Cur	0.215763	0.721080	0.035720		0.219245
5	SNT	0.950652	0.132782	0.294148	0.219245	

Table R7.7A. Kissperi frequencies (probe trial).

Sr	Treatment Groups	Kisseperi - Mean	Kisseperi - SEM
1	ST	4.000000	1.125463
2	VCP	2.166667	0.792324
3	tVCP	8.750000	1.547848
4	Cur	3.333333	1.452966
5	SNT	3.500000	1.384437

Table R7.7B. Kissperi frequencies (probe trial; NK test).

	Treatment Groups	{1} - 4.0000	{2} - 2.1667	{3} - 8.7500	{4} - 3.3333	{5} - 3.5000
1	ST		0.744972	0.015498	0.928572	0.785412
2	VCP	0.744972		0.011205	0.526636	0.745586
3	tVCP	0.015498	0.011205		0.031282	0.021565
4	Cur	0.928572	0.526636	0.031282		0.927698
5	SNT	0.785412	0.745586	0.021565	0.927698	

Table R7.8. Velocities (probe trial).

Sr	Treatment Groups	Velocity - Mean	Velocity - SEM
1	ST	18.17833	1.245125
2	VCP	19.82833	2.128050
3	tVCP	17.34000	0.917778
4	Cur	19.95000	0.712036
5	SNT	21.40167	1.068652

Table R7.9 Escape latencies during Sp RP.

Mean	ST	VCP	tVCP	Cur	SNT
Day 1	53.62583	62.70583	67.32125	60.59333	69.14583
Day 2	65.14000	66.07167	62.86250	72.28333	64.47333
Day 3	62.94444	67.94444	70.16667	58.72222	61.27778
Day 4	70.51944	62.80556	61.13417	62.39722	63.34222
Day 5	69.22222	70.94444	57.50000	71.05556	62.33333
Day 6	69.55556	62.94444	65.83333	61.05556	65.88889
Day 7	69.09667	72.78833	74.58417	73.82500	63.10444
SEM	ST	VCP	tVCP	Cur	SNT
Day 1	9.554241	5.538135	6.337323	5.536590	4.468946
Day 2	3.418929	6.108988	4.135115	2.513780	4.227251
Day 3	7.182498	5.880550	4.833333	8.289850	6.486691
Day 4	2.68250	3.79636	11.72950	9.52675	6.16602
Day 5	3.693504	1.870864	2.119137	2.622434	6.565905
Day 6	2.983494	3.992972	5.403188	6.288922	3.507312
Day 7	2.830527	1.570828	0.415833	1.175000	9.308556

Table R7.10A. The percentage time spent in the central zone of MWM (Sp R P).

Mean	ST	VCP	tVCP	Cur	SNT
Day 1	83.26333	88.13000	76.70125	82.29417	83.69500
Day 2	87.79444	77.26278	71.21167	81.12833	73.14944
Day 7	86.00944	76.57611	68.63667	84.03778	86.13222
SEM	ST	VCP	tVCP	Cur	SNT
Day 1	2.216575	4.012229	8.748572	3.693539	3.099730
Day 2	4.199428	5.495739	5.097702	5.973004	4.617161
Day 7	4.829825	4.494548	4.328959	5.101382	6.280841

Table R 7.10B. Post-hoc analysis for the percentage time spent in the central zone of MWM (Sp R P).

Newman-Keuls test; Percentage time spent in the central zone during Sp R P) (Pooled data, overall mean average % time)				
Sr	Percentage Time	{1} - 82.667	{2} - 78.593	{3} - 66.110
1	Day 1 Central (%)		0.142197	0.000128
2	Day 2 Central (%)	0.142197		0.000151
3	Day 7 Central (%)	0.000128	0.000151	

Table R 7.11A. The percentage time spent in the nearest proximity of the platform during Sp R P.

Sr	Treatment Groups	Sp R P Day 1 - Mean	Sp R P Day 1 - SEM	Sp R P Day 2- Mean	Sp R P Day 2 - SEM	Sp R P Day 7 - Mean	Sp R P Day 7- SEM
1	ST	12.81083	4.953170	7.285556	1.780675	1.776111	0.779891
2	VCP	10.81333	2.217624	6.207778	1.696716	1.228333	0.343968
3	tVCP	8.08500	2.308200	6.490833	0.945259	0.778333	0.638188
4	Cur	8.56917	2.681989	5.624444	1.511142	0.790556	0.271187
5	SNT	6.33667	2.205561	5.682778	0.983105	3.933889	3.160650

Table R 7.11B Post-hoc analysis (NK) for the percentage time spent in the nearest proximity of the platform during Sp R P (Overall pooled average mean data).

Sr	% Time (Nearest Proximity) during Sp R P	{1} - 9.1229	{2} - 6.2417	{3} - 1.7674
1	Proxi Sp R P day 1		0.036658	0.000131
2	Proxi Sp R P day 2	0.036658		0.001771
3	Proxi Sp R P day 7	0.000131	0.001771	

Table R 7.11C. Post-hoc analysis (NK) for the percentage time spent in the nearest proximity of the platform during Sp R P (Within group analysis: ST group).

Newman-Keuls test; Percentage time spent in the nearest proximity [Within group analysis: Only ST values are shown]				
ST	Proxi Sp R D1		0.276076	0.029796
ST	Proxi Sp R D2	0.276076		0.670772
ST	Proxi Sp R D7	0.029796	0.670772	

Table R7.12. Velocities during Sp R P.

Mean	ST	VCP	tVCP	Cur	SNT
Day 1	16.53250	16.33417	14.80125	16.86167	16.81917
Day 2	17.09500	15.56778	14.08667	15.86167	17.37833
Day 7	15.40667	13.15167	13.09167	13.78556	16.81667
SEM	**ST**	**VCP**	**tVCP**	**Cur**	**SNT**
Day 1	0.780166	1.349069	1.040898	1.582944	0.693866
Day 2	0.517879	1.376444	1.092223	1.720890	0.938606
Day 7	0.640090	1.540743	0.381383	1.410284	1.590810

Table R7.13A. Kissperi frequencies during Sp R P.

Sr	Treatment Groups	Kissperi Sp R P Day 1 - Mean	Kissperi Sp R P Day1 - SEM	Kissperi Sp R P Day 2 - Mean	Kissperi Sp R P Day 2 - SEM	Kissperi Sp R P Day 7 - Mean	Kissperi Sp R P Day 7 - SEM
1	ST	3.250000	1.226979	2.833333	1.790492	8.222222	1.666019
2	VCP	1.750000	1.226979	3.722222	1.790492	2.833333	1.666019
3	tVCP	5.500000	1.957666	7.333333	2.119374	9.916667	2.006955
4	Cur	4.500000	1.226979	5.500000	1.790492	6.055556	1.666019
5	SNT	3.416667	1.226979	6.222222	1.790492	7.333333	1.666019

Table R 7.13B. Newman-Keuls test; Kissperi frequencies during Sp R P (Within group: Overall frequencies).

Sr	Kissperi (Sp R P)	{1} - 3.5536	{2} - 4.9643	{3} - 6.6548
1	Day 1		0.086347	0.001136
2	Day 2	0.086347		0.041253
3	Day 7	0.001136	0.041253	

Table R 7.13C. Duncan test; within group Kissperi frequencies during Sp R P (ST).

	Treatment Groups	Sp R P	{1} - 3.2500	{2} - 2.8333	{3} - 8.2222
1	ST	Day1		0.831817	0.024511
2	ST	Day 2	0.831817		0.015795
3	ST	Day 3	0.024511	0.015795	

Table R7.14. A. Percentage time spent in the platform proximity during the reverse probe trial.

Sr	Treatment Groups	Percentage Time (Platform Proximity) - Mean	Percentage Time (Platform Proximity) - SEM
1	ST	0.501667	0.240450
2	VCP	0.278333	0.278333
3	tVCP	1.087500	0.418835
4	Cur	1.378333	0.965756
5	SNT	4.070000	1.147319

Table R7.14 B. Post –hoc analysis for the percentage time spent in the platform proximity during the reverse probe trial (Between group; NK test).

Sr	Treatment Groups	(1) - .50167	(2) - .27833	(3) - 1.0875	(4) - 1.3783	(5) - 4.0700
1	ST		0.838001	0.592591	0.699386	0.015265
2	VCP	0.838001		0.736877	0.740082	0.014608
3	tVCP	0.592591	0.736877		0.790073	0.028785
4	Cur	0.699386	0.740082	0.790073		0.020395
5	SNT	0.015265	0.014608	0.028785	0.020395	

Table R7.15. Percentage time spent in the central zone of MWM (reverse probe trial).

	Treatment Groups	Central (% Duration) - Mean	Central (% Duration) - SEM
1	ST	65.98333	6.60099
2	VCP	78.70833	5.30018
3	tVCP	63.12750	10.08186
4	Cur	68.87167	9.16839
5	SNT	67.50333	5.27805

Table R7.16. Kissperi frequencies during reverse probe trial (Mean and SEM values).

	Treatment Groups	Kissperi - Mean	Kissperi- SEM
1	ST	4.666667	0.760117
2	VCP	1.833333	0.654047
3	tVCP	5.250000	1.314978
4	Cur	2.833333	1.194897
5	SNT	3.500000	1.056724

Table R7.17. Velocities during the reverse probe trial.

Sr	Treatment Groups	Velocity RP - Mean	Velocity RP - SEM
1	ST	18.78833	0.758004
2	VCP	15.16500	1.650191
3	tVCP	15.65000	0.779391
4	Cur	19.13667	1.373955
5	SNT	19.29167	2.054548

Table R7.18A. Percentage time spent in the probe and reverse probe quadrants (reverse probe trial).

Sr	Treatmen t Groups	Probe quadrant - Mean	Probe quadrant - SEM	Reverse probe quadrant (%) - Mean	Reverse probe quadrant (%) - SEM
1	ST	38.81333	7.437716	16.62833	5.110436
2	VCP	32.16333	8.670167	14.71500	5.088527
3	tVCP	48.32750	6.322400	17.47500	5.479788
4	Cur	28.90000	5.520674	20.23000	3.456762
5	SNT	30.26667	7.148080	34.78333	5.403051

Table R 7.18B. Post-hoc for the percentage time spent in the probe and reverse probe quadrants (within group: tVCP; reverse probe trial).

Sr	Percentage Time spent	tVCP	tVCP
1	Probe quadrant		0.021231
2	Reverse probe quadrant (%)	0.021231	

Table R7.18C. Percentage time spent in the probe and reverse probe quadrants (within group: overall pooled mean values; reverse probe trial).

	Percentage Time spent	Overal[Pool ed] Mean
1	Probe quadrant	34.36321
2	Reverse probe quadrant (%)	21.00143

Table R 7.19. Percentage reduction in the escape latencies during the test trials of Sp W P.

Treatment Groups	Day 1	Day 2	Day 3	Day 4	Day 5	Day 6	Day 7
ST	-15.4661	-113.584	12.1111	11.1111	7.2578	23.889	4.1111
VCP	-1.8033	3.741	-43.3072	12.3333	-21.4132	11.015	12.7222
tVCP	24.5200	-3.846	-5.2419	-16.0833	16.8800	23.167	-33.4543
Cur	-18.4851	8.993	7.2996	8.9106	5.4117	-102.861	-24.6667
SNT	18.6444	-10.708	14.1944	-3.3398	6.8044	11.431	-12.9641
SEM values	Day 1	Day 2	Day 3	Day 4	Day 5	Day 6	Day 7
ST	23.66342	123.8655	7.05621	9.36924	4.59051	11.17990	2.90296
VCP	5.31875	6.8629	60.30757	6.54953	20.57568	3.88912	11.94387
tVCP	9.07774	3.8462	5.24194	31.52553	9.27819	9.83333	21.92219
Cur	29.61938	15.5210	12.20158	8.63503	8.07954	94.82949	33.47879
SNT	5.24609	9.2015	9.84250	14.13740	5.46803	11.06488	21.62933

Table R 7.20A. Kissperi frequencies during Sp W P.

Mean	ST	VCP	tVCP	Cur	SNT
Day 1	2.916667	0.944444	5.833333	3.222222	4.000000
Day 6	7.00000	3.11111	12.91667	4.27778	4.11111
Day 11	6.58333	1.38889	14.41667	4.83333	4.33333
SEM	ST	VCP	tVCP	Cur	SNT
Day 1	0.795692	0.309274	1.479102	1.666350	0.720092
Day 6	1.612907	1.434161	1.499228	1.615702	1.107773
Day 11	1.077262	0.612187	1.672864	1.403039	1.336108

Table R 7.20B. Post-hoc analysis for the Kissperi frequencies during Sp W P.

Newman-Keuls test; kissperi frequencies on day 1 of Sp W M.						
Sr	Treatment Groups	{1} - 2.9167	{2} - .94444	{3} - 5.8333	{4} - 3.2222	{5} - 4.0000
1	ST		0.195057	0.226642	0.838082	0.746574
2	VCP	0.195057		0.023171	0.290729	0.193371
3	tVCP	0.226642	0.023171		0.202802	0.227224
4	Cur	0.838082	0.290729	0.202802		0.603710
5	SNT	0.746574	0.193371	0.227224	0.603710	
Newman-Keuls test; Kissperi frequencies on day 5 of SP W M.						
Sr	Treatment Groups	{1} - 7.0000	{2} - 3.1111	{3} - 12.917	{4} - 4.2778	{5} - 4.1111
1	ST		0.269974	0.009451	0.204540	0.364521
2	VCP	0.269974		0.000950	0.842600	0.636031
3	tVCP	0.009451	0.000950		0.001214	0.001823
4	Cur	0.204540	0.842600	0.001214		0.937054
5	SNT	0.364521	0.636031	0.001823	0.937054	
Table 19. Newman-Keuls test; Kissperi frequencies on day 11 of Sp W M.						
	Treatment Groups	{1} - 6.5556	{2} - 1.3889	{3} - 14.417	{4} - 4.8333	{5} - 4.3333
1	ST		0.036697	0.000334	0.341844	0.435439
2	VCP	0.036697		0.000129	0.149913	0.110663
3	tVCP	0.000334	0.000129		0.000173	0.000209
4	Cur	0.341844	0.149913	0.000173		0.780686
5	SNT	0.435439	0.110663	0.000209	0.780685	

Table 7.21A. Velocities during Sp W P.

Sr	Treatment Groups	Velocities Day 1- Mean	Velocities Day 1 – SEM	Velocities Day 5- Mean	Velocities Day 5 – SEM	Velocities Day 11- Mean	Velocities Day 11- SEM
1	ST	16.45000	0.666538	14.30556	0.991287	14.31333	0.316949
2	VCP	13.90111	1.468220	12.49500	1.512495	12.80022	1.643012
3	tVCP	14.83667	0.647768	12.92583	1.493656	11.38917	1.049643
4	Cur	16.13222	1.287383	14.20000	1.018942	14.28056	1.018804
5	SNT	17.45889	1.054647	16.54278	0.945089	15.95028	1.688171

Table 7.21B. Post-hoc analysis of the velocities during Sp W P (Overall Pooled values).

Newman-Keuls test; Mean average Velocity (cm/s)				
Sr	Mean Average Velocity	{1} - 15.607	{2} - 14.197	{3} - 13.921
1	Day 1		0.000736	0.000304
2	Day 5	0.000736		0.476951
3	Day 11	0.000304	0.476951	

Appendix R
Chapter 8.

Table R 8.1A. Pellets consumed during pre-training session.

Sr	Treatment Groups	Day 1 - Mean	Day 1 - SEM	Day 2 pellets - Mean	Day 2 - SEM	Day 3 - Mean	Day 3 - SEM
1	ST	1.800000	1.119034	1.600000	1.275044	2.666667	1.642004
2	VCP	1.166667	0.749074	2.500000	0.621934	4.500000	1.360147
3	tVCP	0.000000		1.250000	0.048466	0.250000	0.250000
4	Cur	1.666667	0.666026	3.500000	1.360147	2.666667	1.021951
5	SNT	1.166667	0.654047	3.833333	1.720788	5.166667	1.027549

Table R 8.1B. Post-hoc analysis for the pellets consumed during pre-training session (Duncan test; Day three).

Sr	Treatment Groups	{1} - 2.6667	{2} - 4.5000	{3} - .25000	{4} - 2.6667	{5} - 5.1667
1	ST		0.335190	0.182490	1.000000	0.205648
2	VCP	0.335190		0.035123	0.307855	0.708048
3	tVCP	0.182490	0.035123		0.206359	0.017903
4	Cur	1.000000	0.307855	0.206359		0.191535
5	SNT	0.205648	0.708048	0.017903	0.191535	

Table R8.2A. Visits to RFs during pre-training session.

Sr	Treatment Groups	Day 1 - Mean	Day 1 - SEM	Day 2 - Mean	Day 2 - SEM	Day 3 - Mean	Day 3 - SEM
1	ST	0.666667	0.333333	0.666667	0.333333	1.000000	0.516398
2	VCP	0.333333	0.210819	1.000000	0.365148	1.500000	0.341565
3	tVCP	0.000000		0.500000	0.289575	0.250000	0.250000
4	Cur	1.166667	0.600925	1.666667	0.614636	0.833333	0.307318
5	SNT	0.500000	0.223607	1.333333	0.494413	2.166667	0.792324

Table R8.2B. Post-hoc analysis of the visits to RFs during pre-training session.

Duncan test; Pre-training session day 3 visits to RFs

	Treatment Groups	{1} - 1.0000	{2} - 1.5000	{3} - .25000	{4} - .83333	{5} - 2.1667
1	ST		0.503466	0.346804	0.822821	0.146480
2	VCP	0.503466		0.132252	0.401462	0.374180
3	tVCP	0.346804	0.132252		0.435666	0.026805
4	Cur	0.822821	0.401462	0.435666		0.109130
5	SNT	0.146480	0.374180	0.026805	0.109130	

Table R8.3A. Time taken for the first visit to RF during pre-training session.

Sr	Treatment Groups	Day 1- Mean	Day 1- SEM	Day 2- Mean	Day 2- SEM	Day 3- Mean	Day 3- SEM
1	ST	156.6667	45.85315	68.3333	41.44126	183.1667	46.56777
2	VCP	185.3333	44.28432	72.1667	32.16563	98.1667	36.75916
3	tVCP	255.0000		133.5000	53.67765	207.0000	49.00000
4	Cur	166.5000	49.71967	23.1667	10.34220	134.5000	46.52671
5	SNT	95.8333	46.80161	27.0000	8.67471	56.8333	14.09117

Table R8.3B. Post-hoc analysis for the time taken for the first visit to RF during pre-training session.

Duncan test; Pre-training Day one (Time taken for the first visit to RF)

	Treatment Groups	{1} - 156.67	{2} - 185.33	{3} - 255.00	{4} - 166.50	{5} - 95.833
1	ST		0.665203	0.156339	0.874547	0.333308
2	VCP	0.665203		0.269412	0.762458	0.195903
3	tVCP	0.156339	0.269412		0.186819	0.027715
4	Curcumin	0.874547	0.762458	0.186819		0.289483
5	SNT	0.333308	0.195903	0.027715	0.289483	

Duncan test; Pre-training Day two (Time taken for the first visit to RF)

	Treatment Groups	{1} - 66.333	{2} - 72.167	{3} - 133.50	{4} - 23.167	{5} - 27.000
1	ST		0.896603	0.165045	0.368045	0.384436
2	VCP	0.896603		0.180040	0.323364	0.346550
3	tVCP	0.165045	0.180040		0.033759	0.036309
4	Curcumin	0.368045	0.323364	0.033759		0.931961
5	SNT	0.384436	0.346550	0.036309	0.931961	

Duncan test; Pre-training Day three (Time taken for the first visit to RF)

	Treatment Groups	{1} - 183.17	{2} - 86.167	{3} - 207.00	{4} - 134.50	{5} - 56.833
1	ST		0.099869	0.661363	0.374235	0.039992
2	VCP	0.099869		0.048894	0.377465	0.590181
3	tVCP	0.661363	0.048894		0.214389	0.017919
4	Curcumin	0.374235	0.377465	0.214389		0.184262
5	SNT	0.039992	0.590181	0.017919	0.184262	

Table R8.4A. Visits to RFs during PAL-ChBM.

Treatment Groups	Day 1	Day 4	Day 8
ST	0.333333	0.000000	0.333333
VCP	0.833333	1.166667	2.333333
tVCP	0.500000	0.000000	0.000000
Cur	0.333333	0.500000	1.000000
SNT	0.833333	2.833333	2.166667
Treatment Groups	SEM values		
ST	0.310835	0.308886	0.394711
VCP	0.310835	0.308886	0.394711
tVCP	0.380893	0.378307	0.483421
Curcumin	0.310835	0.308886	0.394711
SNT	0.310835	0.308886	0.394711

Table R8.4B.Post-hoc analysis for the visits to RFs during PAL-ChBM.

Newman-Keuls test: Visits to Reward Flag day one of PAL-ChBM

	Treatment Groups	{1} - .33333	{2} - .83333	{3} - .50000	{4} - .33333	{5} - .83333
1	ST		0.702318	0.721152	1.000000	0.533063
2	VCP	0.702318		0.752620	0.812615	1.000000
3	tVCP	0.721152	0.752620		0.930804	0.477125
4	Curcumin	1.000000	0.812615	0.930804		0.702318
5	SNT	0.533063	1.000000	0.477125	0.702318	

Newman-Keuls test: Visits to Reward Flag day four of PAL-ChBM

	Treatment Groups	{1} - 0.0000	{2} - 1.1667	{3} - 0.0000	{4} - .50000	{5} - 2.8333
1	ST		0.045874	1.000000	0.286570	0.000181
2	VCP	0.045874		0.078964	0.159293	0.001525
3	tVCP	1.000000	0.078964		0.528960	0.000146
4	Cur	0.286570	0.159293	0.528960		0.000224
5	SNT	0.000181	0.001525	0.000146	0.000224	

Newman-Keuls test: Visits to Reward Flag day eight of PAL-ChBM

	Treatment Groups	{1} - .33333	{2} - 2.3333	{3} - 0.0000	{4} - 1.0000	{5} - 2.1667
1	ST		0.011871	0.574762	0.286684	0.012618
2	VCP	0.011871		0.004877	0.079493	0.778558
3	tVCP	0.574762	0.004877		0.223789	0.006139
4	Curcumin	0.286684	0.079493	0.223789		0.058419
5	SNT	0.012618	0.778558	0.006139	0.058419	

Table R8.5A. Time taken to visit RF during PAL-ChBM.

Mean values			
Treatment Groups	Day 1	Day 4	Day 8
ST	59.76333	60.00000	57.07708
VCP	52.56292	51.37458	41.56625
tVCP	57.85583	60.00000	60.00000
Cur	59.27917	56.11458	53.92583
SNT	54.39083	41.56750	42.64875
SEM			
Treatment Groups	Day one	Day four	Day Eight
ST	1.997213	2.819112	4.294448
VCP	1.997213	2.819112	4.294448
tVCP	2.446076	3.452694	5.259603
Curcumin	1.997213	2.819112	4.294448
SNT	1.997213	2.819112	4.294448

Table R8.5B. Post-hoc analysis (NK) of the time taken to visit RF during PAL-ChBM.

Sr	Treatment Groups	{1} - 60.000	{2} - 51.375	{3} - 60.000	{4} - 56.115	{5} - 41.568
1	ST		0.195230	1.000000	0.627844	0.001841
2	VCP	0.195230		0.120124	0.268788	0.028130
3	tVCP	1.000000	0.120124		0.362584	0.001218
4	Cur	0.627844	0.268788	0.362584		0.005640
5	SNT	0.001841	0.028130	0.001218	0.005640	

Table R8.6A. Visits to RFs during probe trials.

Mean			
Treatment Groups	Type I	Type II	Type III
ST	0.600000	0.666667	0.333333
VCP	1.500000	0.833333	1.166667
tVCP	0.000000	0.000000	0.000000
Cur	0.500000	0.333333	0.666667
SNT	1.333333	1.500000	1.666667
SEM			
Treatment Groups	Type I	Type II	Type III
ST	0.397759	0.442326	0.406766
VCP	0.397759	0.442326	0.406766
tVCP	0.487164	0.541736	0.498185
Cur	0.397759	0.442326	0.406766
SNT	0.397759	0.442326	0.406766

Table R 8.6B. Post-hoc for the visits to RFs during probe trials.

Duncan test: Probe Trial Type I (Probe trials visits to RF)

Sr	Treatment Groups	{1} - .50000	{2} - 1.5000	{3} - 0.0000	{4} - .50000	{5} - 1.3333
1	ST		0.121715	0.432542	1.000000	0.171330
2	VCP	0.121715		0.030285	0.133343	0.780208
3	tVCP	0.432542	0.030285		0.405621	0.048028
4	Cur	1.000000	0.133343	0.405621		0.194587
5	SNT	0.171330	0.780208	0.048028	0.194587	

Duncan test: Probe Trial Type II (Probe trials visits to RF)

Sr	Treatment Groups	{1} - .66667	{2} - .83333	{3} - 0.0000	{4} - .33333	{5} - 1.5000
1	ST		0.801840	0.347677	0.616376	0.242243
2	VCP	0.801840		0.257339	0.479954	0.320265
3	tVCP	0.347677	0.257339		0.616376	0.049972
4	Cur	0.616376	0.479954	0.616376		0.115889
5	SNT	0.242243	0.320265	0.049972	0.115889	

Duncan test: Probe Tiral Type III (Probe trials visits to RF)

Sr	Treatment Groups	{1} - .33333	{2} - 1.1667	{3} - 0.0000	{4} - .66667	{5} - 1.6667
1	ST		0.204388	0.586073	0.586073	0.052904
2	VCP	0.204388		0.088322	0.415940	0.415940
3	tVCP	0.586073	0.088322		0.307766	0.019278
4	Cur	0.586073	0.415940	0.307766		0.129872
5	SNT	0.052904	0.415940	0.019278	0.129872	

Appendix S.

(Solutions, Chemicals and reagents)

Chemicals used for the thesis and Company Names.

HCl = BDH
Acetic acid = BDH
Glycerol = Merck
Triton X 100 = Sigma
Tween-20 = Sigma
Acetone = Sigma
Propanol = Sigma
5000 MW cutoff filter = Amnicon ultra – 15
3000 MW cutoff filter = Centriprep
(Millex GP 0.22μm, Millipore Express PES membrane)
Acetic acid = BDH
Tween-20 = Sigma,
Beta mercaptoethanol = (Merck)
Ammonia = Merck
Propanol = Sigma
Sodium hydroxide = (Merck)
Sodium deoxycholate = (Merck)
SDS = fluka (Sigma)
Sucrose = Saarchem (Merck)
Tris buffer (Merck)
Sodium acetate = (Merck)
Agar = Biolab (Merck)
Paraformaldehyde = (Merck)
Ammonium sulphate = Fluka (Sigma)
Potassium dihydrogen phosphate and dihydrogen potassium phosphate = BDH
Glycine = (Merck)

Preparation of solutions and reagents.

Y = YNB (10X) [Difco]: 134g of YNB was dissolved in 1L of water and filter sterilized, and stored at +4^{O}C. The container was wrapped in an aluminium foil.

B = Biotin (Sigma): 500X B (0.02%) 20mg of Biotin (Sigma) were dissolved in 100 ml deionised double distilled (dd) water, filter sterilized and stored at 4^{O}C.

Preparation of Cur solution.
Cur (Sigma) was dissolved using ice cold 0.5 M sodium hydroxide solution and the final concentration was made to 2mg / ml (Q-sense study = 2mg/ ml; Intranasal administration = saturated and 5 mg / ml) using ice cold PBS (0.154 M; pH). The solution was prepared in the dark and the falcon tubes used for making the solution were covered with an aluminium foil to avoid photo degradation of Cur.
D = Dextrose (Merck) = 10X (20%): 100g dextrose was dissolved in 500ml, filter sterilized, and stored at RT

H = Histidine (Sigma): (100X) 0.4% (L-Histidine) = 40 mg in 100 ml of dd water heated to 45^{O}C, filter sterilized, and store at 4^{O}C.

M = Methanol: (5%) = 5 ml methanol was diluted to 100 ml with dd water; filter sterilized (Millex GP 0.22μm, Millipore Express PES membrane) and stored at 4^{O}C.

G = Glycerol (10X): = 10% = 100 ml glycerol was diluted to 1 L, autoclaved and stored at 4^{O}C.

P = Potassium phosphate buffer: 132 ml of 1M K_2HPO_4 + 832 ml of KH_2PO_4 were mixed, and the pH of the solution was adjusted to 6. The solution was then autoclaved, and stored at RT.

YPD plates = 2.5 g of yeast extract (Difco / Merck) and 5 g of peptone (Merck) was dissolved in 200 ml dd water and 5g of agar was added to this. The volume was made 225 ml with water. To this 25 ml of 10 X **D** was added after autoclaving for 20 min. the plates were poured in the hood. Alternatively, it was also prepared from YPD-Agar (Merck) with the similar composition of yeast extract, peptone, dextrose and Agar.

Minimal methanol + histidine [Sigma] (MMH) plates: 200 ml of water was autoclaved and allowed to cool down to 60^{O}C in water bath. To this, 25 ml of **Y,** 0.5 ml of **B**, and 2.5 ml of **H,** and 1.5 g of agar were added. After mixing, the plates were immediately poured, and stored at 4^{O}C till further use.

Buffered Glycerol-complex Medium (BMGY): 10g of yeast extract, and 20g of peptone were dissolved in 700 ml of water, which was then autoclaved, and cooled to room temperature. To this, 100 ml of **Y**, 100 ml of **G**, 100 ml of **P**, and 2 ml of **B** of the stock solutions were added to make the volume to 1 L. The solution was kept at 4^{O}C till further use.

Buffered Methanol-complex Medium (BMMY): For preparing BMMY, the same procedure that was used for preparing BMGY was followed, but glycerol was replaced by 100 ml of 0.5 % methanol.

Preparation of solutions and reagents for SDS-PAGE analysis: (Ref Sambrook)

Acrylamide mix: 29 g of acrylamide and 0.8 g of bisacrylamide were dissolved in water to make the volume of 100 ml. The solution was filter sterilized, and stored at
4 ^{O}C as a stock solution.

Tris-Cl resolving gel buffer [Merck] (1.5 M): 36.330 g of Tris-base in 150 ml of warm deionised water. Concentrated HCL was added to make pH of 6.8. The volume was adjusted to 200 ml.

Tris-Cl stacking gel buffer: 6.055 g of Tris-base [Merck]was dissolved in 40 ml of warm deionised water, and conc. HCl was added to make the pH of 6.8.The final volume was adjusted to 50 ml.

SDS [Fluka – sigma] (10%): 10g dissolved in 80 g of water (heat at 60^{O}C), and the volume was made upto 100 ml. Alternatively, Extrapure10% SDS solution by GiBco BRL was also used.

Ammonium persulfate [Sigma] (APS): 10 % ammonium persulphate solution was prepared freshly before running SDS-PAGE gel by dissolving 25 to 50 mg in 250 to 500 µl of dd water.

Methanol[koch-light ltd / BDH]: Water: Glacial acetic acid [BDH] (GAA) solution (MWGAA): 500 ml of methanol, 400 ml of methanol and 100 ml of GAA were combined to give 1 L of MWGAA.

Coomassie Brilliant Blue solution: This solution was prepared by dissolving 0.25 g of Coomassie Brilliant Blue was dissolved in 100 ml of MWGAA.

Table S2.1. The compositions of the resolving and running gels for SDS-PAGE.

Solutions / Reagents	Resolving gel	Stacking gel
dd water	1.9 ml	1.9 ml
30 % Acrylamide mix	1.7 ml	1.7 ml
Tris-Cl resolving gel buffer	1.3 ml	0.33 ml
Tris-Cl stacking gel buffer	--------	0.25 ml
SDS (10%)	50 µl	20 µl
APS	50 µl	20 µl
TEMED [Merck]	2 µl	2 µl

Table S3.1. Processing of brain tissue.

Sr.	Treatment	Time	Temperature
1	96% Ethanol	10	31 - 40
2	96% Ethanol	10	31 - 40
3	Absolute alcohol	15	31 - 40
4	Absolute alcohol	15	31 - 40
5	Absolute alcohol	15	31 - 40
6	Absolute alcohol	15	31 - 40
7	Xylol	15	31 - 40
8	Xylol	15	31 - 40
9	Wax	20	60
10	Wax	20	60
11	Wax	25	60
12	Wax	25	60

Brain tissue processing: *dehydration in alcohol at different concentrations, xylol treatment and processing in wax (Sr = serial number, time = time of exposure in minutes, and temperature in* ^{O}C

References.

(Note: "T" after year in references stands for Thesis publication.)

Aberl, F. et al., 1994. HIV serology using piezoelectric immunosensors. Sens. Actuat. B. 18-19:271-275.

AD facts and figures. This is a statistical abstract of U.S. data on Alzheimer's disease published by the Alzheimer's Association. (http://www.alz.org/national/documents/report_alzfactsfigures2008.pdf).

Afagh, A. et al. 1996. Localization and cell association of C1q in Alzheimer's disease brain. Exp. Neurol. 138:22-32.

Aggarwal, B.B. 2008. Prostate cancer and curcumin: Add spice to your life. Cancer Biol. Ther. *In press.*

Aisen, P.S. et al. 2000. A randomized controlled trial of prednisone in Alzheimer's disease. Alzheimer's disease cooperative study. Neurology 54: 588-593.

Aisen, P.S., J. Schmeidler and G.M. Pasinetti. 2002. Randomized pilot study of nimesulide treatment in Alzheimer's disease. Neurology 58: 1050-1054.

Aisen, P.S. et al. 2003. Effects of rofecoxib or naproxen vs placebo on Alzheimer disease progression: a randomized controlled trial. J. Am. Med. Assoc. 289: 2819-2826.

Alisky, J.M. 2007. The coming problem of HIV-associated Alzheimer's disease. Med. Hypotheses. 69:1140-1143.

Al-Mohanna, F., R. Parhar and G. J. Kotwal. 2001. Vaccinia virus complement control protein is capable of protecting xenoendothelial cells from antibody binding and killing by human complement and cytotoxic cells. Transplantation 71:796-801.

Alvarez, P., L. Wendelken and H. Eichenbaum. 2002. hippocampal formation lesions impair performance in an odor–odor association task independently of spatial context. Neurobiol. Learn. Memory. 78: 470-476.

Anderson, J.B. et al. 2003. Vaccinia virus complement control protein inhibits hyperacute xenorejection in a guinea pig-to-rat heterotopic cervical cardiac xenograft model by blocking both xenoantibody binding and complement pathway activation. Transpl. Immunol. 11:129-35.

Andersson, J. et al. 2001. Binding of a model regulator of complement activation (RCA) to a biomaterial surface: surface bound factor H inhibits complement activation. Biomaterials. 22:2435-2443.

Andersson, J. et al. 2002. C3 Adsorbed to a polymer surface can form an initiating alternative pathway convertase. J. Immunol. 168:5786-5791.

Andreas, P. et al. 2008. Native, amyloid fibrils and β-oligomers of the C-terminal domain of human prion protein display differential activation of complement and bind C1q, factor H and C4b-binding protein directly. Mol. Immunol. 45: 3213-3221.

Apostolski, S. 1994. Complement dependent cytotoxicity of sensory ganglion neurons mediated by the gp120 glycoprotein of HIV-1. Immunol. Invest. 23:47-52.

Arendash, G.W. et al. 2001. Progressive, age-related behavioral impairments in transgenic mice carrying both mutant amyloid precursor protein and presenilin-1 transgenes. Brain Res. 891:42-53.

A'vila, J. et al. 2004. Tau in neurodegenerative diseases: tau phosphorylation and assembly. Neurotox. Res. 6:477-482.

Axer, H. et al. 2008. Hereditary Alzheimer's disease with amyloid angiopathy caused by amyloid precursor protein locus. Nervenarzt. *In press.*

Bacskai, B. et al. 2001. Imaging of amyloid-beta deposits in brains of living mice permits direct observation of clearance of plaques with immunotherapy. Nat. Med. 7:369-372.

Bannister, L.H. and H.C. Dodson. 1992. Endocytic pathways in the olfactory and vomeronasal epithelia of the mouse: ultrastructure and uptake of tracers. Microsc. Res. Tech. 23: 128-141.

Bao, Xi. et al. 2008. Effect and mechanism of curcumin on learning and memory dysfunction induced by gp120 in rats. 24:328-331.

Barik, A., K. I. Priyadarsini and H. Mohan. 2003. Photophysical studies on binding of curcumin to bovine serum albumins. Photochem Photobiol. 77:597-603.

Barnes, C.A. 1988. Spatial learning and memory processes: the search for their neurobiological mechanisms in the rat. Trends Neurosci. 11:163-169.

Barnett, E.M., M.D. Cassell and S. Perlman. 1993. Two neurotropic viruses, herpes simplex virus type-1 and mouse hepatitis virus, spread along different neural pathways from the main olfactory bulb. Neuroscience 57:1007-1025.

Barnum, S.R. 1995. Complement biosynthesis in the central nervous system. Crit. Rev. Oral Biol. Med. 6:132-146.

Bertoglio, L.J. and A.P. Carobrez. 2002. Behavioral profile of rats submitted to session 1–session 2 in the elevated plus-maze during diurnal/nocturnal phases and under different illumination conditions. Behav. Brain Res. 132:135-143.

Bhattacharjee, A. et al. 2002. MMP-9 and EBA immunoreactivity after papaverine mediated opening of the blood brain barrier. Neuroreport. 13:32217-32221.

Blake, A.D. 2004. Dipyridamole is neuroprotective for cultured rat embryonic cortical neurons.

Biochem. Biophys. Res. Commun. 314:501-504.

Blennow, K., M.J. de Leon and H. Zetterberg. 2006. Alzheimer's disease. Lancet. 368:387-403.

Bonifati, D.M. and U. Kishore. 2007. Role of complement in neurodegeneration and neuroinflammation. Mol. Immunol. 44:999-1010.

Born, J. et al. 2002. Sniffing neuropeptides: a transnasal approach to the human brain. Nat. Neurosci. 5:514-516.

Bourque, S.L. et al. 2008. Perinatal Iron Deficiency Affects Locomotor Behavior and Water Maze Performance in Adult Male and Female Rats. J. Nutr. 138:931-937.

Bradford, A.A. 1976. A rapid sensitive method for the quantitation of microgram quantities of protein utilising the principle of protein-dye binding. Anal. Biochem. 72:248-254.

Brash, J. L., and T.A Horbett. *In* proteins at interfaces II, ACS symposium series 602. Eds. Brash J. L., Horbett, T. A., Washington DC, 1995.

Brecht, W.J. *et al.* 2004. Neuron-specific apolipoprotein E4 proteolysis is associated with increased tau phosphorylation in brains of transgenic mice. J. Neurosci. 24:2527-2534.

Brew, B.J. et al. 2006. Factors in AIDS dementiacomplex trial design: Results and lessons from the abacavir trial. PLoS Clin Trials 2: e13. doi:10.1371/journal.pctr.0020013

Broadwell, R.D. and Balin, B.J. 1985. Endocytic and exocytic pathways of the neuronal secretory process and trans-synaptic transfer of wheat germ agglutinin-horseradish peroxidase *in vivo*. J. Comp. Neurol. 242:632-650.

Bruce-Keller, A.J. et al. 2000. Antiinflammatory effects of estrogen on microglial activation.

Endocrinology 141:3646-3656.

Bruder, C. 2003. HIV-1 induces complement factor C3 synthesis in astrocytes and neurons by modulation of promoter activity. Mol. Immunol. 40:949-961.

Bussiere, T. et al. 2004. Morphological characterisation of Thioflavine S-positive amyloid plaques in transgenic Alzheimer mice and effect of passive Ab immunotherapy on their clearance. Am. J. Pathol. 65:987-995.

Capsoni, S., S. Giannota and A. Cattaneo. 2002. Nerve growth factor and galantamine ameliorate early signs of neurodegeneration in anti-nerve growth mice. Proc. Natl. Acad. Sci. USA. 99:12432-12437.

Carson, M.J., T. J. Cameron and B. Walter. 2006. The cellular response in neuroinflammation: The role of leukocytes, microglia and astrocytes in neuronal death and survival. Clin. Neurosci. Res. 6:237-245.

Caruso, F., D. N. Furlong and P. Kingshott. 1997. Characterization of Ferritin Adsorption onto Gold. J. Colloid Interface Sci. 186:129-140.

Chainani-Wu, N.J. 2003. Safety and anti-inflammatory activity of curcumin: a component of tumeric (*Curcuma longa*). Alt. Complement Med. 9:161-168.

Chiarugi, A. and M.A. Moskowitz. 2003. Poly(ADP-ribose) polymerase-1 activity promotes NF-kappaB driven transcription and microglial activation: implication for neurodegenerative disorders. J. Neurochem. 85:306-317.

Charneski, L. and P.N. Patel. Eculizumab in paroxysmal nocturnal haemoglobinuria. Drugs. 68:1341-1346.

Chen, C. and N.G. Bazan. 2005. Endogenous PGE2 regulates membrane excitability and synaptic transmission in hippocampal CA1 pyramidal neurons. J. Neurophysiol. 93:929-941.

Cimanga, K. et al. 1995. *In vitro* anticomplementary activity of constituents from Morinda morindoides. J. Nat. Prod. 58:372-378.

Cimanga, K. et al. 2003. Complement-Inhibiting Iridoids from Morinda morindoides. J. Nat. Prod. 66:97-102.

Chou, K.J. and M.D. Donovan. 1998. Lidocaine administration into the CNS following nasal and arterial delivery: a comparisonof local sampling and microdialysis technique. Int. J. Pharm. 171:53-61.

Chun, K.S. et al. 2003. Curcumin inhibits phorbol ester-induced expression of cyclooxygenase-2 in mouse skin through suppression of extracellular signal-regulated kinase activity and NF-κβ activation. Carcinogenesis 24:1515-1524.

Chow, H.S., Z. Chen and G. T. Matsuura. 1999. Direct transport of cocaine from the nasal cavity to the brain following intranasal administration in rats. J. Pharm. Sci. 88:754-758.

Consilvio, C. *et al.* 2004. Neuroinflammation, COX-2, and ALS-a dual role? Exp. Neurol. 187: 1-10.

Constantino, H.R. et al. 2007. Intranasal delivery: Physicochemical and therapeutic aspects. Int. J. Pharmaceutics 337:1-24.

Corder, E.H. et al. 1993. Gene dose of apolipoprotein E type 4 allele and the risk of Alzheimer's disease in late onset families. Science 261: 921-923.

Crawley, L.N. and F.K. Goodwin. 1980. Preliminary report of a simple animal behavior model for the anxiolytic effects of benzodiazepines. Pharmacol Biochem Behav 13: 167-170.

Cutler, P. *et al.* 1997. The recognition of haemoglobin by antibodies raised for the immunoassay of β-amyloid. FEBS Letters 412:341-345.

Dahlin, M. *et al.* 2000. Transfer of dopamine in the olfactory pathway following nasal administration in mice. Pharm Res. 17: 737-742.

Dahlin, M., B. Jansson and E Bjork. 2001. Levels of dopamine in blood and brain following nasal administration to rats. Eur. J. Pharm. Sci. 14:75-80.

Daly, J. and G.J. Kotwal. 1998. Pro-inflammatory complement activation by the Aβ peptide of alzheimer's disease is biologically significant and can be blocked by vaccinia virus complement control protein. Neurobiol. Aging. 19:619-627.

Datta, P.K. and J. Rappaport. 2006. HIV and complement: hijacking an immune defense. Biomed. Pharmacotherapy 60:561-568.

Davoust, N. et al. 1999. Central nervous system-targeted expression of the complement inhibitor sCrry prevents experimental allergic encephalomyelitis. J. Immunol. 163: 6551-6556.

De Felice, F.G. et al. 2007. Aβ oligomers induce neuronal oxidative stress through an N-methyl-D-aspartate receptor-dependent mechanism that is blocked by the Alzheimer drug memantine. J. Biol. Chem. 282:11590-11601.

Depboylu, C. *et al.* 2005. Increase of C1q biosynthesis in brain microglia and macrophages during lentivirus infection in the rhesus macaque is sensitive to antiretroviral treatment with 6-chloro-2′,3′-dideoxyguanosine. Neurobiol. Dis. 20:12-26.

De Simoni, M.G. et al. 2004. The powerful neuroprotective action of C1-inhibitor on brain ischemia-reperfusion injury does not require C1q. Am. J. Pathol. 164:1857-1863.

De Souza Silva, M.A. et al. 1997. Intranasal administration of dopaminergic agonsists L-DOPA, amphetamine, and cocaine increases dopamine activity in the neostriatum: a microdialysis study in the rat. J. Neurochem. 68:233-239.

Earl, P.L. and B. Moss. 1989. Vaccinia virus; in Genetics maps (ed.) S J O'Brian (New York: Cold Spring Harbor Lab), 5:138-148.

Ellis, R.J. 2007. Evidence-based treatment for HIV-associated dementia and cognitive impairment: Why so little? PLOS Clin. Trials. e15: 1-3 (www.plosclinicaltrials.org).

Ewers, M. et al. 2006. Associative and motor learning in 12-month-old transgenic APP + PS1 mice. Neurobiol. Aging 27:1118-1128.

Fan, R., K. DeFilippis, and W. Van Nostrand. 2007. Induction of complement proteins in a mouse model for cerebral microvascular Aβ deposition. J. Neuroinflammation. 4:22 (doi: 10.1073/pnas.0509695103).

Ferri, C.P. et al. 2005. Global prevalence of dementia: a Delphi consensus study. Lancet 366: 2112-2117.

Firat, Y. et al. 2008. Effect of Intranasal Estrogen on Vocal Quality. J Voice. *In press.*

Floyd, R.A. 2002. Nitrones as neuroprotectants and antiaging drugs. Ann. NY. Acad. Sci. 959:321-329.

Fonseca, M.I. et al. 2004. Absence of C1q Leads to less neuropathology in transgenic mouse models of Alzheimer's Disease. J. Neurosci. 24:6457-6465.

Frankmann, S.P. 1986. A technique for repeated sampling of CSF from the anesthetized rat. Physiol. and Behavior, 37: 489-493.

Gafner, S. et al. 2004. Biologic evaluation of curcumin and structural derivatives in cancer chemoprevention model systems. Phytochemistry 65:2849-2859.

Gaillard, P. et al. 2003. Pharmacological investigations on lipopolysaccharide-induced permeability changes in the blood brain barrier in vitro. Microvasc. Res. 65:24-31.

Galvan, V. et al. 2006. Reversal of Alzheimer's-like pathology and behavior in human APP transgenic mice by mutation of Asp664. Proc. Nat. Sci. Acad. 103:7130-7135.

Ganesh,V.K. et al. 2004. Structure of vaccinia complement protein in complex with heparin and potential implications for complement regulation. Proc. Nat. Acad. Sci. 101:8924-8929.

Garcia-Alloza, M. et al. 2006. Characterization of amyloid deposition in the APPswe/PS1dE9 mouse model of Alzheimer disease. Neurobiol. Disease 24:516-524.

Geetha, T. and P. Varalakshmi. 1999. Anticomplement activity of triterpenes from *Crataeva nurvala* stem bark in adjuvant arthritis in rats. Gen. Pharmacol. 32:495-497.

Ghafouri, M. et al. 2006. HIV-1 associated dementia: symptoms and causes. Retrovirology 19:3:28 (doi: 10.1186/1742-4690-3-28).

Ghebremariam, Y.T., et al. 2005. Humanized recombinant vaccinia virus complement control protein (hrVCP) with three amino acid changes, H98Y, E102K, and E120K creating an additional putative heparin binding site, is 100-fold more active than rVCP in blocking both classical and alternative complement pathways. Ann. NY. Acad. Sci. 1056:113-122.

Gibb, S.J., Wolff, M. and J. C. Dalrymple-Alford. 2006. Odour–place paired-associate learning and limbic thalamus: Comparison of anterior, lateral and medial thalamic lesions Behav. Brain Res. 172:155-168.

Gilbert, P.E. and R.P. Kesner. 2002. Role of rodent hippocampus in paired-associate learning involving associations between a stimulus and a spatial location. Behav. Neurosci. 116:63-71.

Goel, A., S. Jhurani and B.B. Aggarwal. 2008a.Multi-targeted therapy by curcumin: how spicy is it? Mol Nutr Food Res. *In press.*

Goel, A., A.B. Kunnumakkara and B.B. Aggarwal. 2008b. Curcumin as "Curecumin": from kitchen to clinic. Biochem Pharmacol. 75:787-809.
Gonzalez-Deniselle, M.C. et al. 2002. Basis of progesterone protection in spinal cord neurodegeneration. J. Steroid Biochem. Mol. Biol. 83:199-209.

Good, M.A. and G. Hale. 2007a. The "Swedish" mutation of the amyloid precursor protein (APPswe) dissociates components of object-location memory in aged Tg2576 mice. Behav Neurosci. 121:1180-1191.

Good, M.A., G. Hale and V. Staal. 2007b. Impaired "episodic-like" object memory in adult APPswe transgenic mice. Behav. Neurosci. 121:443-448.

Goodkin, K. et al. 1997. Subtle neuropsychological impairment and minor cognitive-motor disorder in HIV-1 infection. Neuroradiological, neurophysiological, neuroimmunological, and virological orrelates. Neuroimaging Clin. N. Am. 1997:561-579.

Goodkin, K.*et al.* 1998. Cocaine abuse and HIV-1 infection: Epidemiology and neuropathogenesis. J. Neuroimmunol. 83:88-101.

Griffin, W.S. et al. 1995. Interleukin-1 expression in different plaque types in Alzheimer's disease: significance in plaque evolution. J. Neuropathol. Exp. Neurol. 54:276-281.

Gutman, C.R. et al. 1997. Apolipoprotein E binds to and potentiates the biological activity of ciliary neurotrophic factor. J. Neurosci. 17:6114-6121.

Gozes, I. 2001. Neuroprotective peptide drug delivery and development: potential new therapeutics. Trends Neurosci. 24:700-705.

Gruart, A. *et al.* 2008. Aged wild-type and APP, PS1, and APP+PS1 mice present similar deficits in associative learning and synaptic plasticity independent of amyloid load. Neurobiol Disease. 30:439-450.

Haddad, J.J. et al. 2004. Mitogen activated protein kinases and the evoultion of Alzheimer's: A revolutionary neurogenic axis for therapeutic intervention. Prog. Neurobiol.73:359-377.

Halim, N.D., A.W. Joseph and B.K. Lipska. 2005. A novel ELISA using PVDF microplates. J. Neurosci. Methods 143:163-168.

Hatcher, H. 2008. Curcumin: from ancient medicine to current clinical trials. Cell Mol. Life Sci. 65:1631-1652.

Handley, S.L. and S. Mithani 1984. Effects of alpha-adrenoceptor agonists and antagonists in a maze exploration model for 'fear-motivated' behavior. Naunyn Schmiedebergs Arch. Pharmacol. 327:1-5.

Hardy, J. 2006. A hundred years of Alzheimer's disease research. Neuron 52:3-13.

Harnett, J.J. et al. 2004. Phenolic thiazoles as novel orally-active neuroprotective agents. Bioorganic Medicinal Chem. Lett. 14:157-160.

Hicks, R.H. et al. 2002. Vaccinia virus complement control protein enhances functional recovery after traumatic brain injury. J. Neurotrauma 19:705-714.

Hilton, G.D. et al. 2004. Neuroprotective effects of estradiol in newborn female rat hippocampus. Brain Res. Dev. Brain Res. 150:191-198.

Himmler, A. et al. 1989. Tau consists of a set of proteins with repeated C-terminal microtubule-binding domains and variable N-terminal domains. Mol. Cell Biol. 9:1381-1388.

Hinkin, C.H. et al. 2001. Neuropsychiatric aspects of HIV infection among older adults. J. Clin. Epidemiol. 54:S44-S52.

Hinshelwood, J. et al. 1999. Identification of the C3b Binding Site in a Recombinant vWF-A Domain of Complement Factor B by Surface-enhanced Laser Desorption-ionisation Affinity Mass Spectrometry and Homology Modelling: Implications for the Activity of Factor B. J. Mol. Bio. 294:587-599.

Höök, F. *et al.* 1998a. Energy dissipation kinetics for protein and antibody-antigen adsorption under shear oscillation on a quartz crystal microbalance. Langmuir. 14:729-734.

Höök, F. *et al.* 1998b. Structural changes in hemoglobin during adsorption to solid surfaces: effects of pH, ionic strength, and ligand binding. Proc. Natl. Acad. Sci. USA. 95:12271-122276.

Huber, M. *et al.* 2006. Complement lysis activity in autologous plasma is associated with lower viral loads during the acute phase of HIV-1 infection. PLoS Med. 3: 441. doi:10.1371/journal.pmed.0030441

Huneycutt, B.S. et al. 1994. Distribution of vesicular stomatitis virus proteins in the brains of BALB/c mice following intranasal inoculation: an immunohistochemical analysis. Brain Res. 635:81-95.

Hussain, M.A. et al. 1997. Intranasal absorption of the platelet glycoprotein IIb/IIIa receptor antagonist, DMP 755, and the effect of anesthesia on nasal bioavailability. J. Pharm. Sci. 86:1358-1360.

Hussain, A.A. 1998. Intranasal drug delivery. Adv. Drug Deliv. Rev. 29:39-49.

Höök, F. 2004T. Development of a novel QCM technique for protein adsorption studies. Thesis. Chalmers University of Technology, Goetberg University, Goetberg, Sweden.

Ikeda, M. et al. 2002. Synergistic effect of cold mannitol and Na (+) / C(2+) exchange blocker on the blood brain barrier opening. Biochem. Biophys. Res. Commun. 291:669-674.

Illum, L. 2000. Transport of drugs from the nasal cavity to the central nervous system. Euro. J. Pharma. Sci. 11:1-18.

Isaacs, S.N. et al. 2003. Restoration of complement-enhanced neutralization of vaccinia virus virions by novel monoclonal antibodies raised against the vaccinia virus complement control protein. J Virol.77: 8256-8262.

Jansson, B. and E. Bjork. 2002. Visualisation of in vivo olfactory uptake and transfer using fluorescin dextran. J. Drug Target. 10:379-386.

Jansson, B.2004T. Models for the transfer of drugs from the nasal cavity to the central nervous system. Thesis. Comprehensive summaries of Uppsala Dessertations from the Faculty of Pharmacy, Uppsala, Sweden.

Jarrard, L.E. 1993. On the role of the hippocampus in learning and memory in the rat. Behav. Neural Biol. 60:9-26.

Jha, P. and G.J. Kotwal. 2003.Vaccinia complement control protein: multi-functional protein and a potential wonder drug. J. Biosci. 28:265-271.

Jha, P. et al. 2003. Prolonged retention of vaccinia virus complement control protein following ip injection: implications in blocking xenorejection. Transplant. Proceedings 35:3160-3162.

Jin, K. et al. 2003. Cerebral neurogenesis is induced by intranasal administration of growth factors. Ann Neurol. 53: 405-409.

Jobin, C. et al. 1999. Curcumin blocks cytokine-mediated NF-κB activation and proinflammatory gene expression by inhibiting inhibitory factor i-kb kinase activity. J. Immunol. 163:3474-3483.

Johnston, M. et al. 2004. Evidence of connections between cerebrospinal fluid and nasal lymphatic vessels in humans, non-human primates and other mammalian species. CSF Res. 1:2(doi:10.1186/1743-8454-1-2).

Johnston, M. et al. 2005. Subarachnoid injection of Microfil reveals connections between cerebrospinal fluid and nasal lymphatics in the non-human primate. Neuropathol. Appl. Neurobiol. 31:632-640.

Jones, G. J. et al. 2007. HIV-1 Vpr causes neuronal apoptosis and *in vivo* neurodegeneration. J. Neurosci. 27: 3703-3711.

Jongen, P.J. et al. 2000. Cerebrospinal fluid C3 and C4 indexes in immunological disorders of the central nervous system. Acta. Neurol. Scand. 101:116-21.

Kalaria, R.N. et al. 2008. Alzheimer's disease and vascular dementia in developing countries: prevalence, management, and risk factors. Lancet Neurol. 7:812-826.

Kamatou, G.P. 2005. The in vitro pharmacological activities and a chemical investigation of three South African Salvia species. J. Ethnopharmacol. 102:382-390.

Kaplan, M. 2002. Eculizumab (Alexion) (abstr). Curr. Opin. Invest. Drugs 3:1017-1023.

Kaya, E. et al. 2008. Acute effect of intranasal estrogen on cerebral and cerebellar perfusion in postmenopausal women. 59:72-82.

Karkos, J. 2004. Immunotherapy of Alzheimer's disease. Results of experimental investigations and treatment of perspectives. Fortschritte der Neurologie-Psychiatrie. 72:204-219.

Katsumata, T. et al. 2003. Neuroprotective effect of NS-7, a novel Na and Ca channel blocker, in a focal ischemic model in the rat. Brain Res. 969:168-174.

Kawakami, F., Y. Shimoyama and K. Ohtsuki. 2003. Characterization of complement C3 as a glycyrrhizin (GL)-binding protein and the phosphorylation of C3alpha by CK-2, which is potently inhibited by GL and glycyrrhetinic acid in vitro. J. Biochem. 133:231-237.

Keeling, K.L. et al. 2000. Local neutrophil influx following lateral fluid percussion brain injury in rats is associated with accumulation of complement activation fragments of the third component (C3) of the complement system. J. Neuroimmunol. 105:20-30.

Kesner, R.P., G. Farnsworth and H. Kametani. 1991. Role of parietal cortex and hippocampus in representing spatial information. Cereb. Cortex 1:367-373.

Kesner, R.P., R.F. Berman and R. Tardif. 1992. Place and taste aversion learning: role of basal forebrain, parietal cortex, and amygdala. Brain Res. Bull. 29:345-353.

King, M.E. et al.2006. Tau-dependent microtubule disassembly initiated by prefibrillar beta-amyloid. J. Cell Biol. 175:541-546.

Kößlinger, C. et al. 1995. Comparison of the QCM and the SPR method for surface studies and immunological applications. Sens. Actuat. B24-25:107-112.

Kotwal, G.J. and B. Moss. 1988. Vaccinia virus encodes a secretory polypeptide structurally related to complement control proteins. Nature 335:176-178.

Kotwal, G.J. et al. 1990. Inhibition of the complement cascade by the major secretary protein of vaccinia virus. Science 250:827-830.

Kotwal, G.J. 1994. Purification of virokines using ultrafiltration. Am. Biotechnol. Lab. 12:76-77.

Kotwal, G.J. 2000. Poxviral mimicry of complement and chemokine system components: what's the end game? Immunol. Today 21:242-248.

Kotwal, G.J., D.K. Lahiri and R. Hicks. 2002. Potential intervention by vaccinia virus complement control protein of the signals contributing to the progression of central nervous system injury to Alzheimer's disease. Ann. NY. Acad. Sci. 973:317-322.

Kristensson, K. and Y. Olsson. 1971. Uptake of exogenous proteins in mouse olfactory cells. Acta Neuropathol (Berl). 19:145-154.

Kristin, K.H. et al. 2003. The neuronal nitric oxide synthase inhibitor, TRIM, as a neuroprotective agent: effects in models of cerebral ischaemia using histological and magnetic resonance imaging techniques. Brain Res. 993:42-53.

Kroes, B.H. et al. 1999. Inhibition of human complement by beta-glycyrrhetinic acid. Immunology 90:115-120.

Kubis, A.M. and M. Janusz. 2008. Alzheimer's disease: new prospects in therapy and applied experimental models. Postepy. Hig. Med. Dosw. 62:372-392.

Kunwar et al. 2006. Absorption and fluorescence studies of Curcumin bound to liposome and living cells. BARC Newsletter. 285:213-219.

Lahiri, D.K. *et al.* 2003a. A critical analysis of new molecular targets and strategies for drug developments in Alzheimer's disease. Curr. Drug Targets. 4: 97-112.

Lahiri, D.K. et al. 2003b. Role of cytokines in the gene expression of amyloid β-protein precursor: identification of a 5′-UTR-binding nuclear factor and its implications in Alzheimer's disease. J. Alz. Dis. 5: 81-90.

Lalonde, R., H.D. Kim and K. Fukuchi. 2004. Exploratory activity, anxiety, and motor coordination in bigenic APPswe + PS1/DeltaE9 mice. Neurosci. Lett. 369:156-161.

Laskowitz, D.T. et al. 1997. Apolipoprotein E suppresses glial cell secretion of TNFa. J. Neuroimmunol. 76: 70-74.

Le, G.T., G. Abbenante and D.P. Fairlie. 2007. Profiling the enzymatic properties and inhibition of human complement factor B. J. Biol Chem. 282:34809-34816.

Li, J. et al. 2003. Peroxynitrite induces apoptosis in canine cerebral vascular muscle cells: possible relation to neurodegenerative diseases and strokes. Neurosci. Lett. 350:173-177.

Lindahl, U. 2007. Heparan sulfate-protein interactions--a concept for drug design? Thromb. Haemost. 98:109-115.

Liszewski, M.K. et al. 2006. Structure and regulatory profile of the monkeypox inhibitor of complement: comparison to homologs in vaccinia and variola and evidence for dimer formation. J. Immunol. 176:3725-3734.

Liu, X.F. et al. 2001. Intranasal administration of insulin-like growth factor-I bypasses the blood-brain barrier and protects against focal cerebral ischemic damage. J. Neurol. Sci. 187:91-97.

Liu, L. et al. 2002. Effects of fimbria-fornix lesion and amyloid pathology on spatial learning and memory in transgenic APP+PS1 mice. Behav. Brain Res. 134:433-45.

Loftus, L.T. et al. 2006. *In vivo* protein transduction to the CNS. Neuroscience 139:1061-1067.

Lyncha, J.R. et al. 2001. Apolipoprotein E modulates glial activation and the endogenous central nervous system inflammatory response. J. Neuroimmunol. 114:107-113.

Mactutus, C.F. and R.M. Booze. 1994. Accuracy of spatial navigation: The role of platform and tank size. Soc. Neurosci. Abst. 20:1014.

Mahley, R.W. 1996. Heparan sulfate proteoglycan/low density lipoprotein receptor-related protein pathway involved in type III hyperlipoproteinemia and Alzheimer's disease. Isr. J. Med. Sci. 32:414-429.

Mahley, R.W. and Z.S. Ji. 1999. Remnant lipoprotein metabolism: Key pathways involving cell-surface heparan sulfate proteoglycans and apolipoprotein E. J. Lipid Res. 40:1-16.
Makrides, S.C. 1998. Therapeutic inhibition of the complement system. Pharmacol. Rev. 50: 59-87.

Martinez, R.C.R. et al. 2007. Thermal stress decreases general motor activity of rats in the elevated plus-maze but does not alter aversion to the open arms. Beha. Brain Res. 182:135-139.

Matsuoka, Y. et al. 2001. Inflammatory responses to amyloidosis in a transgenic mouse model of Alzheimer's disease. Am J Pathol. 2001 158:1345-1354.

May, L.A. et al. 2005. Detection and quantitation of curcumin in mouse lung cell cultures by matrix-assisted laser desorption ionization time of flight mass spectrometry. Anal. Biochem. 337:62-69.

McArthur, J.C. 2004. HIV dementia: an evolving disease. J. Neuroimmunol. 157:3-10.

McGeer, P.L. and E.G. McGeer. 1998. Glial cell reactions in neurodegenerative diseases: pathophysiology and therapeutic interventions. Alzh. Dis. Assoc. Disord. 2: S1-S6.

McGeer, P.L. and E.G. McGeer. 2003. Inflammatory processes in Alzheimer's disease. Prog. Neuro-Psychopharmacol. Biol. Psychiat. 27: 741-749.

McKenzie, R. et al. 1992. Regulation of complement activity by vaccinia virus complement-control protein. J. Infect. Dis. 166:1245-1250.

Meilandt, W.J. et al. 2008. Enkephalin elevations contribute to neuronal and behavioral impairments in a transgenic mouse model of Alzheimer's disease.
J Neurosci. 28:5007-5017.

Middei, S. *et al.* 2006. Progressive cognitive decline in a transgenic mouse model of Alzheimer's disease overexpressing mutant hAPPswe. Genes Brain Behav. 3:249-256.

Minghetti, L. 2004. Cyclooxygenase-2 (COX-2) in inflammatory and degenerative brain diseases. J. Neuropathol. Exp. Neurol. 63: 901-910.

Mizuno, T. et al. 2004. Neuroprotective role of phosphodiesterase inhibitor ibudilast on neuronal cell death induced by activated microglia. Neuropharmacology 46: 404−411.

McArthur, J.C. *et al.* 1993. Dementia in AIDS patients: incidence and risk factors. Neurology 43, 2245-2252.

Minagar, A. et al. 2004. HIV-associated dementia, Alzheimer's disease, multiple sclerosis, and schizophrenia: gene expression review J. Neurol. Sci. 224: 3 -17.

Melov, S. *et al.* 2007. Mitochondrial oxidative stress causes hyperphosphorylation of tau. PLoS one. 2:e536 (doi: 10.1371/journal.pone.0000536).

Min, B.S. et al. 2003. Anti-complement activity of constituents from the stem-bark of Juglans mandshurica. Biol. Pharm. Bull. 26:1042-1044.

Mori, I. et al. 2005. The vomeronasal chemosensory system as a route of neuroinvasion by herpes simplex virus. Virology 334:51-58.

Mukherjee, P. and G.M. Pasinetti. 2000. The role of complement anaphylatoxin C5a in neurodegeneration: implications in Alzheimer's disease. J. Neuroimmunol. 105:124-130.

Mukherjee, P. & G.M. Pasinetti. 2001. Complement anaphylatoxin C5a neuroprotects through mitogen-activated protein kinase-dependent inhibition of caspase 3. J. Neurochem. 77: 43-49.

Mukherjee, P., S. Thomas and G. M. Pasinetti 2008. Complement anaphylatoxin C5a neuroprotects through regulation of glutamate receptor subunit 2 in vitro and *in vivo.* J. Neuroinflammation. 29:5-5.

Mukhopadhyay, A. et al. 1982. Anti-inflammatory and irritant activities of curcumin analogues in rats (abstr). Ag. Actions 12:508-515.

Muller-Eberhard, H.J. 1988. Molecular organisation and function of the complement system. Annu. Rev. Biochem. 57: 321−327.

Murthy, K.H.M. et al. 2001. Crystal structure of a complement control protein that regulates both pathways of complement activation and binds heparan sulfate proteoglycans; Cell 104 301-311.

Nath, A. and J. McArthur. 2005. (Epidemiology of HIV dementia: http://hiv.neuro.jhmi.edu/cutaneous/publications/AAN-HIVD2005.pdf

Nicholl, D.S. et al. 2001. In vitro studies on the immunomodulatory effects of extracts of Osbeckia aspera. J. Ethnopharmacol. 78:39-44.

Nixon, R.A. 2007. Autophagy, amyloidogenesis and Alzheimer disease. J. Cell Sci. 120:4081-4091.

Nores, M.M. et al. 1997. Immunomodulatory activities of Cedrela lilloi and Trichilia elegans aqueous leaf extracts. J. Ethnopharmacol. 55:99-106.

Ogawa, S. et al. 1979. Colorimetric determination of boric acid in prawns, shrimp, and salted jelly fish by chelate extraction with 2-ethyl-1,3-hexanediol. J Assoc Off Anal Chem. 62:610-614.

Ohl, F. 2003. Testing for anxiety. Clin. Neurosci. Res. 3:233-238.

Ohl, F. et al. 2002. Cognitive performance in rats differing in their inborn anxiety. Behav Neurosci 116: 464-471.

Ohl, F. et al. 2003. Impact of high and low anxiety on cognitive performance in a modified hole board test in inbred mice strains C57BL/6 and DBA/2. Eur. J. Neurosci.17: 128-36.

Osaka, H. et al. 1999. Complement-derived anaphylatoxin C5a protects against glutamate-mediated neurotoxicity. Cell Biochem. 73:303-311.

O'Callaghan, P. et al. 2008. Heparan sulphate accumulation with Aβ deposits in Alzheimer's disease and Tg2576 mice is contributed by glial cells. Brain Pathol. *In press.*

Oshima, K., H. Uchikado and D.W. Dickson. 2008. Perivascular neuritic dystrophy associated with cerebral amyloid angiopathy in Alzheimer's disease. Int J Clin Exp Pathol. 1: 403-408.

Paxinos, G. and C. Watson. 1982. The rat brain in stereotaxic coordinates, 2nd Ed by, Academic press, Harcourt Brace Jovanovich publishers.

Peake, P.W. et al. 1991. The inhibitory effect of rosmarinic acid on complement involves the C5 convertase (abstr). Int. J. Immunopharmacol. 13: 853–857.

Pérez, M. et al. 2008. Phosphorylated tau in neuritic plaques of APP(sw)/Tau (vlw) transgenic mice and Alzheimer disease.*In press.*

Pellow, S. et al. 1985. Validation of open:closed arm entries in an elevated plus-maze as a measure of anxiety in the rat. J Neurosci Methods. 14: 149-167.

Phillips, R.G. and J.E. LeDoux. 1994. Lesions of the dorsal hippocampal formation interfere with background but not foreground contextual fear conditioning. Learn Mem. 1:34-44.

Phillis, J.W., L. A. Horrocks and A.A. Farooqui. 2006. Cyclooxygenases, lipoxygenases, and epoxygenases in CNS: their role and involvement in neurological disorders.
Brain Res Reviews 52:201-243.

Pieroni, A. et al. 2000. Studies on anti-complementary activity of extracts and isolated flavones from Ligustrum vulgare and *Phillyrea latifolia* leaves (Oleaceae). J. Ethnopharmacol. 70: 213-217.

Pillay, N.S., L.A. Kellaway and G.J. Kotwal. 2005. Administration of vaccinia virus complement control protein shows significant cognitive improvement in a mild injury model. Ann. NY. Acad. Sci. 1056:450-461.

Pillay, N.S. 2006T. An investigation of the in vivo role of vaccinia virus complement control protein in head injury and Alzheimer's Disease. Thesis. University of Cape Town, South Africa.

Pillay, N.S., L.A. Kellaway and G. J. Kotwal. 2007. Vaccinia virus complement control protein significantly improves sensorimotor function recovery after severe head trauma. Brain Res.1153:158-165.

Pillay, N.S., L.A. Kellaway and G.J. Kotwal. 2008. Early detection of memory deficits and memory improvement with vaccinia virus complement control protein in an Alzheimer's disease model. Behav Brain Res. 192:173-177.

Priller, C. et al. 2006. Synapse formation and function is modulated by the amyloid precursor protein. J. Neurosci. 26:7212-7221.

Prince, M. 1997. The need for research on dementia in developing countries. Trop Med Int Health 2:993-1000.

Prince, M. 2000. Methodological issues in population-based research into dementia in developing countries. A position paper from the 10/66 Dementia Research Group. Int. J. Geriatr. Psychiatry. 15: 21-30.

Prince, M. 2006. Epidemiology of dementia. Psychiatry. 6:488-490.

Pryzdial, E.L. and D.E. Isenman. 1986. A reexamination of the role of magnesium in the human alternative pathway of complement. Mol. Immunol. 23: 87–96.

Puoliväli, J. et al. 2002. Hippocampal Aβ-42 levels correlate with spatial memory deficit in APP and PS1 double transgenic mice. 9:339-347.

Quidel corporation: www.quidel.com

Ramsden, J.J. 1993. Experimental Methods for Investigating Protein Adsorption Kinetics at Surface. Quart. Rev. Biophysics. 27: 41-105.

Reichman, W.E. 2000. Alzheimer's disease: clinical treatment options. Am. J. Manag. Care 6: S1125-S1132 [discussion: S1133-S1138].

Reines, S. A. et al. 2004. Rofecoxib: no effect on Alzheimer's disease in a 1-year, randomized, blinded, controlled study. Neurology 62: 66-71.

Reiserer R.S. *et al.* 2007. Impaired spatial learning in the APPSwe + PSEN1DeltaE9 bigenic mouse model of Alzheimer's disease. Genes Brain Behav. 6:54-65.

Rempel, H.C. and L. Pulliam. 2005. HIV-1 Tat inhibits neprilysin and elevates amyloid beta. AIDS. 19:127-135.

Reynolds, D.N. et al. 2000. Heparin binding activity of vaccinia virus complement control protein confers additional properties of uptake by mast cells and attachment to endothelial cells. *In* Advances in animal virology. ed.S Jameel (Villarreal: Science Publishers):337-342.

Reynolds, D.N. et al. 2003. Vaccinia virus complement control protein modulates inflammation following spinal cord injury. Ann N Y Acad Sci. 1010:534-539.

Reynolds, D.N. et al. 2004. Vaccinia virus complement control protein reduces inflammation and improves spinal cord integrity following spinal cord injury. Ann N Y Acad Sci. 1035:165-178.

Robertson, K. *et al.* 2008. Second assessment of NeuroAIDS in Africa. J. Neurovirol. 14: 89-101. (DOI: 10.1080/13550280701829793).

Rodahl, M., F. Höök and B. Kasemo. 1996. QCM Operation in Liquids: An Explanation of Measured Variations in Frequency and Q Factor with Liquid Conductivity. Anal. Chem. 68: 2219 -2227.

Rodahl M. et al. 1997. Simultaneous frequency and dissipation factor QCM measurements of biomolecular adsorption and cell adhesion. Faraday Discuss. 107:229-246.

Rogers, J. et al. 1993. Clinical trial of indomethacin in Alzheimer's disease. Neurology 43: 1609-1611.

Rotilio, G., K. Aquilano, and M.R. Ciriolo. 2003. Interplay of Cu, Zn superoxide dismutase and nitric oxide synthase in neurodegenerative processes. IUBMB Life 55: 629−634.

Ruiz-Opazo, N. et al. 2004. Attenuated hippocampus-dependent learning and memory decline in transgenic TgAPPswe Fischer-344 rats. Mol Med. 10:36-44.

Sacktor, N. et al. 2001. Multicenter AIDS Cohort Study. HIV-associated neurologic disease incidence changes: Multicenter AIDS Cohort Study, 1990-1998. Neurology. 56:257-260.

Saenger, W. 1987. Structure and dynamics of water surrounding biomolecules. Annu. Rev. Biophys. Biophys. Chem. 1987. 16:93-114.

Saha, R.N. and K. Pahan. 2007. Differential regulation of Mn-superoxide dismutase in neurons and astroglia by HIV-1 gp120: Implications for HIV-associated dementia. Free Radic. Biol. Med. 42:1866-1878.

Sahoo, B.K., K.S. Ghosh and S. Dasgupta. 2008. Investigating the binding of curcumin derivatives to bovine serum albumin. Biophys. Chem. 132:81-88.

Sahu, A. and M.K. Pangburn. 1996. Investigation of mechanism-based inhibitors of complement targeting the activated thioester of human C3. Biochem. Pharmacol. 51:797-804.

Sahu, A. et al. 1998. Interaction of vaccinia virus complement control protein with human complement proteins: factor I-mediated degradation of C3b to iC3b1 inactivates the alternative complement pathway. J. Immunol. 160:5596-5604.

Sahu, A., N. Rawal and M.K. Pangburn. 1999. Inhibition of complement by covalent

attachment of rosmarinic acid to activated C3b. Biochem. Pharmacol. 57:1439-1446.

Sakane, T. et al. 1991. Transport of cephalexin to the cerebrospinal fluid directly from the nasal cavity. J. Pharm Pharmacol. 43:449-451.

Sakane, T. et al. 1995. Direct drug transport from the rat nasal cavity to the cerebrospinal fluid: the relation to the molecular weight of drugs. J. Pharm. Pharmacol. 47:379-381.

Sambrook, J. and D.W. Russel. 2001 Molecular Cloning: A laboratory manual, third edition, Cold Spring Harbor laboratory press, Cold spring Harbor, New York.

Sandur, S.K. et al. 2007a. Role of pro-oxidants and antioxidants in the anti-inflammatory and apoptotic effects of curcumin (diferuloylmethane). Free Radic. Biol. Med. 43:568-580.

Sandur, S.K. et al. 2007b. Curcumin, demethoxycurcumin, bisdemethoxycurcumin, tetrahydrocurcumin and turmerones differentially regulate anti-inflammatory and anti-proliferative responses through a ROS-independent mechanism. Carcinogenesis. 28:1765-1773.

Sarne, Y. and O. Keren. 2004. Are cannabinoid drugs neurotoxic or neuroprotective? Med. Hypotheses. 63: 187-192.

Savonenko, A.V. et al. 2003. Normal cognitive behavior in two distinct congenic lines of transgenic mice hyperexpresing APPswe, Neurobiol. Dis. 12:194–211.

Savonenko, A. et al. 2005. Neurobiology of Disease Episodic-like memory deficits in the APPswe/PS1dE9 mouse model of Alzheimer's disease: Relationships to B-amyloid deposition and neurotransmitter abnormalities 18:602-617.

Scharf, S. et al. 1999. A double-blind, placebo-controlled trial of diclofenac/misoprostol in Alzheimer's disease. Neurology 53:197-201.

Seignourel, P.J. et al. 2008. Anxiety in dementia: A critical review. Clin. Psycho. Review. *In press.*

Selkoe, D. 2001. Alzheimer's disease: genes, proteins, and therapy. Physiol Rev 81:741-766.

Shapshak, P. et al. 2006. Bioinformatics models in drug abuse and Neuro-AIDS: Using and developing databases. Bioinformation.1:86-88.

Shapshak, P. et al. 2008. Alzheimer's disease and HIV associated dementia related genes: I. location and function. Bioinformation. 2:348-357.

Shen, Y. et al. 2001. Complement activation by neurofibrillary tangles in Alzheimer's disease. Neurosci. Lett. 305:165-168.

Shen, Y. and S. Meri. 2003. Yin and Yang: Complement activation and regulation in Alzheimer's disease. Prog. Neurobiol. 70:463-472.

Sheng, W.S. et al. 2000. Activation of human microglial cells by HIV-1 gp41 and Tat proteins. Clin. Immunol. 96:243-251.

Sherwin, B.B. 2006. Estrogen and cognitive aging in women. Neuroscience 138:1021-1026.

Shishodia, S., M.M.Chaturvedi and B.B. Aggarwal. 2007. Role of curcumin in cancer therapy. Curr. Probl. Cancer 31:243-305.

Singhrao, S.K. et al. 2000. Spontaneous classical pathway activation and deficiency of membrane regulators render human neurons susceptible to complement lysis. Am. J. Pathol. **157:** 905-918.

Sjöberg, A.P. et al. 2008. Native, amyloid fibrils and beta-oligomers of the C-terminal domain of human prion protein display differential activation of complement and bind C1q, factor H and C4b-binding protein directly. Mol. Immunol. 45:3213-3221.

Smith, S.A. et al. 2000. Conserved surface-exposed K/R-X-K/R motifs and net positive charge on poxvirus complement control proteins serve as putative heparin binding sites and contribute to inhibition of molecular interactions with human endothelial cells: a novel mechanism for evasion of host defense. J. Virol. 74:5659-5666.

Smith, S.A. et al. 2002. Vaccinia virus complement control protein is monomeric, and retains structural and functional integrity after exposure to adverse conditions. Biochim. Biophys. Acta 1598:55-64.

Smith, et al. 2003. Mapping of regions within the vaccinia virus complement control protein involved in dose-dependent binding to key complement components and heparin using surface plasmon resonance. Biochim. Biophys. Acta 1650:30-39.

Snijman, P.W. et al. 2007. The antimutagenic activity of the major flavonoids of rooibos (*Aspalathus linearis*): Some dose-response effects on mutagen activation–flavonoid interactions. Mut. Res. 631:111-123.

Spear, G.T. et al. 1999. Alteration of complement protein levels after antiretroviral therapy in HIV-infected persons. AIDS Res. Hum. Retroviruses 15:1713-1715.

Speth, C. et al. 2002. Mechanism of human immunodeficiency virus-induced complement expression in astrocytes and neurons. J. Virol. 76:3179-3188.

Spielman, L. et al. 2002. Induction of the complement component C1qB in brain of transgenic mice with neuronal overexpression of human cyclooxygenase-2. Acta Neuropathol. 103:157-162.

Stahel, P. et al. 2001. Intrathecal levels of complement-derived soluble membrane attack complex (sC5b-9) correlate with blood-brain barrier dysfunction in patients with traumatic brain injury. J. Neurotrauma.18:773-781.

Stamer, K. et al. 2002. Tau blocks traffic of organelles, neurofilaments, and APP vesicles in neurons and enhances oxidative stress. J. Cell Biol. 156, 1051-1063.
Staub, N. C. 2002. Whole animal physiology redux. Am. J. Physiol. Lung Cell Mol. Physiol. 283:683-687.

Stoiber, H. et al. 2005. Complement-opsonized HIV: the free rider on its way to infection. Mol. Immunol. 42:153-160.

Strimpakos, A.S. and R.A. Sharma. 2008. Curcumin: preventive and therapeutic properties in laboratory studies and clinical trials. Antioxid. Redox Signal. 10:511-545.

Strittmatter,W.J. et al. 1993. Apolipoprotein E: high-avidity binding to beta-amyloid and increased frequency of type 4 allele in late-onset familial Alzheimer disease. Proc. Natl. Acad. Sci.U. S. A. 90: 1977-1981.

Strittmatter,W.J. et al. 1994. Isoform-specific interactions of apolipoprotein E with microtubule-associated protein tau: implications for Alzheimer disease. Proc. Natl. Acad. Sci. USA. 91:11183-11186.

Strohmeyer, R., Y. Shen and J. Rogers. 2000. Detection of complement alternative pathway mRNA and proteins in the Alzheimer's disease brain. Brain Res. Mol. Brain. Res. 81:7-18.

Tacnet-Delorme, P., S. Chevallier and G. J. Arlaud. 2001. β-amyloid fibrils activate the C1 complex of complement under physiological conditions: evidence for a binding site for Aβ on the C1q globular regions. J. Immunol. 167:6374-6381.

Takano, T. et al. 2003. Inhibition of cyclooxygenases reduces complement-induced glomerular epithelial cell injury and proteinuria in passive Heymann nephritis. J. Pharmacol. Exp. Ther. 305:240-249.

Talegaonkar, S. and P.R. Mishra. 2004. Intranasal delivery: An approach to bypass the blood brain barrier. Indian J. Pharmacol. 36:140-147.

Thal, D.R., W.S. Griffin and H. Braak. 2008. Parenchymal and vascular Abeta-deposition and its effects on the degeneration of neurons and cognition in Alzheimer's disease. J. Cell Mol. Med. *In press.*

Thompson, M., C.L. Arthur and G.K. Dhaliwal. 1986. Liquid-phase piezoelectric and acoustic transmission studies of interfacial immunochemistry. Anal. Chem.58:1206-1209.

Thorbjornsdottir, P. et al. 2005. Vaccinia virus complement control protein diminishes formation of atherosclerotic lesions: complement is centrally involved in atherosclerotic disease.
Ann. N.Y. Acad. Sci. 1056:1-15.

Thorne, R.G. and W.H. Frey (2nd). 2001. Delivery of neurotrophic factors to the central nervous system: pharmacokinetic considerations. Clin Pharmacokinet. 40:907-946.

Thorne, R.G. et al. 1995. Quantitative analysis of the olfactory pathway for drug delivery to the brain. Brain Res. 692:278-282.

Thorne, R.G. et al. 2004. Delivery of insulin-like growth factor-I to the rat brain and spinal cord along olfactory and trigeminal pathways following intranasal administration. Neuroscience. 2004:127:481-496.

Tiraboschi, P. et al. 2004. Impact of APOE genotype on neuropathologic and neurochemical markers of Alzheimer disease. Neurology 62:1977-1983.

Tomillero, A. and M.A. Moral. 2008a. Gateways to clinical trials. Methods Find Exp. Clin. Pharmacol. 30:231-251.

Tomillero, A. and M.A. Moral. 2008b. Gateways to clinical trials. Methods Find Exp. Clin. Pharmacol. 30:313-331.

Tonnesen, H.H., J. Karlsen and A. Mostad. 1982. Structural studies of curcuminoids. I. The crystal structure of curcumin. Acta Chem. Scand. B.36: 475–479.

Toyoda, K. et al. 2004. Free radical scavenger, edaravone, in stroke with internal carotid artery occlusion. J. Neurol. Sci. 221:11-17.

Turner, P. R.*et al.* 2003. Roles of amyloid precursor protein and its fragments in regulating neural activity, plasticity and memory. Prog. Neurobiol. 70:1-32.

van Beek, J. et al. 2001. Complement anaphylatoxin C3a is selectively protective against NMDA-induced neuronal cell death. Neuroreport 12:289-293.

van Beek, J., K. Elward and P. Gasque. 2003. Activation of the complement in the central nervous system: roles in neurodegeneration and neuroprotection. Ann. NY. Acad. Sci. 992:56-71.

van de Nes, J.A., R. Nafe and W. Schlote. 2008. Non-tau based neuronal degeneration in Alzheimer's disease-an immunocytochemical and quantitative study in the supragranular layers of the middle temporal neocortex. Brain Res. 1213:152-165.

van den Berg, M.P. et al. 2002. Serial cerebrospinal fluid sampling in a rat model to study drug uptake from the nasal cavity. J. Neurosci. Methods 116:99-107.

van Ginkel, F.W. et al. 2000. Cutting edge: the mucosal adjuvant cholera toxin redirects vaccine proteins into olfactory tissues. J. Immunol. 165:4778-4782.

van Marle, G. et al. 2004. Human immunodeficiency virus type 1 Nef protein mediates neural cell death: a neurotoxic role for IP-10. Virology 329:302-318.

Vehmas, A. et al. 2004. Amyloid precursor protein expression in circulating monocytes and brain macrophages from patients with HIV-associated cognitive impairment. J. Neuroimmunol. 157:99-110.

Vorhees, C. and M. Williams. 2006. Morris water maze: procedures for assessing spatial and related forms of learning and memory. Nat. Protocols. 1:848-858.

Vyas, T.K. et al. 2005. Intranasal drug delivery for brain targeting. Curr. Drug Deliv. 2:165-175.

Wade, L.G. 1995. Additions and condensations of enols and enolate ions. In Organic Chemistry. B.M. Cappuccio, Ed. :1079. Prentice Hall, Inc. A Simon & Schuster Company. New Jersey.

Walf, A.A. and C.A. Frye. 2002. The use of the elevated plus maze as an assay of anxiety-related behavior in rodents. Nature 416:535-539.

Walsh, D.M. et al. 2002. Naturally secreted oligomers of amyloid protein potently inhibit hippocampal long-term potentiation *in vivo.* Acta Neuropathol. 103: 157-162.

Wang, F. et al. 2003. Profiles of methotrexate in blood and CSF following intranasal and intravenous administration of rats. Int. J. Pharm. 263:1-7.

Wang, F. et al. 2006. The sensitive fluorimetric method for the determination of curcumin using the enhancement of mixed micelle. J. Fluoresc. 16:53-59.

Ward, M.D. and D.A. Buttry. 1990. In situ interfacial mass detection with piezoelectric transducers. Science 249:1000-1007.

Webster, S., C. Glabe and J. Rogers. 1995. Multivalent binding of complement protein C1q to the amyloid beta-peptide (A beta) promotes the nucleation phase of Aβ aggregation. Biochem. Biophys. Res. Commun. 217:869-875.

Weisgraber, K.H., A.D. Roses and W.J. Strittmatter. 1994. The role of apolipoprotein E in the nervous system. Curr. Opin. Lipidol. 5:110-116.

Westin, U. et al. 2005. Transfer of morphine along the olfactory pathway to the central nervous system after nasal administration to rodents. Eur. J. Pharm. Sci. 24:565-573.

Westin, U.E. et al. 2006. Direct nose-to-brain transfer of morphine after nasal administration to rats. Pharm. Res. 23:565-572.

Williams, M.T., M.S. Moran and C.V. Vorhees. 2004. Behavioral and growth effects induced by low dose methamphetamine administration during the neonatal period in rats. Int. J. Dev. Neurosci. 22:273-283.

Williamson, R. et al. 2002. Rapid tyrosine phosphorylation of neuronal proteins including tau and focal adhesion kinase in response to amyloid-beta peptide exposure: involvement of Src family protein kinases. J. Neurosci. 22:10-20.

Wilson, M.A. and L. Junor. 2008. The Role of Amygdalar Mu-Opioid Receptors in Anxiety-Related Responses in Two Rat models. Neuropsychopharmacol. *In press*.

Wimo, A. et al. 2003. The magnitude of dementia occurrence in the world. Alz. Dis. Assoc. Disord. 17: 63-67.

Wong, M.H. et al. 2007. Frequency of and risk factors for HIV dementia in an HIV clinic in sub-Saharan Africa. Neurology 68:350-355.

Wyss-Coray, T. et al. 2002. Prominent neurodegeneration and increased plaque formation in complement-inhibited Alzheimer's mice. 99:10837-10842.

Xu, Y., S.V. Narayana and J.E. Volanakis. 2001. Structural biology of the alternative pathway convertase. Immunol. Rev. 180: 123-135.

Yang, F. et al. 2005. Curcumin inhibits formation of amyloid {beta} oligomers and fibrils, binds plaques, and reduces amyloid in vivo. J. Biol. Chem. 280:5892-5901.

Yasojima, K. *et al.* 1999. Up-regulated production and activation of the complement system in Alzheimer's disease brain. Am. J. Pathol. 154:927-936.

Yilmaz, G. *et al.* 2000. Intranasal budesonide spray as an adjunct to oral antibiotic therapy for acute sinusitis in children. Eur. Arch. Otorhinolaryngol. 257:256-259.

Yoshida, M. et al. 1989. Determination of boric acid in biological materials by curcuma paper. Nihon Hoigaku Zasshi. 43:497-501. [Japanese; Pubmed abstract]

Yoshida, M., T. Watabiki and N. Ishida. 1989. Spectrophotometric determination of boric acid by the curcumin method. Nihon Hoigaku Zasshi. 43:490-496. [Japanese; Pubmed abstract]

Zanjani, H. et al. 2005. Complement activation in very early Alzheimer disease. Alzheimer Dis. Assoc. Disord. 19:55-66.

Zetterberg, M. et al. 2008. Association of complement factor H Y402H gene polymorphism with Alzheimer's disease. Am. J. Med. Genet. B. Neuropsychiatr. Genet. 147B:720-726.

Zhou, J. et al. 2008. Complement C3 and C4 expression in C1q sufficient and deficient mouse models of Alzheimer's disease. J. Neurochem.106:2080-2092.